UNIVERSITY OF CALIFORNIA
RIVERSIDE

# Characterization of *Xylella fastidiosa* Virulence Factors and Host Physiological Responses That Contribute to Pierce's Disease in Grapevine

A Dissertation submitted in partial satisfaction
of the requirements for the degree of

Doctor of Philosophy

in

Plant Pathology

by

Brian M. Ingel

December 2019

Dissertation Committee:
Dr. M. Caroline Roper, Chairperson
Dr. Wenbo Ma
Dr. James Borneman

The Dissertation of Brian M. Ingel is approved:

_____

_____

_____

Committee Chairperson

University of California, Riverside

# Acknowledgements

As my time in graduate school comes to an end, I realize that this journey was more of a crucible in which I learned many life skills and discovered more about myself than at any other point in my life. I learned to prioritize, multi-task, manage people, and collaborate. But probably the most important skills I learned were how to accept when something is good enough, how to accept failure, and how to think critically. I learned my personal limits, which ones I could push beyond, and which ones to accept. Ultimately, I learned my own personal philosophies and established the confidence to be comfortable with them around others. But I could not have learned any of this or achieved what I have without the help, support, hard work, kindness, and generosity of others, all of whom I would like to give my sincerest thanks and gratitude.

First and foremost, I would like to thank my graduate advisor, Dr. Caroline Roper. She allowed me the space to become an independent scientist, provided advice when needed, and treated me with respect and consideration. Her values of honesty, scientific integrity, and employee advocacy are those that I wish to emulate in my career.

I would also like to thank the Roper lab members, both past and present, especially my good friends Lindsey Burbank, Claudia Castro, Nichole Ginnan, and Polrit Viravathana. Lindsey, thanks for being a great mentor when I was starting my journey in the Roper lab. Claudia, thanks for all the great life conversations, and for being my "battle buddy" in the grapevine jungles of UCR greenhouses. Nichole, thanks for listening when I needed to vent and for all the statistics and coding consultations. And Pol, thank you for all your generosity and for the numerous and lengthy consultations about proteomics. I

sincerely wish all of you the best in your future endeavors. And to my Manosalva lab friends, Rod and Aidan, thanks for all your support and for the great times at the Getaway.

I would also like to thank Dr. Richard Stouthamer for his support and help navigating graduate school. Our conversations about my work and his wise and timely advice were critical to my completion of this degree, and for that, I am truly grateful.

To my parents, thank you for fostering my scientific interests and for helping me achieve my goals. From science fairs to college admission, you've always supported me. And to my brother, thanks for all the great times we've had over the years. They definitely helped keep me going during graduate school.

And most importantly, I am deeply and sincerely grateful for my wonderful wife Claire, who has helped me through all the ups and downs of this tumultuous journey, talked me down from the metaphorical ledge more times than I care to remember, and stood by me during my darkest hours, all while being a full-time scientist and mother. Her fierce independence, intelligence, kindness, optimism, and enthusiasm have been truly inspirational and are traits I strive to emulate. Claire, you are my rock and the love of my life. Thank you. To my son Rowan, thank you for all of your smiles, laughter, and hugs. They are the highlights of my day and have helped me get through the end of this journey. I hope that one day you too will find the joy that I have in exploring the wonders of this world through science.

I would like to thank all of my collaborators whose work has made this dissertation possible: Dr. Daniel Jeske for his contribution of the Generalized Estimating

Equations model and the statistical analysis, Dr. Armann Andaya of the UC Davis Mass Spectrometry Facility for his work extracting and analyzing my secretome samples, Dr. Lindsey Burbank for her help with bacterial RNAseq, Clarissa Reyes, Dr. Mason Earles, and Dr. Andrew McElrone for their work using microCT and machine-learning algorithms to assess starch depletion, and Dr. Melanie Massonnet and Dr. Dario Cantu for their work using RNAseq to assess the grapevine transcriptome. And lastly, I would like to give special thanks to Dr. Qiang Sun, whose masterful Scanning Electron Microscopy work contributed significantly to Chapters 2 and 4.

As I move forward into the next chapter of my life, I will remember all of those who helped make this possible, and I will strive to help others in the way you all have helped me.

The text of Chapter 1, in full, is a reprint of parts of the material as they appear in the review article "*Xylella fastidiosa*: an examination of a re-emerging plant pathogen" (Rapicavoli, J., Ingel, B., Blanco-Ulate, B., Cantu, D. and Roper, C. 2018. Molecular plant pathology. 19(4):786-800). The co-author, Dr. Caroline Roper, listed in that publication directed and supervised the research which forms the basis for this chapter. Dr. Jeannette Rapicavoli and Brian Ingel contributed equally as co-first authors.

The text of Chapter 2, in full, is a reprint of the material as it appears in "*Xylella fastidiosa* Endoglucanases Mediate the Rate of Pierce's Disease Development in *Vitis vinifera* in a Cultivar-Dependent Manner" (Ingel, B., Jeske, D.R., Sun, Q., Grosskopf, J.

and Roper, C. 2019. Molecular Plant-Microbe Interactions). The co-author, Dr. Caroline Roper, listed in that publication directed and supervised the research which forms the basis for this chapter.

ABSTRACT OF THE DISSERTATION

Characterization of *Xylella fastidiosa* Virulence Factors and Host Physiological Responses That Contribute to Pierce's Disease in Grapevine

by

Brian M. Ingel

Doctor of Philosophy, Graduate Program in Plant Pathology
University of California, Riverside, December 2019
Dr. M. Caroline Roper, Chairperson

*Xylella fastidiosa* is a xylem-limited bacterium that causes Pierce's Disease (PD) in grapevine. PD symptom progression is correlated with systemic colonization by *X. fastidiosa*, which occurs via pit membrane degradation. Previous studies determined that a polygalacturonase, one of several cell wall degrading enzymes (CWDEs) secreted by *X. fastidiosa*, is necessary for pit membrane degradation. Here, it is demonstrated that the loss of two *X. fastidiosa* β-1,4-endoglucanases (EGases) in tandem causes significantly slower PD symptom development and progression, and reduces *X. fastidiosa* virulence and population size. Furthermore, differences in the PD symptom progression rate between two cultivars appear to be caused by variations in pit membrane carbohydrate composition, which influence the rate of enzymatic degradation, and subsequently, the rate of systemic colonization.

How these CWDEs and other virulence factors are secreted has not been fully elucidated. However, several are predicted to be secreted via the Type II secretion system

(T2SS). T2SS-deficient *X. fastidiosa* mutants did not induce PD symptoms, and the mutant bacteria were not recovered from infected vines, indicating that the T2SS and its secreted substrates are necessary for virulence and survival. Analysis of wild type *X. fastidiosa* and T2SS-deficient mutant secretomes found six potential Type II secreted proteins for further characterization, including three lipases, a β-1,4-cellobiohydrolase, a protease, and a hypothetical protein. However, none of the CWDEs were present in the secretomes, but their high transcript abundance indicates that these enzymes could be post-transcriptionally regulated.

Several PD symptoms appear similar to drought stress symptoms. Under drought conditions, decreased photosynthesis, cessation of plant growth, and carbon starvation occur. Tylose formation in response to *X. fastidiosa* infection occludes vessels to prevent the spread of pathogens and air embolisms. Interestingly, genes involved in photosynthesis and plant growth are down-regulated during PD symptom development, and tylose formation increases significantly. This increased vessel occlusion in the absence of new vessel formation over time could cause prolonged water stress. Furthermore, starch in the ray parenchyma depletes as PD symptoms progress, indicating that carbon starvation occurs. These results indicate that, along with *X. fastidiosa*-mediated virulence factors, host responses also contribute to PD.

## Table of Contents

## List of Figures

## List of Tables

# 1. Chapter 1 Introduction

In the late 1800's, Newton B. Pierce described a severe grapevine disease occurring in Anaheim, California. This disease was initially called Anaheim disease (Pierce 1892) and was first attributed to a viral infection because (i) no causal microorganism could be cultured from the infected vines, and (ii) the disease was graft transmissible. However, electron micrographs indicated bacterial-like bodies in the xylem of infected plants (Hopkins and Mollenhauer 1973). A bacterium was subsequently cultured from infected plants (Davis et al. 1978). Koch's postulates were then completed, ultimately confirming *X. fastidiosa* as the causal agent of what was eponymously named Pierce's disease (PD). In addition to PD, this bacterium has been implicated as the causal agent of many other significant plant diseases. The severity of the Citrus Variegated Chlorosis (CVC) epidemic in Brazil (Bove and Ayres 2007) and PD epidemic in Southern California (Siebert 2001) prompted sequencing of the 9a5c CVC strain genome (Simpson et al. 2000), followed by other PD strains of *X. fastidiosa* (Van Sluys et al. 2003, Chen et al. 2016). Notably, *X. fastidiosa* was the first plant pathogenic bacterium to have its genome sequenced. Subsequently, genomes of other *X. fastidiosa* isolates have been sequenced (Chen et al. 2010, Guan et al. 2014, Giampetruzzi et al. 2015, Chen et al. 2016), providing a robust database for genome mining and comparative genomics.

*X. fastidiosa* has a marked capacity to engage in inter-strain recombination that can effectively result in new strains with different host ranges than the original parent strains (Nunney et al. 2014). This has allowed *X. fastidiosa* to have a broad host range that includes both monocots and dicots. Although all *X. fastidiosa* isolates were initially assigned to the same species, they have been further classified to the subspecies level

(Scally et al. 2005, Schuenzel et al. 2005). Historically, *X. fastidiosa* has been limited to the Americas (Janse and Obradovic 2010). Three clades of *X. fastidiosa* have been identified in North America, corresponding to the different subspecies: *X. fastidiosa* subsp. *fastidiosa*, which is found in grapevines, almond, and alfalfa; *X. fastidiosa* subsp. *multiplex*, which can be found in almond, peach, plum, and oak; *X. fastidiosa* subsp. *sandyi*, which thus far has only been found in oleander; and *X. fastidiosa* subsp. *pauca*, which is primarily found in citrus and coffee in South America (Scally et al. 2005). The strain associated with Olive Quick Decline Syndrome (OQDS) was recently identified in olive trees in Salento (Lecce district), of the Apulia region of Italy, and was found to be genetically related to the *pauca* subsp. (Giampetruzzi et al. 2015). This represents the first confirmed detection of *X. fastidiosa* in the European Union (Loconsole et al. 2014). An understanding of OQDS epidemiology is just emerging. Thus far, the meadow spittlebug, *Philaenus spumarius*, has been identified as the primary insect vector (Saponari et al. 2014). The recent outbreak of OQDS in Italy presents a formidable threat to European agriculture. Olive trees are an essential part of the Mediterranean landscape and culture, and olive farming in Southern Italy's Apulia region currently accounts for nearly 40% of Italy's olive oil production (Strona et al. 2017). The European Food Safety Authority (EFSA) recently stated that the dissemination of *X. fastidiosa* to other European countries is very likely, since many other olive-growing regions (e.g. Spain, Portugal, Greece) match the climatic conditions of Apulia (Luvisi et al. 2017). Currently, nearly 10,000 ha of olive trees have been destroyed, which amounts to millions of dollars in damages (Martelli et al. 2016). *X. fastidiosa* can also reside in a wide range of plants as

a harmless endophyte, and has been detected in hundreds of asymptomatic plant species (Raju et al. 1980, Hopkins and Purcell 2002, Chatterjee et al. 2008a). Most *X. fastidiosa* strains do not move systemically in symptomless hosts (Hill and Purcell 1995, Purcell and Saunders 1999), but these plants could still serve as sources of inoculum (Hill and Purcell 1997).

*X. fastidiosa* subsp. *fastidiosa*, the causal agent of PD, colonizes two environments: the grapevine host xylem and the mouthparts of its insect vectors, *Homalodisca vitripennis*, Glassy winged sharpshooter (GWSS) and *Graphocephala atropunctata*, Blue green sharpshooter (BGSS), both of which are members of the sharpshooter subfamily of leafhoppers (Cicadellidae) (Hewitt et al. 1946). *X. fastidiosa* has a persistent and propagative, but non-circulative, relationship in adult sharpshooters, which is the only described vector-microbe relationship of this sort. An adult sharpshooter remains infective throughout its life, while infective nymphs lose the ability to transmit when they molt and shed the cuticular lining of the foregut (Purcell and Finlay 1979). Sharpshooters acquire *X. fastidiosa* by feeding on infected hosts and can immediately transmit *X. fastidiosa* to a new plant host with no latent period. A possible explanation for the absence of a latent period is the ability of sharpshooters to transiently hold a column of fluid containing *X. fastidiosa* cells in their stylets without swallowing it, allowing the fluid to be immediately egested during feeding (Backus et al. 2015). Over time, the bacteria colonize the insect foregut (namely the cibarium and precibarium regions) by attaching to the cuticular lining and forming biofilms (Brlansky et al. 1983).

Inoculation occurs through a combined egestion/salivation mechanism that dislodges the bacteria from the cuticular lining of the foregut.

Generally speaking, the ability to form a robust surface-attached community (biofilm) directly correlates with virulence for many bacterial pathogens (Danhorn and Fuqua 2007). Formation of a biofilm plays an important role in colonization of the insect and plant environments for *X. fastidiosa*. The surface, in this case, is either the wall of the xylem or the cuticular lining of the insect foregut. *X. fastidiosa* has never been found outside of the plant host or its insect vector. In the insect environment, it is clear that attachment and formation of biofilm-like structures within the foregut are tightly associated with acquisition, retention (and ultimately transmission) of *X. fastidiosa* by sharpshooters (Killiny and Almeida 2014). However, the role of biofilm formation in the plant environment is much more nuanced. In heavily infected plants, *X. fastidiosa* biofilms are abundant (Newman et al. 2003, Roper et al. 2007a), thus, attachment to the xylem wall is a key aspect of establishment *in planta*. However, to move systemically in the plant, the bacteria must enter an exploratory, motile state. There are several examples of mutants that are defective in surface/cell-cell attachment, but display hypervirulent phenotypes (Guilhabert and Kirkpatrick 2005, Chatterjee et al. 2008b). Thus, it has been proposed that *X. fastidiosa* forms biofilms partially to attenuate its own virulence by controlling rampant systemic colonization. Logically, it would benefit the bacterium not to kill its host immediately, and this model also explains how *X. fastidiosa* can exist as a commensal endophyte in many plant species (Chatterjee et al. 2008a, Roper and Lindow 2014). To be effectively acquired from the plant by the insect, the bacteria must be in the

adhesive state. Taken together, this requires that *X. fastidiosa* fluctuate between an exploratory (non-adhesive) state and an insect-acquirable (adhesive) state. We will focus this review on the latest information regarding the factors governing plant and insect colonization.

In the xylem, *X. fastidiosa* produces prolific amounts of outer membrane vesicles (OMVs) as compared to other bacterial species. For *X. fastidiosa*, OMVs hinder attachment to glass and xylem surfaces suggesting that they serve to prevent attachment during the exploratory phase of xylem colonization. Blocking attachment is a novel function described for OMVs in bacteria (Ionescu et al. 2014). Afimbrial hemagglutinin adhesins, HxfA and HxfB, facilitate cell-cell attachment (Guilhabert and Kirkpatrick 2005) and are found in both the outer membrane of *X. fastidiosa* cells and as cargo in OMVs that are shed from the cells (Voegel et al. 2010). Loss of function mutations in both the *hxfA* and *hxfB* genes resulted in hypervirulent phenotypes after inoculation into grapevines, supporting the hypothesis that *X. fastidiosa* uses adhesion to control the dynamics of systemic colonization to attenuate its own virulence. XatA, an autotransported protein related to surface adhesion and cell-cell aggregation, is also found in OMVs (Matsumoto et al. 2012), but a knockout mutation in *xatA* resulted in a significant decrease in virulence rather than the hypervirulent phenotype that resulted from mutations in the hemagglutinin adhesins. It is tempting to speculate that altering OMV cargo and OMV production is a mechanism used by *X. fastidiosa* to adjust its adhesiveness during plant colonization to either facilitate systemic plant movement or enable insect acquisition.

After attaching to the xylem vessel wall, *X. fastidiosa* produces an exopolysaccharide (EPS), termed fastidian gum to form a biofilm. Fastidian gum is predicted to be similar in structure to xanthan gum (da Silva et al. 2001), but the polymer has yet to be fully characterized. Spatiotemporal localization of EPS during the different stages of biofilm formation indicated that there is very little EPS associated with initial biofilm stages (microcolony formation), but EPS can be seen intercalating the mature biofilm structure. Thus, EPS contributes more to maintenance of three-dimensional biofilm architecture, and stability of the mature biofilm, as opposed to initial surface attachment (Roper et al. 2007a). Findings by Souza et al. (2006) corroborate this, as EPS mutants in the CVC strain of *X. fastidiosa* were not affected in surface attachment but showed a reduced capacity to form biofilms. Immunolocalization in PD-infected grapevines showed that an EPS matrix was associated with *X. fastidiosa* cell aggregates in the plant xylem vessels, where it also contributed to xylem vessel occlusions (Roper et al. 2007a). *X. fastidiosa* mutants compromised in EPS production had reduced virulence in grapes and were poorly acquired by insects (Killiny et al. 2013).

In an exploratory state, either after insect transmission or dispersion from a biofilm, *X. fastidiosa* must move from one xylem vessel to another to systemically colonize the grapevine host. The xylem in grapevines is comprised of many interconnected vessels that are finite, but variable in length, and any one vessel rarely spans the entire length of the stem (Tyree and Zimmermann 2002, Thorne et al. 2006b). These xylem vessels are connected to each other by scalariform bordered pits that separate vessel elements from one another via pit membranes, which are composed of primary plant cell wall material

(cellulose microfibrils embedded in a meshwork of hemicellulose and pectin) (Buchanan et al. 2000, Choat et al. 2004). The pores within the pit membrane range from 5 – 20 nm in diameter and allow for the flow of water and small solutes from one vessel to another, but block air embolisms and pathogen movement (Tyree and Zimmermann 2002, Stevenson et al. 2004). *X. fastidiosa* is too large to passively move through the pores of the pit membranes (Mollenhauer and Hopkins 1974). Therefore, it uses enzymatic degradation of the pit membranes as its primary means of achieving systemic colonization. *X. fastidiosa* utilizes an endo-polygalacturonase (PG) to digest polymers with a pectin backbone and requires this endo-PG to systemically colonize grapevines. A deletion mutation in the gene encoding endo-PG resulted in complete loss of pathogenicity (Roper et al. 2007b). Interestingly, effective degradation of the pit membranes requires a concerted effort with an endo-PG and at least one endoglucanase (EGase), EngXCA2, indicating that effective degradation of the plant cell wall mesh work is a cooperative effort between at least two classes of cell wall degrading enzymes (CWDEs). EngXCA2 is a prototypical EGase that degrades both carboxymethylcellulose and xyloglucan substrates (Perez-Donoso et al. 2010). *engXCA1* (PD1856) and *egl* (PD2061) putatively encode two additional EGases. Egl is comprised of a putative glycosyl hydrolase domain. EngXCA1 is comprised of a putative N-terminal glycosyl hydrolase domain and a putative C-terminal expansin domain. The expansin domain is unique because expansins are typically described as non-enzymatic plant proteins that facilitate cell wall expansion during plant cell growth (Cosgrove 2000). However, a few phytopathogenic bacteria have expansin proteins or EGases with expansin domains (e.g.

*Xanthomonas campestris*, *Clavibacter michiganensis*, and *Ralstonia solanacearum*) that were likely acquired from plants via cross-kingdom horizontal gene transfer (Nikolaidis et al. 2013, Georgelis et al. 2014). It is notable that all of these organisms have a significant xylem-dwelling phase, suggesting that bacterial expansins evolved as a result of association with the plant xylem tissue. The expansin domain from EngXCA1 has yet to be characterized, and its role in pit membrane degradation is still unknown.

It is estimated that only 10-15% of the vessels are heavily colonized by *X. fastidiosa* (Newman et al. 2003) and that the majority of colonized vessels contain only a few cells. Too many cells in one vessel would block or limit the flow of xylem sap in that particular vessel and, presumably, the nutrients necessary for bacterial survival (Newman et al. 2003). The current model of cell-density-regulated host colonization (Chatterjee et al. 2008a) indicates that when vessels do become heavily occluded, the Rpf high cell density system down-regulates genes conducive to systemic spread (i.e. motility and cell wall degrading enzymes (CWDEs), via accumulation of a diffusible signaling factor (DSF) (Newman et al. 2004). This accumulation of DSF activates the RPF signaling system enhances the production of various adhesins that increase cell "stickiness" (Chatterjee et al. 2008a). This would allow the cells in heavily occluded vessels to enter the insect-acquirable state to increase the chances of acquisition and, subsequently, transmission to a new plant by an insect vector. OMV production, which is also linked to adhesiveness, is regulated by cyclic di-GMP signaling via the Rpf diffusible signal factor (Ionescu et al. 2014). Disruption of the Rpf system results in hyper-vesiculation (Ionescu et al. 2014), making *X. fastidiosa* less adhesive and, subsequently, hypervirulent *in planta*

(Newman et al. 2004). Please see past reviews (Chatterjee et al. 2008b and Roper and Lindow, 2014) for extensive reviews on the gene regulation hierarchy in *X. fastidiosa*.

*X. fastidiosa* secretes several proteins when interfacing with its host, but unlike many other phytopathogenic bacteria, *X. fastidiosa* does not possess a Type III secretion system, which is commonly used to secrete protein effectors that enhance virulence and/or suppress plant defenses (Dow and Daniels 2000). However, *X. fastidiosa* does possess operons containing the genes necessary to produce components of the Type I, II, and V secretion systems (Simpson et al. 2000, Van Sluys et al. 2003). The Type I secretion system is a general secretory pathway that has many functions, including multidrug resistance efflux and secretion of various proteases, hydrolases, and toxins (Delepelaire 2004). The Type I translocator channel is ATP-dependent and is comprised two inner membrane proteins that attach to TolC, a periplasm/outer membrane protein that is highly conserved among many phytopathogenic bacteria (Holland et al. 2005). A mutation in *tolC* caused a loss of pathogenicity (Reddy et al. 2007). However, bacteria could not be isolated from grapevines inoculated with the mutant strain, suggesting that the *tolC* mutation is actually lethal *in planta*. The mutant strain also displayed a high level of sensitivity to several phytochemicals, detergents, and crude plant extracts, highlighting the necessity of TolC for multidrug efflux and viability of *X. fastidiosa* in plants.

The Type V secretion system is comprised of a family of autotransporter proteins that transport themselves out of the cell without requiring any energy input (van Ulsen et

al. 2014). *X. fastidiosa* has six genes predicted to encode members of the AT-1 autotransporter family, one of which is XatA (Matsumoto et al. 2012). Its C-terminal helper domain interacts with the bacterial outer membrane and with OMVs, and its passenger domain is released into the extracellular environment. A *xatA* mutant formed smaller bacterial aggregates and produced less biofilm relative to the wild type parent strain, indicating an important role of XatA in the adhesion for *X. fastidiosa*. When inoculated into grapevines, the mutant strain did not induce symptoms of PD, or systemically colonize plants, and was compromised in colonization at the point of inoculation (Matsumoto et al. 2012).

*X. fastidiosa* possesses a 12-protein Type II secretion system (T2SS) that is closely related to those found in *Xanthamonas campestris* pv. *campestris* and *Xanthomonas oryzae* pv. *oryzae* (Jha et al. 2005). The T2SS is made up of three parts: the outer membrane pore, the inner membrane complex, and the pseudopilin complex (Sandkvist 2001). Pseudopilin formation is driven by XpsE: an ATPase that facilitates the stacking of additional pseudopilin subunits that push the loaded protein out into the extracellular environment (Jha et al. 2005). Proteins secreted by the T2SS are often proteases and plant cell wall degrading enzymes (CWDEs) that utilize a secretion signal to direct their transport (Sandkvist 2001). The majority of the proteases and CWDEs in *X. fastidiosa* are predicted to be secreted via the T2SS. Mutations in *xpsE* in *X. fastidiosa* cause a non-pathogenic phenotype similar to the *pglA* mutant (Peng, 2014) indicating a strong connection between the T2SS and secretion of critical CWDEs in *X. fastidiosa*.

Obstruction of xylem vessels by gums and tyloses are a common plant response designed to restrict the movement and systemic infection of vascular pathogens (Clerivet et al. 2000, Tyree and Zimmermann 2002, Sun et al. 2008, Yadeta and Thomma 2013). Tyloses are produced in response to cavitation within the xylem, which occurs as the result of vascular damage, such as pit membrane degradation, and are found in abundance when PD symptoms are evident (Zimmerman 1979, Sun et al. 2013, De Micco et al. 2016). Tyloses are outgrowths of xylem-associated parenchyma cell walls into the neighboring vessel that expand by incorporating new cell wall materials (cellulose, hemicellulose, and pectin) in the presence of ethylene (Esau 1977). High ethylene levels have been reported in grape tissues infected with *X. fastidiosa* (Perez-Donoso et al. 2007, Sun et al. 2007), which can partially explain the extensive induction of tylose formation during PD.

Tyloses can efficiently block *X. fastidiosa* movement in the stem vasculature and prevent systemic infection if the disassembly of pit membranes in the vessel-xylem parenchyma interface occurs faster than the breakdown of the inter-vessel pit membrane system (Sun et al. 2013). Tyloses form faster in PD resistant species of grapevines, such as species of native muscadine and wild grapevines (e.g. *Vitis rotundifolia* and *Vitis arizonica*, respectively), than in susceptible species (*Vitis vinifera*). The formation of these occlusions restricts the movement of *X. fastidiosa* into vessel segments beyond the inoculation point (Mollenhauer and Hopkins 1976, Fry and Milholland 1990b, Fry and Milholland 1990a, Sun et al. 2013). Conversely, it appears that the enzymatic breakdown of pit membranes facilitated by *X. fastidiosa* takes place more quickly in the PD

susceptible genotype, which allows the pathogen to move systemically before tyloses seal the vessels. Although tylose formation could be a successful mechanism for restricting bacterial spread, it has the negative side effect of blocking water flux within the affected xylem vessel (Stevenson et al. 2004). In fact, whether tyloses in *X. fastidiosa*-infected grapevines contribute to disease resistance (i.e. preventing pathogen movement) or susceptibility (i.e. by reducing water movement) continues to be a matter of debate (Cantu et al. 2016). Numerous observations have confirmed that extensive tylose formation in compatible *X. fastidiosa*-host interactions has an impact on the plant water transport, which in turn worsens the symptoms of the disease (Machado and Tyree 1994, Perez-Donoso et al. 2007, Choi et al. 2013, Sun et al. 2013). Additionally, *X. fastidiosa* cells and/or their secretions may also contribute to the blockage of vascular tissues. It is well established that plants affected by *X. fastidiosa* infections are more vulnerable to water stress, possibly due to the decrease in xylem hydraulic conductivity, a consequence of stomatal closure and blockage of the vessels (De Souza et al. 2009).

It was proposed that PD symptoms resulted solely from the water deficit caused by xylem occlusions, instead of the bacterial infection itself. However, this hypothesis has been refuted by several studies. For example, Thorne et al. (2006a) exposed 'Chardonnay' grapevines to water stress, inoculation with *X. fastidiosa*, and a combination of both treatments to determine whether symptoms of PD mimicked those of water deficit. The results showed that visual symptoms of PD were qualitatively and quantitatively different than those caused by water stress. *X. fastidiosa*-inoculated vines showed several PD-specific symptoms, such as green islands, matchstick petioles, and

patchy leaf necrosis; while vines exposed to water deficits did not develop any of these hallmark symptoms. Using a similar experimental design, Choi et al. (2013) evaluated the transcriptional response of 'Cabernet Sauvignon' grapevines to *X. fastidiosa* inoculation, water deficit, and a combination of the two stresses. This report indicated that gene expression changes associated with bacterial inoculation were clearly distinct from those related to water stress. Notably, vines experiencing both pathogen infection and water deficit presented more pronounced expression changes of genes involved in *X. fastidiosa*-unique responses, supporting the idea of a direct interaction between PD and grapevine water stress.

PD has been in California for many years, but typically it spread slowly and did not cause significant damage in most viticultural areas of the state. However, in the late 1990's, PD became an acute concern in California. To understand why the disease incidence increased to epidemic levels, one must consider the behavior of the insect vectors. Historically, the BGSS has been the most important vector in California coastal vineyards, whereas the red headed (*Carneocephala fulgida*) and green (*Draeculacephala minerva*) sharpshooters have been most significant in the San Joaquin Valley (Hewitt 1949). These native vectors overwinter in riparian habitats (e.g. streambeds), and in the spring and summer, move from riparian habitats to vineyards where they feed on grapevines. Native sharpshooters exclusively feed on succulent new growth (Purcell 1975). Once in the plant, the bacteria move basipetally from the point of inoculation down to the vine cordon and trunk where they overwinter. Infections that occur in spring or early summer become chronic because the bacteria have adequate time to migrate

down to these permanent parts of the vine (i.e. the cordon and trunk are not pruned annually). Infections occurring late in the season do not have a chance to become chronic because severe winter pruning removes infected parts of the vine before *X. fastidiosa* can migrate into the cordon to overwinter. Because they fly from their preferred habitats only into the edge of the vineyards, native sharpshooters do not spread PD from one vine to another (Purcell 1974, Purcell 1975). In the Northern coastal regions of California, PD persists mainly in "PD hot spots" along parts of the vineyard adjacent to riparian areas (e.g. streambeds). The dominant vector in this region is the native BGSS, which enters vineyards from these riparian areas in the spring and summer, following overwintering, to feed and reproduce. PD incidence is the highest in these hot spots, creating what is known as the PD "edge effect" (Hopkins and Purcell 2002), meaning that infection remains primarily along the edges of the vineyard. In addition, BGSS prefer to feed on succulent, new growth, so any *X. fastidiosa* that has not reached the vine's permanent arms or trunk will likely be pruned out when vines enter dormancy in the winter. Thus, PD does not typically persist from year to year in these areas and is a monocyclic disease. This lack of spread within vineyards was an essential feature of PD epidemiology because it has limited occurrence and distribution of the disease (Hopkins and Purcell 2002).

The epidemiology of PD changed drastically in the southern regions of California due to the introduction of the polyphagous GWSS. It is hypothesized that the GWSS was introduced into California from Texas on nursery stock. The GWSS and *X. fastidiosa* are endemic to Texas and the southeastern United States, and they are the primary reason that

these regions lack a major *Vitis vinifera* grape industry. The GWSS was first spotted in 1990 in Southern California. Soon after, PD became a polycyclic disease and reached epidemic proportions, causing millions of dollars of damage to Temecula Valley vineyards (Blua et al. 1999). Furthermore, the presence of GWSS brought about a new *X. fastidiosa*-related disease in Southern California called Oleander Leaf Scorch. The disease was first noticed in the Palm Springs-Indio area of Riverside County in 1994 and spread to adjacent areas in the years following (Blua et al. 1999).

This change in PD epidemiology results from differences in the feeding, flying, and breeding behavior of the GWSS. Unlike native sharpshooters, the GWSS can feed on both succulent new growth and woody stems. Woody stems are closer to the cordons and main trunk, and bacteria introduced here require less time to reach the cordon and trunk to overwinter. Therefore, GWSS feeding behavior increases the incidence of chronic infections. In addition, the GWSS is a much stronger flier than the native sharpshooters and can fly faster and further into the vineyard. The final property of the GWSS that contributes to the increase of PD is its breeding behavior. In contrast with native sharpshooters (which preferentially feed and reproduce on riparian plants), GWSS can reproduce on numerous plant species, with special preference for citrus. Citrus groves support enormous populations of these insects, and in Southern California, many citrus groves are planted adjacent to vineyards (Perring et al. 2001). This unfortunate situation allows the GWSS easy access to vineyards and increases the spread and incidence of PD. The introduction of the GWSS into Southern California effectively shifted PD from a monocyclic to a polycyclic disease. With the establishment of the GWSS, PD became so

severe in Southern California that it threatened to eliminate viticulture in some areas. The potential impact it may have in Central and Northern grape growing regions of California is unknown. Most of the economically important diseases caused by *X. fastidiosa* occur mainly in parts of North America that do not experience cold winters (Hopkins and Purcell 2002). Therefore, if the GWSS migrates into Northern California, the incidence and distribution of PD could reach the same levels experienced in the southern part of the state.

Because *X. fastidiosa* causes diseases in economically valuable crops, the occurrence of these epidemics are typically accompanied by substantial economic consequences. The California table, raisin, and wine grape industries were valued at over $5 billion in 2014 (CDFA 2014). Following the introduction of GWSS into Southern California, losses were estimated to be $37.9 million dollars annually (Siebert 2001). Despite the presence of the PD/GWSS Control Program, established in 2001, PD costs producers over 100 million dollars per year in crop loss and replanting expenses. This amount excludes an additional $50 million per year spent on preventative measures, including vector control (Alston et al. 2015). Alston et al. (2013) evaluated the costs and benefits of PD research in the wine grape industry, and they estimated that PD would cost an additional $189 million per year if the PD Control Program (PDCP) ended. Therefore, the benefits of PD research clearly outweigh the costs in terms of preventing another major outbreak.

Currently, there are no effective PD control methods that target the pathogen. The most widely used methods of control for PD are i) severe pruning and roguing of infected

vines and ii) control of the insect vector via insecticide applications. Insecticides are currently the most important facet of PD control in California, and have generally been successful at managing the insect vector populations. For instance, coordinated area wide-insecticide sprays for GWSS were able to restore grape production to economically viable levels in the Temecula valley. Growers often apply within-vineyard applications of the insecticide imidacloprid to complement area-wide control applications to control GWSS. It is not clear if within-vineyard applications are necessary for control of PD or if a grower can rely solely on area-wide management for sufficient PD control. However, modeling of vector behavior in the context of climate change suggests that warmer temperatures would favor an increase in PD incidence (Daugherty et al. 2017).

A robust grapevine breeding program has also been established to evaluate germplasm for PD resistance. Although no *V. vinifera* genotypes resistant to PD have been identified, genetic sources of disease resistance are present in the *Vitis* germplasm. Wild *Vitis* populations with varying degrees of PD resistance or tolerance have been identified in the Southeastern United States and North of Mexico (Krivanek et al. 2005). The availability of genetic transformation approaches for *V. vinifera* has opened up the possibilities of using biotechnology to improve PD resistance in susceptible genotypes (Aguero et al. 2005, Dandekar et al. 2012). Because of the negative perception of genetically modified organisms, various strategies have been suggested to use biotechnology techniques for traditional breeding and viticulture practices. One example is trans-grafting, which refers to the grafting of non-transgenic scions to transgenic rootstocks (Song et al. 2015). This approach is based on the hypothesis that rootstocks

expressing different PD resistance-associated transgenes could potentially confer resistance to the non-transgenic scion. Moreover, stacking resistance genes (or transgenes) could also be accomplished by crossing plants of the same rootstock variety. Therefore, if transgenic rootstock strategies for PD defense prove effective, then it is likely that only a few particular rootstock genotypes would be needed for deployment with numerous *V. vinifera* grape scion varieties (Cantu et al. 2016).

Because of its capacity to undergo inter-strain recombination and its incredibly wide host range, *X. fastidiosa* remains a formidable threat to many susceptible agricultural crops and, perhaps, in plant species where a pathogenic relationship has yet to be described. Because there are no effective control measures that target the bacterium itself, this is an open area of research. To this end, understanding the biology of X. fastidiosa with regards to virulence and determining which bacterial processes are most important for disease development may facilitate the discovery of viable bacterial targets for direct *X. fastidiosa* control measures. Therefore, this dissertation seeks to further the understanding of *X. fastidiosa* virulence factors, the mechanisms by which *X. fastidiosa* disseminates these virulence factors, and the host physiological responses to *X. fastidiosa* infection.

## Literature Cited


Agueero, C. B., Uratsu, S. L., Greve, C., Powell, A. L., Labavitch, J. M., Meredith, C. P. and Dandekar, A. M. 2005. Evaluation of tolerance to Pierce's disease and Botrytis in transgenic plants of *Vitis vinifera* L. expressing the pear PGIP gene. Molecular Plant Pathology. 6(1): 43-51.

Alston, J. M., Fuller, K. B., J. D. Kaplan, J. D. and Tumber K. P. 2013. Economic Consequences of Pierce's Disease and Related Policy in the California Winegrape Industry. Journal of Agricultural and Resource Economics. 38(2): 269-297.

Alston, J. M., Fuller, K. B., J. D. Kaplan, J. D. and Tumber K. P. 2013. Assessing the returns to R&D on perennial crops: the costs and benefits of Pierce's disease research in the California winegrape industry. Australian Journal of Agricultural and Resource Economics. 59(1): 95-115.

Backus, E. A. and Morgan, D. J. W. 2011. Spatiotemporal Colonization of *Xylella fastidiosa* in its Vector Supports the Role of Egestion in the Inoculation Mechanism of Foregut-Borne Plant Pathogens. Phytopathology. 101(8): 912-922.

Backus, E. A., H. J. Shugart, H. J., Rogers, E. E., Morgan J. K., and Shatters R. 2015. Direct Evidence of Egestion and Salivation of *Xylella fastidiosa* Suggests Sharpshooters Can Be Flying Syringes. Phytopathology. 105(5): 608-620.

Blua, M., Phillips, P. and Redak, R. 1999. A new sharpshooter threatens both crops and ornamentals. California Agriculture. 53(2): 22-25.

Bove, J. M. and Ayres, A. J. 2007. Etiology of three recent diseases of citrus in Sao Paulo State: Sudden death, variegated chlorosis and huanglongbing. Iubmb Life. 59(4-5): 346-354.

Brlansky, R. H., Timmer, L. W., French, W. J. and Mccoy, R. E. 1983. Colonization of the sharpshooter vectors, *Oncometopia nigricans* and *Homalodisca coagulata*, by xylem-limited bacteria. Phytopathology. 73(4):530-535.

Buchanan, B. B., Gruissem, W. and Jones, R. L. 2000. Biochemistry & molecular biology of plants. American Society of Plant Physiologists, Rockville, Md.

Cantu, D., Roper, M.C., Powell A. L. and Labavitch, J. M. 2016. Problematic Crops: 1. Grape: To long life and good health: untangling the complexity of grape diseases to develop pathogen-resistant varieties. Plant Pathogen Resistance Biotechnology: 193.

Chatterjee, S., Almeida, R. P. P. and Lindow, S. 2008a. Living in two worlds: The plant and insect lifestyles of *Xylella fastidiosa*. Annual Review of Phytopathology. 46:243-271.

Chatterjee, S., Wistrom, C. and Lindow, S. E. 2008b. A cell-cell signaling sensor is required for virulence and insect transmission of *Xylella fastidiosa*. Proceedings of the National Academy of Sciences of the United States of America. 105(7):2670-2675.

Chen, J., Wu, F., Zheng, Z., Deng, X., Burbank, L. P. and Stenger, D. C. 2016. Draft Genome Sequence of *Xylella fastidiosa* subsp. *fastidiosa* Strain Stag's Leap. Genome Announc 4(2).

Chen, J., Xie, G., Han, S., Chertkov, O., Sims, D. and Civerolo, E. L. 2010. Whole genome sequences of two *Xylella fastidiosa* strains (M12 and M23) causing almond leaf scorch disease in California. J Bacteriol. 192(17):4534.

Choat, B., Jansen, S., Zwieniecki, M. A., Smets, E. and Holbrook, N. M. 2004. Changes in pit membrane porosity due to deflection and stretching: the role of vestured pits. Journal of Experimental Botany. 55(402):1569-1575.

Choi, H. K., Iandolino, A., da Silva, F. G. and Cook, D. R. 2013. Water Deficit Modulates the Response of *Vitis vinifera* to the Pierce's Disease Pathogen *Xylella fastidiosa*. Mol Plant-Microbe Interacts. 26(6):643-657.

Clerivet, A., Deon, V., Alami, I., Lopez, F., Geiger, J. P. and Nicole, M. 2000. Tyloses and gels associated with cellulose accumulation in vessels are responses of plane tree seedlings (*Platanus* x *acerifolia*) to the vascular fungus *Ceratocystis fimbriata* f. sp *platani*. Trees-Structure and Function. 15(1):25-31.

Cosgrove, D. J. 2000. Loosening of plant cell walls by expansins. Nature 407(6802):321-326.

da Silva, F. R., Vettore, A. L., Kemper, E. L., Leite, A. and Arruda, P. 2001. Fastidian gum: the *Xylella fastidiosa* exopolysaccharide possibly involved in bacterial pathogenicity. Fems Microbiology Letters. 203(2):165-171.

Dandekar, A. M., Gouran, H., Ibanez, A. M., Uratsu, S. L., Aguero, C. B., McFarland, S., Borhani, Y., Feldstein, P. A., Bruening, G., Nascimento, R., Goulart, L. R., Pardington, P. E., Chaudhary, A., Norvell, M., Civerolo E. and Gupta, G. 2012. An engineered innate immune defense protects grapevines from Pierce disease. Proc Natl Acad Sci U S A. 109(10):3721-3725.

Danhorn, T. and Fuqua, C. 2007. Biofilm formation by plant-associated bacteria. Annual Review of Microbiology. 61:401-422.

Daugherty, M., Zeilinger, A. R. and Almeida, R. 2017. Conflicting effects of climate and vector behavior on the spread of a plant pathogen. Phytobiomes. 1(1):46-53.

Davis, M. J., Purcell, A. H. and Thomson, S. V. 1978. Pierce's disease of grapevines: isolation of the causal bacterium. Science. 199(4324):75-77.

De Micco, V., Balzano, A., Wheeler, E.A. and Baas, P. 2016. Tyloses and gums: a review of structure, function and occurrence of vessel occlusions. IAWA journal. 37(2):186-205.

De Souza, A. A., Takita, M. A., Amaral, A. d., Coletta-Filho, H. and Machado, M. A. 2009. Citrus responses to *Xylella fastidiosa* infection, the causal agent of citrus variegated chlorosis. Tree For Sci Biotech. 2(3):957-964.

Delepelaire, P. 2004. Type I secretion in gram-negative bacteria. Biochimica Et Biophysica Acta-Molecular Cell Research. 1694(1-3):149-161.

Dow, J. M. and Daniels, M. J. 2000. *Xylella* genomics and bacterial pathogenicity to plants. Yeast. 17(4):263-271.

Esau, K. 1977. Anatomy of Seed Plants. 2'ed. New York.

Fry, S. and Milholland, R. 1990a. Multiplication and translocation of *Xylella fastidiosa* in petioles and stems of grapevine resistant, tolerant, and susceptible to Pierce's disease. Phytopathology. 80(1):61-65.

Fry, S. and Milholland, R. 1990b. Response of resistant, tolerant, and susceptible grapevine tissues to invasion by the Pierce's disease bacterium, *Xylella fastidiosa*. Phytopathology. 80(1):66-69.

Georgelis, N., Nikolaidis, N. and Cosgrove, D. J. 2014. Biochemical analysis of expansin-like proteins from microbes. Carbohydr Polym. 100:17-23.

Giampetruzzi, A., Chiumenti, M., Saponari, M., Donvito, G., Italiano, A., Loconsole, G., Boscia, D., Cariddi, C., Martelli, G. P. and Saldarelli, P. 2015. Draft Genome Sequence of the *Xylella fastidiosa* CoDiRO Strain. Genome Announc 3(1).

Guan, W., Shao, J., Zhao, T. and Huang, Q. 2014. Genome Sequence of a *Xylella fastidiosa* Strain Causing Mulberry Leaf Scorch Disease in Maryland. Genome Announc 2(2).

Guilhabert, M. R. and Kirkpatrick, B. C. 2005. Identification of *Xylella fastidiosa* antivirulence genes: Hemagglutinin adhesins contribute to *X. fastidiosa* biofilm maturation and colonization and attenuate virulence. Mol Plant-Microbe Interacts. 18(8):856-868.

Hewitt, W. B., Houston, B. R. and et al. 1946. Leafhopper transmission of the virus causing Pierce's disease of grape and dwarf of alfalfa. Phytopathology. 36:117-128.

Hewitt, W. B., Frazier, N. W., Freitag, J. H. and Winkler, A. J. 1949. Pierce's disease investigations. California Agriculture. 19(7):207-264.

Hill, B. and Purcell, A. 1995. Multiplication and movement of *Xylella fastidiosa* within grapevine and four other plants. Phytopathology. 85(11):1368-1372.

Hill, B. L. and Purcell, A. H. 1997. Populations of *Xylella fastidiosa* in plants required for transmission by an efficient vector. Phytopathology. 87(12):1197-1201.

Holland, I. B., Schmitt, L. and Young, J. 2005. Type 1 protein secretion in bacteria, the ABC-transporter dependent pathway (Review). Molecular Membrane Biology. 22(1-2):29-39.

Hopkins, D. L. and Mollenhauer, H. H. 1973. Rickettsia-like Bacterium Associated with Pierce's Disease of Grapes. Science. 179(4070):298-300.

Hopkins, D. L. and Purcell, A. H. 2002. *Xylella fastidiosa*: Cause of Pierce's disease of grapevine and other emergent diseases. Plant Disease. 86(10):1056-1066.

Ionescu, M., Zaini, P. A., Baccari, C., Tran, S., da Silva, A. M. and Lindow, S. E. 2014. *Xylella fastidiosa* outer membrane vesicles modulate plant colonization by blocking attachment to surfaces. Proceedings of the National Academy of Sciences of the United States of America. 111(37):E3910-E3918.

Janse, J. D. and Obradovic, A. 2010. *Xylella Fastidiosa*: Its Biology, Diagnosis, Control and Risks. Journal of Plant Pathology. 92(1):S35-S48.

Jha, G., Rajeshwari, R. and Sonti, R. V. 2005. Bacterial type two secretion system secreted proteins: double-edged swords for plant pathogens. Mol Plant Microbe Interacts. 18(9):891-898.

Killiny, N. and Almeida, R. P. P. 2014. Factors Affecting the Initial Adhesion and Retention of the Plant Pathogen *Xylella fastidiosa* in the Foregut of an Insect Vector. Applied and Environmental Microbiology. 80(1):420-426.

Killiny, N., Martinez, R. H., Dumenyo, C. K., Cooksey, D. A. and Almeida, R. P. P. 2013. The Exopolysaccharide of *Xylella fastidiosa* Is Essential for Biofilm Formation, Plant Virulence, and Vector Transmission. Mol Plant-Microbe Interacts. 26(9):1044-1053.

Krivanek, A., Famula, T., Tenscher, A. and Walker, M. 2005. Inheritance of resistance to *Xylella fastidiosa* within a *Vitis rupestris*× *Vitis arizonica* hybrid population. Theoretical and applied genetics. 111(1):110-119.

Loconsole, G., Potere, O., Boscia, D., Altamura, G., Djelouah, K., Elbeaino, T., Frasheri, D., Lorusso, D., Palmisano, F., Pollastro, P., Silletti, M. R., Trisciuzzi, N., Valentini, F., Savino, V. and Saponari, M. 2014. Detection of *Xylella Fastidiosa* in Olive Trees by Molecular and Serological Methods. Journal of Plant Pathology. 96(1):7-14.

Luvisi, A., Nicolì, F., and De Bellis, L. 2017. Sustainable Management of Plant Quarantine Pests: The Case of Olive Quick Decline Syndrome. Sustainability. 9(4):659.

Machado, J.-L. and Tyree, M. T. 1994. Patterns of hydraulic architecture and water relations of two tropical canopy trees with contrasting leaf phenologies: *Ochroma pyramidale* and *Pseudobombax septenatum*. Tree physiology. 14(3):219-240.

Martelli, G. P., Boscia, D., Porcelli, F. and Saponari, M. 2016. The olive quick decline syndrome in south-east Italy: a threatening phytosanitary emergency. European Journal of Plant Pathology. 144(2):235-243.

Matsumoto, A., Huston, S. L., Killiny, N. and Igo, M. M. 2012. XatA, an AT-1 autotransporter important for the virulence of *Xylella fastidiosa* Temecula1. Microbiologyopen. 1(1):33-45.

Meng, Y., Li, Y., Galvani, C. D., Hao, G., Turner, J. N., Burr, T. J. and Hoch, H. C. 2005. Upstream migration of *Xylella fastidiosa* via pilus-driven twitching motility. J Bacteriol. 187(16):5560-5567.

Mollenhauer, H. H. and Hopkins, D. L. 1974. Ultrastructural Study of Pierces Disease Bacterium in Grape Xylem Tissue. Journal of Bacteriology. 119(2):612-618.

Mollenhauer, H. H. and Hopkins, D. L. 1976. Xylem morphology of Pierce's disease-infected grapevines with different levels of tolerance. Physiological Plant Pathology. 9(1):95IN2597-2596IN27100.

Newman, K. L., Almeida, R. P., Purcell, A. H., and Lindow, S. E. 2003. Use of a green fluorescent strain for analysis of *Xylella fastidiosa* colonization of *Vitis vinifera*. Applied and Environmental Microbiology. 69(12):7319-7327.

Newman, K. L., Almeida, R. P. P., Purcell, A. H. and Lindow, S. E. 2004. Cell-cell signaling controls *Xylella fastidiosa* interactions with both insects and plants. Proceedings of the National Academy of Sciences of the United States of America. 101(6):1737-1742.

Nikolaidis, N., Doran, N., and Cosgrove, D. J. 2013. Plant Expansins in Bacteria and Fungi: Evolution by Horizontal Gene Transfer and Independent Domain Fusion. Mol Biol Evol. 31(2):376-86.

Nunney, L., Hopkins, D. L., Morano, L. D., Russell, S. E. and Stouthamer, R. 2014. Intersubspecific Recombination in *Xylella fastidiosa* Strains Native to the United States: Infection of Novel Hosts Associated with an Unsuccessful Invasion. Applied and Environmental Microbiology. 80(3):1159-1169.

Perez-Donoso, A. G., Greve, L. C., Walton, J. H., Shackel, A. K. and Labavitch, J. M. 2007. *Xylella fastidiosa* infection and ethylene exposure result in xylem and water movement disruption in grapevine shoots. Plant Physiology. 143(2):1024-1036.

Perez-Donoso, A. G., Sun, Q., Roper, M. C., Greve, L. C., Kirkpatrick, B. and Labavitch, J. M. 2010. Cell Wall-Degrading Enzymes Enlarge the Pore Size of Intervessel Pit Membranes in Healthy and *Xylella fastidiosa*-Infected Grapevines. Plant Physiology. 152(3):1748-1759.

Perring, T., Farrar, C. and Blua, M. 2001. Proximity to citrus influences Pierce's disease in Temecula Valley vineyards. California agriculture. 55(4):13-18.

Pierce, N. B. 1892. The California vine disease: a preliminary report of investigations, US Government Printing Office.

Purcell, A. 1974. Spatial patterns of Pierce's disease in the Napa Valley. American Journal of Enology and Viticulture. 25(3):162-167.

Purcell, A. H. 1975. Role of the blue-green sharpshooter, *Hordnia circellata*, in the epidemiology of Pierce's disease of grapevines. Environmental Entomology. 4(5):745-752.

Purcell, A. H. and Finlay, A. 1979. Evidence for noncirculative transmission of Pierce's disease bacterium by sharpshooter leafhoppers. Phytopathology. 69(4):393-395.

Purcell, A. H. and Saunders, S. R. 1999. Fate of Pierce's disease strains of *Xylella fastidiosa* in common riparian plants in California. Plant Disease. 83(9):825-830.

Raju, B., Goheen, A., Teliz, D. and Nyland, G. 1980. Pierce's disease of grapevines in Mexico. Plant Disease. 64(3):280-282.

Reddy, J. D., Reddy, S. L., Hopkins, D. L. and Gabriel, D. W. 2007. TolC is required for pathogenicity of *Xylella fastidiosa* in *Vitis vinifera* grapevines. Mol Plant Microbe Interacts. 20(4):403-410.

Roper, M. C., Greve, L. C., Labavitch, J. M. and Kirkpatrick, B. C. 2007a. Detection and visualization of an exopolysaccharide produced by *Xylella fastidiosa* in vitro and in planta. Applied and Environmental Microbiology. 73(22):7252-7258.

Roper, M. C., Greve, L. C., Warren, J. G., Labavitch, J. M. and Kirkpatrick, B. C. 2007b. *Xylella fastidiosa* requires polygalacturonase for colonization and pathogenicity in *Vitis vinifera* grapevines. Mol Plant-Microbe Interacts. 20(4):411-419.

Roper, M. C. and Lindow, S. 2014. *Xylella fastidiosa*: Insights into the lifestyle of a xylem-limited bacterium. Virulence mechanisms of plant pathogenic bacteria. eds. de la Fuente, L. and Wang., N. St. Paul, Minnesota, American Phytopathological Society Press.

Sandkvist, M. 2001. Biology of type II secretion. Mol Microbiol. 40(2):271-283.

Saponari, M., Boscia, D., Loconsole, G., Palmisano, F., Savino, V., Potere, O. and Martelli, G. P. 2014. New Hosts of *Xylella Fastidiosa* Strain Codiro in Apulia. Journal of Plant Pathology. 96(3):611-611.

Scally, M., Schuenzel, E. L., Stouthamer, R. and Nunney, L. 2005. Multilocus sequence type system for the plant pathogen *Xylella fastidiosa* and relative contributions of recombination and point mutation to clonal diversity. Applied and Environmental Microbiology. 71(12):8491-8499.

Schuenzel, E. L., Scally, M., Stouthamer, R. and Nunney, L. 2005. A multigene phylogenetic study of clonal diversity and divergence in North American strains of the plant pathogen *Xylella fastidiosa*. Applied and Environmental Microbiology. 71(7):3832-3839.

Siebert, J. 2001. Economic impact of Pierce's disease on the California grape industry. California Department of Food and Agriculture Pierce's Disease Research Symposium.

Simpson, A. J. G., Reinach, F. D. C., Arruda, P., Abreu, F. A. D., Acencio, M., Alvarenga, R., Alves, L. M. C., Araya, J. E., Baia, G. S., Baptista, C. S., Barros, M. H. D., Bonaccorsi, E. D., Bordin, S., Bové J. M., Briones, M. R. S., Bueno, M. R. P., Camargo, A. A., Camargo, L. E. A., Carraro, D. M., Carrer, H., Colauto, N. B., Colombo, C., Costa, F. F., Costa, M. C. R., Costa-Neto, C. M., Coutinho, L. L., Cristofani, M., Dias-Neto, E., Docena, C., El-Dorry, H., Facincani, A. P., Ferreira, A. J. S., Ferreira, V. C. A., Ferro, J. A., Fraga, J. S., França, S. C., Franco, M. C., Frohme, M., Furlan, L. R., Garnier, M., Goldman, G. H., Goldman, M. H. S., Gomes, S. L., Gruber, A., Ho, P. L., Hoheisel, J. D., Junqueira, M. L., Kemper, E. L., Kitajima, J.P., Krieger, J. E., Kuramae, E. E., Laigret, F., Lambais, M. R., Leite, L. C. C., Lemos, E. G. M., Lemos, M. V. F., Lopes, S. A., Lopes, C. R., Machado, J. A., Machado, M. A., Madeira, A. M. B. N., Madeira, H. M. F., Marino, C. L., Marques, M. V., Martins, E. A. L., Martins, E. M. F., Matsukuma, A. Y., Menck, C. F. M., Miracca, E. C., Miyaki, C. Y., Monteiro-Vitorello, C. B., Moon, D. H., Nagai, M. A., Nascimento, A. L. T. O., Netto, L. E. S., Nhani Jr, A., Nobrega, F. G., Nunes, L. R., Oliveira, M. A., de Oliveira, M. C., de Oliveira, R. C., Palmieri, D. A., Paris, A., Peixoto, B. R., Pereira, G. A. G., Pereira Jr, H. A., Pesquero, J. B., Quaggio, R. B., Roberto, P. G., Rodrigues, V., de M. Rosa, A. J., de Rosa Jr, V. E., de Sá, R. G., Santelli, R. V., Sawasaki, H. E., da Silva, A. C. R., da Silva, A. M., da Silva, F. R., Silva, W. A., da Silveira, J. F., Silvestri, M. L. Z., Siqueira, W. J., de Souza, A. A., de Souza, A. P., Terenzi, M. F., Truffi, D., Tsai, S. M., Tsuhako, M. H., Vallada, H., Van Sluys, M. A., Verjovski-Almeida, S., Vettore, A. L., Zago, M. A., Zatz, M., Meidanis J., and Setubal J. C. 2000. The genome sequence of the plant pathogen *Xylella fastidiosa*. Nature. 406:151-157.

Song, G. Q., Walworth, A. E. and Loescher, W. H. 2015. Grafting of Genetically Engineered Plants. Journal of the American Society for Horticultural Science. 140(3):203-213.

Souza, L. C. A., Wulff, N. A., Gaurivaud, P., Mariano, A. G., Virgilio, A. C. D., Azevedo, J. L. and Monteiro, P. B. 2006. Disruption of *Xylella fastidiosa* CVC *gumB* and *gumF* genes affects biofilm formation without a detectable influence on exopolysaccharide production. Fems Microbiology Letters. 257(2):236-242.

Stevenson, J. F., Matthews, M. A. and Rost, T. L. 2004. Grapevine susceptibility to Pierce's disease I: Relevance of hydraulic architecture. American Journal of Enology and Viticulture. 55(3):228-237.

Strona, G., Carstens, C. J. and Beck, P. S. A. 2017. Network analysis reveals why *Xylella fastidiosa* will persist in Europe. Scientific Reports. 7.

Sun, Q., Rost, T. L. and Matthews, M. A. 2008. Wound-Induced Vascular Occlusions in *Vitis Vinifera* (Vitaceae): Tyloses in Summer and Gels in Winter. American Journal of Botany. 95(12):1498-1505.

Sun, Q., Rost, T. L., Reid, M. S. and Matthews, M. A. 2007. Ethylene and not embolism is required for wound-induced tylose development in stems of grapevines. Plant Physiology. 145(4):1629-1636.

Sun, Q., Sun, Y. L., Walker, M. A. and Labavitch, J. M. 2013. Vascular Occlusions in Grapevines with Pierce's Disease Make Disease Symptom Development Worse. Plant Physiology. 161(3):1529-1541.

Thorne, E. T., Stevenson, J. F., Rost, T. L., Labavitch, J. M. and Matthews, M. A. 2006a. Pierce's disease symptoms: comparison with symptoms of water deficit and the impact of water deficits. American Journal of Enology and Viticulture. 57(1):1-11.

Thorne, E. T., Young, B. M., Young, G. M., Stevenson, J. F., Labavitch, J. M., Matthews, M. A. and Rost, T. L. 2006b. The structure of xylem vessels in grapevine (vitaceae) and a possible passive mechanism for the systemic spread of bacterial disease. American Journal of Botany. 93(4):497-504.

Tyree, M. T. and Zimmermann, M. H. 2002. Hydraulic architecture of whole plants and plant performance. Xylem structure and the ascent of sap, Springer:175-214.

Van Sluys, M. A., de Oliveira, M. C., Monteiro-Vitorello, C. B., Miyaki, C. Y., Furlan, L. R., Camargo, L. E. A., da Silva, A. C. R., Moon, D. H., Takita, M. A., Lemos, E. G. M., Machado, M. A., Ferro, M. I. T., da Silva, F. R., Goldman, M. H. S., Goldman, G. H., Lemos, M. V. F., El-Dorry, H., Tsai, S. M., Carrer, H., Carraro, D. M., de Oliveira, R. C., Nunes, L. R., Siqueira, W. J., Coutinho, L. L., Kimura, E. T., Ferro, E. S., Harakava, R., Kuramae, E. E., Marino, C. L., Giglioti, E., Abreu, I. L., Alves, L. M. C., do Amaral, A. M., Baia, G. S., Blanco, S. R., Brito, M. S., Cannavan, F. S., Celestino, A. V., da Cunha, A. F., Fenille, R. C., Ferro, J. A., Formighieri, E. F., Kishi, L. T., Leoni, S. G., Oliveira, A. R., Rosa Jr., V. E., Sassaki, F. T., Sena, J. A. D., de Souza, A. A., Truffi, D., Tsukumo, F., Yanai, G. M., Zaros, L. G., Civerolo, E. L., Simpson, A. J. G., Almeida Jr., N. F., Setubal, J. C., and Kitajima J. P. 2003. Comparative analyses of the complete genome sequences of Pierce's disease and citrus variegated chlorosis strains of *Xylella fastidiosa*. Journal of Bacteriology. 185:101-1026.

van Ulsen, P., Rahman, S., Jong, W. S., Daleke-Schermerhorn, M. H. and Luirink, J. 2014. Type V secretion: from biogenesis to biotechnology. Biochim Biophys Acta. 1843(8):1592-1611.

Voegel, T. M., Warren, J. G., Matsumoto, A., Igo, M. M., and Kirkpatrick, B. C. 2010. Localization and characterization of *Xylella fastidiosa* haemagglutinin adhesins. Microbiology-Sgm. 156:2172-2179.

Wang, P. 2014. Characterization of the Oxidative Stress Response and the Type II Secretion System for the Phytopathogen, *Xylella fastidiosa* (Doctoral dissertation, UC Riverside).

Yadeta, K. and Thomma, B. P. H. J. 2013. The xylem as battleground for plant hosts and vascular wilt pathogens. Frontiers in Plant Science. 4.

Zimmermann, M. H. 1979. The discovery of tylose formation by a Viennese lady in 1845. IAWA Bull. 1979:51–56.

# 2. Chapter 2

# *Xylella fastidiosa* Endoglucanases Mediate the Rate of Pierce's Disease Development in *Vitis vinifera* in a Cultivar-Dependent Manner

## Abstract

*Xylella fastidiosa* is a Gram-negative bacterium that causes Pierce's Disease (PD) in grapevine. *X. fastidiosa* is xylem-limited and interfaces primarily with pit membranes (PMs) that separate xylem vessels from one another and from adjacent xylem parenchyma cells. PMs are comprised of both pectic and cellulosic substrates, and dissolution of PMs is facilitated by *X. fastidiosa* cell wall degrading enzymes (CWDEs). A polygalacturonase, which hydrolyzes the pectin component of PMs, is required for both movement and pathogenicity in grapevines. Here, we demonstrate that two *X. fastidiosa* β-1,4-endoglucanases (EGases), EngXCA1 and EngXCA2, also play a role in how *X. fastidiosa* interfaces with grapevine PMs. The loss of EngXCA1 and EngXCA2 in tandem reduces both *X. fastidiosa* virulence and population size, and slows the rate of PD symptom development and progression. Moreover, we demonstrate that single and double EGase mutants alter the rate of PD progression differently in two grapevine cultivars, Cabernet sauvignon and Chardonnay, and that Chardonnay is significantly more susceptible to PD than Cabernet sauvignon. Interestingly, we determined that there are quantitative differences in the amount of fucosylated xyloglucans that make up the surface of the PMs in these cultivars. Fucosylated xyloglucans are targets of the *X. fastidiosa* EGases and xyloglucan abundance could impact PM dissolution and affect PD symptom development. Taken together, these results indicate that *X. fastidiosa* EGases and PM carbohydrate composition of different grape cultivars are important factors that influence PD symptom development and progression.

# Introduction

*Xylella fastidiosa* is a gram-negative, xylem-limited bacterium that causes disease in many economically important crops across several continents. *X. fastidiosa* strains have been assigned to different subspecies that generally align with host specificity (Almeida and Nunney 2015; Schuenzel et al. 2005). In the United States, *X. fastidiosa* subsp. *fastidiosa* is the implicated causal agent of Pierce's disease (PD) of grapevine. In Central and South America, the citrus and coffee industries have been severely affected by *X. fastidiosa* subsp. *pauca*, which causes citrus variegated chlorosis and coffee leaf scorch, respectively (Chang et al. 1993; Li et al. 2001). Recently, *X. fastidiosa* subsp. *pauca* has been implicated as the causal agent of Olive Quick Decline Syndrome in Southern Italy (Saponari et al. 2013) as one of the first reports of *X. fastidiosa* in Europe. Symptoms of PD include leaf scorching, irregular lignification (green islands) and matchstick petioles, followed by fruit desiccation, cordon dieback and vine death (Goheen and Hopkins 1988; Purcell 1986; Stevenson et al. 2005; Varela, 1996). *X. fastidiosa* resides exclusively within the xylem of plant hosts, with symptoms similar to, but not exactly like, water stress imparted by xylem disruption (McElrone et al. 2001; McElrone et al. 2003; Thorne et al. 2006a). *X. fastidiosa* is transmitted by xylem-feeding hemipteran leafhopper insects including *Graphocephala atropunctata*, the blue-green sharpshooter and *Homalodisca vitripennis*, the glassy-winged sharpshooter (Hill and Purcell 1995).

PD symptom severity is highly correlated with the ability of the bacterium to proliferate within the xylem and systemically colonize the grapevine host (Chatterjee et

al. 2008a, Sun et al. 2011). *X. fastidiosa* is strictly limited to the xylem tissue, a nutrient-poor niche with few available carbon sources dissolved as solutes in the xylem sap or in the primary cell wall material that comprises pit membranes (PMs). The xylem in grapevines is built of many interconnected vessels that are finite, but variable in length, and vessels rarely span the entire length of the vine (Thorne et al. 2006b, Tyree and Zimmerman 2002). Xylem vessels are connected to each other by scalariform bordered pits that contain PMs (Brett and Waldron 1996). PMs are porous primary cell wall-middle lamella structures that allow water and small solutes to pass between vessels, but also serve to prevent the movement of disruptive elements such as air embolisms or pathogens (Stevenson et al. 2004, Tyree and Zimmerman 2002). *X. fastidiosa* must traverse PMs to move systemically within the grapevine xylem. However, grapevine PM pores have a diameter of 5 – 20 nm, and the rod-shaped *X. fastidiosa* cells, having a width of 250 – 500 nm and length of 1000 – 4000 nm, are too large to passively move through these small pores (Buchanan et al. 2000, Choat et al. 2004, Mollenhauer and Hopkins 1974). Grapevine PMs are comprised of cellulose microfibrils, xyloglucan (hemicellulose) and pectin (Brett and Waldron 1996, Dickison 2007). These polysaccharides can serve as the substrates of cell wall-degrading enzymes (CWDEs) produced by pathogenic bacteria and fungi as these invading pathogens navigate and proliferate within the xylem (Bateman 1976, Hématy et al. 2009, Popeijus et al. 2000, Ward et al. 1989). The *X. fastidiosa* genome encodes several genes annotated as CWDEs, including one polygalacturonase (PG), three β-1,4-endoglucanases (EC 3.2.1.4) (EGases), a cellobiohydrolase and a xylanase (Simpson et al. 2000, Van Sluys et al. 2003). PGs

facilitate the hydrolytic cleavage of pectin, and a *X. fastidiosa* mutant lacking one PG (PglA) failed to move beyond the point of inoculation and did not induce PD symptoms, indicating that the PG is required for systemic colonization (Roper et al. 2007).

EGases are hydrolytic enzymes that cleave β-1,4 glycosidic linkages, such as those found in cellulose and the cross-linking glycans (hemicellulose) that are both constituents of the vascular plant cell wall (Buchanan et al. 2000, Larner J 1960). Of the three annotated *X. fastidiosa* EGases, EngXCA2 (PD1851) is the only prototypical EGase comprised of an N-terminal glycosyl hydrolase domain and a C-terminal carbohydrate binding module. *X. fastidiosa* EngXCA2 hydrolyzes cellulosic substrates, such as carboxymethylcellulose (CMC) and xyloglucan (Perez-Donoso et al. 2010). EngXCA1 (PD1856) has a predicted N-terminal glycosyl hydrolase domain homologous to that of EngXCA2, and a predicted C-terminal expansin domain. The expansin domain is notable because expansins are considered to be plant proteins. Expansins are non-enzymatic and bind to cellulose and hemicellulose to facilitate cell wall expansion during plant cell growth, and were likely acquired from plants via cross-kingdom horizontal gene transfer (Cosgrove 2000, Nikolaidis et al. 2014). Interestingly, with a few exceptions, expansins are found in genera of bacteria that dwell in plant xylem tissue, such as *Bacillus*, *Clavibacter*, *Ralstonia*, *Xanthomonas*, *Pectobacterium* and *Dickeya*, suggesting that expansins are advantageous for bacteria inhabiting the xylem (Georgelis et al. 2014, Kerff et al. 2008, Tancos et al. 2018, Tovar-Herrera et al. 2018). The third EGase, Egl (PD2061), has a predicted N-terminal glycosyl hydrolase domain, but does not have domains related to carbohydrate binding.

EGases are important enzymatic virulence factors for several bacterial phytopathogens. For necrotrophic bacteria such as *Pectobacterium* (*Erwinia*) *caratovorum*, EGases contribute to virulence and nutrient acquisition by inducing soft rot (Barras et al. 1994, Walker et al. 1994). For bacteria with a significant xylem-dwelling phase, such as *Pantoea stewartii* subsp. *stewartii*, *Ralstonia solanacearum* and *Xanthomonas campestris* pv. *campestris*, EGases play an important role in virulence and host colonization (Gough 1988, Roberts et al. 1988, Saile et al. 1997, Mohammadi et al. 2012). Moreover, it has been suggested that xylem-dwelling bacteria use EGases to degrade PMs as a means of acquiring nutrients (Fatima and Senthil-Kumar 2015, Perez-Donoso et al. 2010, Pieretti et al. 2012).

The mechanisms by which *X. fastidiosa* acquires carbon in the xylem have not been fully elucidated, and it is unclear if carbon released as a consequence of PM degradation is utilized by the bacterium as a nutrient source. In addition, differences in PD severity and symptom progression rate have been noted in different cultivars of *Vitis vinifera*, but little is known about host physiological properties or bacterial molecular mechanisms underlying these observations. This study was structured to examine host PM composition as a factor in cultivar susceptibility, as well as to test the role of *X. fastidiosa* EGases in plant colonization and disease symptom development. This work demonstrates that there are quantitative differences in the hemicellulosic component of PMs, namely the fucosylated xyloglucans, of two cultivars, Chardonnay and Cabernet sauvignon, and that Chardonnay develops PD at a significantly faster rate than Cabernet sauvignon. Furthermore, a *X. fastidiosa* mutant lacking two of the EGases is severely impacted in

virulence in both cultivars, but significantly more so in Cabernet sauvignon. These results support our hypothesis that composition of the hemicellulosic content of xylem PMs affects the rate of PD development and is one of the determinants of PD severity among grapevine cultivars. Collectively, two *X. fastidiosa* EGases (EngXCA1 and EngXCA2) also support bacterial growth in the xylem, suggesting EGases play a major role in nutrient acquisition in the xylem environment.

## Materials and Methods

**Bacterial strains.** All bacterial strains, plasmids and primers for this study are listed in Table 2.4.

**Media and bacterial growth conditions.** *X. fastidiosa* strains were grown at 28°C in PD3 broth and solid medium (Davis et al. 1981). *E. coli* strains were grown at 37°C in Luria-Bertani medium. Selection of *X. fastidiosa* transformants was performed on PD3 with 5 μg/ml of kanamycin or gentamicin, and sub-culturing of transformants was performed on PD3 with 30 μg/ml of kanamycin or 10 μg/ml of gentamicin, when appropriate. For selection of *E. coli* transformants, kanamycin or gentamicin were added at 30 or 10 μg/ml, respectively.

**Construction of the Δ*engXCA1*, Δ*engXCA2*, and Δ*engXCA1/2* mutants.** Overlap extension polymerase chain reaction was used to combine 5' and 3' flanking regions adjacent to the target gene (*engXCA1* or *engXCA2*) with an antibiotic resistance gene to

create a deletion construct. Homologous recombination between flanking regions of the deletion construct and the same regions within the *X. fastidiosa* chromosome facilitated complete removal of the target gene and subsequent insertion of the antibiotic resistance gene. The 5' and 3' flanking regions adjacent to *engXCA1* were amplified from the *X. fastidiosa* chromosome via polymerase chain reaction (PCR) using primer pairs engXCA1_LF_fwd and engXCA1_LF-rev, and engXCA1_RF_fwd and engXCA1_RF_rev, respectively. The kanamycin resistance gene was amplified from pCR2.1 TOPO (Invitrogen) using primers engXCA1_kan_fwd and engXCA1_kan_rev. The 5' and 3' flanking regions adjacent to *engXCA2* were amplified from the *X. fastidiosa* chromosome via PCR using primer pairs engXCA2_LF_fwd and engXCA2_LF-rev, and engXCA2_RF_fwd and engXCA2_RF_rev, respectively. The gentamicin resistance gene was amplified from the pBBR1-MCS5 plasmid (Kovach et al. 1995) using primers engXCA2_gent_fwd and engXCA2_gent_rev. Individual fragments for each deletion construct were amplified using Ex Taq DNA polymerase (Takara) and 30 PCR cycles: denaturation at 95℃ for 1 minute; primer annealing at 60℃ for 1 minute; extension at 72℃ for 2 minutes. The three fragments for each deletion construct were assembled by overlap extension PCR and the resulting products were cloned into pCR8/GW/TOPO (Invitrogen) following the manufacturer's instructions to create plasmids pBI1 and pBI2. The Δ*engXCA1* construct was verified by sequencing using primers GW1 and GW2 (Invitrogen), and engXCA1_kan_fwd and engXCA1_kan_rev. The Δ*engXCA2* construct was verified by sequencing using primers GW1 and GW2 (Invitrogen), and engXCA2_gent_fwd and engXCA2_gent_rev. Either pBI1 or pBI2

were transformed into *X. fastidiosa* by electroporation. Electrocompetent *X. fastidiosa* cells were prepared according to Matsumoto et al. (2009), and 200 ng of pBI1 or pBI2 and 1 µl of TypeOne Restriction Inhibitor (Epicentre) were electroporated (3.0 kV, 300 Ω, 25 µF) into *X. fastidiosa* using a 0.2 cm cuvette (Bio-Rad) and the GenePulser X-cell (Bio-Rad). Positive transformants were validated via sub-culturing onto PD3 agar containing the appropriate antibiotics. Genomic DNA from *X. fastidiosa* Δ*engXCA1* and *X. fastidiosa* Δ*engXCA2* positive transformants was extracted using the DNeasy Blood and Tissue Kit (Qiagen). Δ*engXCA1* was verified by sequencing using primers engXCA1_XfgenDNA_For_seq, engXCA1_XfgenDNA_Rev_seq, engXCA1mut_Kan_For_seq, and engXCA1mut_Kan_Rev_seq. Δ*engXCA2* was verified by sequencing using primers Xf_engXCA2_PCR_fwd, Xf_engXCA2_PCR_rev, Xf_engXCA2seq_92outLF, Xf_engXCA2seq_71intLF, Gent_seq_fwd, and Xf_engXCA2seq_33intRF. The *X. fastidiosa* Δ*engXCA1/2* double mutant strain was created by transforming electrocompetent *ΔengXCA1* cells with 200 ng of the pBI2 plasmid and 1 µl of TypeOne Restriction Inhibitor (Epicentre). Positive transformants were obtained and screened as described above. All relevant primers can be found in Table 2.4. Complementation tools are limited for *X. fastidiosa* and repeated attempts to obtain transformants for complementation of the EGase mutants were unsuccessful.

**Recombinant EngXCA1 and EngXCA2 protein expression.** The *engXCA1* gene was inserted into the pET20b(+) protein expression vector to create pBI3 (Genscript USA Inc.). The gene was inserted between the SacI and XhoI restriction sites, and the codon

sequence was aligned to include a histidine (His) tag and the periplasmic localization signal peptide. The pBI3 plasmid was used to transform *E. coli* BL21 DE3. Single colonies of *E. coli* harboring either pBI3, pMCR7 (Perez-Donoso et al. 2010), or empty vector (pET20b(+)) were grown in 5 ml of liquid LB media containing 100 µg/ml of ampicillin at 37°C while shaking at 200 rpm overnight. Four ml of each overnight culture was added to 400 ml of liquid LB media containing 100 µg/ml of ampicillin, and each culture was incubated at 37°C while shaking at 200 rpm until each $OD_{600}$ = 0.5. The cultures were centrifuged at 5,000 rpm for 10 minutes, the supernatant was discarded, and cell pellets were re-suspended in 400 ml of fresh LB media containing 100 µg/ml of ampicillin and 0.6 mM isopropyl β-D-1-thiogalactopyranoside to induce protein production. The cultures were incubated at 4°C while shaking at 200 rpm overnight. After protein induction, the cultures were split in half to assess both protein expression via Western Blotting and EGase activity.

Cell cultures (200 ml) expressing recombinant EngXCA1, recombinant EngXCA2, or the pET20b(+) empty vector was centrifuged at 5,000 rpm for 10 minutes. Cell pellets were freeze-thawed twice at -80°C, then lysed using the B-PER Complete lysis reagent (Thermo Scientific), following manufacturer's instructions. A protease inhibitor was added during cell lysis to prevent protein degradation. Lysed samples were mixed 1:1 with 2X Laemmli Buffer (Bio Rad), boiled for 5 minutes, and subjected to SDS-PAGE using a 10% polyacrylamide gel. The protein was then transferred to a 0.45 µm nitrocellulose membrane overnight. The membrane was blocked with 5% non-fat milk and then probed with an α-His tag primary monoclonal antibody (Thermo

Scientific), followed by a goat α-mouse secondary polyclonal antibody conjugated with alkaline phosphatase (Thermo Scientific). The blot was developed using the AP Development Kit (Bio Rad), following the manufacturer's instructions.

**Endoglucanase activity assay.** Cell cultures (200 ml) expressing recombinant EngXCA1, recombinant EngXCA2, or the pET20b(+) empty vector were centrifuged at 5,000 rpm for 10 minutes, and cell pellets were each re-suspended in 1 ml of 1X PBS (pH 7.4). Each cell re-suspension (50 µl) was placed onto the center of a respective plate containing 1% agarose (medium EEO, Fisher Scientific) and 0.2% carboxymethyl cellulose (CMC) (Sigma Aldrich) in phosphate buffer (pH 6.0), and incubated at 37°C for 48 hours. After incubation, the perimeter of each cell droplet was marked, the diameter was measured using calipers, and then the cells were removed with copious amounts of water. Each plate was flooded with 0.1% Congo Red dye (Sigma Aldrich), followed by flooding with 1 M sodium chloride twice, and then flooding with 5% acetic acid (Carder 1986). The perimeter of each zone of hydrolysis was marked, and the diameter was measured using calipers. The area of each zone of hydrolysis was calculated and normalized by subtracting the area of the associated cell droplet. The assay was performed with three biological replicates containing three technical replicates of each treatment. Statistical significance between treatments was determined using the Kruskal-Wallis rank sum test for non-parametric data. Pairwise comparisons were made using Dunn's multiple comparison test, and *p*-values were adjusted using the Benjamini-Hochberg FDR method.

***In planta* virulence assays.** *Vitis vinifera* cv. Cabernet sauvignon and cv. Chardonnay were propagated from cuttings (generously provided by Foundation Plant Services (UC Davis)). Vines were mechanically inoculated following the methodology outlined by Purcell and Saunders (1999). Briefly, a 20 µl drop of a $10^8$ colony forming units per ml (CFU/ml) of *X. fastidiosa* inoculum was placed on the stem between the third and fourth node. The stem was pierced through the drop using a 20-gauge needle and the drop was drawn into the xylem. Grapevines were inoculated with either wild type, Δ*engXCA1*, Δ*engXCA2*, or the Δ*engXCA1/2 X. fastidiosa* strains. Grapevines inoculated with 1× PBS served as negative controls. Within trials, each strain was inoculated into ten vines and the experiment was repeated three times for a total of thirty replicates per strain (or 1× PBS) inoculation. All trials were randomized in the greenhouse, and vines were given a weekly PD symptom score based on the established rating scale from 0 – 5 as described in Guilhabert and Kirkpatrick (2005) where 0= a healthy vine, 1= one or two leaves with scorching at the margins, 2= two or three leaves with more developed scorching, 3= all leaves with some scorching and a few matchstick petioles, 4= all leaves with heavy scorching and many matchstick petioles, and 5= a dead or dying vine. Each trial compared PD symptom scores over a 20-week period in Cabernet sauvignon and Chardonnay grapevines inoculated with either wild type or one mutant strain. Each trial was completed twice over a two-year period, for a total of six pathogenicity assays: two comparing wild type and Δ*engXCA1*, two comparing wild type and Δ*engXCA2*, and two comparing wild type and Δ*engXCA1/2*. Because wild type was present in every trial, data

for wild type-inoculated vines was combined for each vine type and used as a reference to make comparisons to data from vines inoculated with each of the mutants across multiple trials and years. The mean PD symptom score per week was calculated, and comparisons between wild type and each of the mutants were made at 5 WPI (early-stage PD), 10 WPI (mid-stage PD), 15 WPI (late-stage PD), and 20 WPI (endpoint). The rate of PD symptom progression was assessed within the linear portion of the disease curve (5-15 WPI) by calculating the slopes between early-stage and mid-stage PD (5-10 WPI) and mid-stage and late-stage PD (10-15 WPI).

**Local and distal xylem colonization assays.** Grapevines were inoculated as described above. To determine the contribution of EGases in local xylem colonization, wild-type, Δ*engXCA1*, Δ*engXCA2*, and Δ*engXCA1/2* populations per gram of tissue were quantified by isolating *X. fastidiosa* from the first intact petiole closest to the point of inoculation. Additionally, isolations were performed on petioles from the 20th node distal to the point of inoculation to determine if the EGases (singly or in tandem) had an impact on movement. Petioles were collected from every vine in each of the six trials after the late-stage infection time point, surface sterilized (30 seconds in 70% ethanol, 30 seconds in 10% bleach, and twice for 1 min in sterile deionized water) and ground in 2 ml of sterile 1× PBS. The resulting suspension was diluted and the dilution series were plated on solid PD3 medium according to standard methods (Roper et al. 2007). *X. fastidiosa* titers were normalized by dividing colony counts (CFU) by the weight of the corresponding petiole (CFU/g tissue). The titers for wild type-inoculated vines from all trials were combined for

each vine type and used as a reference, and wild type titers were compared to the titers of each mutant.

**Integrity and polysaccharide composition of intervessel PMs.** An immunogold-scanning electron microscopy (SEM) technique was used to reveal intervessel PM structure and immuno-localize fucosylated xyloglucans on the PMs of Chardonnay and Cabernet sauvignon vines at the late-stage time point of PD symptom development. Details of the technique can be found in Sun et al (2017). In brief, the third internode above the inoculated internode of each vine was fixed in 4% paraformaldehyde in PEM buffer (50 mM PIPES, 5 mM EGTA, 5 mM MgSO4, pH 6.9) for at least 24 hrs. Each internode was then trimmed into 3 mm wide x 5 mm long x 1 mm thick longitudinal segments, exposing either a radial or tangential surface of the secondary xylem. Trimmed specimens were washed twice with 50 mM PIPES and once with 0.2 M PBS with 3% non-fat milk powder (MP/PBS, pH 7.4) with 30 minutes each wash. Subsequently, specimens were divided into three groups with one as the immune-localization treatment and the other two as controls. A monoclonal antibody (mAb, CCRC-M1) and a corresponding secondary Ab (gold-conjugated goat anti-mouse IgG) were used to detect fucosylated xyloglucans on intervessel PMs. Specimens for each treatment were incubated at 4 $^{0}$C overnight in a 3-fold dilution of the original mAb mouse hybridoma supernatant in 3 % MP/PBS. After three PBS washes of 10 minutes each, specimens were incubated at room temperature (RT) for 1 hour with a 50-fold dilution in 3 % MP/PBS of the original colloidal gold-conjugated goat anti-mouse IgG. Incubation was followed by

three 10 minute washes of deionized water and one 15 minute silver enhancement treatment. Silver enhanced specimens were washed twice in deionized water (10 minutes each), and dehydrated via an ethanol series. Dehydrated specimens were critical-point dried, sputter-coated with gold-palladium and then examined at an accelerating voltage of 5 kV or 8 kV under a Hitachi 3400N SEM in the UWSP Biology Department. The other two sets of specimens for controls were processed in the same way described above, except that the mAb or secondary Ab incubation step was replaced with the 3 % MP/PBS incubation with in either of the two sets of specimens, respectively. Silver-enhanced gold particles appear as bright particles and indicate the presence, quantity and distribution of fucosylated xyloglucans on intervessel PMs of the polysaccharide group. Specimens of either treatment or controls also were examined with SEM to reveal structural features of intervessel PMs.

**Statistical analyses.** Longitudinal disease ratings are discrete, non-Gaussian, observations. Therefore, a Generalized Estimating Equations (GEE) model was used for this analysis (Liang and Zeger 1986). The time trend was captured by using a quadratic spline with knots at 5 weeks and 10 weeks. A GEE model with a quadratic spline time trend provided a robust approach to the data analysis. A full model with year, cultivar, strain and time as main effects, cultivar*strain, cultivar*time and strain*time as 2-factor interactions, and cultivar*strain*time as a 3-factor interaction was fit to the complete data set of disease ratings. The 3-factor interaction was significant in the model, and therefore

least squares means (LSMs), standard errors, and 95% confidence intervals for the mean disease rating at each combination of cultivar, strain, and time were obtained.

For each strain, contrasts between cultivars at each time point were carried out using two-sided asymptotic Z-tests based upon the LSMs. Within a cultivar, the three mutants were contrasted with wild type at each time point using a 2-sided asymptotic Z-test. The LSMs were used to estimate rates of PD symptom progression as the slopes between times 5 and 10, and between times 10 and 15. The two slopes were similarly contrasted between cultivar and within cultivar using 2-sided asymptotic Z-tests.

Bacterial titer is an integer valued count that was highly variable and contained several zeros. Therefore, a negative binomial generalized linear model (GLM) was used to analyze bacterial titer (McCullagh and Nelder 1989). Between cultivar comparisons utilized a negative binomial GLM for each combination of strain and colonization location, and which coded cultivar using two dummy variables. Cultivars were compared using a 2-sided asymptotic Wald test. Within cultivar comparisons utilized a negative binomial GLM for each colonization location, and which coded strain with four dummy variables. Because mutant counts were expected to be lower than wild type counts, contrasts of each mutant with wild type were carried out with lower 1-sided asymptotic Wald tests.

All analyses were performed in SAS 9.4 (SAS Institute, Cary NC) using the GENMOD procedure.

## Results

**Grapevine cultivar is a factor in rate and severity of PD symptom development**. PD symptoms were monitored weekly for 20 weeks post-inoculation (WPI), and observed PD symptom scores were used to generate a Generalized Estimating Equations (GEE) model to compare PD symptom development in Chardonnay and Cabernet sauvignon. From the GEE model, PD symptom development was divided into stages: early stage PD (5 WPI), mid-stage PD (10 WPI), late-stage PD (15 WPI), and the endpoint of the experiment (20 WPI). Wild type-inoculated Chardonnay vines exhibit significantly higher PD symptom scores than wild type-inoculated Cabernet sauvignon vines at early-, mid-, and late-stage PD, and at the endpoint of the experiment (Fig. 2.1A). To further understand the rate of disease manifestation, the GEE model was used to assess differences in the rate of PD symptom development in Cabernet sauvignon and Chardonnay by calculating the change in PD symptom score over time between early-stage PD and late-stage PD (5-15 WPI) where symptom progression was linear (PD symptom progression rate). The PD symptom progression rate is significantly faster in Chardonnay than in Cabernet sauvignon between early- and mid-stage PD (5-10 WPI), and between mid- and late-stage PD (10-15 WPI) (Table 2.1). However, wild type titers at the POI and at 20 nodes distal to the POI were statistically similar in Chardonnay and Cabernet sauvignon at the late stage of infection (Fig 2.1B), indicating that symptom severity is decoupled from bacterial titer at this stage of disease. These trends were also seen in vines inoculated with Δ*engXCA1*, Δ*engXCA2*, or Δ*engXCA1/2* (Table 2.1, Fig.

2.6). All *p*-values, estimated mean differences, and statistical significance are summarized in Tables 2.5 and 2.6.

**The fucosylated xyloglucan component of xylem pit membranes differs between cultivars.** Immunogold-scanning electron microscopy (SEM) was used to detect fucosylated xyloglucans in the surface layer of intervessel PMs in Cabernet sauvignon and Chardonnay grapevines to determine if there were qualitative differences between the two cultivars with regard to the fucosylated xyloglucan component of PMs. After immunogold labeling, relatively few gold particles were bound to Cabernet sauvignon PMs (Fig. 2.1C), indicating that the surface layer is sparsely populated with fucosylated xyloglucans. Conversely, many gold particles were detected for Chardonnay PMs (Fig. 2.1D), indicating that the surface layer is densely populated with fucosylated xyloglucans.

**EGases are required for full virulence and affect rate of PD symptom development in a cultivar-dependent manner.** PD symptoms were monitored weekly over a 20-week period, and observed PD symptom scores were used to generate a GEE model to compare PD symptom development at early-, mid-, and late-stage PD in wild type and EGase mutant-inoculated vines (Fig. 2.7). Subsequently, to better understand when EGases play the largest role, the GEE model was used to analyze the PD symptom progression rate between early- and late-stage PD (Table 2.2, 2.3). Cabernet sauvignon vines inoculated with the Δ*engXCA1/2* double mutant had significantly lower PD symptom scores than

wild type-inoculated vines during all stages of PD and at the 20-week endpoint (Fig. 2.2). Not only were symptoms less severe overall, but the PD symptom progression rate was significantly slower in Δ*engXCA1/2*-inoculated vines than in wild type-inoculated vines between early-stage and late-stage PD (Table 2.2), indicating that disease manifests more slowly in Cabernet sauvignon vines inoculated with Δ*engXCA1/2*.

To better understand how individual EGases contribute to disease, we also tested single Δ*engXCA1* and Δ*engXCA2* mutants *in planta*. In Cabernet sauvignon, Δ*engXCA1*-inoculated vines had significantly lower disease ratings than wild type-inoculated vines during early-stage PD, but there were no differences in PD symptom scores during mid- and late-stage PD, or at the endpoint (Fig. 2.2B). The PD symptom progression rate was not statistically different between Δ*engXCA1*-inoculated vines and wild type-inoculated vines between early-stage and late-stage PD, indicating that while Δ*engXCA1* initially elicits fewer symptoms *in planta* during the early-stage, PD develops at the same rate as in wild type-inoculated vines with symptom severity eventually equaling wild type levels (Fig. 2.2B, Table 2.2). Δ*engXCA2*-inoculated vines had significantly higher PD symptom scores than wild type-inoculated vines during all stages of PD and the endpoint, and the PD symptom progression rate was faster in Δ*engXCA2*-inoculated vines than in wild type-inoculated vines between early-stage and late-stage PD (Fig. 2.2C, Table 2.2).

Similar to what was observed in Cabernet sauvignon, Chardonnay vines inoculated with the Δ*engXCA1/2* double mutant had significantly lower PD symptom scores than wild type-inoculated vines during all stages of PD and the endpoint (Fig. 2.2D), and the PD symptom progression rate in Δ*engXCA1/2*-inoculated vines was

significantly slower than in wild type-inoculated vines between early-stage and mid-stage PD (Table 2.3). However, there was a notable difference in the rate at which PD symptoms developed in Δ*engXCA1/2*-inoculated Chardonnay as compared to Cabernet sauvignon. A continually lower rate of PD symptom progression was observed between early-stage and late-stage PD in Cabernet sauvignon vines inoculated with Δ*engXCA1/2* as compared to wild type inoculated vines, whereas, in Chardonnay, there was no difference in the rate of PD symptom development between mid- and late-stage PD (Table 2.2, 2.3). These data taken together indicate that *X. fastidiosa* virulence is dependent on EngXCA1 and EngXCA2 in both Chardonnay and Cabernet sauvignon, but the rate at which PD symptoms develop in absence of EngXCA1 and EngXCA2 is cultivar-dependent.

The Δ*engXCA1* single mutant also behaved differently in Chardonnay as compared to Cabernet sauvignon. Δ*engXCA1*-inoculated Chardonnay vines only displayed PD symptom scores similar to wild type-inoculated vines at late-stage PD, while PD symptom scores in Δ*engXCA1*-inoculated Cabernet sauvignon vines were similar to wild type-inoculated vines at mid- and late-stage PD (Fig. 2.2B, E). Furthermore, the PD symptom progression rate for Δ*engXCA1*-inoculated Chardonnay vines was significantly faster between mid-stage and late-stage PD as compared to wild type-inoculated vines (Table 2.3), whereas the PD symptom progression rate for Δ*engXCA1*-inoculated Cabernet sauvignon vines was consistently similar to wild type-inoculated vines (Table 2.2).

Δ*engXCA2*-inoculated Chardonnay vines had PD symptom scores that were similar to those for wild type-inoculated vines during early-stage and mid-stage PD, but the Δ*engXCA2* mutant elicited significantly higher PD symptom scores than wild type *X. fastidiosa* during late-stage PD and at the endpoint (Fig. 2.2F), which differed from its behavior in Cabernet sauvignon where it was hypervirulent at all stages of PD (Fig. 2.2C). Moreover, PD symptoms in Chardonnay progressed at a similar rate between early-stage and mid-stage PD in Δ*engXCA2*- and wild type-inoculated vines, but progressed faster between mid-stage and late-stage PD in Δ*engXCA2*-inoculated vines, whereas in Cabernet sauvignon, PD symptoms progressed faster in Δ*engXCA2*-inoculated vines at all stages of PD (Table 2.2, 2.3).

In all trials, the disease ratings for PBS-inoculated vines (negative controls) for each week were zero. All *p*-values, estimated mean differences, and statistical significance are summarized in Tables 2.7 and 2.8.

**EngXCA1 and EngXCA2 are required for complete pit membrane degradation.** SEM was used to analyze the structural integrity of PMs in both Cabernet sauvignon and Chardonnay vines inoculated with either wild type or Δ*engXCA1/2* during late-stage PD. At this stage of PD, PMs of vines inoculated with wild type were completely dismantled in both cultivars (Fig. 2.3A, C). In contrast, the PMs of vines inoculated with Δ*engXCA1/2* were still present and were only partially degraded in both cultivars (Fig. 2.3B, D). The PMs of the PBS-inoculated control vines for both cultivars remained fully intact (Fig. 2.1C, D).

**Bacterial colonization of the xylem is EngXCA1/EngXCA2-dependent.** In both Cabernet sauvignon and Chardonnay, Δ*engXCA1/2* titers were significantly lower than wild type titers at the POI and at 20 nodes distal to the POI, indicating that both EngXCA1 and EngXCA2 are concomitantly required to achieve maximal xylem colonization at both points. Δ*engXCA1* and Δ*engXCA2* single mutant titers at the POI and at 20 nodes distal to the POI were statistically similar to wild type titers in both cultivars, indicating that deletion of EngXCA1 or EngXCA2 in singlet does not have a quantifiable impact on the ability of *X. fastidiosa* to proliferate at the point of inoculation or to move away from the point of inoculation during the late phase of infection (Fig. 2.4). In all trials, bacterial extractions from PBS-inoculated vines (negative controls) did not yield any *X. fastidiosa* colonies. All *p*-values, estimated mean differences, and statistical significance are summarized in Tables 2.9 and 2.10.

**EngXCA1 has a marginal amount of endoglucanase activity as compared to EngXCA2.** Initial attempts to measure EGase activity from *X. fastidiosa* itself were unsuccessful, thus, recombinant expression was used to characterize the activities of EngXCA1 and EngXCA2. Previous studies indicated that recombinant EngXCA2 expressed in *E. coli* possesses robust EGase activity *in vitro* when using both carboxymethylcellulose (CMC) and xyloglucan as substrates (Pérez-Donoso et al. 2010). A radial diffusion assay was used to determine the zones of CMC hydrolysis for recombinant EngXCA1 using differential staining with Congo Red (Fig. 2.5A).

EngXCA2 was included as a positive EGase control and *E. coli* harboring the empty pET20b(+) plasmid vector served as a negative control. The area of the zone of hydrolysis for EngXCA1 was determined to be significantly different from that of the pET20b(+) empty vector control ($p=0.02217$) and from that of EngXCA2 ($p=0.01881$) (Fig. 2.5B). Additionally, the area of the zone of hydrolysis for EngXCA2 also was determined to be significantly different from the pET20b(+) empty vector control ($p<0.0001$). Western blotting confirmed the expression of recombinant EngXCA1 and EngXCA2, as well as the absence of expressed protein from the pET20b(+) empty vector control (Fig. 2.8). Initial attempts to measure EGase activity from *X. fastidiosa* itself were unsuccessful, thus, we opted for recombinant expression to characterize the activities of EngXCA1 and EngXCA2.

## Discussion

Xyloglucans are the most abundant portion of hemicellulose in dicotyledonous plants and can make up as much as 20% of the dry weight of the primary plant cell wall (Buchanan et al. 2000, Scheller and Ulvskov 2010). Xyloglucans are comprised of 1,4-linked β-D-pyranosyl glucan backbone substituted with 1,6-linked xylose side chains. EGases can digest xyloglucans by cleaving linkages in the glucan backbone, and the *X. fastidiosa* EngXCA2 protein has known EGase activity when using xyloglucan as a target substrate (Perez-Donoso et al. 2010). The *X. fastidiosa* EGase mutants tested in this study, particularly the Δ*engXCA1/2* mutant, collectively affected the rate of PD symptom progression in a cultivar-dependent manner, indicating that enzymatic targets of the

EGases are a determining factor in the observed differences in cultivar susceptibility. Because the PM surface is a major interface between pathogen and host, we explored the content of potential hemicellulosic target substrates of X. *fastidiosa* EGases in xylem PMs of these two cultivars. Indeed, qualitative analyses of the PM surface layer of the highly susceptible Chardonnay cultivar and more tolerant Cabernet sauvignon cultivar indicate that Chardonnay PM surfaces contain a higher abundance of fucosylated xyloglucans than the surface of PMs in Cabernet sauvignon, which contained a relatively low abundance of fucosylated xyloglucans. The rate of PD symptom progression and the overall PD symptom scores were significantly different between Chardonnay and Cabernet sauvignon and quantitatively confirmed field observations that Chardonnay is significantly more susceptible to PD than Cabernet sauvignon.

Interestingly, Sun et al. (2011) determined that the pectin component of Chardonnay PMs is almost exclusively weakly methyl-esterified. PGs are more effective at hydrolyzing pectin with low degrees of methyl esterification and the effectiveness of PGs in hydrolyzing pectin is inversely proportional to the degree of methyl-esterification (Lionetti et al. 2012). Our data combined with the Sun et al (2011) study indicate that Chardonnay PMs offer more available targets substrates for *X. fastidiosa* CWDEs in the form of weakly methyl-esterified pectins and high abundances of fucosylated xyloglucans that are readily digested by *X. fastidiosa*. It is tempting to speculate that Cabernet sauvignon PMs contain pectin with high levels of methyl esterification and this feature, coupled with low levels of fucosylated xyloglucans, leads to less efficient PM dissolution in Cabernet sauvignon and could explain why this cultivar is significantly less susceptible

to PD when compared to Chardonnay. Scanning electron micrographs of PMs in vines inoculated with the Δ*engXCA1/2* mutant indicate that this mutant does not rupture PMs as readily as its wild type parent supporting our hypothesis that EGases target the hemicellulosic content of PMs. Taken together, these data support previous findings that PG is the major enzymatic determinant for movement in grapevine xylem and that EGases are accessory enzymes that facilitate PM dissolution (Roper et al. 2007).

The bacterial titer at the POI for each mutant strain was similar to the respective bacterial titer 20 nodes distal to the POI, indicating that none of the EGase mutants were hindered in movement. However, these assays were performed during the late stage of PD when the vines had a PD symptom score of ≥3 (all leaves have some scorching with a few matchstick petioles), which was at the end of the linear portion of the PD symptom curve. It is possible that movement could be delayed for certain EGase mutants during the earlier phases of infection and the timing of the colonization assay did not capture this delay. Several attempts to isolate *X. fastidiosa* from grapevines at earlier time points were not successful. Our own previous work (Clifford et al. 2013, Wang et al. 2017) and work performed by other research groups indicates that *X. fastidiosa* cannot be consistently quantified in grapevines with PD symptom scores below 3 (Deyett et al. 2019).

Soluble carbohydrates in xylem sap are in relatively low abundance and the carbohydrate composition of xylem sap fluctuates over the course of the growing season (Roper 2006). Thus, soluble carbohydrates are likely to be an inconsistent source of carbon for a microorganism living in the xylem (Andersen and Brodbeck 1989, Hardy and Possingham 1969, Loescher et al. 1990). The carbohydrate content of PMs may serve

as a reliable and sustainable source of carbon that *X. fastidiosa* utilizes to augment any carbon obtained from xylem sap. Neither Δ*engXCA1* nor Δ*engXCA2* were impaired in population growth when compared to wild type in both cultivars, but the Δ*engXCA1/2* mutant was significantly impaired in proliferating within the xylem, supporting the hypothesis that these two EGases play a collective role in harvesting carbon in the xylem environment. However, despite this impairment, the Δ*engXCA1/2* mutant population did increase, indicating that the PG may also have a role in carbon acquisition. It is possible that the different roles of these EGases allow them to act synergistically to degrade PMs and harvest carbon. However, our data suggest that these EGases act in a redundant manner where one can compensate for the loss of the other.

In accordance with this carbon acquisition hypothesis, we expected that there would be a significant difference in bacterial titer in Chardonnay and Cabernet sauvignon, with the less susceptible variety harboring less *X. fastidiosa*. However, both cultivars supported similar populations of bacteria at the POI and at 20 nodes distal to the POI. As mentioned above, this result is likely due to the inability to quantify *X. fastidiosa* titer in grapevine tissue during the early phases of *X. fastidiosa* infection when bacterial titer is below the threshold of reliable detection. Thus, it appears that the *X. fastidiosa* titer is lower in the less susceptible Cabernet sauvignon cultivar at earlier time points.

EngXCA1 is predicted to be a chimeric protein comprised of an EGase domain and an expansin domain (Cosgrove 2017). There are only a few examples of bacterial expansins and they are almost exclusively found in bacteria that have a xylem-dwelling component of their lifestyle and have varying roles in virulence (Cosgrove 2017;

Nikolaidis et al. 2014). Deletion of one expansin in *C. michiganensis* subsp. michiganensis resulted in a hypervirulent phenotype in tomato whereas, deletion of one expansin in *R. solanacearum* resulted in a hypovirulent phenotype for root inoculations (Tancos et al. 2018). EngXCA1 digested a β-1,4 linked glucan backbone (CMC) indicating that it does possess EGase activity. However, the zone of hydrolysis of the CMC substrate was significantly smaller relative to a lower concentration of EngXCA2 indicating that EngXCA1 is a less potent EGase than EngXCA2 *in vitro*. Additionally, the loss of only EngXCA1 had a small, but significant impact on *X. fastidiosa* virulence in the early stages of infection in Chardonnay. This leads us to speculate that the primary role of EngXCA1 is to function as an expansin rather than an EGase *in vivo*. Expansins disrupt the bonds between hemicellulosic xyloglucans and the hydrophobic regions of cellulose microfibrils, allowing relaxation of the cell wall and subsequent extension (Cosgrove 2018). EngXCA1 could aid PM degradation process by acting as an expansin and disrupting the bonds between cellulose and xyloglucans, thereby providing other CWDEs, such as EngXCA2 and PG, with easier access to target substrates. This effect would be most evident in highly susceptible varieties (e.g. Chardonnay) that contain high amounts of fucosylated xyloglucans in PMs. Deletion of EngXCA1 had little effect on PD severity in Cabernet sauvignon for which PMs have a lower abundance of fucosylated xyloglucans relative to Chardonnay, supporting the hypothesis that amount of cross-linking glycans mediates PM integrity.

In an *ex vivo* study in grapevine stem explants, purified recombinant *X. fastidiosa* EngXCA2 was required for PM dissolution in collaboration with a purified PG. Thus, it

was surprising that the *X. fastidiosa ΔengXCA2* mutant was hypervirulent and had a faster PD symptom progression rate in both Cabernet sauvignon and Chardonnay. Hypervirulent phenotypes have been documented for mutant strains of *X. fastidiosa* that do not aggregate or form biofilms and are locked in the planktonic, exploratory state in the xylem (Burbank and Stenger 2017; Chatterjee et al. 2008b; Gouran et al. 2016; Guilhabert and Kirkpatrick 2005; Newman et al. 2004). Interestingly, the Δ*engXCA2* mutant had a mucoid colony morphotype on solid medium when compared to wild type *X. fastidiosa* cells that have a comparatively drier colony phenotype. Furthermore, the Δ*engXCA2* mutant did not aggregate in liquid cultures (*data not shown*). Overproduction or de-regulation of exopolysaccharides (EPS) can have an adverse effect on the ability of bacteria to attach to surfaces and self-aggregate, both of which are hallmarks of the regimented developmental processes related to biofilm formation (Dertli et al. 2015; Koutsoudis et al. 2006; Rendueles et al. 2013). Therefore, it is likely that excessive EPS accumulation in the Δ*engXCA2* mutant disrupts cell-cell adhesion and, subsequently, early biofilm developmental processes that are known to be an important factor in attenuating *X. fastidiosa* virulence early in the xylem colonization process (Guilhabert and Kirkpatrick 2005, Rapicavoli et al. 2018), which leads to the observed hypervirulent phenotype for the Δ*engXCA2 mutant.* The *X. fastidiosa* EPS molecule is predicted to be comprised of a β-1,4 linked glucan backbone, which could be a substrate of EngXCA2. Our data indicate that EngXCA2 could play a dual role in *X. fastidiosa's* biology, one of which is that of a traditional plant CWDE that targets primary plant cell walls, and the

other in facilitating the turnover of EPS. Further studies on the role of EngXCA2 in EPS processing and biofilm development are warranted.

Our findings indicate PM composition is an important component of the plant-microbe interaction between cultivated grapevines and *X. fastidiosa*. In highly susceptible cultivars, the abundance of readily accessible carbohydrates in PMs that are compatible with *X. fastidiosa* CWDEs facilitates a greater PD symptom progression rate. In contrast, PD symptom progression is slower in more tolerant varieties that have lower abundances of substrates that are compatible with CWDEs of *X. fastidiosa*. Little is known about PM composition in the many plant hosts where *X. fastidiosa* resides as a commensal bacterium without causing disease (Freitag, 1951). Our data suggest that carbohydrate composition of PMs in tolerant grapevines may be less compatible with *X. fastidiosa* CWDEs than the PM carbohydrate composition found in susceptible hosts. Furthermore, PM carbohydrate composition may be a factor in plant-microbe interactions that determines where bacteria fall on the symbiosis spectrum of commensalism or parasitism.

## Literature Cited


Almeida, R. P. P., and Nunney, L. 2015. How do plant diseases caused by *Xylella fastidiosa* emerge?. Plant Disease. 99:1457-1467.

Andersen, P. C., and Brodbeck, B. V. 1989. Diurnal and temporal changes in the chemical profile of xylem exudate from *Vitis rotundifolia*. Physiologia Plantarum. 75:63-70.

Barras, F., van Gijsegem, F. and Chatterjee, A. K. 1994. Extracellular enzymes and pathogenesis of soft-rot *Erwinia*. Annual review of phytopathology. 32(1):201-234.

Bateman, D. F. 1976. Plant cell wall hydrolysis by pathogens. Pages 79–103 in: Biochemical Aspects of Plant-Parasite Relationships, J. Friend and D.R. Threlfall, eds. Academic Press, London.

Brett, C. T., and Waldron, K. W. 1996. *Physiology and biochemistry of plant cell walls*. Springer Science & Business Media, Heidelberg.

Buchanan, B. B., Gruissem, W., and Jones, R. L. 2000. The Cell Wall. Pages 52–100 in: Biochemistry and Molecular Biology of Plants, American Society of Plant Physiologists, Rockville, MD.

Burbank, L. P. Stenger, D. C. 2017. The DinJ/RelE Toxin-Antitoxin System Suppresses Bacterial Proliferation and Virulence of *Xylella fastidiosa* in Grapevine. Phytopathology. 107:388–394.

Carder, J. H. 1986. Detection and quantitation of cellulase by Congo red staining of substrates in a cup-plate diffusion assay. Analytical Biochemistry. 153:75-79.

Chang, C. J., Garnier, M., Zreik, L., Rossetti, V., and Bové, J. M. 1993. Culture and serological detection of the xylem-limited bacterium causing citrus variegated chlorosis and its identification as a strain of *Xylella fastidiosa*. Current Microbiology. 27:137-142.

Chatterjee, S., Almeida, R. P. P., and Lindow, S. 2008a. Living in two worlds: The plant and insect lifestyles of *Xylella fastidiosa*. Annual Review of Phytopathology. 46:243-271.

Chatterjee, S., Wistrom, C., and Lindow, S.E. 2008b. A cell–cell signaling sensor is required for virulence and insect transmission of Xylella fastidiosa. Proceedings of the National Academy of Sciences. 105:2670-2675.

Choat, B., Jansen, S., Zwieniecki, M. A., Smets, E., and Holbrook, N. M. 2004. Changes in pit membrane porosity due to deflection and stretching: the role of vestured pits. Journal of Experimental Botany. 55:1569-1575.

Clifford, J. C., Rapicavoli, J. N., and Roper, M. C. 2013. A rhamnose-rich O-antigen mediates adhesion, virulence, and host colonization for the xylem-limited phytopathogen *Xylella fastidiosa*. Mol Plant-Microbe Interacts. 26:676-685.

Cosgrove, D. J. 2000. Loosening of plant cell walls by expansins. Nature. 407:321-326.

Cosgrove, D. J. 2017. Microbial expansins. Annual Review of Microbiology. 71:479-497.

Cosgrove, D. J. 2018. Diffuse growth of plant cell walls. Plant Physiology. 176:16-27.

Davis, M. J., French, W. J. and Schaad, N. W. 1981. Axenic culture of the bacteria associated with phony disease of peach and plum leaf scald. Current Microbiology. 6:309-314.

Dertli, E., Mayer, M. J., and Narbad, A. 2015. Impact of the exopolysaccharide layer on biofilms, adhesion and resistance to stress in *Lactobacillus johnsonii* FI9785. BMC Microbiology. 15:8.

Deyett, E., Pouzoulet, J., Yang, J.I., Ashworth, V.E., Castro, C., Roper, M.C. and Rolshausen, P.E. 2019. Assessment of Pierce's disease susceptibility in *Vitis vinifera* cultivars with different pedigrees. Plant Pathology. 68(6): 1079-1087.

Dickison, W. C. 2007. Integrative Plant Anatomy. Harcourt/Academic Press, San Diego, CA.

Fatima, U. and Senthil-Kumar, M. 2015. Plant and pathogen nutrient acquisition strategies. Frontiers in plant science. 6:750.

Freitag, J. H. 1951. Host range of the Pierce's disease virus of grapes as determined by insect transmission. Phytopathology. 41:920-934.

Georgelis, N., Nikolaidis, N., Cosgrove, D. J. 2014. Biochemical analysis of expansin-like proteins from microbes. Carbohydrate Polymers. 100:17-23.

Goheen, A. C., and Hopkins, D. L. 1988. Pierce's disease. Pages 44–45 in: Compendium of Grape Diseases, A.C. Goheen and R.C. Pearson, eds. American Phytopathological Society Press, St. Paul, MN.

Gough, C. L., Dow, J. M., Barber, C. E. and Daniels, M. J. 1988. Cloning of two endoglucanase genes of *Xanthomonas campestris* pv. *campestris*: analysis of the role of the major endoglucanase in pathogenesis. Mol Plant-Microbe Interacts. 1(7):275-281.

Gouran, H., Gillespie, H., Nascimento, R., Chakraborty, S., Zaini, P. A., Jacobson, A., Phinney, B. S., Dolan, D., Durbin-Johnson, B. P., Antonova, E. S., Lindow, S. E., Mellema, M. S., Goulart, L. R., and Dandekar, A. M. 2016. The secreted protease PrtA controls cell growth, biofilm formation and pathogenicity in *Xylella fastidiosa*. Scientific Reports. 6:31098.

Guilhabert, M. R., and Kirkpatrick, B. C. 2005. Identification of *Xylella fastidiosa* antivirulence genes: hemagglutinin adhesins contribute to biofilm maturation to *X. fastidiosa* and colonization and attenuate virulence. Molecular Plant-Microbe Interactions. 18:856–868.

Hardy, P. J., and Possingham, J. V. 1969. Studies on translocation of metabolites in the xylem of grapevine shoots. Journal of Experimental Botany. 20:325-335.

Hématy, K., Cherk, C. and Somerville, S. 2009. Host–pathogen warfare at the plant cell wall. Current Opinion in Plant Biology. 12:406-413.

Hill, B. L., and Purcell, A. H. 1995. Acquisition and retention of *Xylella fastidiosa* by an efficient vector, *Graphocephala atropunctata*. Phytopathology. 85:209-212.

Kerff, F., Amoroso, A., Herman, R., Sauvage, E., Petrella, S., Filee, P., Charlier, P., Joris, B., Tabuchi, A., Nikolaidis, N., and Cosgrove, D. J. 2008. Crystal structure and

activity of Bacillus subtilis YoaJ (EXLX1), a bacterial expansin that promotes root colonization. Proceedings of the National Academy of Sciences. 105:16876-16881.

Koutsoudis, M. D., Tsaltas, D., Minogue, T. D., and von Bodman, S. B. 2006. Quorum-sensing regulation governs bacterial adhesion, biofilm development, and host colonization in *Pantoea stewartii* subspecies *stewartii*. Proceedings of the National Academy of Sciences. 103:5983-5988.

Kovach, M. E., Elzer, P. H., Hill, D. S., Robertson, G. T., Farris, M. A., Roop II, R. M., and Peterson, K. M. 1995. Four new derivatives of the broad-host-range cloning vector pBBR1MCS, carrying different antibiotic-resistance cassettes. Gene. 166:175-176.

Larner, J. 1960. Other glucosidases. Pages 369–378 in: The Enzymes, P. D. Boyer, H. Lardy, and K. Myrbäck, eds. Academic Press, New York, NY.

Li, W. B., Pria Jr, W. D., Teixeira, D. C., Miranda, V. S., Ayres, A. J., Franco, C. F., Costa, M. G., He, C. X., Costa, P. I., and Hartung, J. S., 2001. Coffee leaf scorch caused by a strain of *Xylella fastidiosa* from citrus. Plant Disease. 85:501-505.

Liang, K. Y., and Zeger, S. L. 1986. Longitudinal Data Analysis Using Generalized Linear Models. Biometrika. 73:13–22.

Lionetti, V., Cervone, F., and Bellincampi, D. 2012. Methyl esterification of pectin plays a role during plant–pathogen interactions and affects plant resistance to diseases. Journal of Plant Physiology. 169:1623-1630.

Loescher, W. H., McCamant, T., and Keller, J. D. 1990. Carbohydrate reserves, translocation, and storage in woody plant roots. HortScience. 25:274-281.

Matsumoto, A., Young, G. M.. and Igo, M. M. 2009. Chromosome-based genetic complementation system for *Xylella fastidiosa*. Applied Environmental Microbiology. 75:1679-1687.

McCullagh, P., and Nelder, J. A. 1989. *Generalized Linear Models*. 2nd ed. Chapman & Hall, London.

McElrone, A. J., Sherald, J. L., and Forseth, I. N. 2001. Effects of water stress on symptomatology and growth of *Parthenocissus quinquefolia* infected by *Xylella fastidiosa*. Plant Disease. 85:1160-1164.

McElrone, A. J., Sherald, J. L., and Forseth, I. N. 2003. Interactive effects of water stress and xylem-limited bacterial infection on the water relations of a host vine. Journal of Experimental Botany. 54:419-430.

Mohammadi, M., Burbank, L. and Roper, M.C. 2012. *Pantoea stewartii* subsp. *stewartii* produces an endoglucanase that is required for full virulence in sweet corn. Mol plant-microbe Interacts. 25(4):463-470.

Mollenhauer H. H., and Hopkins D. L. 1974. Ultrastructural study of Pierce's disease bacterium in grape xylem tissue. Journal of Bacteriology. 119:612-618.

Newman, K. L., Almeida, R. P. P., Purcell, A. H., and Lindow, S. E. 2004. Cell-cell signaling controls *Xylella fastidiosa* interactions with both insects and plants. Proceedings of the National Academy of Sciences. 101:1737–1742.

Nikolaidis, N., Doran, N., Cosgrove, D. J. 2014. Plant expansins in bacteria and fungi: evolution by horizontal gene transfer and independent domain fusion. Molecular Biology and Evolution. 31:376-386.

Perez-Donoso, A. G., Sun, Q., Roper, M. C., Greve, L. C., Kirkpatrick B. C., and Labavitch, J. M. 2010. Cell Wall-Degrading Enzymes Enlarge the Pore Size of Intervessel Pit Membranes in Healthy and *Xylella fastidiosa*-Infected Grapevines. Plant Physiology. 152:1748-1759.

Pieretti, I., Royer, M., Barbe, V., Carrere, S., Koebnik, R., Couloux, A., Darrasse, A., Gouzy, J., Jacques, M. A., Lauber, E. and Manceau, C. 2012. Genomic insights into strategies used by *Xanthomonas albilineans* with its reduced artillery to spread within sugarcane xylem vessels. BMC genomics. 13(1):658.

Popeijus, H., Overmars, H., Jones, J., Blok, V., Goverse, A., Helder, J., Schots, A., Bakker, J., and Smant, G. 2000. Enzymology: degradation of plant cell walls by a nematode. Nature. 406:36.

Purcell, A. H. 1986. Pierce's disease. Pages 62–69 in: Grape Pest Management, D.L. Flaherty, ed. Cooperative Extension University of California, Division of Agriculture and Natural Resources, Oakland, CA.

Purcell, A. H., and Saunders, S. R. 1999. Fate of Pierce's disease strains of *Xylella fastidiosa* in common riparian plants in California. Plant Disease. 83:825-830.

Rapicavoli, J., Ingel, B., Blanco-Ulate, B., Cantu, D., and Roper, C. 2018. *Xylella fastidiosa*: an examination of a re-emerging plant pathogen. Molecular Plant Pathology. 19:786-800.

Rendueles, O., Kaplan, J. B., and Ghigo, J. M. 2013. Antibiofilm polysaccharides. Environmental Microbiology. 15:334-346.

Roberts, D. P., Denny, T. P. and Schell, M. A. 1988. Cloning of the *egl* gene of *Pseudomonas solanacearum* and analysis of its role in phytopathogenicity. Journal of Bacteriology. 170(4):1445-1451.

Roper, M. C. 2006. The characterization and role of *Xylella fastidiosa* plant cell wall degrading enzymes and exopolysaccharide in Pierce's disease of grapevine. University of California, Davis.

Roper, M. C., Greve, L. C., Warren, J. G., Labavitch, J. M., and Kirkpatrick, B. C. 2007. *Xylella fastidiosa* requires polygalacturonase for colonization and pathogenicity in *Vitis vinifera* grapevines. Mol Plant Microbe Interacts. 20:411-419.

Saile, E., McGarvey, J. A., Schell, M. A. and Denny, T. P. 1997. Role of extracellular polysaccharide and endoglucanase in root invasion and colonization of tomato plants by *Ralstonia solanacearum*. Phytopathology. 87(12):1264-1271.

Saponari, M., Boscia, D., Nigro, F., and Martelli, G. P. 2013. Identification of DNA sequences related to *Xylella fastidiosa* in oleander, almond and olive trees exhibiting leaf scorch symptoms in Apulia (Southern Italy). Journal of Plant Pathology. 95:659-668.

Scheller, H. V., and Ulvskov, P. 2010. Hemicelluloses. Annual Review of Plant Biology. 61:263-289.

Schuenzel, E. L., Scally, M., Stouthamer, R., and Nunney, L. 2005. A multigene phylogenetic study of clonal diversity and divergence in North American strains of the plant pathogen *Xylella fastidiosa*. Applied and Environmental Microbiology. 71:3832-3839.

Simpson, A. J. G., Reinach, F. D. C., Arruda, P., Abreu, F. A. D., Acencio, M., Alvarenga, R., Alves, L. M. C., Araya, J. E., Baia, G. S., Baptista, C. S., Barros, M. H. D., Bonaccorsi, E. D., Bordin, S., Bové J. M., Briones, M. R. S., Bueno, M. R. P., Camargo, A. A., Camargo, L. E. A., Carraro, D. M., Carrer, H., Colauto, N. B., Colombo, C., Costa, F. F., Costa, M. C. R., Costa-Neto, C. M., Coutinho, L. L., Cristofani, M., Dias-Neto, E., Docena, C., El-Dorry, H., Facincani, A. P., Ferreira, A. J. S., Ferreira, V. C. A., Ferro, J. A., Fraga, J. S., França, S. C., Franco, M. C., Frohme, M., Furlan, L. R., Garnier, M., Goldman, G. H., Goldman, M. H. S., Gomes, S. L., Gruber, A., Ho, P. L., Hoheisel, J. D., Junqueira, M. L., Kemper, E. L., Kitajima, J.P., Krieger, J. E., Kuramae, E. E., Laigret, F., Lambais, M. R., Leite, L. C. C., Lemos, E. G. M., Lemos, M. V. F., Lopes, S. A., Lopes, C. R., Machado, J. A., Machado, M. A., Madeira, A. M. B. N., Madeira, H. M. F., Marino, C. L., Marques, M. V., Martins, E. A. L., Martins, E. M. F., Matsukuma, A. Y., Menck, C. F. M., Miracca, E. C., Miyaki, C. Y., Monteiro-Vitorello, C. B., Moon, D. H., Nagai, M. A., Nascimento, A. L. T. O., Netto, L. E. S., Nhani Jr, A., Nobrega, F. G., Nunes, L. R., Oliveira, M. A., de Oliveira, M. C., de Oliveira, R. C., Palmieri, D. A., Paris, A., Peixoto, B. R., Pereira, G. A. G., Pereira Jr, H. A., Pesquero, J. B., Quaggio, R. B., Roberto, P. G., Rodrigues, V., de M. Rosa, A. J., de Rosa Jr, V. E., de Sá, R. G., Santelli, R. V., Sawasaki, H. E., da Silva, A. C. R., da Silva, A. M., da Silva, F. R., Silva, W. A., da Silveira, J. F., Silvestri, M. L. Z., Siqueira, W. J., de Souza, A. A., de Souza, A. P., Terenzi, M. F., Truffi, D., Tsai, S. M., Tsuhako, M. H., Vallada, H., Van Sluys, M. A., Verjovski-Almeida, S., Vettore, A. L., Zago, M. A., Zatz, M., Meidanis J., and Setubal J. C. 2000. The genome sequence of the plant pathogen *Xylella fastidiosa*. Nature. 406:151-157.

Stevenson, J. F., Matthews, M. A., and Rost, T. L. 2004. Grapevine susceptibility to Pierce's disease I: relevance of hydraulic architecture. American Journal of Enology and Viticulture. 55:228-237.

Stevenson, J. F., Matthews, M. A., and Rost, T. L. 2005. The developmental anatomy of green islands and matchsticks as symptoms of Pierce's disease of grapevines. Plant Disease. 89:543-548.

Sun, Q., Greve, C. L., and Labavitch, J. M. 2011. Polysaccharide compositions of intervessel pit membranes contribute to Pierce's disease resistance of grapevines. Plant Physiology. 155:1976-1987.

Sun. Q., Sun. Y., Juzenas, K. 2017. Immunogold scanning electron microscopy can reveal the polysaccharide architecture of xylem cell walls. Journal of Experimental Botany. 68:2231-2244.

Tancos, M. A., Lowe-Power, T. M., Peritore-Galve, F. C., Tran, T. M., Allen, C., and Smart, C. D. 2018. Plant-like bacterial expansins play contrasting roles in two tomato vascular pathogens. Molecular Plant Pathology. 19:1210-1221.

Thorne, E. T., Stevenson, J. F., Rost, T. L., Labavitch, J. M., and Matthews, M. A. 2006a. Pierce's disease symptoms: comparison with symptoms of water deficit and the impact of water deficits. American Journal of Enology and Viticulture. 57:1-11.

Thorne, E. T., Young, B. M., Young, G. M., Stevenson, J. F., Labavitch, J. M., Matthews, M. A., and Rost, T. L. 2006b. The structure of xylem vessels in grapevine (Vitaceae) and a possible passive mechanism for the systemic spread of bacterial disease. American Journal of Botany. 93:497-504.

Tovar-Herrera, O. E., Rodríguez, M., Olarte-Lozano, M., Sampedro-Guerrero, J. A., Guerrero, A., Pinto-Cámara, R., Alvarado-Affantranger, X., Wood, C. D., Moran-Mirabal, J. M., Pastor, N. and Segovia, L. 2018. Analysis of the Binding of Expansin Exl1, from *Pectobacterium carotovorum*, to Plant Xylem and Comparison to EXLX1 from *Bacillus subtilis*. ACS Omega. 3:7008-7018.

Tyree, M. T., and Zimmermann, M. H. 2002. Hydraulic architecture of whole plants and plant performance. Pages 175–214 in: Xylem Structure and the Ascent of Sap, Springer-Verlag Berlin Heidelberg, Berlin.

Van Sluys, M. A., de Oliveira, M. C., Monteiro-Vitorello, C. B., Miyaki, C. Y., Furlan, L. R., Camargo, L. E. A., da Silva, A. C. R., Moon, D. H., Takita, M. A., Lemos, E. G. M., Machado, M. A., Ferro, M. I. T., da Silva, F. R., Goldman, M. H. S., Goldman, G. H., Lemos, M. V. F., El-Dorry, H., Tsai, S. M., Carrer, H., Carraro, D. M., de Oliveira, R. C., Nunes, L. R., Siqueira, W. J., Coutinho, L. L., Kimura, E. T., Ferro, E. S., Harakava, R., Kuramae, E. E., Marino, C. L., Giglioti, E.,

Abreu, I. L., Alves, L. M. C., do Amaral, A. M., Baia, G. S., Blanco, S. R., Brito, M. S., Cannavan, F. S., Celestino, A. V., da Cunha, A. F., Fenille, R. C., Ferro, J. A., Formighieri, E. F., Kishi, L. T., Leoni, S. G., Oliveira, A. R., Rosa Jr., V. E., Sassaki, F. T., Sena, J. A. D., de Souza, A. A., Truffi, D., Tsukumo, F., Yanai, G. M., Zaros, L. G., Civerolo, E. L., Simpson, A. J. G., Almeida Jr., N. F., Setubal, J. C., and Kitajima J. P. 2003. Comparative analyses of the complete genome sequences of Pierce's disease and citrus variegated chlorosis strains of *Xylella fastidiosa*. Journal of Bacteriology. 185:101-1026.

Varela, L. G. 1996. Pierce's Disease in the North Coast. University of California Cooperative Extension & Statewide IPM Project: 1Y11.

Walker, D. S., Reeves, P. J. and Salmond, G. P. 1994. The major secreted cellulase, CelV, of *Erwinia carotovora* subsp. *carotovora* is an important soft rot virulence factor. Mol Plant Microbe Interacts. 7:425-425.

Wang, P., Lee, Y., Igo, M. M. and Roper, M. C. 2017. Tolerance to oxidative stress is required for maximal xylem colonization by the xylem-limited bacterial phytopathogen, *Xylella fastidiosa*. Molecular Plant Pathology. 18:990-1000.

Ward, O. P., Moo-Young, M., and Venkat, K. 1989. Enzymatic degradation of cell wall and related plant polysaccharides. Critical Reviews in Biotechnology. 8:237-274.

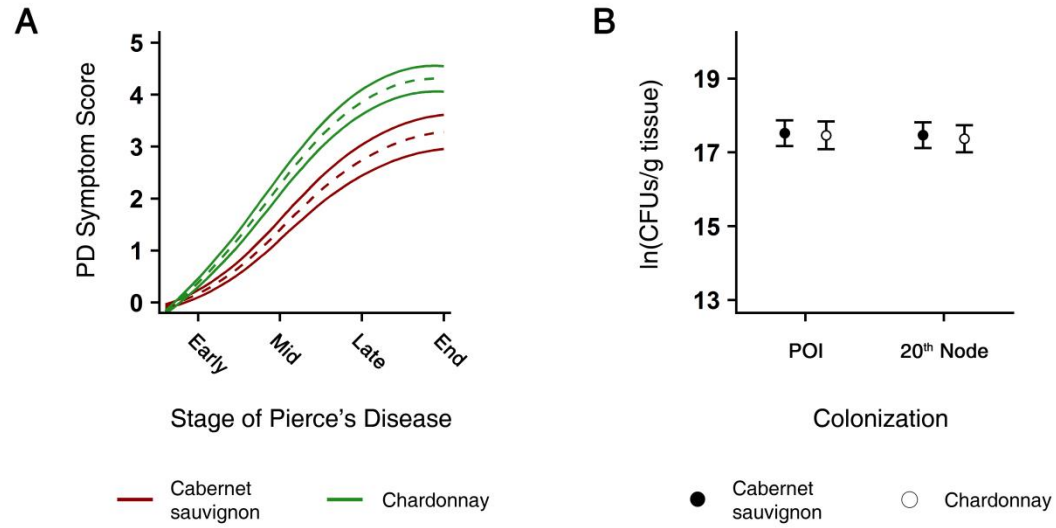
A
PD Symptom Score
5
4
3
2
1
0
Early
Mid
Late
End
Stage of Pierce's Disease
Cabernet sauvignon
Chardonnay
B
ln(CFUs/g tissue)
19
17
15
13
POI
20th Node
Colonization
Cabernet sauvignon
Chardonnay

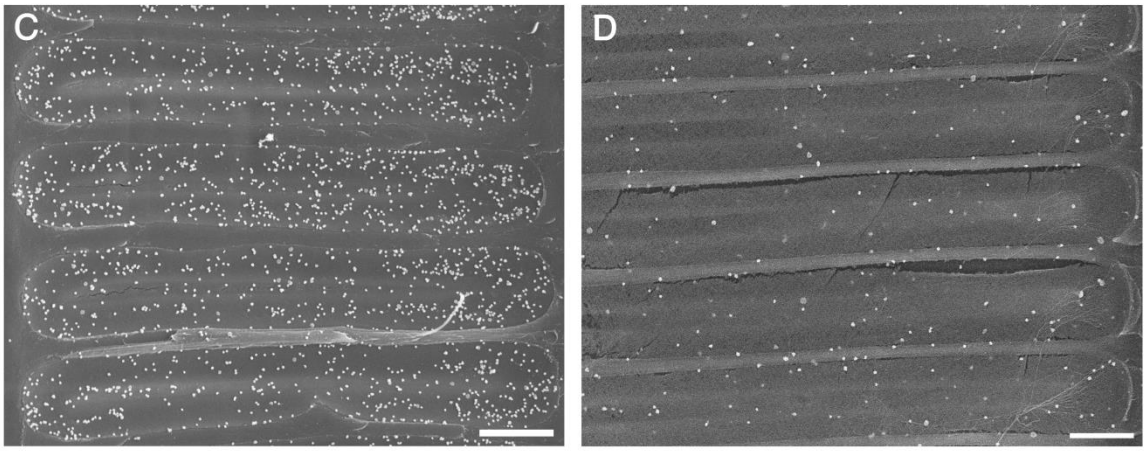
C
D

Figure 2.1 Grapevine cultivar affects PD symptom development and is mediated by differences in pit membrane composition. A) Overall PD symptom severity is greater in Chardonnay (green) than in Cabernet sauvignon (red). A Generalized Estimating Equations (GEE) model was used to determine the estimated mean PD symptom scores per week (dashed lines) and calculate 95% confidence intervals (solid lines). B) *X. fastidiosa* titers at the POI and at 20 nodes distal to the POI are not significantly different between Cabernet sauvignon and Chardonnay. Colony Forming Units were normalized per gram of petiole tissue and transformed using the natural log (ln). Statistical comparisons were made using a generalized negative binomial regression model. Error bars represent the standard error of the mean. C) Intervessel pit membranes of PBS-inoculated Chardonnay have a dense distribution of silver-enhanced particles, indicating an abundance of fucosylated xyloglucans. D) Intervessel pit membranes of PBS-inoculated Cabernet sauvignon have a moderate amount of silver-enhanced particles indicating the presence of some fucosylated xyloglucans. Fucosylated xyloglucans were detected using the CCRC-M1 antibody, and intervessel pit membranes were imaged using immunogold-scanning electron microscopy. Scale bars are equal to 5 µm.

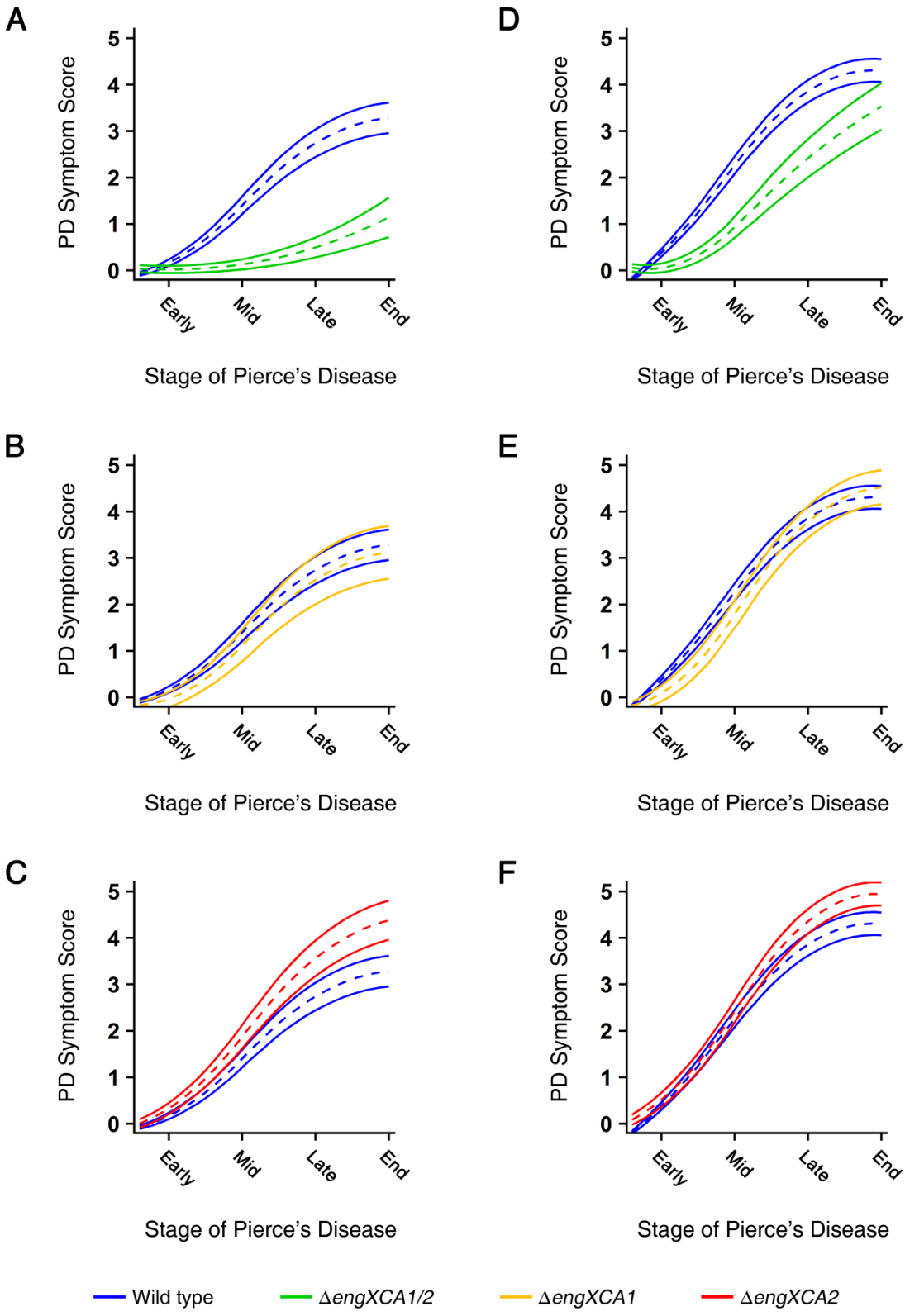
A
B
C
D
E
F
PD Symptom Score
0
1
2
3
4
5
Early
Mid
Late
End
Stage of Pierce's Disease
Wild type
ΔengXCA1/2
ΔengXCA1
ΔengXCA2

Figure 2.2 *X. fastidiosa* endoglucanases affect PD severity and the rate of PD symptom development in a cultivar-dependent manner. Estimated mean PD symptom scores generated by the Generalized Estimating Equations model for Δ*engXCA1* (yellow), Δ*engXCA2* (red), and Δ*engXCA1/2* (green) were compared to wild type (blue) in Cabernet sauvignon (A – C) and in Chardonnay (D – F) at early-, mid-, and late-stages of PD. A) Δ*engXCA1/2* induces milder PD symptoms than wild type in Cabernet sauvignon. B) Δ*engXCA1* and wild type induce similar PD symptoms in Cabernet sauvignon. C) Δ*engXCA2* induces more severe PD symptoms than wild type in Cabernet sauvignon. D) Δ*engXCA1/2* induces milder PD symptoms than wild type in Chardonnay, but to a lesser degree than in Cabernet sauvignon. E) Δ*engXCA1* induces milder symptoms than wild type at the early- and mid-stages of PD, but has similar symptom severity to wild type at the late stage of PD. F) Δ*engXCA2* and wild type induce similar symptoms at the early and mid-stages of PD, but induces more severe symptoms than wild type at the late-stage of PD. Estimated mean PD symptom scores per week are represented by dashed lines and 95% confidence intervals are represented by solid lines.

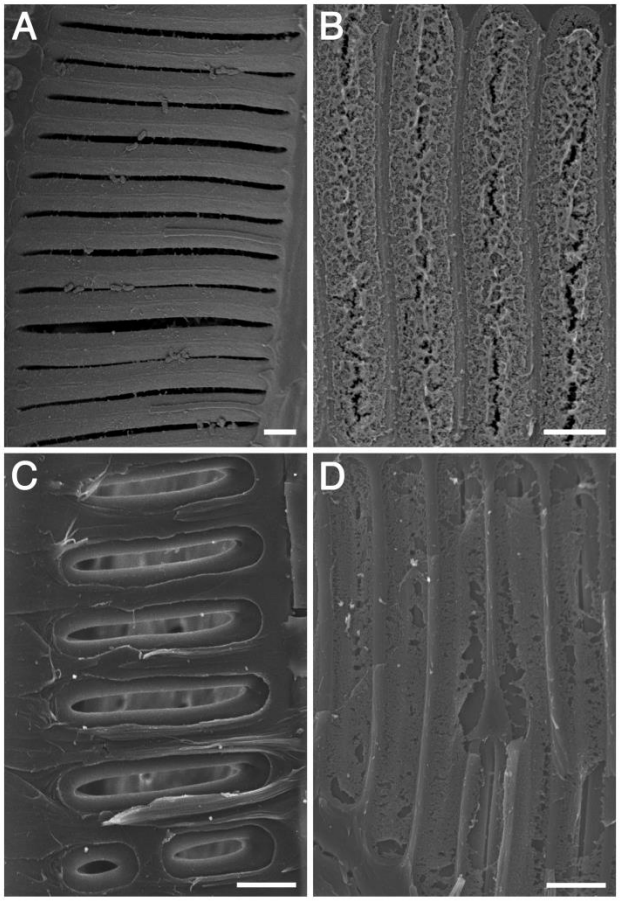


Figure 2.3 The Δ*engXCA1/2* double mutant is impaired in pit membrane dissolution. Integrity of intervessel pit membranes in Chardonnay (A and B) and Cabernet sauvignon (C and D) vines inoculated with wild-type (A and C) and Δ*engXCA1/2* (B and D) during late-stage infection. A and C) All of the intervessel PMs have been completely degraded. B and D) Intervessel PMs are still in place, but display partial degradation. Scale bar in each panel equals to 5 µm.

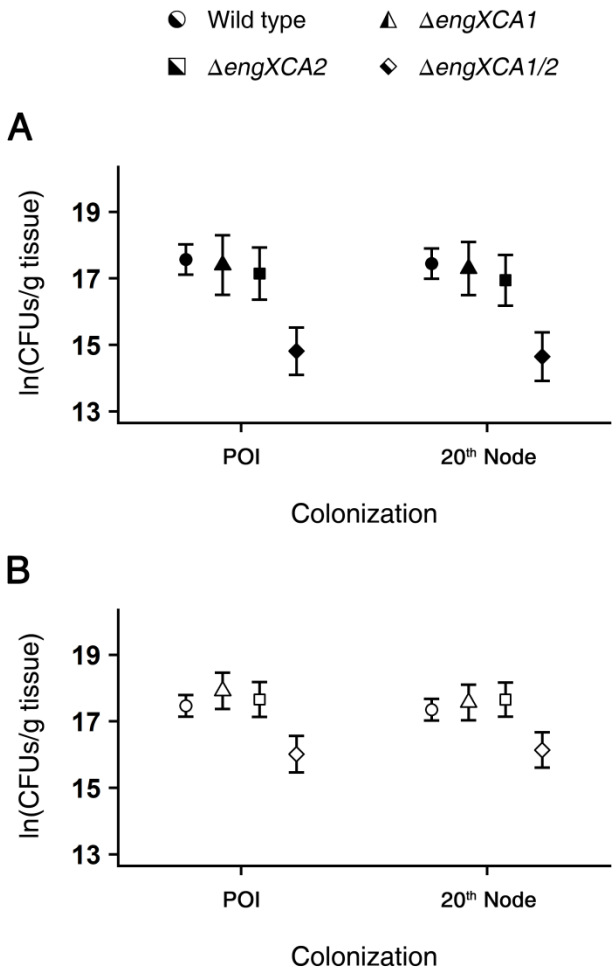


Figure 2.4 *X. fastidiosa* colonization is dependent on both EngXCA1 and EngXCA2. Colonization at the point of inoculation (POI) and at 20 nodes distal to the POI in A) Cabernet sauvignon (black) and B) Chardonnay (white) by Δ*engXCA1*(triangle) or Δ*engXCA2* (square) was similar to wild type (circle), while colonization by Δ*engXCA1/2* (diamond) at both locations was significantly reduced. Colony Forming Units were normalized per gram of petiole tissue and transformed using the natural log (ln). Statistical comparisons were made using a generalized negative binomial regression model. Error bars represent the standard error of the mean.

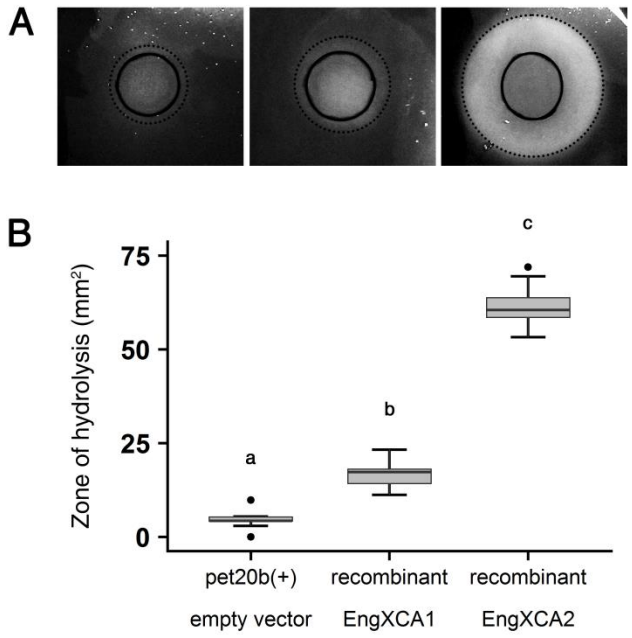


Figure 2.5 EngXCA1 has marginal endoglucanase activity. A) A radial diffusion assay shows that recombinant EngXCA1 is able to hydrolyze carboxymethylcellulose (CMC), but much less than the previously-characterized *X. fastidiosa* endoglucanase, EngXCA2. B) Recombinant EngXCA1 hydrolyzes significantly more CMC than the empty vector control, but significantly less than EngXCA2. Trials consisted of three biological replicates, each consisting of three technical replicates per treatment. Boxplot whiskers represent the minimum and maximum values per treatment, and black dots represent outliers. Letters indicate statistical significance.

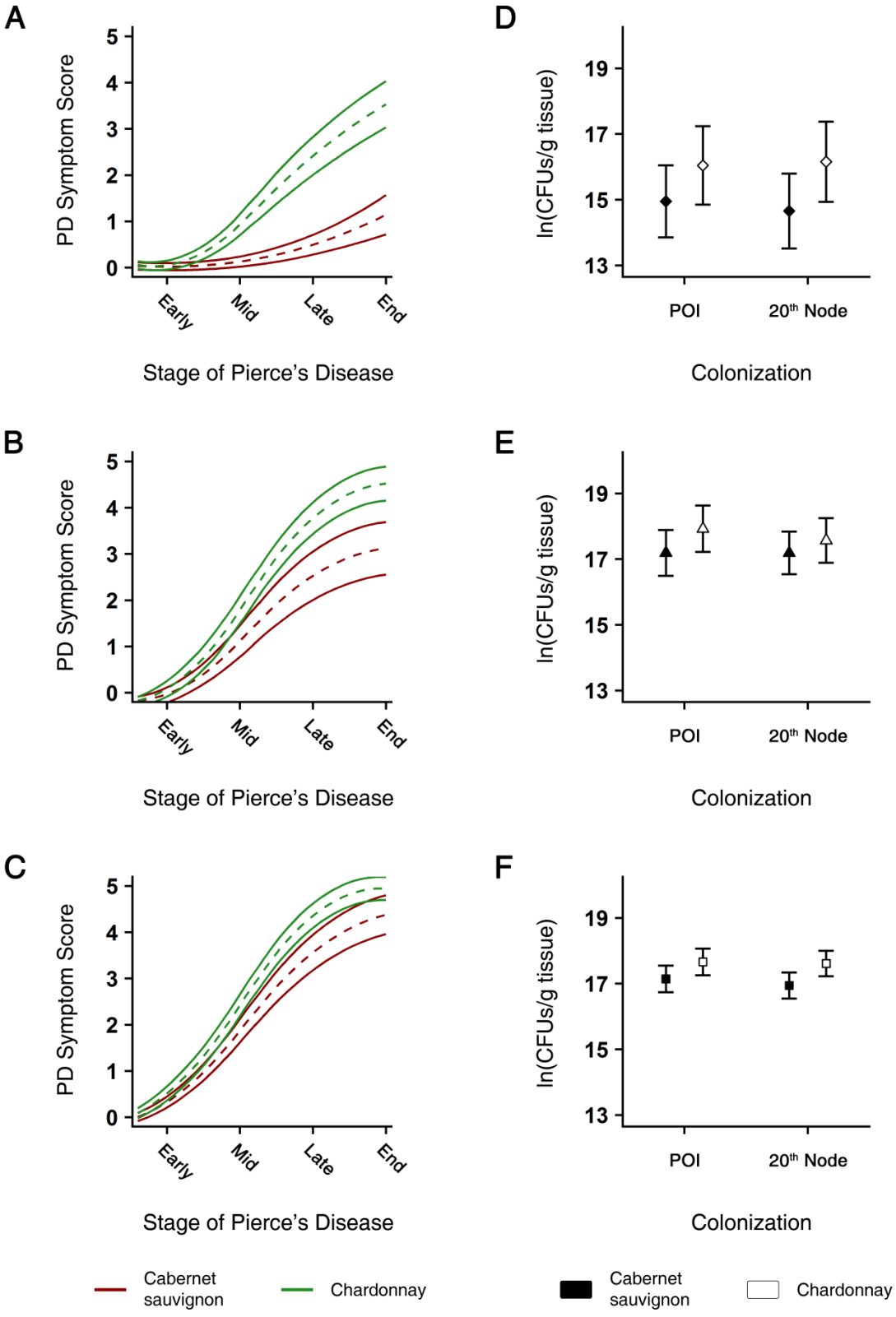
A
B
C
D
E
F
PD Symptom Score
0
1
2
3
4
5
Early
Mid
Late
End
Stage of Pierce's Disease
ln(CFUs/g tissue)
13
15
17
19
POI
20th Node
Colonization
Cabernet sauvignon
Chardonnay
Cabernet sauvignon
Chardonnay

Figure 2.6 Grapevine cultivar affects PD symptom development in mutant-inoculated vines. PD symptoms were more severe in Chardonnay (green) than in Cabernet sauvignon (red) when inoculated with A) Δ*engXCA1/2*, B) Δ*engXCA1*, or C) Δ*engXCA2*. A Generalized Estimating Equations (GEE) model was used to determine the estimated mean PD symptom scores per week (dashed lines) and calculate 95% confidence intervals (solid lines). Colonization at both the POI and at 20 nodes distal to the POI for D) Δ*engXCA1/2* (diamond), E) Δ*engXCA1* (triangle), and F) Δ*engXCA2* (square) were similar in both Cabernet sauvignon (black) and Chardonnay (white). Colony Forming Units were normalized per gram of petiole tissue and transformed using the natural log (ln). Statistical comparisons of bacterial titer were made using a generalized negative binomial regression model. Error bars represent the standard error of the mean.

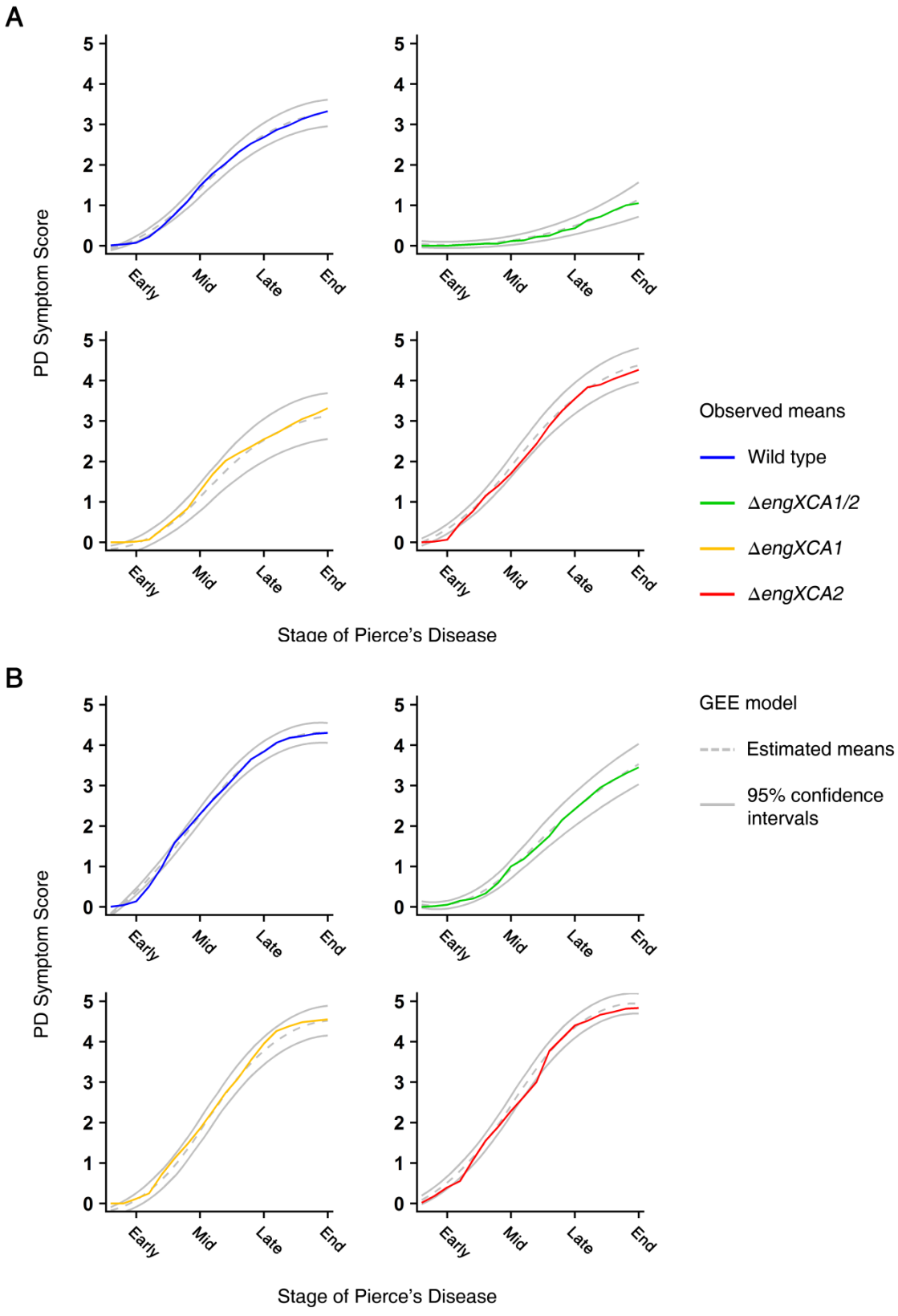
A
PD Symptom Score
0
1
2
3
4
5
Early
Mid
Late
End
Stage of Pierce's Disease
Observed means
Wild type
ΔengXCA1/2
ΔengXCA1
ΔengXCA2
B
PD Symptom Score
Stage of Pierce's Disease
GEE model
Estimated means
95% confidence intervals

Figure 2.7 The Generalized Estimating Equations model is validated by the goodness-of-fit of the observed PD symptom score means. The observed PD symptom score means were used to generate the Generalized Estimating Equations (GEE) model for A) Cabernet sauvignon and B) Chardonnay. Colored lines represent to observed means for grapevines inoculated with wild type (blue), Δ*engXCA1/2* (green), Δ*engXCA1* (yellow), or Δ*engXCA2* (red). The observed means are overlaid on top of the estimated PD symptom score means (dashed gray lines) and the 95% confidence intervals (solid gray lines) generated by the GEE model for each strain to show goodness-of-fit.

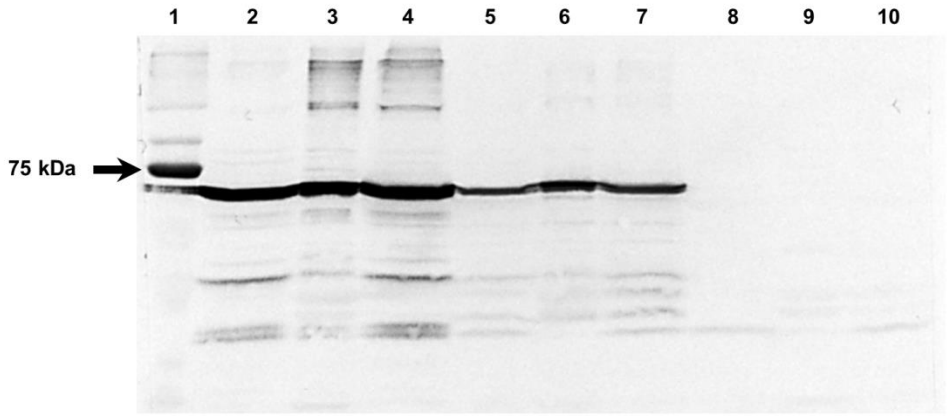


Figure 2.8 Western blot analysis of *Escherichia coli* cell lysates after transformation with pBI3, pMCR7, or the empty pET20b(+) vector. Lane 1, Molecular weight ladder; lane 2, *E. coli* transformed with pBI3 soluble fraction of cell lysate; lane 3, *E. coli* transformed with pBI3 insoluble fraction of cell lysate; lane 4, *E. coli* transformed with pBI3 whole cell lysate; lane 5 *E. coli* transformed with pMCR7 soluble fraction of cell lysate; lane 6, *E. coli* transformed with pMCR7 insoluble fraction of cell lysate; lane 7, *E. coli* transformed with pMCR7 whole cell lysate; lane 8, *E. coli* transformed with empty pET20b(+) vector soluble fraction of cell lysate; lane 9, *E. coli* transformed with empty pET20b(+) vector insoluble fraction of cell lysate; lane 10, *E. coli* transformed with empty pET20b(+) vector whole cell lysate. The molecular masses of EngXCA1 and EngXCA2 are 63 kDa and 62 kDa, respectively.

| | Pierce's Disease Stage Interval | | | | | | | | |
|---|---|---|---|---|---|---|---|---|---|
| | Early-stage to Mid-Stage | | | | | Mid-stage to Late-Stage | | | |
| | Rate | | Comparison | | | Rate | | Comparison | | |
| Strain | Cabernet sauvignon | Chardonnay | Rate Difference | *p*-value | | Cabernet sauvignon | Chardonnay | Rate Difference | *p*-value | |
| Wild type | 0.25 | 0.39 | -0.14 ±0.02 | <0.0001 | *** | 0.27 | 0.32 | -0.05 ±0.02 | 0.0139 | * |
| Δ*engXCA1* | 0.23 | 0.35 | -0.12 ±0.04 | 0.0013 | ** | 0.28 | 0.40 | -0.12 ±0.04 | 0.0016 | ** |
| Δ*engXCA2* | 0.32 | 0.39 | -0.07 ±0.03 | 0.0087 | ** | 0.34 | 0.39 | -0.05 ±0.03 | 0.0525 | ns |
| Δ*engXCA1/2* | 0.02 | 0.17 | -0.15 ±0.02 | <0.0001 | *** | 0.07 | 0.30 | -0.23 ±0.03 | <0.0001 | *** |



Table 2.1 Comparing the rate of Pierce's Disease symptom progression in Cabernet sauvignon and Chardonnay between early- and mid-stages of PD (5-10 weeks post-inoculation) and between mid- and late-stages of PD (10-15 weeks post-inoculation). The estimated rates of Pierce's Disease symptom progression were generated from the Generalized Estimated Equations model for each strain. Negative rate values indicate that Pierce's Disease progresses slower in Cabernet sauvignon than in Chardonnay and positive rate values indicate that Pierce's Disease progresses faster in Cabernet sauvignon than in Chardonnay. *p*-values of the estimated rate differences were generated using 95% confidence intervals in the Generalized Estimated Equations model; ns = no significance, * = $p<0.05$, ** = $p<0.01$, *** = $p<0.001$.

| | Pierce's Disease Stage Interval | | | | | | | |
|---|---|---|---|---|---|---|---|---|
| | Early-stage to Mid-Stage | | | | Mid-stage to Late-Stage | | | |
| Strain | Rate | Rate Difference | *p*-value | | Rate | Rate Difference | *p*-value | |
| Wild type | 0.25 | N/A | N/A | | 0.27 | N/A | N/A | |
| Δ*engXCA1* | 0.23 | -0.02 ±0.03 | 0.54 | ns | 0.28 | 0.01 ±0.03 | 0.64 | ns |
| Δ*engXCA2* | 0.32 | 0.06 ±0.21 | 0.023 | * | 0.34 | 0.07 ±0.03 | 0.0053 | ** |
| Δ*engXCA1/2* | 0.02 | -0.23 ±0.02 | <0.0001 | *** | 0.07 | -0.20 ±0.02 | <0.0001 | *** |

Table 2.2 Comparing the rate of Pierce's Disease symptom progression for wild type and mutant strains in Cabernet sauvignon between early- and mid-stages of PD (5-10 weeks post-inoculation) and between mid- and late-stages of PD (10-15 weeks post-inoculation). The estimated rates of Pierce's Disease symptom progression were generated from the Generalized Estimated Equations model for each strain. Negative values indicate rates for mutant strains are slower than wild type and positive values indicate rates for mutant strains are faster than wild type. *p*-values of the estimated rate differences were generated using 95% confidence intervals in the Generalized Estimated Equations model; ns = no significance, * = $p<0.05$, ** = $p<0.01$, *** = $p<0.001$.

| | Pierce's Disease Stage Interval | | | | | | | |
|---|---|---|---|---|---|---|---|---|
| | Early-stage to Mid-Stage | | | | Mid-stage to Late-Stage | | | |
| Strain | Rate | Rate Difference | *p*-value | | Rate | Rate Difference | *p*-value | |
| Wild type | 0.39 | N/A | N/A | | 0.32 | N/A | N/A | |
| Δ*engXCA1* | 0.35 | -0.04 ±0.03 | 0.0735 | ns | 0.40 | 0.08 ±0.03 | 0.0023 | ** |
| Δ*engXCA2* | 0.39 | 0.00 ±0.02 | 0.85 | ns | 0.39 | 0.07 ±0.02 | 0.008 | ** |
| Δ*engXCA1/2* | 0.17 | -0.22 ±0.03 | <0.0001 | *** | 0.30 | -0.02 ±0.03 | 0.46 | ns |

Table 2.3 Comparing the rate of Pierce's Disease symptom progression for wild type and mutant strains in Chardonnay between early- and mid-stages of PD (5-10 weeks post-inoculation) and between mid- and late-stages of PD (10-15 weeks post-inoculation). The estimated rates of Pierce's Disease symptom progression were generated from the Generalized Estimated Equations model for each strain. Negative values indicate rates for mutant strains are slower than wild type and positive values indicate rates for mutant strains are faster than wild type. *p*-values of the estimated rate differences were generated using 95% confidence intervals in the Generalized Estimated Equations model; ns = no significance, * = $p<0.05$, ** = $p<0.01$, *** = $p<0.001$.

| Strains, plasmids, and primers | Relevant characteristics or primer sequence | Source |
|---|---|---|
| Strains | | |
| *Escherichia coli* TOP10 | F- *mcr*A Δ(*mrr-hsd*RMS-*mcr*BC) Φ80*lacZ*ΔM15 Δ*lac*X74 *rec*A1 *ara*D139 Δ(*araleu*)7697 *gal*U *gal*K *rps*L (*Str*R) *end*A1 nup*G* | Invitrogen |
| *X. fastidiosa* Temecula 1 | | Temecula, CA |
| *X. fastidiosa* Δ*engXCA1* | *engXCA1* deletion in Temecula 1 background | This study |
| *X. fastidiosa* Δ*engXCA2* | *engXCA2* deletion in Temecula 1 background | This study |
| *X. fastidiosa* Δ*engXCA1/2* | *engXCA1* and *engXCA2* deletions in Temecula 1 background | This study |
| Plasmids | | |
| pCR8/GW/TOPO | pUC19 derivative, $Spn^r$ | Invitrogen |
| pCR2.1 TOPO | $Km^r$ | Invitrogen |
| pBBR1-MCS5 | $Gm^r$ | Kovach et al. (1995) |
| BI1 | pCR8/GW/TOPO with Δ*engXCA1* deletion construct | This study |
| BI2 | pCR8/GW/TOPO with Δ*engXCA2* deletion construct | This study |
| BI3 | pET20b(+) protein expression vector with *engXCA1* gene | This Study |
| MCR7 | pET20b(+) protein expression vector with *engXCA2* gene | Perez-Donoso et al. (2010) |
| Primers | | |
| engXCA1_LF_fwd | CGATCCGCCACGCTTCAGTATTGCC | This study |
| engXCA1_LF_rev | GGGCTTCCCAACCTTGACCGTGACT | This study |
| engXCA1_kan_fwd | AGTCACGGTCAAGGTTGGGAAGCCC | This study |
| engXCA1_kan_rev | GCAACATCCGGTTGCTACTTTCACCAG | This study |
| engXCA1_RF_fwd | CTGGTGAAAGTAGCAACCGGATGTTGC | This study |
| engXCA1_RF_rev | CCACACTCGCAGTGGCGCTTATTGG | This study |
| engXCA2_LF_fwd | TGCGTCCATAGACGCTTGCCATC | This study |
| engXCA2_LF_rev | CCACGGTGTGCGTCTAAGTATCCTTAATAGG | This study |
| engXCA2_gent_fwd | CCTATTAAGGATACTTAGACGCACACCGTGG | This study |
| engXCA2_gent_rev | GGAATAGAAAATGCACTTTAGGTGGCGGTAC TTG | This study |
| engXCA2_RF_fwd | CAAGTACCGCCACCTAAAGTGCATTTTCTAT TCC | This study |
| engXCA2_RF_rev | GTTCCGAGACCGAGAATACCGATGATGAG | This study |
| GW1 | GTTGCAACAAATTGATGAGCAATGC | Invitrogen |
| GW2 | TAATTGCTCATCAATTTGTTGCAAC | Invitrogen |
| engXCA1_XfgenDNA_For_ seq | CCTCAGGCGATACAGGCTAATCAGC | This study |
| engXCA1_XfgenDNA_Rev _seq | CGCTCAGGTCATTCGTGATACACC | This study |
| engXCA1mut_Kan_For_seq | ATCGCCTTCTTGACGAGTTCTTCTG | This study |
| engXCA1mut_Kan_Rev_seq | CTGCGTGCAATCCATCTTGTTCAATC | This study |
| Xf_engXCA2_PCR_fwd | CCGGTTTCAAAGTCGGGATC | This study |
| Xf_engXCA2_PCR_rev | ATGTGCGAACCCAGTTTTCC | This study |
| Xf_engXCA2seq_92outLF | CCTGCCCCTGAGTCAAAGAG | This study |
| Xf_engXCA2seq_71intLF | CCCTAACGGCGTTTGAATCAC | This study |
| Gent_seq_fwd | GACGCACACCGTGGAAACGGATGAAG | This study |
| Xf_engXCA2seq_33intRF | CGGAGTGGTAACGATGGCAT | This study |

Table 2.4 Strains, plasmids, and primer sequences used in this chapter. Primer sequences are presented 5' to 3'. $Spn^r$, $Kan^r$, and $Gm^r$ indicate spectinomycin, kanamycin, and gentamicin resistance genes, respectively.

| Stage of Pierce's Disease | | | | | |
|---|---|---|---|---|---|
| **Early-Stage** | | | | | |
| Strain | Mean Cabernet sauvignon | Mean Chardonnay | Difference | *p*-value | |
| Wild type | 0.14 | 0.30 | -0.16 | <0.0001 | *** |
| Δ*engXCA1* | 0.00 | 0.06 | -0.06 | 0.1142 | ns |
| Δ*engXCA2* | 0.29 | 0.48 | -0.19 | 0.0027 | ** |
| Δ*engXCA1/2* | 0.03 | 0.07 | -0.04 | 0.1958 | ns |
| **Mid-Stage** | | | | | |
| Strain | Mean Cabernet sauvignon | Mean Chardonnay | Difference | *p*-value | |
| Wild type | 1.40 | 2.27 | -0.87 | <0.0001 | *** |
| Δ*engXCA1* | 1.12 | 1.79 | -0.67 | 0.0016 | ** |
| Δ*engXCA2* | 1.87 | 2.42 | -0.55 | 0.008 | ** |
| Δ*engXCA1/2* | 0.13 | 0.93 | -0.80 | <0.0001 | *** |
| **Late-Stage** | | | | | |
| Strain | Mean Cabernet sauvignon | Mean Chardonnay | Difference | *p*-value | |
| Wild type | 2.74 | 3.86 | -1.12 | <0.0001 | *** |
| Δ*engXCA1* | 2.53 | 3.78 | -1.25 | <0.0001 | *** |
| Δ*engXCA2* | 3.56 | 4.36 | -0.80 | 0.0006 | *** |
| Δ*engXCA1/2* | 0.50 | 2.42 | -1.92 | <0.0001 | *** |
| **Endpoint** | | | | | |
| Strain | Mean Cabernet sauvignon | Mean Chardonnay | Difference | *p*-value | |
| Wild type | 3.28 | 4.30 | -1.02 | <0.0001 | *** |
| Δ*engXCA1* | 3.12 | 4.52 | -1.40 | <0.0001 | *** |
| Δ*engXCA2* | 4.38 | 4.94 | -0.56 | 0.0224 | * |
| Δ*engXCA1/2* | 1.14 | 3.53 | -2.39 | <0.0001 | *** |

Table 2.5 Comparison of Symptom Scores for each *X. fastidiosa* strain at each Stage of Pierce's Disease in Cabernet sauvignon and Chardonnay. Pierce's Disease Symptom Scores are based on the 0-5 rating scale (Guilhabert and Kirkpatrick 2005) at Early-, Mid-, and Late-Stages of Pierce's Disease, and at the Endpoint of the experiment (5, 10, 15, and 20 weeks post-inoculation, respectively). Estimated mean Pierce's Disease Symptom Scores for Cabernet sauvignon and Chardonnay were generated from the Generalized Estimated Equations model for each strain at each Stage of Pierce's Disease. A positive Pierce's Disease symptom score differential indicates mean symptom scores in Cabernet sauvignon are greater than in Chardonnay, while a negative differential indicates mean symptom scores in Cabernet sauvignon are less than in Chardonnay. *p*-values of the estimated mean differences were generated using 95% confidence intervals in the Generalized Estimated Equations model; ns = no significance, * = $p<0.05$, ** = $p<0.01$, *** = $p<0.001$.

| Bacterial Titer | | | | | | | |
|---|---|---|---|---|---|---|---|
| **Point of Inoculation** | | | | | | | |
| | **CFUs/g tissue** | | **ln(CFUs/g tissue)** | | | | |
| Strain | Mean Cabernet sauvignon | Mean Chardonnay | Mean Cabernet sauvignon | Mean Chardonnay | Difference | *p*-value | |
| Wild type | 4.07 (±1.42) × $10^7$ | 3.83 (±1.46) × $10^7$ | 17.52±0.35 | 17.46 ±0.38 | 0.06 ±0.03 | 0.90 | ns |
| Δ*engXCA1* | 2.91 (±2.01) × $10^7$ | 6.08 (±2.02) × $10^7$ | 17.19±0.70 | 17.92 ±0.71 | -0.73 ±0.01 | 0.46 | ns |
| Δ*engXCA2* | 2.79 (±1.50) × $10^7$ | 4.67 (±1.50) × $10^7$ | 17.14±0.41 | 17.66 ±0.41 | -0.52 ±0.00 | 0.37 | ns |
| Δ*engXCA1/2* | 3.11 (±3.00) × $10^6$ | 9.27 (±3.29) × $10^6$ | 14.95±1.10 | 16.04 ±1.19 | -1.09 ±0.09 | 0.50 | ns |
| **20$^{th}$ Node** | | | | | | | |
| | **CFUs/g tissue** | | **ln(CFUs/g tissue)** | | | | |
| Strain | Mean Cabernet sauvignon | Mean Chardonnay | Mean Cabernet sauvignon | Mean Chardonnay | Difference | *p*-value | |
| Wild type | 3.84 (±1.42) × $10^7$ | 3.49 (±1.44) × $10^7$ | 17.47 ±0.35 | 17.37 ±0.37 | 0.10 ±0.02 | 0.85 | ns |
| Δ*engXCA1* | 2.91 (±1.91) × $10^7$ | 4.26 (±1.97) × $10^7$ | 17.19 ±0.65 | 17.57 ±0.68 | -0.38 ±0.03 | 0.68 | ns |
| Δ*engXCA2* | 2.28 (±1.49) × $10^7$ | 4.46 (±1.47) × $10^7$ | 16.94 ±0.40 | 17.61 ±0.39 | -0.67 ±0.01 | 0.23 | ns |
| Δ*engXCA1/2* | 2.32 (±3.12) × $10^6$ | 1.04 (±3.39) × $10^7$ | 14.66 ±1.14 | 16.16 ±1.22 | -1.50 ±0.08 | 0.37 | ns |

Table 2.6 Comparison of Bacterial Titer for each *X. fastidiosa* strain in Cabernet sauvignon and Chardonnay at the point of inoculation and at 20 nodes above the point of inoculation. The estimated mean bacterial titer and standard error were generated by a negative binomial regression model comparing each strain in Cabernet sauvignon and Chardonnay and expressed as the natural log transformation of colony-forming units per gram of tissue. Negative values indicate mean bacterial titers in Cabernet sauvignon are less than in Chardonnay, and positive values indicate mean bacterial titers in Cabernet sauvignon are greater than in Chardonnay. *p*-values of the estimated mean differences were generated by the negative binomial regression model; ns = no significance, * = $p<0.05$, ** = $p<0.01$, *** = $p<0.001$.

| | Stage of Pierce's Disease | | | | | | | | | | | |
|---|---|---|---|---|---|---|---|---|---|---|---|---|
| | Early-stage | | | Mid-stage | | | Late-stage | | | Endpoint | | |
| Strain | Mean | Difference | *p*-value | Mean | Difference | *p*-value | Mean | Difference | *p*-value | Mean | Difference | *p*-value |
| Wild type | 0.14 | N/A | N/A | 1.40 | N/A | N/A | 2.74 | N/A | N/A | 3.28 | N/A | N/A |
| Δ*engXCA1* | 0.00 | -0.14 | 0.0043 ** | 1.12 | -0.28 | 0.14 ns | 2.53 | -0.21 | 0.49 ns | 3.12 | -0.16 | 0.63 ns |
| Δ*engXCA2* | 0.29 | 0.15 | 0.019 * | 1.87 | 0.47 | 0.0038 ** | 3.56 | 0.82 | 0.0009 ** | 4.38 | 1.10 | <0.0001 *** |
| Δ*engXCA1/2* | 0.03 | -0.11 | 0.0037 ** | 0.13 | -1.27 | <0.0001 *** | 0.50 | -2.24 | <0.0001 *** | 1.14 | -2.14 | <0.0001 *** |

Table 2.7 Symptom scores for each *X. fastidiosa* strain at each Stage of Pierce's Disease in Cabernet sauvignon based on the 0-5 rating scale (Guilhabert and Kirkpatrick 2005) at Early-, Mid-, and Late-Stages of Pierce's Disease, and at the Endpoint of the experiment (5, 10, 15, and 20 weeks post-inoculation, respectively). The estimated mean Pierce's Disease Symptom Scores were generated from the Generalized Estimated Equations model for each strain at each Stage of Pierce's Disease. Negative values indicate means less than wild type and positive values indicate means greater than wild type. *p*-values of the estimated mean differences were generated using 95% confidence intervals in the Generalized Estimated Equations model; ns = no significance, * = $p<0.05$, ** = $p<0.01$, *** = $p<0.001$.

| | Stage of Pierce's Disease | | | | | | | | | | | |
|---|---|---|---|---|---|---|---|---|---|---|---|---|
| | Early-stage | | | Mid-stage | | | Late-stage | | | Endpoint | | |
| Strain | Mean | Difference | *p*-value | Mean | Difference | *p*-value | Mean | Difference | *p*-value | Mean | Difference | *p*-value |
| Wild type | 0.30 | N/A | N/A | 2.27 | N/A | N/A | 3.86 | N/A | N/A | 4.30 | N/A | N/A |
| Δ*engXCA1* | 0.06 | -0.24 | 0.0023 ** | 1.79 | -0.48 | 0.0069 ** | 3.78 | -0.08 | 0.7 ns | 4.52 | 0.22 | 0.33 ns |
| Δ*engXCA2* | 0.48 | 0.18 | 0.0255 * | 2.42 | 0.15 | 0.32 ns | 4.36 | 0.50 | 0.0072 ** | 4.94 | 0.64 | 0.0005 *** |
| Δ*engXCA1/2* | 0.07 | -0.23 | <0.0001 *** | 0.93 | -1.34 | <0.0001 *** | 2.42 | -1.44 | <0.0001 *** | 3.53 | -0.77 | 0.0079 ** |

Table 2.8 Symptom scores for each *X. fastidiosa* strain at each Stage of Pierce's Disease in Chardonnay based on the 0-5 rating scale (Guilhabert and Kirkpatrick 2005) at Early-, Mid-, and Late-Stages of Pierce's Disease, and at the Endpoint of the experiment (5, 10, 15, and 20 weeks post-inoculation, respectively). The estimated mean Pierce's Disease Symptom Scores were generated from the Generalized Estimated Equations model for each strain at each Stage of Pierce's Disease. Negative values indicate means less than wild type and positive values indicate means greater than wild type. *p*-values of the estimated mean differences were generated using 95% confidence intervals in the Generalized Estimated Equations model; ns = no significance, * = $p<0.05$, ** = $p<0.01$, *** = $p<0.001$.

| Bacterial Titer | | | | | |
|---|---|---|---|---|---|
| **Point of Inoculation** | | | | | |
| | **CFUs/g tissue** | **ln(CFUs/g tissue)** | | | |
| Strain | Mean | Mean | Difference | *p*-value | |
| Wild type | 4.25 (±1.58) × $10^7$ | 17.56 ±0.46 | N/A | N/A | |
| Δ*engXCA1* | 3.61 (±2.45) × $10^7$ | 17.40 ±0.90 | -0.16 ±0.44 | 0.44 | ns |
| Δ*engXCA2* | 2.79 (±2.19) × $10^7$ | 17.14 ±0.78 | -0.42 ±0.32 | 0.32 | ns |
| Δ*engXCA1/2* | 2.71 (±2.04) × $10^6$ | 14.81 ±0.71 | -2.75 ±0.25 | 0.0006 | *** |
| **20$^{th}$ Node** | | | | | |
| | **CFUs/g tissue** | **ln(CFUs/g tissue)** | | | |
| Strain | Mean | Mean | Difference | *p*-value | |
| Wild type | 3.76 (±1.58) × $10^7$ | 17.44 ±0.46 | N/A | N/A | |
| Δ*engXCA1* | 3.24 (±2.22) × $10^7$ | 17.29 ±0.80 | -0.15 ±0.34 | 0.44 | ns |
| Δ*engXCA2* | 2.28 (±2.14) × $10^7$ | 16.94 ±0.76 | -0.50 ±0.30 | 0.29 | ns |
| Δ*engXCA1/2* | 2.29 (±2.08) × $10^6$ | 14.64 ±0.73 | -2.80 ±0.27 | 0.0006 | *** |

Table 2.9 Comparison of bacterial titer for wild type and each mutant strain in Cabernet sauvignon at the point of inoculation and at 20 nodes above the point of inoculation. The estimated mean bacterial titer and standard error were generated by a negative binomial regression model comparing wild type to each mutant strain and expressed as the natural log transformation of colony-forming units per gram of tissue. Negative values indicate mean bacterial titers for a mutant strain are less than wild type, and positive values indicate mean bacterial titers for a mutant strain are greater than wild type. *p*-values of the estimated mean differences were generated by the negative binomial regression model; ns = no significance, * = $p<0.05$, ** = $p<0.01$,
*** = $p<0.001$.

| Bacterial Titer | | | | | |
|---|---|---|---|---|---|
| **Point of Inoculation** | | | | | |
| | **CFUs/g tissue** | **ln(CFUs/g tissue)** | | | |
| Strain | Mean | Mean | Difference | *p*-value | |
| Wild type | 3.84 (±1.39) × $10^7$ | 17.46 ±0.33 | N/A | N/A | |
| Δ*engXCA1* | 6.04 (±1.73) × $10^7$ | 17.92 ±0.55 | 0.46 ±0.22 | 0.76 | ns |
| Δ*engXCA2* | 4.66 (±1.69) × $10^7$ | 17.66 ±0.53 | 0.20 ±0.20 | 0.62 | ns |
| Δ*engXCA1/2* | 9.02 (±1.73) × $10^6$ | 16.02 ±0.55 | -1.44 ±0.22 | 0.012 | * |
| **20$^{th}$ Node** | | | | | |
| | **CFUs/g tissue** | **ln(CFUs/g tissue)** | | | |
| Strain | Mean | Mean | Difference | *p*-value | |
| Wild type | 3.43 (±1.38) × $10^7$ | 17.35 ±0.32 | N/A | N/A | |
| Δ*engXCA1* | 4.26 (±1.71) × $10^7$ | 17.57 ±0.54 | 0.22 ±0.22 | 0.64 | ns |
| Δ*engXCA2* | 4.63 (±1.67) × $10^7$ | 17.65 ±0.51 | 0.30 ±0.19 | 0.69 | ns |
| Δ*engXCA1/2* | 1.02 (±1.70) × $10^7$ | 16.14 ±0.53 | -1.21 ±0.21 | 0.026 | * |

Table 2.10 Comparison of bacterial titer for wild type and each mutant strain in Chardonnay at the point of inoculation and at 20 nodes above the point of inoculation. The estimated mean bacterial titer and standard error were generated by a negative binomial regression model comparing wild type to each mutant strain and expressed as the natural log transformation of colony-forming units per gram of tissue. Negative values indicate mean bacterial titers for a mutant strain are less than wild type, and positive values indicate mean bacterial titers for a mutant strain are greater than wild type. *p*-values of the estimated mean differences were generated by the negative binomial regression model; ns = no significance, * = $p<0.05$, ** = $p<0.01$, *** = $p<0.001$.

# 3. Chapter 3

# The Type II secretion system and its secreted substrates are necessary for *Xylella fastidiosa* pathogenicity and survival in grapevine

# Abstract

*Xylella fastidiosa* is a xylem-limited bacterial pathogen that causes Pierce's Disease (PD) in grapevine. The severity and progression of PD is significantly influenced by known virulence factors that *X. fastidiosa* produces. Many of these virulence factors are hydrolytic enzymes including as glycosyl hydrolases, which dismantle pit membranes between xylem vessels, proteases, and lipases, and are predicted to be secreted via the Type II secretion system (T2SS). The T2SS is the main terminal branch of the Sec-dependent general secretory pathway, and one of only three secretion systems maintained by *X. fastidiosa*. In this study, we demonstrate that *X. fastidiosa* T2SS-deficient mutants are non-pathogenic and unable to survive *in planta*, indicating that the proteins secreted via this pathway are involved in both virulence and survival. To discern which proteins might be Type II secreted, mass spectrometry was used to identify potential Type II secretion candidates and provide direction for future characterization via biochemical and molecular assays. We compared the extracellular proteomic profiles of wild type, the T2SS-deficient mutants, and the respective complements across three trials. Six proteins including three lipases, a β-1,4-cellobiohydrolase, a protease, and a hypothetical protein, had a consistently lower number of matched peptides in T2SS mutant profiles than in wild type profiles, and at least one complement strain conferred either partial or full complementation for each protein. Furthermore, a differential gene expression analysis determined that the differences seen in the proteomic profiles are not the result of significantly different gene expression.

# Introduction

*Xylella fastidiosa* (*X. fastidiosa*) is a gram-negative bacterium that exclusively colonizes the xylem of a wide range of hosts either as endophyte or as a pathogen (Hopkins 1989). In North America, *X. fastidiosa* is the causal agent of Pierce's Disease (PD) in grapevine, inducing symptoms such as leaf scorching leaf drop and matchstick petioles, fruit shriveling, incomplete lignification of vascular tissue (green islands), and eventually vine death (Davis et al. 1978, Goheen and Hopkins 1988; Purcell 1986; Stevenson et al. 2005; Varela, 1996). *X. fastidiosa* is also the causal agent of notable diseases on other continents such as citrus variegated chlorosis and coffee leaf scorch in South America, and Olive Quick Decline syndrome in Europe (Chang et al. 1993; Li et al. 2001, Saponari et al. 2013). In grapevine, the xylem-limited nature of *X. fastidiosa* implies that it must successfully survive in an environment where nutrients are diverse, but transient (Andersen and Brodbeck, 1989). Therefore, *X. fastidiosa* must be able to move freely within the xylem to take advantage of as many nutrient sources as possible. However, xylem vessels are connected by bordered pits that contain pit membranes, which are primary cell wall structures comprised of cellulose, hemicellulose, and pectin (Brett and Waldron 1996, Dickison 2007). These pit membranes are porous and allow water and small solutes to move freely between vessels, but serve as a barrier to air embolisms and pathogens (Stevenson et al. 2004, Tyree and Zimmerman 2002). Indeed, pit membranes in grapevines, for which the average pore diameter is 5-20 nm, adequately prevent the passive movement of *X. fastidiosa* from one vessel to the next, given that the average size of *X. fastidiosa* is 250-500 nm wide by 1000-4000 nm long (Buchanan et al.

2000, Choat et al. 2004, Mollenhauer and Hopkins 1974). Nevertheless, *X. fastidiosa* is able to circumvent these barriers by utilizing several cell wall-degrading enzymes (CWDEs), which have been implicated as virulence factors, to hydrolyze the carbohydrates within pit membranes and simultaneously facilitate both access to adjacent vessels and nutrient acquisition (Ingel et al. 2019, Perez-Donoso et al. 2010, Roper et al. 2007). *X. fastidiosa* also maintains genes for several potentially secreted proteases and lipases that could be involved in nutrient acquisition (Simpson et al. 2000, Van Sluys et al. 2003). Pit membranes contain an abundance of proteins that could serve as a nitrogen source in an environment where nitrogen is the scarcest resource (Fisher 2000, Schenk et al. 2018). Furthermore, pit membranes and the xylem vessel lumen are replete with lipids, and likely serve as a major carbon source alongside the carbohydrates from pit membranes (Schenk et al. 2018). Many of these proteases and lipases still have unclear functions, though some have been documented as important virulence factors (Gouran et al. 2016, Nascimento et al. 2016).

The importance of these CWDEs, proteases, and lipases as virulence factors highlights the importance of understanding their secretion mechanisms. Unlike many other phytopathogenic bacteria with a significant xylem-dwelling phase, *X. fastidiosa* does not have a Type III secretion system to deliver virulence factors directly into host cells, and instead only maintains operons for three secretion systems: Type I, Type II, and Type V (Simpson et al. 2000, Van Sluys et al. 2003). Some *X. fastidiosa* proteases have already been implicated as Type V autotransporters, but the secretion mechanisms for the CWDEs and other proteases and lipases remains unclear (Chen et al. 2008). Several other

gram-negative phytopathogenic bacteria also secrete these types of enzymes, and they do so via the Type II secretion system (T2SS). *Erwinia carotovora*, *Erwinia chrysanthemi*, and *Ralstonia solancearum* utilize the T2SS to secrete CWDEs such as β-1,4-endoglucanases and polygalacturonases (Chapon et al. 2001, Kang et al. 1994, Palomäki et al. 2002). *Xanthomonas campestris* and *Xanthomonas oryzae*, both closely-related to *X. fastidiosa*, utilize the T2SS to secrete β-1,4-endoglucanases, proteases, xylanases, lipases, and cellobiohydrolases (Jha et al. 2007, Rajeshwari et al. 2005, Ray et al. 2000, Solé et al. 2015, Sun et al. 2005). Given the homology of these proteins with those from *X. fastidiosa*, it stands to reason that *X. fastidiosa* could also secrete its CWDEs, proteases, and lipases via the T2SS.

The T2SS serves as the main terminal branch of the General secretory pathway (Gsp) that relies on the Sec-dependent pathway to translocate target substrates across the inner membrane and into the periplasm (Pugsley 1993a). It is comprised of 12-15 proteins depending on species, but the 12 core components (GspCDEFGHIJKLMO) are required for full function (Cianciotto 2005). These 12 core components are used to construct four subassemblies: the outer membrane complex, the inner membrane platform, the secretion ATPase, and the pseudopilus (Korotkov et al. 2012). The outer membrane complex consists of multiple copies of GspD, which forms a channel in the outer membrane, often referred to as the secretin (Nouwen et al. 2000, Korotkov et al. 2009). In some species, GspD must interact with GspS (referred to as the pilotin) for insertion into the outer membrane, while GspS is not required in other species (Hu et al. 1995, Nouwen et al. 1999). The inner membrane platform is formed by GspC, F, L, and

M, while the secretion ATPase is formed by a GspE hexamer (Patrick et al. 2011, Possot et al. 2000, Py et al. 2001). The pseudopilus is primarily comprised of the major pseudopilin protein (GspG), while the tip of the pseudopilus consists of a trimer of the minor pseudopilin proteins GspI, J, and K (Korotkov et al. 2008, Sauvonnet et al. 2000). The minor pseudopilin protein GspH likely acts as an adapter between GspG and the pseudopilus tip (Yanez et al. 2008).

GspE associates with the cytoplasmic side of the inner membrane and interacts with the inner membrane platform via the transmembrane proteins GspL and GspF (Py et al. 2001, Sandkvist et al. 1995). GspL forms a complex with GspM, GspF, and GspC, the latter of which extends into the periplasm and binds to GspD in the outer membrane complex (Korotkov et al. 2006, Possot et al. 2000, Py et al. 2001). Some species utilize an additional protein (GspN) in conjunction with GspC to link the inner membrane platform and the outer membrane complex, while others use GspN instead of GspC (Lee et al. 2000, Possot et al. 2000). Prior to pilus formation, GspG, H, I, J, and K are translocated to the periplasm via the Sec-dependent pathway and inserted into the inner membrane (Francetic et al. 2007). Release of GspH, I, J, and K from the inner membrane by the prepilin peptidase GspO allows for the formation of tip of the pseudopilus (GspIJK trimer) and subsequent GspH recruitment at the inner membrane platform, which initiates pseudopilus formation after a T2SS substrate protein has been loaded (Cisneros et al. 2012, Nunn and Lory 1993). GspO-mediated release of GspG from the inner membrane and ATP hydrolysis via GspE drive the GspL-mediated incorporation of multiple GspG copies beneath the tip, thereby extending the pseudopilus through the outer membrane

complex channel and expelling the loaded protein into the extracellular matrix (Gray et al. 2011, Pugsley 1993b).

*X. fastidiosa* maintains both the Sec-dependent pathway and a fully functional T2SS comprised of 12 proteins, and uses the *Xanthomonas* designation (Xps) instead of Gsp (Simpson et al. 2000, Van Sluys et al. 2003). The genes for 11 of these proteins (*xps*EFGHIJKLMND) are part of an operon (PD0732-PD0742), while *xps*O (PD1922) exists outside the operon, likely due to its shared role with the Type IV pilus, which has significant structural and functional homology with the T2SS (Peabody et al. 2003). Therefore, we hypothesized that *X. fastidiosa* uses the T2SS to secrete several known virulence factors, including CWDEs, proteases, and lipases. To test this hypothesis, we constructed two T2SS-deficient *X. fastidiosa* mutants: an energy utilization mutant (Δ*xpsE*), which is missing the ATPase that drives pseudopilus formation, and a structural mutant (Δ*xpsG*), which is missing the major pseudopilin protein necessary for pseudopilus extension. In this study, we demonstrate that the T2SS is necessary for *X. fastidiosa* pathogenicity and survivability in grapevine. Furthermore, we identify six possible Type II-secreted proteins including three lipases, a protease, a cellobiohydrolase, and a hypothetical protein.

## Materials and Methods

**Bacterial strains.** All bacterial strains, plasmids and primers for this study are listed in Table 3.1.

**Media and bacterial growth conditions.** For *X. fastidiosa* mutant construction, *in planta* assays and *in vitro* assays, *X. fastidiosa* strains were propagated on PD3 solid medium at 28℃ (Davis et al. 1981). Selection of *X. fastidiosa* mutant transformants was performed on PD3 with 5 μg/ml of gentamicin, kanamycin, or chloramphenicol. Sub-culturing of mutant transformants was performed on PD3 with 10 μg/ml of gentamicin, 30 μg/ml of kanamycin, or 25 μg/ml of chloramphenicol. *E. coli* strains were grown in Luria-Bertani medium at 37℃, and selection of *E. coli* transformants was performed in the presence of 10 μg/ml gentamicin, 30 μg/ml kanamycin, or 25 μg/ml of chloramphenicol, where applicable.

A modified XFM minimal medium was used for *in vitro* assays and was adapted from Almeida et al. (2004). The medium was comprised of final concentrations of Potassium phosphate dibasic (8.6 mM, Fisher Scientific), Potassium phosphate monobasic (7.4 mM, Fisher Scientific), Magnesium sulfate heptahydrate (4.1 mM, Sigma Aldrich), Sodium succinate hexahydrate (5.6 mM, Fisher Scientific), Trisodium citrate dihydrate (5.1 mM, Calbiochem), polygalacturonic acid (0.02% [w/v], Megazyme), xyloglucan (0.02% [w/v], Megazyme), and carboxymethylcellulose (0.02% [w/v], Sigma Aldrich). For the RNAseq assay, final concentrations of Bovine Serum Albumin (0.003% [w/v], Sigma Aldrich) and Hemin chloride (0.0005% [w/v], Millipore) were added. For the Mass Spectrometry assay, a final concentration of Casamino acids (0.003% [w/v], Acros Organics) was used as a substitute for the Bovine Serum Albumin, and the final concentration of Hemin chloride was reduced to $5\times10^{-6}$% [w/v].

**Construction of mutant and complementation strains.** The Δ*xpsE* mutant strain was constructed by Wang (2014). Briefly, the Δ*xpsE* deletion construct was created by combining the adjacent 5' and 3' gene flanking regions with a gentamicin resistance gene via overlap extension polymerase chain reaction. The flanking regions in the deletion construct undergo homologous recombination with the same regions on the *X. fastidiosa* chromosome and facilitate the removal of the *xpsE* gene while simultaneously inserting the gentamicin resistance gene. Polymerase chain reaction (PCR) was used to amplify the 5' and 3' flanking regions adjacent to *xpsE* from the *X. fastidiosa* chromosome using the primer pairs XpsE LF fwd EcoRI and XpsE LF rev Gm, and XpsE RF fwd Gm and XpsE RF rev HindIII, respectively. The gentamicin resistance gene was amplified from the pBBR1-MCS5 plasmid (Kovach et al. 1995) using primers XpsE Gm fwd and XpsE Gm rev. The individual fragments were each amplified using PCR, and the three fragments were assembled by overlap extension PCR to create the Δ*xpsE* deletion construct, which was cloned into pUC19 to create the pPW04 plasmid and verified by sequencing. To create the *xpsE*+/- complementation construct, the *xpsE* gene, native promoter, and terminator sequence were amplified via PCR from *X. fastidiosa* genomic DNA using primers XpsE_pXf20pemIK-GW_F and XpsE_pXf20pemIK-GW_R. The amplified fragment was cloned into pCR8/GW/TOPO (Invitrogen) to create the pCC1 plasmid, and the fragment was sub-cloned into the pXf20pemIK-GW plasmid (Burbank and Stenger 2016) to create pCC2 using Gateway LR Clonase II Enzyme Mix (Invitrogen).

The *ΔxpsG* deletion construct and the *xpsG*+/- complementation construct were created by the Gene Synthesis service provided by Genscript USA Inc. The *ΔxpsG*

construct consisted of the 5' and 3' *xpsG* flanking regions from the *X. fastidiosa* chromosome and the kanamycin resistance gene from the pCR2.1 TOPO vector (Invitrogen), and was inserted into the pUC19 vector to create the pBI4 plasmid. The *xpsG*+/- complementation construct consisted of the pAX1cm cassette (Matsumoto et al. 2009), the *xpsG* gene, and 200 bp upstream of the *xps* operon to include the operon promoter. The complementation construct was inserted into the pUC19 vector to create the pBI5 plasmid. Both constructs were verified by Genscript USA Inc.

The pPW04 and pBI4 plasmids were transformed into electrocompetent wild type *X. fastidiosa* cells, the pBI5 plasmid was transformed into electrocompetent *ΔxpsG X. fastidiosa* cells, and the pCC2 plasmid was transformed into electrocompetent Δ*xpsE X. fastidiosa* cells, according to the methods presented by Matsumoto et al. (2009). Briefly, 200 ng of pPW04, pBI4, pBI5, or pCC2 and 1 µl of the TypeOne Restriction Inhibitor (Epicentre) were electroporated (3.0 kV, 300 Ω, 25 µF) into *X. fastidiosa* cells using a 0.2 cm cuvette (Bio-Rad) and the GenePulser X-cell (Bio-Rad). Validation of positive transformants was performed by sub-culturing onto PD3 agar containing the appropriate antibiotics. Genomic DNA from *X. fastidiosa* Δ*xpsE*, Δ*xpsG*, and *xpsG*+/- positive transformants was extracted using the DNeasy Blood and Tissue Kit (Qiagen). Δ*xpsE*, Δ*xpsG*, and *xpsG*+/- constructs were amplified via PCR using the respective primer sets XpsEoutfwd and XpsEoutrev, xpsG_LF_fwd and xpsG_RF_rev, and Xf-pAXinsert_seq_fwd and Xf-pAXinsert_seq_rev, and were verified by the size of each amplified PCR fragment, and by sequencing. The pCC2 plasmid was extracted from

*xpsE*+/- positive transformants using the DNeasy Blood and Tissue Kit (Qiagen), and the *xpsE*+/- construct was verified by sequencing.

***In planta* virulence assays.** *Vitis vinifera* cv. Cabernet sauvignon, kindly provided by Foundation Plant Services (UC Davis), were propagated from cuttings. Grapevines were mechanically inoculated according to Purcell and Saunders (1999), where a 20 µl drop of *X. fastidiosa* inoculum ($10^8$ colony forming units (CFU/ml)) was placed on the stem between the third and fourth node, and the stem was pierced through the drop using a 20-gauge needle. The drop was drawn into the xylem, and the inoculation site was covered with parafilm. Grapevines were inoculated with wild type, Δ*xpsE*, or Δ*xpsG X. fastidiosa* strains and grapevines inoculated with 1× PBS served as negative controls. Each strain (or 1× PBS) was inoculated into ten vines and the experiment was repeated three times for a total of thirty replicates. Trials were performed under greenhouse conditions and all grapevines were randomized. PD symptom development was assessed weekly over a 20-week period using a rating scale from 0 – 5 where 0= a healthy vine, 1= one or two leaves with scorching at the margins, 2= two or three leaves with more developed scorching, 3= all leaves with some scorching and a few matchstick petioles, 4= all leaves with heavy scorching and many matchstick petioles, and 5= a dead or dying vine (Guilhabert and Kirkpatrick 2005).

**Local and distal xylem colonization assays.** Petioles at the point of inoculation (POI) and at the $20^{th}$ node distal to the POI were collected from five randomly-chosen vines of

each biological replicate for each inoculated strain, and from all ten negative control vines, at 13 weeks post-inoculation when the average disease rating for wild type-inoculated vines was between 3 and 4. The petioles were surface sterilized (30 seconds in 70% ethanol, 30 seconds in 10% bleach and twice for 1 min in sterile deionized water) and ground in 2 ml of sterile 1× PBS. A dilution series of each petiole suspension was plated on solid PD3 medium and incubated at 28°C for 7 – 14 days per standard methods (Roper et al. 2007). *X. fastidiosa* colonies were counted (CFU), and titers were normalized per gram of petiole tissue (CFU/g tissue).

**Protein precipitation from XFM media.** 60 ml of XFM minimal media (described above) was inoculated with three independent replicates of either wild type, Δ*xpsE*, *xpsE*+/-, Δ*xpsG*, or *xpsG*+/- *X. fastidiosa* strains (final $OD_{600}$ = 0.05), and incubated at 28°C and 180 rpm for five days. Cultures were vortexed briefly and then centrifuged at 7,000 rpm for 20 minutes at 4°C to separate the *X. fastidiosa* cells from the culture media. The supernatants were carefully collected and centrifuged again using the same conditions to ensure all *X. fastidiosa* cells were removed. The supernatants from the second centrifugation were carefully collected for protein precipitation using the pyrogallol red-molybdate-methanol (PRMM) method as described by Caldwell and Lattemann (2004). Briefly, pryogallol red (0.05 mM; Sigma Aldrich), sodium molybdate (0.16 mM; Sigma Aldrich), sodium oxalate (1.0 mM; Sigma Aldrich), succinic acid (50 mM; Sigma Aldrich), and methanol (20% [v/v]; Fisher Scientific) were mixed to create the PRMM solution and the pH was adjusted to 2.0. The supernatants from the second

centrifugation were mixed 1:1 with the PRMM solution and the pH was immediately adjusted to 2.8. The precipitation mixtures were gently mixed via stirring for two hours at room temperature and then overnight at 4℃. The precipitation mixtures were then centrifuged at 10,000 x g for one hour at 4℃ and the supernatants were discarded. The pellets were rinsed twice with cold acetone, resuspended in a 1:1 mixture of saturated Tris (pH 8.0) and 2X Laemmli buffer (Bio Rad), and then incubated at 95°C for 15 minutes. The absorbance at 600 nm was measured for each sample to determine protein concentration via the amount of protein-bound pyrogallol red (Fujita et al. 1983), and the samples were normalized to the lowest concentration.

**Preparation of samples for Mass Spectrometry.** SDS polyacrylamide gel electrophoresis was performed using the Mini-PROTEAN Electrophoresis system (Bio Rad). SDS-polyacrylamide gels (5% stacking gel; 12% resolving gel) were immersed in Tris-glycine running buffer (25 mM Tris, 192 mM glycine, 0.1% [w/v] SDS; pH8.3) according to the manufacturer's instructions, and 100 ul of each normalized samples was loaded onto the gel. The electrophoresis system was run at 60V until the samples entered the resolving gel, and then the voltage was increased to 120V until the samples reached the end of the resolving gel. Gels were stained with Coomassie Blue R250 (Fisher Scientific) in 45% [v/v] methanol and 10% [v/v] glacial acetic acid overnight, and then de-stained with 45% [v/v] methanol and 10% [v/v] glacial acetic acid.

Each gel lane was cut out with a sterile razor, and the protein bands were excised and cut into small pieces. The gel pieces were washed with 50 mM ammonium

bicarbonate and incubated with acetonitrile. Disulfide bonds were reduced by incubating the gel pieces with 10 mM dithiothreitol (DTT) in 50 mM ammonium bicarbonate for 30 minutes at 56℃. The gel pieces were incubated again with acetonitrile and then with 55 mM iodoacetamide in 50 mM ammonium bicarbonate for 20 minutes at room temperature in the dark. The iodoacetamide was discarded and the gel pieces were washed with 50 mM ammonium bicarbonate, followed by incubation in acetonitrile. The gel pieces were then dried using a speed vac. A mixture of trypsin (Promega) and ProteaseMAX solution (Promega) was added to the dried gel following the manufacturer's instructions and incubated at 50°C for four hours. After incubation, formic acid was added to each trypsinized sample followed by centrifugation and collection of the supernatant.

**Mass spectrometry.** The mass spectrometry instrument used to analyze the samples was a Xevo G2 QTof coupled to a nanoAcquity UPLC system (Waters, Milford, MA). Samples were loaded onto a C18 Waters Trizaic nanotile of 85 um × 100 mm; 1.7 µm (Waters, Milford, MA). The column temperature was set to 45℃ with a flow rate of 0.45 mL/min. The mobile phase consisted of A (water containing 0.1% formic acid) and B (acetonitrile containing 0.1% formic acid). A linear gradient elution program was used: 0–40 min, 3–40 % (B); 40-42 min, 40–85 % (B); 42-46 min, 85 % (B); 46-48 min, 85-3 % (B); 48-60 min, 3% (B).

Mass spectrometry data were recorded for 60 minutes for each run and controlled by MassLynx 4.1 (Waters, Milford, MA). Acquisition mode was set to positive polarity

under resolution mode. Mass range was set form 50 – 2000 Da. Capillary voltage was 3.5 kV, sampling cone at 25 V, and extraction cone at 2.5 V. Source temperature was held at 110C. Cone gas was set to 25 L/h, nano flow gas at 0.10 Bar, and desolvation gas at 1200 L/h. Leucine–enkephalin at 720 pmol/ul (Waters, Milford, MA) was used as the lock mass ion at m/z 556.2771 and introduced at 1 uL/min at 45 second intervals with a 3 scan average and mass window of +/- 0.5 Da. The MSe data were acquired using two scan functions corresponding to low energy for function 1 and high energy for function 2. Function 1 had collision energy at 6 V and function 2 had a collision energy ramp of 18 − 42 V.

**Mass spectrometry data analysis.** RAW MSe files were processed using Protein Lynx Global Server (PLGS) version 2.5.3 (Waters, Milford, MA). Processing parameters consisted of a low energy threshold set at 200.0 counts, an elevated energy threshold set at 25.0 counts, and an intensity threshold set at 1500 counts. The databank used was constructed from the NCBI *X. fastidiosa* Temecula 1 protein reference sequence (NC_004556.1) plus other random proteins as well as common contaminants including human keratins, porcine trypsin, bovine serum albumin, bovine beta-casein, as well as their randomized sequences. Searches were performed with trypsin specificity and allowed for three missed cleavages. Possible structure modifications included for consideration were methionine oxidation and carbamidomethylation of cysteine.

PLGS search results were exported to Scaffold v4.9.0 (Proteome Software Inc., Portland, OR) for data analysis. Within Scaffold, the threshold for the calculated

probability of correct protein identification was set to 50%, the threshold for the certainty of peptide identification was set to 20% and the minimum number of matched peptides required for positive protein identification was set to 2. The total number of matched peptides for each protein within a gel lane was calculated by adding the matched peptides from all of the gel slices related to that gel lane. The overall percent coverage and Scaffold Probability score for each protein within a gel lane was determined by calculating the respective averages weighted by the number of matched peptides from each individual gel slice related to that gel lane. For all samples across all trials, proteins that did not obtain a Scaffold Probability weighted average score of $\geq 90\%$ were discarded. Proteins that remained were screened *in silico* for predicted signal sequences (SignalP 5.0; SecretomeP 2.0) and predicted subcellular localization (pSORTb 3.02), and proteins without predicted signal sequences were discarded. Of the remaining proteins, any that had < 20 matched peptides in the wild type samples from any of the three trials were also discarded. When making comparisons between wild type, the T2SS-deficient mutants, and the respective complement strains, this list was further filtered to omit proteins with known secretion mechanisms, and proteins known to be imbedded in the outer membrane, such as receptors, channel proteins, or porins, to help focus on potential type II-secreted proteins.

For each protein on the filtered list, the number of matched peptides found in each mutant sample was compared to the number of matched peptides found in the wild type sample within trial by calculating the fold-change to determine possible T2SS candidates. Proteins were considered possible T2SS candidates if the number of matched peptides for

a protein in the wild type samples had a fold-change of ≥ 2 when compared to the number of matched peptides for that protein in both mutant samples across all three trials. Proteins where the fold-change in the number of matched peptides between wild type and one mutant was ≥ 2 across all three trials, but ≥ 1.5 between wild type and the second mutant across all three trials were also considered.

Complementation of these possible T2SS candidates was determined by two criteria: 1) a matched peptide fold-change of ≥ 2 when comparing the complement strain to the respective mutant strain within a trial, and 2) a matched peptide fold-change of < 1.5 when comparing the wild type strain to the complement strains within a trial. Full complementation of a mutant was considered with these criteria were met across all three trials. Partial complementation was considered if: 1) a complement strain had a matched peptide fold-change of ≥ 2 compared to its respective mutant strain across all three trials, but did not have a matched peptide fold-change of < 1.5 when compared to the wild type strain, or 2) a complement strain had a matched peptide fold-change of ≥ 2 compared to its respective mutant strain in two of the three trials, and had a matched peptide fold-change of < 1.5 when compared to the wild type strain in those two trials.

**RNA extraction and library preparation.** 60 ml of modified XFM minimal medium was inoculated with three independent replicates of either wild type or Δ*xpsE X. fastidiosa* strains (final $OD_{600}$ = 0.05), and incubated at 28°C and 180 rpm for five days. RNA was extracted from both strains following the hot SDS/hot phenol methodology outlined in Jahn et al. (2008). RNAseq libraries were constructed using the Truseq stranded mRNA kit HT (Illumina Inc.) following the manufacturer's instructions, and the

quality and fragment size of each sample in the library was assessed using the 2100 Bioanalyzer (Agilent Technologies Inc.).

**RNA sequencing and analysis.** The libraries were multiplexed, and RNA 1 x 75 single-end sequencing was performed using the NextSeq500 DNA Sequencer (Illumina Inc.). The resulting reads were de-multiplexed and the barcodes were trimmed. Within the Pathosystems Resource Integration Center (PATRIC), Rockhopper (version 3.5.26) was used to align the reads to the *X. fastidiosa* genome, assemble the transcripts, and quantify transcript abundance (McClure et al. 2013, Tjaden, B 2015, Wattam et al. 2016). Differential expression testing was performed using limma-voom (version 3.38.3) within Galaxy (version 19.01) (Law et al. 2014, Liu et al. 2015, Afgan et al. 2018).

## Results

**T2SS-deficient mutants lose pathogenicity *in planta*.** PD symptoms were rated over a period of 20 weeks using the 0 – 5 rating scale outlined in the methods. Over that period, the average PD symptom score for wild type-inoculated vines progressed from zero to 4.6, while the average PD symptom scores both Δ*xpsE*- and Δ*xpsG*-inoculated vines remained between 0.2 and 0.3 (Fig. 3.1). Negative control vines did not display any PD symptoms and over the same 20-week period. Furthermore, 29 of the 30 wild type-inoculated vines were rating a 4 or higher at 20 weeks post inoculation, while 29 of the 30 vines inoculated with either mutant, respectively, were rating 0 or 1.

**T2SS-deficient mutants fail to colonize the grapevine xylem.** Isolation of *X. fastidiosa* from petioles at the POI and at the 20$^{th}$ node distal to the POI was performed at 13 weeks post-inoculation when the average PD symptom score for wild type-inoculated vines was between 3 and 4. At the POI, *X. fastidiosa* was isolated from 5 of the 15 wild type-inoculated vines, and the average titer was 7.6 (±4.4) × $10^6$ CFU/g tissue. At the 20$^{th}$ node distal to the POI, *X. fastidiosa* was isolated from 9 of the 15 wild type-inoculated vines, and the average titer was 1.3 (±0.7) × $10^7$ CFU/g tissue. *X. fastidiosa* was not isolated from any of the Δ*xpsE*- or Δ*xpsG*- inoculated vines at either the POI or at the 20$^{th}$ node distal to the POI. *X. fastidiosa* was not isolated from any of the negative control vines.

**Lipases, proteases, and a glycosyl hydrolase are among the most abundant *X. fastidiosa* proteins.** Across all three trials, 47 proteins with predicted secretion signals and ≥ 20 matched peptides were found in the extracellular fraction of wild type cultures (Table 3.2). Of these proteins, 13 are related to the outer membrane, including six TonB receptors, five porins, and two surface assembly factors. Another 13 proteins identified have hydrolytic functions including nine proteases, three lipases, and one β-1,4-cellobiohydrolase. Other proteins identified included four adhesins, three hemolysins, two chaperones, two oxidoreductases, and singular proteins related to Type IV pili, DNA uptake, isoprenoid metabolism, an aconitase, a polysaccharide deacetylase, a histidine kinase, and an RNase. Three of the identified proteins are uncharacterized and considered hypothetical, though one has been listed as a putative autotransporter.

12 proteins listed are known to be embedded in the outer membrane and are not secreted extracellularly. Six proteins listed are known to be Type V autotransporters, while three others are known to be Type I-secreted. Furthermore, two proteins listed are known to be associated with Type IV and Type I pili (PD0023 and PD0058, respectively) and are not secreted via the general pathways. The remaining 24 proteins listed have unknown secretion mechanisms.

**Seven proteins have consistently fewer matched peptides in mutant extracellular fractions.** From the list of most abundant wild type proteins in the extracellular fraction, the 24 proteins with unknown secretion mechanisms were selected for comparison between wild type and the T2SS-deficient mutants to determine if any might be Type II-secreted. Comparisons were made by calculating the fold-change in the number of matched peptides between wild type and each mutant over three trials. A protein was considered a possible candidate for Type II secretion if the number of matched peptides was at least 2-fold less for both mutants across all three trials. Three of the 24 proteins compared met this criteria, including the β-1,4-cellobiohydrolase (PD0529), a lipase (PD1211), and a hypothetical protein (PD1299), while four other proteins were close to meeting the criteria in that there was a fold-change of greater than 2 between wild type and one mutant across all three trials, but greater than 1.5 between wild type and the second mutant across all three trials. These proteins included two lipases (PD1702 and PD1703), a protease (PD1934), and a DNA uptake protein (PD1558) (Fig. 3.2). The

number of matched peptides, percent sequence coverage, and Scaffold Probability scores for these proteins from Δ*xpsE* and Δ*xpsG* cultures are summarized in Tables 3.5 and 3.6.

**Complementation strains partially or fully restore peptide abundance for six of the Type II secretion candidates.** The seven proteins that were selected as possible Type II secretion candidates were further analyzed for complementation. Full complementation was based on two criteria: 1) the number of matched peptides for a protein was least two-fold higher for a complement strain relative to its respective mutant strain across all three trials (Fig. 3.3A), and 2) the number of matched peptides for that same protein had a fold-change of less than 1.5 between the complement strain and the wild type across all three trials (Fig. 3.3B). Partial complementation was considered if: 1) a complement strain had a two-fold greater number of matched peptides relative to its respective mutant strain across all three trials, but did not have a fold-change of less than 1.5 when compared to wild type, or 2) a complement strain had a two-fold greater number of matched peptides relative to its respective mutant strain in two of the three trials and had a fold change of less than 1.5 when compared to wild type for those two trials.

Based on these criteria, partial complementation of Δ*xpsE* was seen for PD0529, where the number of matched peptides for Δ*xpsE* was at least 2-fold lower than *xpsE*+/- in all three trials, but the number of matched peptides for *xpsE*+/- only resembled that of wild type in two of those trials. Partial complementation of Δ*xpsG* was seen for PD1299, PD1702, and PD1934. For PD1299, the number of matched peptides for Δ*xpsG* was at least 2-fold lower than *xpsG*+/- in all three trials, but the number of matched peptides for

*xpsG*+/- only resembled that of wild type in two of those trials. For PD1702 and PD1934, the number of matched peptides for Δ*xpsG* was at least 2-fold lower than *xpsG*+/- in only two trials, but the number of matched peptides for *xpsG*+/- resembled that of wild type in both of those trials. Full complementation of Δ*xpsG* was seen for PD1211 and PD1703, while no complementation was seen for PD1558 (Fig. 3.3). The number of matched peptides, percent sequence coverage, and Scaffold Probability scores for these proteins from *xpsE*+/- and *xpsG*+/- cultures are summarized in Tables 3.7 and 3.8.

**Wild type and Δ*xpsE* maintain similar transcript levels for all of the Type II secretion candidates.** RNAseq was performed to determine if the differences seen in these seven potential Type II secretion candidates were the result of differential gene expression. As these seven candidates displayed a marked reduction in the number of matched peptides in both mutants relative to wild type, Δ*xpsE* was chosen for RNAseq analysis as the differences in matched peptide number between Δ*xpsE* and wild type were more severe. For all seven candidates, the differential gene expression analysis between Δ*xpsE* and wild type indicated that there were no significant differences in transcript abundance (Table 3.3).

**Other predicted Type II secretion proteins not present despite abundant transcript levels.** Several other proteins predicted to be Type II secreted did not appear in the extracellular fraction of wild type cultures, or appeared transiently, and could not be analyzed for potential secretion. These proteins all have predicted signal peptides and are

predicted to be extracellular, including a polygalacturonase (PglA, PD1485), a β-1,4-endoglucanase (EngXCA2, PD1851), a β-1,4-endoglucanase-expansin (EngXCA1, PD1856), and a cellulase (Egl, PD2061). EngXCA1 and Egl appeared transiently, having fewer than 10 matched peptides with a Scaffold Probability score greater than 90% in only one trial, while matched peptides for PglA and EngXCA2 were not present in any trial. However, the RNAseq analysis indicated that the mRNA transcripts for these proteins are abundant, especially for PglA and EngXCA1 (Table 3.4).

## Discussion

The T2SS is considered the main branch of the general secretory pathway and has been shown in several bacterial pathosystems to secrete a diversity of virulence factors (Pugsley 1993a, Cianciotto 2005). These virulence factors include CWDEs, which are important for *X. fastidiosa* virulence in grapevines. Thus, analysis of the T2SS in *X. fastidiosa* could provide further insight into how these virulence factors are able to move into the xylem and interface with the grapevine host. In studying the *X. fastidiosa* T2SS, it was desirable to make a mutation that fully disabled the secretion system while minimizing adverse secondary effects. Removal of The ATPase gene (*xpsE*) had the benefit of completely disabling the T2SS, but also had the potential of causing adverse secondary effects as this ATPase has been known function with the Type IV pilus. Removal of the major pseudopilin gene (*xpsG*) had the benefit of minimal adverse secondary effects, but also had the potential of not completely disabling the T2SS. Thus,

we opted to create both mutants and use both in determining the importance of the T2SS in *X. fastidiosa*, and which proteins might be Type II secreted.

In contrast to wild type-inoculated grapevines, both Δ*xpsE*- and Δ*xpsG*-inoculated grapevines did not show PD symptoms over a period of 20 weeks. Furthermore, *X. fastidiosa* could not be isolated from Δ*xpsE*- or Δ*xpsG*-inoculated vines. The *in planta* phenotypes for both mutants are the same and provides a good indication that the T2SS in both strains was successfully disrupted. More importantly, these results indicate that the T2SS is necessary for *X. fastidiosa* pathogenicity and survivability *in planta*.

Because the T2SS is a mechanism for moving certain proteins into the extracellular environment, it could be inferred that these proteins are actually the necessary factors for pathogenicity and survivability, and the inability to secrete them is facilitating the *in planta* phenotype of Δ*xpsE* and Δ*xpsG*. Therefore, we sought to identify these proteins to provide directions for further study. Cultures were grown in modified XFM minimal media instead of PD3 in an attempt to provide *X. fastidiosa* with a closer approximation of its native environment and the extracellular fractions were analyzed by mass spectrometry. This was a label-free experiment and direct comparisons between strains could not be made due to high variability in the digestion, extraction, and physical data collection processes. Instead, we sought to identify consistent trends that could elucidate possible Type II secretion candidates for further study. Of the 47 most abundant proteins consistently found in wild type extracellular fractions across all three trials, 24 of these proteins did not have known secretion mechanisms. Seven of those proteins were found

to be of consistently lower abundance in both T2SS-deficient mutants and were considered as possible Type II secretion candidates.

Three of these proteins are predicted to be lipases, of which only PD1703 has been characterized as such and has been shown to be an important virulence factor. Of these lipases, only PD1211 abundance shows a consistently marked reduction in both T2SS-deficient mutants and *xpsG*+/- displayed full complementation, indicating that it is a probable Type II secretion candidate for further analysis. Both PD1702 and PD1703 were still found with some abundance in the extracellular fractions of the Δ*xpsG* mutant cultures, albeit between 1.5 and 2–fold lower than their respective abundances in wild type extracellular fractions, and only PD1703 displayed full complementation while PD1702 had partial complementation. Interestingly, Nascimento et al. (2016) found PD1703 both in outer membrane vesicles (OMVs) and on the surface of OMVs. Given the data acquired in this study, it is possible that some copies of PD1702 and PD1703 are secreted via the T2SS and anchored to the outer membrane surface while those remaining in the periplasm are secreted via OMVs. Taken together with the high abundance of these proteins and the importance of PD1703 as a virulence factor, further characterization of their secretion methods is warranted.

The abundance of peptides matching the sole β-1,4-cellobiohydrolase (PD0529) maintained by *X. fastidiosa* was markedly decreased consistently in both T2SS-deficient mutants. PD0529 has yet to be fully characterized, but its predicted extracellular localization and its function as a β-1,4-cellobiohydrolase suggests the possibility that it plays a role in nutrient acquisition by hydrolyzing the polysaccharide dimers created by

the EngXCA1- and EngXCA2-meditated dismantling of pit membranes. *xpsE*+/- provided partial complementation, restoring the abundance of PD0529-related peptides back to wild type levels in two of the three trials, thus indicating that this protein is a probable Type II secretion candidate that requires further characterization.

Interestingly, the abundance of peptides matching a relatively unknown protein (PD1299) was also markedly decreased consistently in both T2SS-deficient mutants. PD1299 is predicted to be a PQQ-like beta-propeller repeat protein, of which the most studied are polyvinylalcohol dehydrogenases, which function by employing the cofactor pyrroloquinoline quinone to oxidize polyvinyl alcohols. Very little information exists about these proteins with respect to gram-negative bacteria with the exception of the Pseudomonads where the genes *pvaA* and *pvaB* encode a polyvinylalcohol dehydrogenase and polyvinylalcohol hydrolase, respectively (Shimao et al. 2000). However, a protein BLAST search yielded no similarity of PD1299 with any Pseudomonad-related proteins, indicating that the function of PD1299 remains fully uncharacterized. *xpsG*+/- provided partial complementation, restoring the abundance of PD1299 back to wild type levels in two of the three trials, indicating the possibility that this protein is Type II secreted. This data, along with its predicted extracellular localization, warrants further examination of this unknown protein and its potential as a virulence factor.

Peptides matching PD1934 were not present in any of the Δ*xpsG* extracellular fractions. Similarly, two of the three Δ*xpsE* extracellular fractions were devoid of peptides matching PD1934, and the number of matching peptides in the third Δ*xpsE*

extracellular fraction was nearly two-fold lower than in the corresponding wild type extracellular fraction. PD1934 is predicted to be a serine protease of the S9 family, which is classified by the MEROPS database as a group consisting of oligopeptidases, dipeptidyl-peptidases, acylaminoacyl-peptidases, and glutamyl endopeptidases. However, its function and its subcellular localization remain uncharacterized in the *X. fastidiosa* pathosystem. *xpsG*+/- did provide partial complementation, restoring the abundance of PD1934 back to wild type levels in two of the three trials, indicating that this protein is potentially Type II secreted. The absence of any other information in addition to the data presented here indicates that it cannot be determined whether or not PD1934 is Type II secreted. However, Type II-secreted proteases have been documented in several other bacterial pathosystems, so further study and characterization of this protease is warranted.

Δ*xpsE* extracellular fractions were devoid of peptides matching PD1558, which is a predicted DNA uptake protein. However, peptides matching this protein were found in Δ*xpsG* extracellular fractions at 1.5 – 1.9 fold lower levels relative to wild type extracellular fractions in two of the three trials, and neither complement strain provided any complementation. DNA uptake proteins have not been characterized as Type II secreted proteins in any bacterial system, and are typically associated with a separate DNA uptake system (Dubnau 1999). Interestingly, DNA uptake systems in gram-negative bacteria are similar in structure to the T2SS (Hobbs and Mattick 1993). Given this similarity, it is possible that disruption of the T2SS inadvertently disrupted the *X. fastidiosa* DNA uptake system, and could account for the reduction in peptides matching this protein in the extracellular fractions of both mutants. However, this explanation is

speculative and any potential interconnections between these two systems would require further experimentation. Thus, the data presented here combined with the current and extensive knowledge of DNA uptake systems presented in the literature indicate that this protein is unlikely to be Type II secreted.

CWDEs have been identified as Type II-secreted for several other bacterial phytopathogens, and it is predicted that the CWDEs produced by *X. fastidiosa* are also Type II-secreted. However, two of these CWDEs, PglA and EngXCA2, were not present in any of the wild type extracellular fractions. Furthermore, EngXCA1 and Egl appeared in the wild type extracellular fraction of only one trial, with relatively few matching peptides. Thus, any determination of Type II secretion for these CWDEs could not be made in this study. Interestingly, there was an abundance of transcripts corresponding to these CWDEs, indicating that the genes encoding these CWDEs were expressed, but possibly being subjected to various regulatory mechanisms. Indeed, several of these types of CWDEs are known only to be activated by the presence of specific substrates, at specific population densities, or under specific environmental conditions, all of which could influence both transcription and translation of these genes (Allen et al. 1997, Linden and Shiang 1991, Hugouvieux-Cotte-Pattat et al. 2002). Given the data presented here, it is possible that some or all of these CWDEs could maintain a basal level of transcription, but have regulation at the transcriptional and secretory levels in a process similar to that in *Pectobacterium carotovorum* (formerly *Erwinia carotovorum*) (Chatterjee et al. 1995). As *X. fastidiosa* resides in an environment with transient nutrients, it could be speculated that maintaining a basal level of readily available CWDE

transcripts would be advantageous for quick activation of these enzymes when nutrients, such as the polysaccharides in pit membranes, are discovered. However, this line of reasoning requires further study.

From the data presented here, three proteins are considered likely candidates for Type II secretion: a β-1,4-cellobiohydrolase (PD0529), a lipase (PD1211), and a hypothetical protein (PD1299). Two additional lipases, PD1702 and PD1703, may also be Type II secreted in addition to secretion via OMVs. The sixth potential candidate is a family S9 protease (PD1934), though little is known about the extracellular nature of this family of proteases. An RNAseq differential expression analysis comparing transcript abundance in wild type and the Δ*xpsE* mutant strain did not reveal any significant differences, implying that the consistent decreases in matched peptides for these proteins in mutant extracellular fractions is likely due to secretion-related deficiencies. The possibility exists that several other *X. fastidiosa* proteins omitted in the strict filtering process could also be Type II secreted, and secretion-related analyses for predicted Type II secretion substrates not presented here should be considered.

The experiments presented in this study were designed to provide direction for further studies related to *X. fastidiosa* Type II-secreted virulence factors, and the data presented should be viewed solely in terms of probability. Therefore, further analysis of each of these candidates via molecular and biochemical experimentation are required.

## Literature Cited


Afgan E., Baker D., Batut B., van den Beek M., Bouvier D., Čech M., Chilton J., Clements D., Coraor N., Grüning B., Guerler A., Hillman-Jackson J., Jalili V., Rasche H., Soranzo N., Goecks J., Taylor J., Nekrutenko A., and Blankenberg D. 2018. The Galaxy platform for accessible, reproducible and collaborative biomedical analyses: 2018 update. Nucleic Acids Res. 46(1):537-544.

Allen, C., Gay, J. and Simon-Buela, L. 1997. A regulatory locus, *pehSR*, controls polygalacturonase production and other virulence functions in *Ralstonia solanacearum*. Mol Plant Microbe Interact. 10(9):1054-1064.

Andersen, P. C. and Brodbeck, B. V. 1989. Chemical composition of xylem exudate from bleeding spurs of *Vitis rotundifolia* Noble and *Vitis* hybrid Suwannee in relation to pruning date. American journal of enology and viticulture. 40(3):155-160.

Brett, C. T., and Waldron, K. W. 1996. Physiology and biochemistry of plant cell walls. Springer Science & Business Media, Heidelberg.

Buchanan, B. B., Gruissem, W., and Jones, R. L. 2000. The Cell Wall. Pages 52–100 in: Biochemistry and Molecular Biology of Plants, American Society of Plant Physiologists, Rockville, MD.

Burbank, L. P. and Stenger, D. C. 2016. Plasmid vectors for *Xylella fastidiosa* utilizing a toxin-antitoxin system for stability in the absence of antibiotic selection. Phytopathology. 106(8):928-936.

Caldwell, R. B. and Lattemann, C. T., 2004. Simple and reliable method to precipitate proteins from bacterial culture supernatant. Appl. Environ. Microbiol. 70(1):610-612.

Chang, C. J., Garnier, M., Zreik, L., Rossetti, V., and Bové, J. M. 1993. Culture and serological detection of the xylem-limited bacterium causing citrus variegated chlorosis and its identification as a strain of *Xylella fastidiosa*. Current Microbiology. 27:137-142.

Chapon, V., Czjzek, M., El Hassouni, M., Py, B., Juy, M. and Barras, F. 2001. Type II protein secretion in gram-negative pathogenic bacteria: the study of the

structure/secretion relationships of the cellulase Cel5 (formerly EGZ) from *Erwinia chrysanthemi*. Journal of molecular biology. 310(5):1055-1066.

Chatterjee, A., Cui, Y., Liu, Y., Dumenyo, C. K. and Chatterjee, A. K. 1995. Inactivation of *rsmA* leads to overproduction of extracellular pectinases, cellulases, and proteases in *Erwinia carotovora* subsp. *carotovora* in the absence of the starvation/cell density-sensing signal, N-(3-oxohexanoyl)-L-homoserine lactone. Appl. Environ. Microbiol. 61(5):1959-1967.

Chen, J., Civerolo, E., Tubajika, K., Livingston, S. and Higbee, B. 2008. Hypervariations of a protease-encoding gene, PD0218 (pspB), in *Xylella fastidiosa* strains causing almond leaf scorch and Pierce's disease in California. Appl. Environ. Microbiol. 74(12):3652-3657.

Choat, B., Jansen, S., Zwieniecki, M. A., Smets, E., and Holbrook, N. M. 2004. Changes in pit membrane porosity due to deflection and stretching: the role of vestured pits. Journal of Experimental Botany. 55:1569-1575.

Cianciotto, N. P. 2005. Type II secretion: a protein secretion system for all seasons. Trends in microbiology. 13(12):581-588.

Cisneros, D. A., Bond, P. J., Pugsley, A. P., Campos, M. and Francetic, O. 2012. Minor pseudopilin self-assembly primes type II secretion pseudopilus elongation. The EMBO journal. 31(4):1041-1053.

Davis, M. J., Purcell, A. H. and Thomson, S. V. 1978. Pierce's disease of grapevines: isolation of the causal bacterium. Science. 199(4324): 75-77.

Dickison, W. C. 2007. Integrative Plant Anatomy. Harcourt/Academic Press, San Diego, CA.

Dubnau, D. 1999. DNA uptake in bacteria. Annual Reviews in Microbiology 53(1):217-244.

Fisher, D. B. 2000. Long-distance transport. In Biochemistry and Molecular Biology of Plants (Buchanan, B.B., Gruissem, W. and Jones, R.L., eds). Rockville: American Society of Plant Physiologists. 730–784.

Francetic, O., Buddelmeijer, N., Lewenza, S., Kumamoto, C. A. and Pugsley, A. P. 2007. Signal recognition particle-dependent inner membrane targeting of the PulG pseudopilin component of a type II secretion system. Journal of bacteriology. 189(5):1783-1793.

Fujita, Y., Mori, I. and Kitano, S. 1983. Color reaction between pyrogallol red-molybdenum (VI) complex and protein. Bunseki Kagaku 32(12):379-386.

Goheen, A. C., and Hopkins, D. L. 1988. Pierce's disease. Pages 44–45 in: Compendium of Grape Diseases, A.C. Goheen and R.C. Pearson, eds. American Phytopathological Society Press, St. Paul, MN.

Gouran, H., Gillespie, H., Nascimento, R., Chakraborty, S., Zaini, P. A., Jacobson, A., Phinney, B. S., Dolan, D., Durbin-Johnson, B. P., Antonova, E. S., Lindow, S. E., Mellema, M. S., Goulart, L. R., and Dandekar, A. M. 2016. The secreted protease PrtA controls cell growth, biofilm formation and pathogenicity in *Xylella fastidiosa*. Scientific Reports. 6:31098.

Gray, M. D., Bagdasarian, M., Hol, W. G. and Sandkvist, M. 2011. In vivo cross-linking of EpsG to EpsL suggests a role for EpsL as an ATPase-pseudopilin coupling protein in the Type II secretion system of *Vibrio cholerae*. Molecular microbiology. 79(3):786-798.

Guilhabert, M. R. and Kirkpatrick, B. C. 2005. Identification of *Xylella fastidiosa* antivirulence genes: Hemagglutinin adhesins contribute to *X. fastidiosa* biofilm maturation and colonization and attenuate virulence. Mol Plant-Microbe Interacts. 18(8):856-868.

Hobbs, M. and Mattick, J. S. 1993. Common components in the assembly of type 4 fimbriae, DNA transfer systems, filamentous phage and protein-secretion apparatus: a general system for the formation of surface-associated protein complexes. Molecular microbiology. 10(2):233-243.

Hopkins, D. L. 1989. *Xylella fastidiosa*: xylem-limited bacterial pathogen of plants. Annual review of phytopathology. 27(1):271-290.

Hu, N. T., Hung, M. N., Liao, C. T. and Lin, M. H. 1995. Subcellular location of XpsD, a protein required for extracellular protein secretion by *Xanthomonas campestris* pv. *campestris*. Microbiology. 141(6):1395-1406.

Hugouvieux-Cotte-Pattat, N., Shevchik, V. E. and Nasser, W. 2002. PehN, a polygalacturonase homologue with a low hydrolase activity, is coregulated with the other *Erwinia chrysanthemi* polygalacturonases. Journal of bacteriology. 184(10):2664-2673.

Ingel, B., Jeske, D. R., Sun, Q., Grosskopf, J. and Roper, C. 2019. *Xylella fastidiosa* Endoglucanases Mediate the Rate of Pierce's Disease Development in *Vitis vinifera* in a Cultivar-Dependent Manner. Mol Plant Microbe Interact. (ja).

Jha, G., Rajeshwari, R. and Sonti, R. V. 2007. Functional interplay between two *Xanthomonas oryzae* pv. *oryzae* secretion systems in modulating virulence on rice. Mol Plant Microbe Interact. 20(1):31-40.

Kang Y., Huang J., Mao G., He L-Y., Schell M. A. 1994. Dramatically reduced virulence of mutants of Pseudomonas solanacearum defective in export of extracellular proteins across the outer membrane. Mol Plant Microbe Interact. 7:370–377.

Korotkov, K. V., Krumm, B., Bagdasarian, M. and Hol, W. G. 2006. Structural and functional studies of EpsC, a crucial component of the type 2 secretion system from *Vibrio cholerae*. Journal of molecular biology. 363(2):311-321.

Korotkov, K. V. and Hol, W. G. 2008. Structure of the GspK–GspI–GspJ complex from the enterotoxigenic Escherichia coli type 2 secretion system. Nature structural & molecular biology. 15(5):462.

Korotkov, K. V., Pardon, E., Steyaert, J. and Hol, W. G. 2009. Crystal structure of the N-terminal domain of the secretin GspD from ETEC determined with the assistance of a nanobody. Structure. 17(2):255-265.

Korotkov, K. V., Sandkvist, M. and Hol, W. G. 2012. The type II secretion system: biogenesis, molecular architecture and mechanism. Nature Reviews Microbiology, 10(5), p.336.

Kovach, M. E., Elzer, P. H., Hill, D. S., Robertson, G. T., Farris, M. A., Roop II, R. M., and Peterson, K. M. 1995. Four new derivatives of the broad-host-range cloning vector pBBR1MCS, carrying different antibiotic-resistance cassettes. Gene. 166:175-176.

Law C. W., Chen Y., Shi W., and Smyth G. K. 2014. Voom: precision weights unlock linear model analysis tools for RNA-seq read counts. Genome Biology. 15:29.

Lee, H. M., Wang, K. C., Liu, Y. L., Yew, H. Y., Chen, L. Y., Leu, W. M., Chen, D. C. and Hu, N. T. 2000. Association of the cytoplasmic membrane protein XpsN with the outer membrane protein XpsD in the type II protein secretion apparatus of *Xanthomonas campestris* pv. *campestris*. Journal of Bacteriology. 182(6):1549-1557.

Li, W. B., Pria Jr, W. D., Teixeira, D. C., Miranda, V. S., Ayres, A. J., Franco, C. F., Costa, M. G., He, C. X., Costa, P. I., and Hartung, J. S. 2001. Coffee leaf scorch caused by a strain of *Xylella fastidiosa* from citrus. Plant Disease. 85:501-505.

Linden, J. C. and Shiang, M. 1991. Bacterial cellulases: regulation of synthesis. Pages 331-348 in: Enzymes in Biomass Conversion, American Chemical Society, Washington D.C.

Matsumoto, A., Young, G. M.. and Igo, M. M. 2009. Chromosome-based genetic complementation system for *Xylella fastidiosa*. Applied Environmental Microbiology. 75:1679-1687.

McClure R., Balasubramanian D., Sun Y., Bobrovskyy M., Sumby P., Genco C. A., Vanderpool C. K., and Tjaden B. 2013. Computational analysis of bacterial RNA-seq data. Nucleic Acids Res. 41(14):140.

Liu R., Holik A. Z., Su S., Jansz N., Chen K., Leong H. S., Blewitt M. E., Asselin-Labat M. L., Smyth G. K., and Ritchie M. E. 2015. Why weight? Modelling sample and observational level variability improves power in RNA-seq analyses. Nucleic Acids Res. 43(15):97.

Mollenhauer H. H., and Hopkins D. L. 1974. Ultrastructural study of Pierce's disease bacterium in grape xylem tissue. Journal of Bacteriology. 119:612-618.

Nascimento, R., Gouran, H., Chakraborty, S., Gillespie, H. W., Almeida-Souza, H. O., Tu, A., Rao, B. J., Feldstein, P. A., Bruening, G., Goulart, L. R. and Dandekar, A. M. 2016. The type II secreted lipase/esterase LesA is a key virulence factor required for *Xylella fastidiosa* pathogenesis in grapevines. Scientific reports. 6:18598.

Norrander, J., Kempe, T. and Messing, J. 1983. Construction of improved M13 vectors using oligodeoxynucleotide-directed mutagenesis. Gene. *26*(1):101-106.

Nouwen, N., Ranson, N., Saibil, H., Wolpensinger, B., Engel, A., Ghazi, A. and Pugsley, A. P. 1999. Secretin PulD: association with pilot PulS, structure, and ion-conducting channel formation. Proceedings of the National Academy of Sciences. 96(14):8173-8177.

Nouwen, N., Stahlberg, H., Pugsley, A. P. and Engel, A. 2000. Domain structure of secretin PulD revealed by limited proteolysis and electron microscopy. The EMBO journal. 19(10):2229-2236.

Nunn, D. N. and Lory, S. 1993. Cleavage, methylation, and localization of the *Pseudomonas aeruginosa* export proteins XcpT,-U,-V, and-W. Journal of bacteriology. 175(14):4375-4382.

Palomäki, T., Pickersgill, R., Riekki, R., Romantschuk, M. and Saarilahti, H. T. 2002. A putative three-dimensional targeting motif of polygalacturonase (PehA), a protein secreted through the type II (GSP) pathway in *Erwinia carotovora*. Molecular microbiology. 43(3):585-596.

Patrick, M., Korotkov, K. V., Hol, W. G. and Sandkvist, M. 2011. Oligomerization of EpsE coordinates residues from multiple subunits to facilitate ATPase activity. Journal of Biological Chemistry. 286(12):10378-10386.

Peabody, C. R., Chung, Y. J., Yen, M. R., Vidal-Ingigliardi, D., Pugsley, A. P. and Saier Jr, M. H. 2003. Type II protein secretion and its relationship to bacterial type IV pili and archaeal flagella. Microbiology. 149(11):3051-3072.

Perez-Donoso, A. G., Sun, Q., Roper, M. C., Greve, L. C., Kirkpatrick B. C., and Labavitch, J. M. 2010. Cell Wall-Degrading Enzymes Enlarge the Pore Size of

Intervessel Pit Membranes in Healthy and *Xylella fastidiosa*-Infected Grapevines. Plant Physiology. 152:1748-1759.

Possot, O. M., Vignon, G., Bomchil, N., Ebel, F. and Pugsley, A. P. 2000. Multiple interactions between pullulanase secreton components involved in stabilization and cytoplasmic membrane association of PulE. Journal of Bacteriology. 182(8):2142-2152.

Pugsley, A. P. 1993a. The complete general secretory pathway in gram-negative bacteria. Microbiology and Molecular Biology Reviews. 57(1):50-108.

Pugsley, A. P. 1993b. Processing and methylation of PulG, a pilin-like component of the general secretory pathway of Klebsiella oxytoca. Molecular microbiology. 9(2):295-308.

Purcell, A. H. 1986. Pierce's disease. Pages 62–69 in: Grape Pest Management, D.L. Flaherty, ed. Cooperative Extension University of California, Division of Agriculture and Natural Resources, Oakland, CA.

Py, B., Loiseau, L. and Barras, F. 2001. An inner membrane platform in the type II secretion machinery of Gram-negative bacteria. EMBO reports. 2(3):244-248.

Rajeshwari, R., Jha, G. and Sonti, R. V. 2005. Role of an in planta-expressed xylanase of *Xanthomonas oryzae* pv. *oryzae* in promoting virulence on rice. Mol Plant Microbe Interact. 18(8):830-837.

Ray, S. K., Rajeshwari, R. and Sonti, R. V. 2000. Mutants of *Xanthomonas oryzae* pv. *oryzae* deficient in general secretory pathway are virulence deficient and unable to secrete xylanase. Mol Plant Microbe Interact. 13(4):394-401.

Roper, M. C., Greve, L. C., Warren, J. G., Labavitch, J. M., and Kirkpatrick, B. C. 2007. *Xylella fastidiosa* requires polygalacturonase for colonization and pathogenicity in *Vitis vinifera* grapevines. Mol Plant Microbe Interact. 20:411-419.

Sandkvist, M., Bagdasarian, M., Howard, S. P. and DiRita, V. J. 1995. Interaction between the autokinase EpsE and EpsL in the cytoplasmic membrane is required for extracellular secretion in *Vibrio cholerae*. The EMBO journal. 14(8):1664-1673.

Saponari, M., Boscia, D., Nigro, F., and Martelli, G. P. 2013. Identification of DNA sequences related to *Xylella fastidiosa* in oleander, almond and olive trees exhibiting leaf scorch symptoms in Apulia (Southern Italy). Journal of Plant Pathology. 95:659-668.

Sauvonnet, N., Vignon, G., Pugsley, A. P. and Gounon, P. 2000. Pilus formation and protein secretion by the same machinery in *Escherichia coli*. The EMBO journal. 19(10):2221-2228.

Schenk, H. J., Espino, S., Rich-Cavazos, S. M. and Jansen, S. 2018. From the sap's perspective: The nature of vessel surfaces in angiosperm xylem. American journal of botany. 105(2):172-185.

Shimao, M., Tamogami, T., Kishida, S. and Harayama, S. 2000. The gene *pvaB* encodes oxidized polyvinyl alcohol hydrolase of *Pseudomonas* sp. strain VM15C and forms an operon with the polyvinyl alcohol dehydrogenase gene *pvaA*. Microbiology. 146(3):649-657.

Simpson, A. J. G., Reinach, F. D. C., Arruda, P., Abreu, F. A. D., Acencio, M., Alvarenga, R., Alves, L. M. C., Araya, J. E., Baia, G. S., Baptista, C. S., Barros, M. H. D., Bonaccorsi, E. D., Bordin, S., Bové J. M., Briones, M. R. S., Bueno, M. R. P., Camargo, A. A., Camargo, L. E. A., Carraro, D. M., Carrer, H., Colauto, N. B., Colombo, C., Costa, F. F., Costa, M. C. R., Costa-Neto, C. M., Coutinho, L. L. Cristofani, M., Dias-Neto, E., Docena, C., El-Dorry, H., Facincani, A. P., Ferreira, A. J. S., Ferreira, V. C. A., Ferro, J. A., Fraga, J. S., França, S. C., Franco, M. C., Frohme, M., Furlan, L. R., Garnier, M., Goldman, G. H., Goldman, M. H. S., Gomes, S. L., Gruber, A., Ho, P. L., Hoheisel, J. D., Junqueira, M. L., Kemper, E. L., Kitajima, J.P., Krieger, J. E., Kuramae, E. E., Laigret, F., Lambais, M. R., Leite, L. C. C., Lemos, E. G. M., Lemos, M. V. F., Lopes, S. A., Lopes, C. R., Machado, J. A., Machado, M. A., Madeira, A. M. B. N., Madeira, H. M. F., Marino, C. L., Marques, M. V., Martins, E A. L., Martins, E. M. F., Matsukuma, A. Y., Menck, C. F. M., Miracca, E. C., Miyaki, C. Y., Monteiro-Vitorello, C. B., Moon, D. H., Nagai, M. A., Nascimento, A. L. T. O., Netto, L. E. S., Nhani Jr, A., Nobrega, F. G., Nunes, L. R., Oliveira, M. A., de Oliveira, M. C., de Oliveira, R. C., Palmieri, D. A., Paris, A., Peixoto, B. R., Pereira, G. A. G., Pereira Jr, H. A., Pesquero, J. B., Quaggio, R. B., Roberto, P. G., Rodrigues, V., de M. Rosa, A. J., de Rosa Jr, V. E., de Sá, R. G., Santelli, R.

V., Sawasaki, H. E., da Silva, A. C. R., da Silva, A. M., da Silva, F. R., Silva, W. A., da Silveira, J. F., Silvestri, M. L. Z., Siqueira, W. J., de Souza, A. A., de Souza, A. P., Terenzi, M. F., Truffi, D., Tsai, S. M., Tsuhako, M. H., Vallada, H., Van Sluys, M. A., Verjovski-Almeida, S., Vettore, A. L., Zago, M. A., Zatz, M., Meidanis J., and Setubal J. C. 2000. The genome sequence of the plant pathogen *Xylella fastidiosa*. Nature. 406:151-157.

Solé, M., Scheibner, F., Hoffmeister, A. K., Hartmann, N., Hause, G., Rother, A., Jordan, M., Lautier, M., Arlat, M. and Büttner, D. 2015. *Xanthomonas campestris pv. vesicatoria* secretes proteases and xylanases via the Xps type II secretion system and outer membrane vesicles. Journal of bacteriology. 197(17):2879-2893.

Stevenson, J. F., Matthews, M. A., and Rost, T. L. 2004. Grapevine susceptibility to Pierce's disease I: relevance of hydraulic architecture. American Journal of Enology and Viticulture. 55:228-237.

Stevenson, J. F., Matthews, M. A., and Rost, T. L. 2005. The developmental anatomy of green islands and matchsticks as symptoms of Pierce's disease of grapevines. Plant Disease. 89:543-548.

Sun, Q. H., Hu, J., Huang, G. X., Ge, C., Fang, R. X. and He, C. Z. 2005. Type-II secretion pathway structural gene xpsE, xylanase-and cellulase secretion and virulence in *Xanthomonas oryzae* pv. *oryzae*. Plant pathology. 54(1):15-21.

Tjaden B. 2015. De novo assembly of bacterial transcriptomes from RNA-seq data. Genome Biology. 16:1.

Tyree, M. T., and Zimmermann, M. H. 2002. Hydraulic architecture of whole plants and plant performance. Pages 175–214 in: Xylem Structure and the Ascent of Sap , Springer-Verlag Berlin Heidelberg, Berlin.

Van Sluys, M. A., de Oliveira, M. C., Monteiro-Vitorello, C. B., Miyaki, C. Y., Furlan, L. R., Camargo, L. E. A., da Silva, A. C. R., Moon, D. H., Takita, M. A., Lemos, E. G. M., Machado, M. A., Ferro, M. I. T., da Silva, F. R., Goldman, M. H. S., Goldman, G. H., Lemos, M. V. F., El-Dorry, H., Tsai, S. M., Carrer, H., Carraro, D. M., de Oliveira, R. C., Nunes, L. R., Siqueira, W. J., Coutinho, L. L., Kimura, E. T., Ferro, E. S., Harakava, R., Kuramae, E. E., Marino, C. L., Giglioti, E., Abreu, I. L., Alves, L. M. C., do Amaral, A. M., Baia, G. S., Blanco, S. R., Brito,

M. S., Cannavan, F. S., Celestino, A. V., da Cunha, A. F., Fenille, R. C., Ferro, J. A., Formighieri, E. F., Kishi, L. T., Leoni, S. G., Oliveira, A. R., Rosa Jr., V. E., Sassaki, F. T., Sena, J. A. D., de Souza, A. A., Truffi, D., Tsukumo, F., Yanai, G. M., Zaros, L. G., Civerolo, E. L., Simpson, A. J. G., Almeida Jr., N. F., Setubal, J. C., and Kitajima J. P. 2003. Comparative analyses of the complete genome sequences of Pierce's disease and citrus variegated chlorosis strains of *Xylella fastidiosa*. Journal of Bacteriology. 185:1018-1026.

Varela, L. G. 1996. Pierce's Disease in the North Coast. University of California Cooperative Extension & Statewide IPM Project: 1Y11.

Wang, P., 2014. Characterization of the Oxidative Stress Response and the Type II Secretion System for the Phytopathogen, *Xylella fastidiosa* (Doctoral dissertation, UC Riverside).

Wattam A. R., Davis J. J., Assaf R., Boisvert S., Brettin T., Bun C., Conrad N., Dietrich E. M., Disz T., Gabbard J. L., Gerdes S., Henry C. S., Kenyon R. W., Machi D., Mao C., Nordberg E. K., Olsen G. J., Murphy-Olson D. E., Olson R., Overbeek R., Parrello B., Pusch G. D., Shukla M., Vonstein V., Warren A., Xia F., Yoo H., Stevens R. L. 2017. Improvements to PATRIC, the all-bacterial Bioinformatics Database and Analysis Resource Center. Nucleic Acids Res. 4(45):535-542.

Yanez, M. E., Korotkov, K. V., Abendroth, J. and Hol, W. G. 2008. Structure of the minor pseudopilin EpsH from the Type 2 secretion system of *Vibrio cholerae*. Journal of molecular biology. 377(1):91-103.

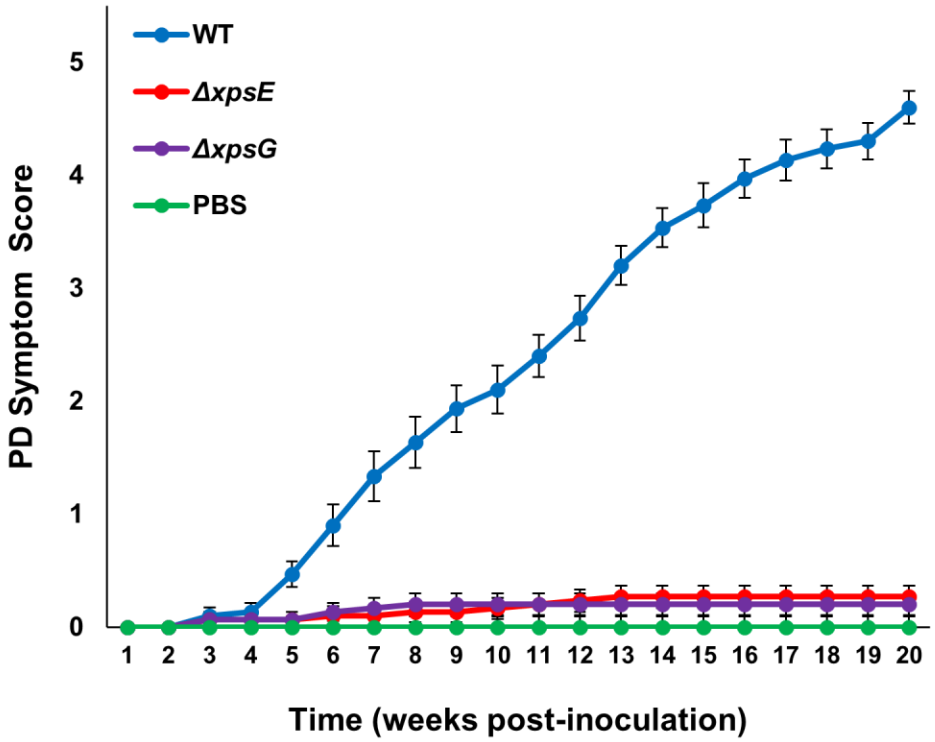


Figure 3.1 Pierce's Disease symptom development over 20 weeks comparing wild type (WT) *X. fastidiosa* to the T2SS-deficient mutant strains Δ*xpsE* (red) and Δ*xpsG* (purple). 1× PBS (green) was used as a negative control. Ratings were performed using the 0 – 5 Pierce's Disease rating index developed by Guilhabert and Kirkpatrick (2005). For wild type, Δ*xpsE*, and Δ*xpsG*, each data point represents the mean PD symptom score of 30 vines. Each data point for 1×PBS represents the mean PD symptom score of 10 vines. Bars represent the standard error of the mean.

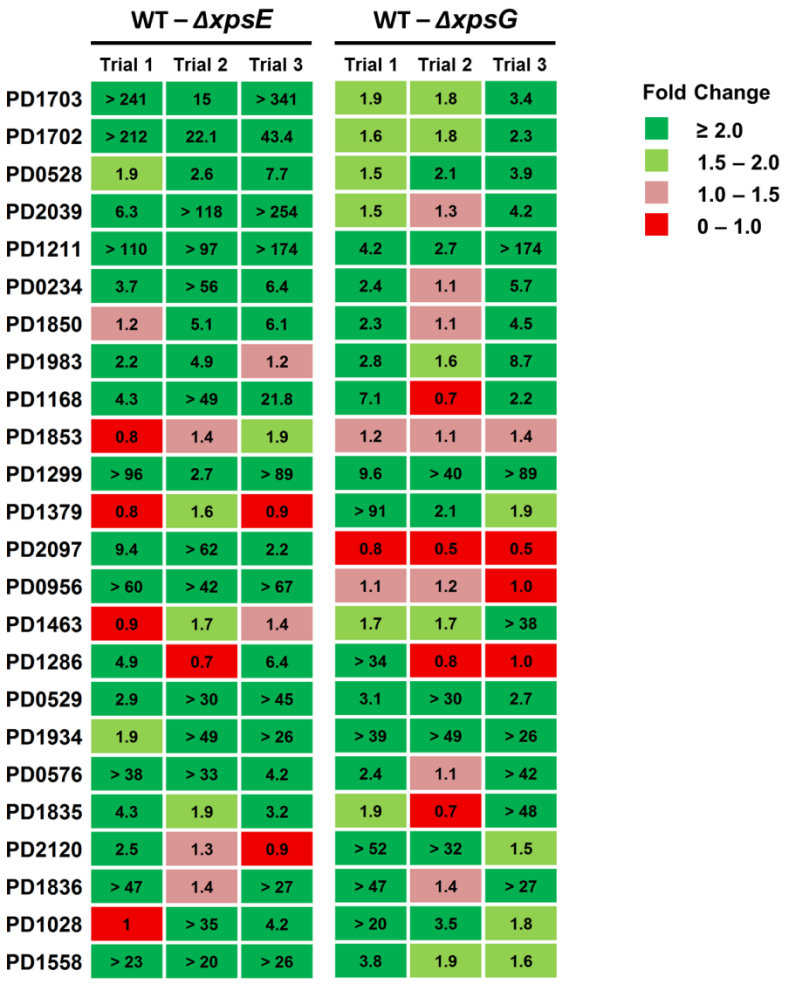


Figure 3.2 Fold change in the number of matched peptides per trial between wild type and Δ*xpsE* (*left*) and wild type and Δ*xpsG* (*right*), for 24 abundant proteins present in wild type extracellular fractions that have unknown secretion mechanisms. Green and light green indicate that the number of matched peptides for a protein was ≥ 2-fold greater and 1.5 – 2-fold greater, respectively, in wild type extracellular fractions. Light red indicates that the number of matched peptides for a protein was between 1.0 and 1.5-fold greater in wild type extracellular fractions, and red indicates no difference or a greater number of matched peptides for a protein in mutant extracellular fractions.

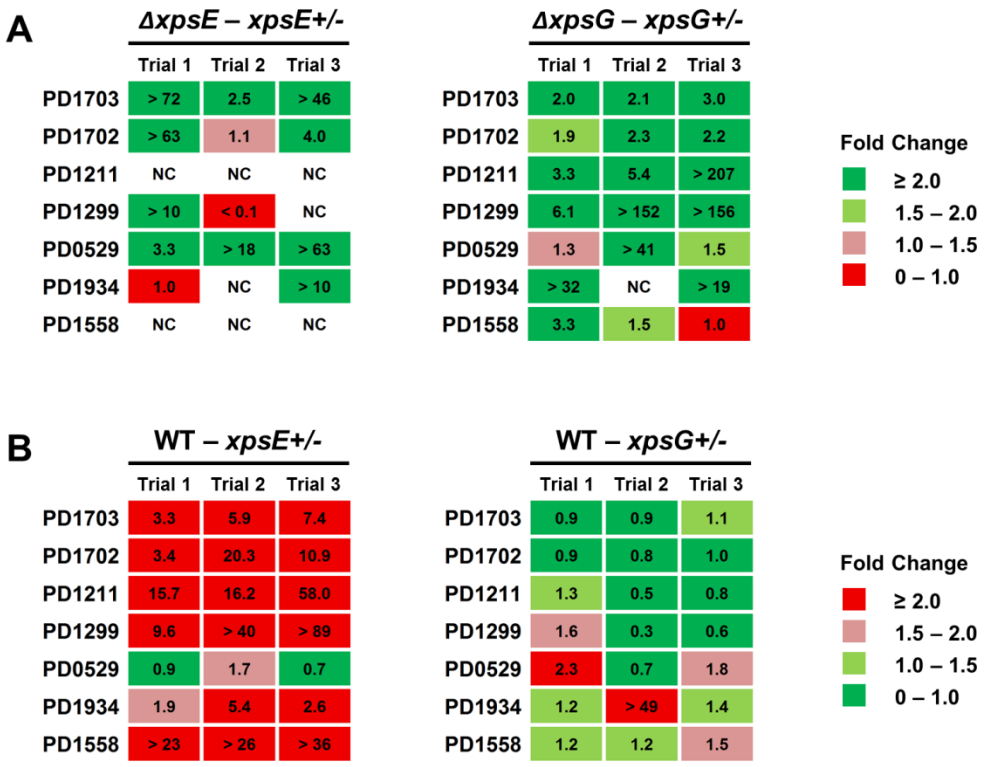


Figure 3.3 Fold change in the number of matched peptides per trial between mutant and complement strains and wild type and complement strains for the seven Type II secretion candidate proteins. A) Fold change between *xpsE* +/- and Δ*xpsE* (*left*) and *xpsG* +/- and Δ*xpsG* (*right*). Green and light green indicate that the number of matched peptides for a protein was ≥ 2-fold greater and 1.5 – 2-fold greater, respectively, in complement extracellular fractions. Light red indicates that the number of matched peptides for a protein was between 1.0 and 1.5-fold greater in complement extracellular fractions, and red indicates no difference or a greater number of matched peptides for a protein in mutant extracellular fractions. B) Fold change between wild type and *xpsE* +/- (*left*) and wild type and *xpsG* +/- (*right*). Red and light red indicate that the number of matched peptides for a protein was ≥ 2-fold greater and 1.5 – 2-fold greater, respectively, in wild type extracellular fractions, suggesting that the complement did not restore protein abundance to wild type levels. Light green indicates that the number of matched peptides for a protein was between 1.0 and 1.5-fold greater in wild type extracellular fractions, and green indicates no difference or a greater number of matched peptides for a protein in complement extracellular fractions, suggesting partial or full complementation, respectively. NC indicates the fold change was not calculated due to the absence of peptides in both extracellular fractions being compared.

| Strains, plasmids, and primers | Relevant characteristics or primer sequence | Source |
|---|---|---|
| Strains | | |
| *Escherichia coli* TOP10 | F- *mcr*A Δ(*mrr-hsd*RMS-*mcr*BC) Φ80*lac*ZΔM15 Δ*lac*X74 *rec*A1 *ara*D139 Δ(*araleu*)7697 *gal*U *gal*K *rps*L (*Str*R) *end*A1 nup*G* | Invitrogen |
| *X. fastidiosa* Temecula 1 | | Temecula, CA |
| *X. fastidiosa* Δ*xpsE* | *xpsE* deletion in Temecula 1 background | Wang (2014) |
| *X. fastidiosa xpsE*+/- | Addition of pCC2 plasmid to Δ*xpsE* strain | This study |
| *X. fastidiosa* Δ*xpsG* | *xpsG* deletion in Temecula 1 background | This study |
| *X. fastidiosa xpsG*+/- | Addition of *xpsG* to neutral site between PD0702 and PD0703 in Δ*xpsE* background | This study |
| Plasmids | | |
| pCR8/GW/TOPO | pUC19 derivative, $Spn^r$ | Invitrogen |
| pCR2.1 TOPO | $Km^r$ | Invitrogen |
| pBBR1-MCS5 | $Gm^r$ | Kovach et al. (1995) |
| pUC19 | $Amp^r$ | Norrander et al. (1983) |
| pAX1cm | pAX1 with $Cm^r$ cassette and multiple-cloning site | Matsumoto et al. (2009) |
| pXf20pemIK-GW | *pemI*/*pemK* stability factor, $Kan^r$, $Amp^r$, Gateway cloning compatible, requires ccdB strain for propagation | Burbank and Stenger (2016) |
| pPW04 | pUC19 with Δ*xpsE* deletion construct | Wang (2014) |
| pBI4 | pUC19 with Δ*xpsG* deletion construct | This study |
| pBI5 | pUC19 with *xpsG* gene, *xps* operon promoter, and pAX1cm cassette | This study |
| pCC2 | pXf20pemIK-GW with *xpsE* gene and *xps* operon promoter | This study |
| Primers | | |
| XpsE LF fwd EcoRI | GCTGTGAATTCGAATGGACAGATGCGTCGGC | Wang (2014) |
| XpsE LF rev Gm | TTCCACGGTGTGCGTCATTCGGACACCATAAA | Wang (2014) |
| XpsE Gm fwd | TTTATGGTGTCCGAATGACGCACACCGTGGAA | Wang (2014) |
| XpsE Gm rev | ATTGGCAACCACACCTTTAGGTGGCGGTACTT | Wang (2014) |
| XpsE RF fwd Gm | AAGTACCGCCACCTAAAGGTGTGGTTGCCAAT | Wang (2014) |
| XpsE RF rev HindIII | TCTACAAGCTTAATCAGCCAGCCGCTGCAG | Wang (2014) |
| XpsEoutfwd | CAATGCGCAGGTGTTGTCCAAAGA | Wang (2014) |
| XpsEoutrev | ATTAATCACCTTGGCACGCACCAC | Wang (2014) |
| xpsG_LF_fwd | TGCAGCGTTGGTGGATGATCTTGG | This study |
| xpsG_RF_rev | CTTCCCAACCTTCGCTACGACCTCA | This study |
| XpsE_pXf20pemIK-GW_F | GGCTTCCAGAATGGTCAGGCAGCAC | This study |
| XpsE_pXf20pemIK-GW_R | CTTGCGTGTGACGGAGGAAGGCTGA | This study |
| Xf-pAXinsert_seq_fwd | TTGCGTAATGAGGTGATGCCTAAGAAC | This study |
| Xf-pAXinsert_seq_rev | GTCCATGCGATTTCTATCGTGGCAC | This study |
| GW1 | GTTGCAACAAATTGATGAGCAATGC | Invitrogen |
| GW2 | TAATTGCTCATCAATTTGTTGCAAC | Invitrogen |

Table 3.1 Strains, plasmids, and primer sequences used in this chapter. Primer sequences are presented 5' to 3'. $Amp^r$, $Cm^r$, $Gm^r$, $Kan^r$, and $Spn^r$ indicate ampicillin, chloramphenicol, gentamicin, kanamycin, and spectinomycin resistance genes, respectively.

| | | Predictions | | | Matched peptides | | | Seq. Coverage (%) | | | Scaffold Prob. (%) | | |
|---|---|---|---|---|---|---|---|---|---|---|---|---|---|
| PD # | Description | Sec. Signal | Prot. Local. | EC Sec. | Trial 1 | Trial 2 | Trial 3 | Trial 1 | Trial 2 | Trial 3 | Trial 1 | Trial 2 | Trial 3 |
| PD0731 | Outer mem. prot. XadA1 | SecP | U | T5SS | 343 | 321 | 447 | 56.2 | 52.2 | 54.8 | 100 | 100 | 100 |
| PD1427 | Hemolysin | SecP | EC | T1SS | 288 | 286 | 398 | 32.5 | 32.2 | 36.3 | 100 | 100 | 100 |
| PD1506 | Hemolysin-type $Ca^{2+}$-binding prot. | SecP | EC | T1SS | 262 | 271 | 425 | 29.1 | 30.6 | 36.8 | 100 | 100 | 99.9 |
| PD0744 | Outer mem. prot. XadA2 | SPI | OM | T5SS | 276 | 264 | 377 | 22.6 | 23.6 | 23.9 | 99.9 | 100 | 100 |
| PD1703 | Lipase | SPI | U | U | 241 | 255 | 341 | 69.5 | 66.8 | 70.1 | 100 | 100 | 100 |
| PD1702 | Lipase | SPI | U | U | 212 | 243 | 304 | 64.0 | 65.7 | 65.2 | 100 | 100 | 100 |
| PD0305 | Hemolysin | SecP | EC | T1SS | 246 | 192 | 277 | 27.5 | 26.7 | 28.8 | 100 | 100 | 100 |
| PD1711 | TonB-dependent receptor | SPI | OM | NS | 175 | 164 | 297 | 54.9 | 44.7 | 51.4 | 99.5 | 99.7 | 99.8 |
| PD0528 | Hypothetical protein | SPI | U | U | 131 | 189 | 277 | 66.2 | 53.7 | 68.4 | 100 | 100 | 99.4 |
| PD2039 | L-ascorbate oxidase | SPI | U | U | 133 | 118 | 254 | 47.3 | 38.0 | 47.1 | 99.4 | 99.8 | 100 |
| PD0218 | Serine protease | SPII | OM | T5SS | 121 | 159 | 191 | 42.8 | 33.6 | 36.8 | 97.0 | 99.6 | 98.6 |
| PD0824 | XadA-like adhesin | SecP | OM | T5SS | 158 | 66 | 232 | 31.6 | 18.1 | 34.3 | 99.7 | 99.3 | 99.3 |
| PD1709 | Outer mem. prot. OprF | SPI | OM | NS | 123 | 124 | 188 | 57.7 | 46.7 | 51.4 | 100 | 99.8 | 100 |
| PD0313 | Serine protease | SPII | OM | T5SS | 116 | 131 | 186 | 36.8 | 36.8 | 37.4 | 98.3 | 99.4 | 99.9 |
| PD1211 | Lipase | SPI | U | U | 110 | 97 | 174 | 58.9 | 60.4 | 59.6 | 100 | 99.9 | 100 |
| PD1283 | TonB-dependent receptor | SPI | OM | NS | 100 | 55 | 175 | 39.4 | 38.9 | 41.9 | 99.7 | 98.5 | 99.7 |
| PD0234 | Aconitate hydratase | SecP | C | U | 85 | 56 | 154 | 41.2 | 46.6 | 49.0 | 98.9 | 97.8 | 95.1 |
| PD1850 | Peptidase M20 | SPI | U | U | 100 | 72 | 121 | 56.4 | 46.7 | 56.8 | 100 | 99.1 | 100 |
| PD1589 | TonB-dependent receptor | SPI | OM | NS | 95 | 97 | 96 | 32.7 | 31.9 | 59.6 | 99.7 | 97.4 | 96.7 |
| PD1983 | Ribonuclease E/G | SecP | U | U | 90 | 127 | 52 | 25.0 | 29.7 | 25.5 | 99.1 | 98.7 | 99.9 |
| PD1168 | Prolyl isomerase | SPI | OM | U | 100 | 49 | 109 | 59.8 | 50.1 | 49.9 | 100 | 99.3 | 99.2 |
| PD1853 | Peptidase M16 | SPI | U | U | 68 | 101 | 87 | 27.2 | 34.5 | 26.7 | 98.2 | 98.8 | 100 |
| PD0318 | TonB-dependent receptor | SPI | OM | NS | 100 | 68 | 61 | 33.6 | 27.2 | 42.1 | 99.9 | 99.3 | 99.9 |
| PD1299 | Hypothetical protein | SecP | EC | U | 96 | 40 | 89 | 43.8 | 40.1 | 30.9 | 99.8 | 100 | 100 |
| PD1379 | Putat. autotransporter prot. | SPI | OM | U | 91 | 78 | 50 | 32.2 | 35.2 | 33.6 | 98.3 | 99.4 | 100 |
| PD2097 | Peptidase M23 | SecP | EC | U | 66 | 62 | 66 | 23.6 | 23.2 | 34.2 | 98.8 | 96.6 | 100 |
| PD0326 | Outer mem. prot. BamA | SPI | OM | NS | 65 | 84 | 44 | 41.5 | 32.0 | 37.8 | 99.2 | 98.8 | 98.9 |
| PD2065 | TonB-dependent receptor | SPI | OM | NS | 58 | 39 | 90 | 32.8 | 27.3 | 30.6 | 97.2 | 99.9 | 99.4 |
| PD1699 | Cell env. biogen. prot. OmpA | SPII | OM | NS | 53 | 41 | 84 | 58.8 | 45.8 | 61.6 | 99.8 | 98.1 | 99.7 |
| PD0956 | Peptidase | SPI | U | U | 60 | 42 | 67 | 45.0 | 48.1 | 50.7 | 98.9 | 100 | 99.6 |
| PD0950 | Serine protease | SecP | OM | T5SS | 71 | 33 | 61 | 33.9 | 31.4 | 26.5 | 96.9 | 99.9 | 100 |

| | | Predictions | | | Matched peptides | | | Seq. Coverage (%) | | | Scaffold Prob. (%) | | |
|---|---|---|---|---|---|---|---|---|---|---|---|---|---|
| PD # | Description | Sec. Signal | Prot. Local. | EC Sec. | Trial 1 | Trial 2 | Trial 3 | Trial 1 | Trial 2 | Trial 3 | Trial 1 | Trial 2 | Trial 3 |
| PD1463 | Hypothetical protein | SPI | IM | U | 59 | 63 | 38 | 21.8 | 22.3 | 13.7 | 99.4 | 99.8 | 99.9 |
| PD1807 | Outer mem. prot. OmpW | SPI | OM | NS | 42 | 46 | 57 | 51.8 | 57.8 | 59.0 | 99.3 | 93.5 | 99.8 |
| PD1550 | Outer mem. prot. UptE | SPI | U | NS | 43 | 42 | 47 | 44.3 | 54.1 | 57.5 | 97.6 | 100 | 100 |
| PD1200 | Putat. siderophore receptor | SPI | OM | NS | 36 | 44 | 43 | 19.0 | 25.4 | 38.4 | 96.3 | 99.8 | 100 |
| PD1286 | Peptidase S1 | SPII | P | U | 34 | 25 | 64 | 34.0 | 38.7 | 35.7 | 100 | 96.5 | 100 |
| PD0529 | β-1,4-cellobiosidase | SPI | EC | U | 46 | 30 | 45 | 24.8 | 29.9 | 30.2 | 98.4 | 93.9 | 98.8 |
| PD1934 | Peptidase S9 | SPI | U | U | 39 | 49 | 26 | 17.8 | 35.9 | 21.5 | 94.9 | 97.1 | 97.1 |
| PD0576 | Histidine kinase | SPI | IM | U | 38 | 33 | 42 | 13.3 | 16.0 | 21.5 | 94.9 | 100 | 100 |
| PD1835 | Chaperone SurA | SPII | P | U | 34 | 31 | 48 | 46.6 | 38.9 | 49.7 | 99.6 | 96.8 | 96.1 |
| PD2120 | Putat. polysaccharide deacetylase | SPII | C | U | 52 | 32 | 21 | 21.1 | 19.7 | 16.5 | 95.7 | 100 | 96.7 |
| PD0270 | Porin | SPI | OM | NS | 20 | 21 | 63 | 38.6 | 37.2 | 44.5 | 99.7 | 100 | 100 |
| PD1836 | LPS-assembly protein LptD | SPI | OM | U | 47 | 21 | 27 | 21.2 | 33.2 | 24.4 | 96.7 | 96.7 | 96.2 |
| PD1028 | Polyisoprenoid-binding protein | SPII | U | U | 20 | 35 | 38 | 40.1 | 47.4 | 47.4 | 97.0 | 100 | 95.4 |
| PD0023 | Type IV pilus biogen. prot. PilY | SPI | U | T4P | 33 | 33 | 26 | 14.0 | 26.3 | 35.0 | 93.7 | 100 | 100 |
| PD1558 | DNA uptake protein | SPI | IM | U | 23 | 26 | 36 | 60.9 | 43.3 | 46.5 | 100 | 93.2 | 100 |
| PD0058 | Fimbrial adhesin protein | SecP | EC | T1P | 20 | 29 | 21 | 44.8 | 45.8 | 45.1 | 98.3 | 100 | 100 |

Table 3.2 Most abundant proteins with secretion signals in wild type extracellular fractions. Secretion signal prediction was performed using SignalP 5.0 and SecretomeP 2.0. SPI indicates standard Sec signal peptides; SPII indicates lipoprotein Sec signal peptides. SecP indicates non-standard secretion. Predicted subcellular localization was performed using PSORTb v. 3.0.2. C = cyltoplasm; IM = inner membrane; P = periplasm; OM = outer membrane; EC = extracellular; U = unknown. Number of matched peptides, Sequence coverage, and protein probability scores were generated using Scaffold v4.9.0 (Proteome Software Inc., Portland, OR). The Scaffold Probability Score is the percentage of confidence in the identified protein based on matched peptides.

| | | WT – Δ*xpsE* | |
|---|---|---|---|
| PD # | Description | Log2FC | Adj. *P*-value |
| PD1703 | Lipase | 2.83 | 0.51 |
| PD1702 | Lipase | 1.88 | 0.71 |
| PD1211 | Lipase | -0.53 | 0.86 |
| PD1299 | Hypothetical protein | 0.08 | 0.99 |
| PD0529 | β-1,4-cellobiosidase | 2.30 | 0.63 |
| PD1934 | Peptidase S9 | -0.09 | 0.98 |
| PD1558 | DNA uptake protein | 3.55 | 0.74 |

Table 3.3 Differential gene expression of Type II secretion candidates between wild type and Δ*xpsE* using RNAseq. Reads were aligned to the *X. fastidiosa* genome and transcripts were assembled and quantified using Rockhopper (version 3.5.26) within the Pathosystems Resource Integration Center (PATRIC). Differential expression testing was performed using limma-voom (version 3.38.3) within Galaxy (version 19.01) to generate Log2 Fold Change and adjusted *p*-values. Data used to generate the differential expression analysis consisted of three biological replicates of wild type and Δ*xpsE*.

| PD # | Description | Matched peptides | | | Avg. transcript abundance |
|---|---|---|---|---|---|
| | | Trial 1 | Trial 2 | Trial 3 | |
| PD1485 | Polygalacturonase | -- | -- | -- | 186 ± 71 |
| PD1851 | β-1,4-endoglucanase | -- | -- | -- | 21 ± 5 |
| PD1856 | β-1,4-endoglucanase-expansin | -- | 6 | -- | 145 ± 26 |
| PD2061 | Putat. cellulase | -- | 7 | -- | 52 ± 8 |

Table 3.4 Matched peptides and transcript abundances for other predicted Type II-secreted proteins in wild type cultures. Number of matched peptides was generated using Scaffold v4.9.0 (Proteome Software Inc., Portland, OR). Average transcript abundance and standard deviation were calculated from total transcript abundances across three biological replicates. Total transcript abundances were quantified using Rockhopper (version 3.5.26) within the Pathosystems Resource Integration Center (PATRIC).

| | | Predictions | | | Matched peptides | | | Seq. Coverage (%) | | | Scaffold Prob. (%) | | |
|---|---|---|---|---|---|---|---|---|---|---|---|---|---|
| PD # | Description | Sec. Signal | Prot. Local. | EC Sec. | Trial 1 | Trial 2 | Trial 3 | Trial 1 | Trial 2 | Trial 3 | Trial 1 | Trial 2 | Trial 3 |
| PD1703 | Lipase | SPI | U | U | -- | 17 | -- | -- | 42.7 | -- | -- | 90.3 | -- |
| PD1702 | Lipase | SPI | U | U | -- | 11 | 7 | -- | 32.4 | 34.3 | -- | 100 | 100 |
| PD0528 | Hypothetical protein | SPI | U | U | 69 | 74 | 36 | 38.0 | 50.2 | 41.3 | 98.3 | 100 | 99.1 |
| PD2039 | L-ascorbate oxidase | SPI | U | U | 21 | -- | -- | 35.3 | -- | -- | 90.0 | -- | -- |
| PD1211 | Lipase | SPI | U | U | -- | -- | -- | -- | -- | -- | -- | -- | -- |
| PD0234 | Aconitate hydratase | SecP | C | U | 23 | -- | 24 | 24.2 | -- | 27.6 | 96.3 | -- | 97.6 |
| PD1850 | Peptidase M20 | SPI | U | U | 82 | 14 | 20 | 42.2 | 55.6 | 32.5 | 99.2 | 100 | 100 |
| PD1983 | Ribonuclease E/G | SecP | U | U | 41 | 26 | 45 | 16.9 | 26.8 | 24.1 | 95.2 | 99.4 | 95.4 |
| PD1168 | Prolyl isomerase | SPI | OM | U | 23 | -- | 5 | 50.1 | -- | 36.5 | 98.3 | -- | 100 |
| PD1853 | Peptidase M16 | SPI | U | U | 81 | 72 | 47 | 32.5 | 39.7 | 25.8 | 99.8 | 100 | 100 |
| PD1299 | Hypothetical protein | SecP | EC | U | -- | 15 | -- | -- | 46.0 | -- | -- | 97.1 | -- |
| PD1379 | Putat. autotransporter prot. | SPI | OM | U | 114 | 49 | 57 | 51.0 | 47.5 | 42.9 | 99.7 | 100 | 98.6 |
| PD2097 | Peptidase M23 | SecP | EC | U | 7 | -- | 30 | 24.0 | -- | 26.9 | 97.0 | -- | 100 |
| PD0956 | Peptidase | SPI | U | U | -- | -- | -- | -- | -- | -- | -- | -- | -- |
| PD1463 | Hypothetical protein | SPI | IM | U | 69 | 38 | 27 | 24.6 | 34.1 | 33.9 | 95.1 | 100 | 99.0 |
| PD1286 | Peptidase S1 | SPII | P | U | 7 | 38 | 10 | 26.7 | 34.1 | 15.4 | 99.0 | 97.1 | 98.0 |
| PD0529 | β-1,4-cellobiosidase | SPI | EC | U | 16 | -- | -- | 33.7 | -- | -- | 95.9 | -- | -- |
| PD1934 | Peptidase S9 | SPI | U | U | 21 | -- | -- | 26.0 | -- | -- | 99.7 | -- | -- |
| PD0576 | Histidine kinase | SPI | IM | U | -- | -- | 10 | -- | -- | 24.2 | -- | -- | 100 |
| PD1835 | Chaperone SurA | SPII | P | U | 8 | 16 | 15 | 35.2 | 54.0 | 52.0 | 100 | 100 | 90.7 |
| PD2120 | Putat. polysaccharide deacetylase | SPII | C | U | 21 | 24 | 23 | 17.7 | 27.6 | 27.4 | 91.7 | 96.2 | 100 |
| PD1836 | LPS-assembly protein LptD | SPI | OM | U | -- | 15 | -- | -- | 28.0 | -- | -- | 100 | -- |
| PD1028 | Polyisoprenoid-binding protein | SPII | U | U | 21 | -- | 9 | 35.2 | -- | 37.8 | 90.2 | -- | 99.7 |
| PD1558 | DNA uptake protein | SPI | IM | U | -- | -- | -- | -- | -- | -- | -- | -- | -- |

Table 3.5 Mass spectrometry data for the 24 proteins with unknown secretion mechanisms in Δ*xpsE* extracellular fractions. Secretion signal prediction was performed using SignalP 5.0 and SecretomeP 2.0. SPI indicates standard Sec signal peptides; SPII indicates lipoprotein Sec signal peptides. SecP indicates non-standard secretion. Predicted subcellular localization was performed using PSORTb v. 3.0.2. C = cyltoplasm; IM = inner membrane; P = periplasm; OM = outer membrane; EC = extracellular; U = unknown. Number of matched peptides, Sequence coverage, and protein probability scores were generated using Scaffold v4.9.0 (Proteome Software Inc., Portland, OR). The Scaffold Probability Score is the percentage of confidence in the identified protein based on matched peptides.

| | | Predictions | | | Matched peptides | | | Seq. Coverage (%) | | | Scaffold Prob. (%) | | |
|---|---|---|---|---|---|---|---|---|---|---|---|---|---|
| PD # | Description | Sec. Signal | Prot. Local. | EC Sec. | Trial 1 | Trial 2 | Trial 3 | Trial 1 | Trial 2 | Trial 3 | Trial 1 | Trial 2 | Trial 3 |
| PD1703 | Lipase | SPI | U | U | 130 | 140 | 101 | 48.0 | 57.7 | 45.3 | 99.3 | 99.9 | 100 |
| PD1702 | Lipase | SPI | U | U | 131 | 132 | 133 | 46.5 | 47.3 | 47.2 | 99.5 | 99.9 | 100 |
| PD0528 | Hypothetical protein | SPI | U | U | 89 | 91 | 71 | 54.4 | 44.7 | 41.0 | 100 | 99.4 | 99.8 |
| PD2039 | L-ascorbate oxidase | SPI | U | U | 90 | 90 | 61 | 35.8 | 35.4 | 24.1 | 99.9 | 100 | 100 |
| PD1211 | Lipase | SPI | U | U | 26 | 36 | -- | 36.3 | 56.2 | -- | 91.4 | 99.9 | -- |
| PD0234 | Aconitate hydratase | SecP | C | U | 36 | 53 | 27 | 35.0 | 33.5 | 52.1 | 97.5 | 96.9 | 100 |
| PD1850 | Peptidase M20 | SPI | U | U | 43 | 67 | 27 | 39.0 | 57.8 | 49.7 | 97.8 | 100 | 93.3 |
| PD1983 | Ribonuclease E/G | SecP | U | U | 32 | 80 | 6 | 25.3 | 25.0 | 10.4 | 98.3 | 100 | 100 |
| PD1168 | Prolyl isomerase | SPI | OM | U | 14 | 73 | 49 | 36.5 | 47.4 | 43.8 | 96.0 | 99.9 | 99.4 |
| PD1853 | Peptidase M16 | SPI | U | U | 55 | 94 | 62 | 28.2 | 37.2 | 24.6 | 98.5 | 100 | 100 |
| PD1299 | Hypothetical protein | SecP | EC | U | 10 | -- | -- | 29.8 | -- | -- | 100 | -- | -- |
| PD1379 | Putat. autotransporter prot. | SPI | OM | U | -- | 37 | 27 | -- | 32.7 | 33.0 | -- | 100 | 100 |
| PD2097 | Peptidase M23 | SecP | EC | U | 86 | 121 | 123 | 33.9 | 30.7 | 32.3 | 98.9 | 99.9 | 100 |
| PD0956 | Peptidase | SPI | U | U | 55 | 35 | 70 | 48.4 | 42.8 | 41.7 | 100 | 98.4 | 100 |
| PD1463 | Hypothetical protein | SPI | IM | U | 34 | 38 | -- | 21.3 | 22.6 | -- | 99.0 | 95.7 | -- |
| PD1286 | Peptidase S1 | SPII | P | U | -- | 32 | 62 | -- | 39.4 | 30.9 | -- | 99.7 | 100 |
| PD0529 | β-1,4-cellobiosidase | SPI | EC | U | 15 | -- | 17 | 20.1 | -- | 28.3 | 97.6 | -- | 100 |
| PD1934 | Peptidase S9 | SPI | U | U | -- | -- | -- | -- | -- | -- | -- | -- | -- |
| PD0576 | Histidine kinase | SPI | IM | U | 16 | 31 | -- | 20.3 | 23.2 | -- | 97.4 | 100 | -- |
| PD1835 | Chaperone SurA | SPII | P | U | 18 | 43 | -- | 31.6 | 42.0 | -- | 99.5 | 97.9 | -- |
| PD2120 | Putat. polysaccharide deacetylase | SPII | C | U | -- | -- | 14 | -- | -- | 16.8 | -- | -- | 90.0 |
| PD1836 | LPS-assembly protein LptD | SPI | OM | U | -- | 15 | -- | -- | 31.4 | -- | -- | 100 | -- |
| PD1028 | Polyisoprenoid-binding protein | SPII | U | U | -- | 10 | 21 | -- | 56.1 | 42.4 | -- | 100 | 100 |
| PD1558 | DNA uptake protein | SPI | IM | U | 6 | 14 | 23 | 41.3 | 47.5 | 40.3 | 100 | 100 | 100 |

Table 3.6 Mass spectrometry data for the 24 proteins with unknown secretion mechanisms in Δ*xpsG* extracellular fractions. Secretion signal prediction was performed using SignalP 5.0 and SecretomeP 2.0. SPI indicates standard Sec signal peptides; SPII indicates lipoprotein Sec signal peptides. SecP indicates non-standard secretion. Predicted subcellular localization was performed using PSORTb v. 3.0.2. C = cyltoplasm; IM = inner membrane; P = periplasm; OM = outer membrane; EC = extracellular; U = unknown. Number of matched peptides, Sequence coverage, and protein probability scores were generated using Scaffold v4.9.0 (Proteome Software Inc., Portland, OR). The Scaffold Probability Score is the percentage of confidence in the identified protein based on matched peptides.

| | | Predictions | | | Matched peptides | | | Seq. Coverage (%) | | | Scaffold Prob. (%) | | |
|---|---|---|---|---|---|---|---|---|---|---|---|---|---|
| PD # | Description | Sec. Signal | Prot. Local. | EC Sec. | Trial 1 | Trial 2 | Trial 3 | Trial 1 | Trial 2 | Trial 3 | Trial 1 | Trial 2 | Trial 3 |
| PD1703 | Lipase | SPI | U | U | 72 | 43 | 46 | 39.5 | 56.1 | 46.9 | 98.6 | 97.3 | 96.2 |
| PD1702 | Lipase | SPI | U | U | 63 | 12 | 28 | 45.3 | 37.5 | 43.2 | 97.3 | 93.8 | 98.2 |
| PD0528 | Hypothetical protein | SPI | U | U | 92 | 21 | 58 | 49.2 | 40.2 | 46.6 | 100 | 100 | 99.5 |
| PD2039 | L-ascorbate oxidase | SPI | U | U | 45 | -- | 14 | 31.2 | -- | 13.9 | 94.9 | -- | 100 |
| PD1211 | Lipase | SPI | U | U | 7 | 6 | 3 | 30.0 | 21.2 | 19.8 | 97.0 | 92.0 | 100 |
| PD0234 | Aconitate hydratase | SecP | C | U | 59 | 38 | 38 | 24.0 | 34.0 | 30.1 | 95.7 | 95.5 | 100 |
| PD1850 | Peptidase M20 | SPI | U | U | 55 | 39 | 37 | 53.5 | 57.3 | 41.2 | 100 | 100 | 100 |
| PD1983 | Ribonuclease E/G | SecP | U | U | 107 | 47 | 69 | 29.5 | 30.1 | 25.7 | 99.9 | 100 | 99.9 |
| PD1168 | Prolyl isomerase | SPI | OM | U | 34 | 34 | 27 | 61.1 | 55.2 | 40.5 | 97.8 | 100 | 100 |
| PD1853 | Peptidase M16 | SPI | U | U | 103 | 61 | 68 | 33.2 | 41.0 | 32.9 | 99.0 | 95.9 | 100 |
| PD1299 | Hypothetical protein | SecP | EC | U | 10 | -- | -- | 21.0 | -- | -- | 90.8 | -- | -- |
| PD1379 | Putat. autotransporter prot. | SPI | OM | U | 110 | 85 | 113 | 40.0 | 45.2 | 36.8 | 99.8 | 99.2 | 100 |
| PD2097 | Peptidase M23 | SecP | EC | U | 50 | -- | 35 | 36.0 | -- | 26.1 | 99.4 | -- | 99.7 |
| PD0956 | Peptidase | SPI | U | U | 19 | -- | -- | 48.8 | -- | -- | 99.7 | -- | -- |
| PD1463 | Hypothetical protein | SPI | IM | U | 83 | 53 | -- | 27.9 | 34.2 | -- | 99.9 | 99.7 | -- |
| PD1286 | Peptidase S1 | SPII | P | U | 18 | 35 | 54 | 28.9 | 29.4 | 32.2 | 99.7 | 100 | 100 |
| PD0529 | β-1,4-cellobiosidase | SPI | EC | U | 52 | 18 | 63 | 24.3 | 24.9 | 31.2 | 95.2 | 100 | 99.9 |
| PD1934 | Peptidase S9 | SPI | U | U | 21 | 9 | 10 | 23.3 | 30.9 | 26.2 | 96.2 | 100 | 100 |
| PD0576 | Histidine kinase | SPI | IM | U | 43 | -- | 7 | 20.8 | -- | 10.3 | 97.4 | -- | 99.0 |
| PD1835 | Chaperone SurA | SPII | P | U | 73 | 18 | 33 | 44.9 | 59.0 | 42.7 | 100 | 100 | 97.7 |
| PD2120 | Putat. polysaccharide deacetylase | SPII | C | U | 86 | 8 | -- | 26.2 | 17.3 | -- | 97.9 | 100 | -- |
| PD1836 | LPS-assembly protein LptD | SPI | OM | U | 65 | -- | -- | 26.6 | -- | -- | 97.5 | -- | -- |
| PD1028 | Polyisoprenoid-binding protein | SPII | U | U | -- | -- | 9 | -- | -- | 26.5 | -- | -- | 100 |
| PD1558 | DNA uptake protein | SPI | IM | U | -- | -- | -- | -- | -- | -- | -- | -- | -- |

Table 3.7 Mass spectrometry data for the 24 proteins with unknown secretion mechanisms in *xpsE*+/- extracellular fractions. Secretion signal prediction was performed using SignalP 5.0 and SecretomeP 2.0. SPI indicates standard Sec signal peptides; SPII indicates lipoprotein Sec signal peptides. SecP indicates non-standard secretion. Predicted subcellular localization was performed using PSORTb v. 3.0.2. C = cyltoplasm; IM = inner membrane; P = periplasm; OM = outer membrane; EC = extracellular; U = unknown. Number of matched peptides, Sequence coverage, and protein probability scores were generated using Scaffold v4.9.0 (Proteome Software Inc., Portland, OR). The Scaffold Probability Score is the percentage of confidence in the identified protein based on matched peptides.

| | | Predictions | | | Matched peptides | | | Seq. Coverage (%) | | | Scaffold Prob. (%) | | |
|---|---|---|---|---|---|---|---|---|---|---|---|---|---|
| PD # | Description | Sec. Signal | Prot. Local. | EC Sec. | Trial 1 | Trial 2 | Trial 3 | Trial 1 | Trial 2 | Trial 3 | Trial 1 | Trial 2 | Trial 3 |
| PD1703 | Lipase | SPI | U | U | 261 | 296 | 305 | 67.2 | 72.8 | 71.6 | 100 | 100 | 100 |
| PD1702 | Lipase | SPI | U | U | 250 | 303 | 290 | 61.1 | 63.8 | 61.2 | 100 | 100 | 100 |
| PD0528 | Hypothetical protein | SPI | U | U | 22 | 130 | 87 | 30.8 | 60.9 | 66.1 | 98.7 | 100 | 100 |
| PD2039 | L-ascorbate oxidase | SPI | U | U | 26 | 23 | 15 | 33.7 | 30.9 | 35.8 | 99.7 | 100 | 100 |
| PD1211 | Lipase | SPI | U | U | 86 | 194 | 207 | 59.6 | 63.3 | 58.7 | 100 | 99.9 | 100 |
| PD0234 | Aconitate hydratase | SecP | C | U | 28 | 50 | 85 | 30.8 | 33.8 | 43.6 | 100 | 99.3 | 99.2 |
| PD1850 | Peptidase M20 | SPI | U | U | 56 | 64 | 43 | 57.5 | 57.9 | 59.7 | 100 | 100 | 100 |
| PD1983 | Ribonuclease E/G | SecP | U | U | 87 | 82 | 52 | 26.1 | 29.1 | 27.2 | 99.1 | 100 | 97.9 |
| PD1168 | Prolyl isomerase | SPI | OM | U | -- | -- | -- | -- | -- | -- | -- | -- | -- |
| PD1853 | Peptidase M16 | SPI | U | U | 72 | 58 | 58 | 37.9 | 33.4 | 33.3 | 100 | 100 | 100 |
| PD1299 | Hypothetical protein | SecP | EC | U | 61 | 152 | 156 | 43.1 | 52.6 | 51.7 | 98.4 | 100 | 100 |
| PD1379 | Putat. autotransporter prot. | SPI | OM | U | 46 | 34 | 60 | 40.9 | 33.0 | 37.5 | 99.1 | 100 | 100 |
| PD2097 | Peptidase M23 | SecP | EC | U | 76 | 161 | 51 | 32.4 | 39.4 | 27.6 | 99.9 | 99.7 | 97.3 |
| PD0956 | Peptidase | SPI | U | U | 32 | 20 | 15 | 41.8 | 53.7 | 37.3 | 97.9 | 100 | 100 |
| PD1463 | Hypothetical protein | SPI | IM | U | 39 | 5 | 29 | 34.4 | 16.7 | 26.3 | 96.1 | 95.0 | 99.2 |
| PD1286 | Peptidase S1 | SPII | P | U | -- | -- | 8 | -- | -- | 28.2 | -- | -- | 99.0 |
| PD0529 | β-1,4-cellobiosidase | SPI | EC | U | 20 | 41 | 25 | 22.4 | 28.4 | 30.9 | 96.1 | 95.0 | 96.2 |
| PD1934 | Peptidase S9 | SPI | U | U | 32 | -- | 19 | 34.3 | -- | 20.0 | 99.7 | -- | 93.2 |
| PD0576 | Histidine kinase | SPI | IM | U | 28 | 37 | -- | 20.7 | 21.5 | -- | 98.1 | 96.9 | -- |
| PD1835 | Chaperone SurA | SPII | P | U | -- | 10 | -- | -- | 35.6 | -- | -- | 100 | -- |
| PD2120 | Putat. polysaccharide deacetylase | SPII | C | U | 46 | 38 | 18 | 20.0 | 22.0 | 42.3 | 95.3 | 93.7 | 100 |
| PD1836 | LPS-assembly protein LptD | SPI | OM | U | 20 | 15 | 21 | 31.2 | 27.3 | 20.6 | 96.0 | 97.9 | 97.4 |
| PD1028 | Polyisoprenoid-binding protein | SPII | U | U | -- | 5 | 7 | -- | 40.5 | 47.3 | -- | 100 | 100 |
| PD1558 | DNA uptake protein | SPI | IM | U | 20 | 21 | 24 | 47.4 | 45.0 | 33.5 | 100 | 100 | 100 |

Table 3.8 Mass spectrometry data for the 24 proteins with unknown secretion mechanisms in *xpsG*+/- extracellular fractions. Secretion signal prediction was performed using SignalP 5.0 and SecretomeP 2.0. SPI indicates standard Sec signal peptides; SPII indicates lipoprotein Sec signal peptides. SecP indicates non-standard secretion. Predicted subcellular localization was performed using PSORTb v. 3.0.2. C = cyltoplasm; IM = inner membrane; P = periplasm; OM = outer membrane; EC = extracellular; U = unknown. Number of matched peptides, Sequence coverage, and protein probability scores were generated using Scaffold v4.9.0 (Proteome Software Inc., Portland, OR). The Scaffold Probability Score is the percentage of confidence in the identified protein based on matched peptides.

# 4. Chapter 4

# Pierce's Disease symptom progression in *Vitis vinifera* is accompanied by increased tylose-mediated vessel occlusion and starch depletion

## Abstract

Prolonged water stress and carbon starvation are two hallmarks of plant decline. Symptoms of Pierce's disease (PD) in grapevine (*Vitis vinifera*) caused by the xylem-limited bacterial pathogen, *Xylella fastidiosa* (*X. fastidiosa*), have similarities to drought stress. Several studies have shown that tylose-mediated vessel occlusion occurs in grapevines infected with *X. fastidiosa*, though their role in PD symptom progression has been a subject of debate. In this study, we used scanning electron microscopy (SEM) to visualize tylose formation and *X. fastidiosa* presence during different phases of PD symptom progression. Likewise, we used X-ray computed microtomography (microCT) to assess starch depletion and RNAseq to assess *Vitis vinifera* transcriptomic changes during *X. fastidiosa* infection. Genes related to tylose formation, including those involved in ethylene signaling and cell wall biogenesis, and genes related to drought stress were consistently up-regulated. The percentage of vessels occluded with tyloses increased as PD symptoms progressed over an extended period of time, suggesting that PD induces prolonged water stress. A majority of vessels with tyloses were devoid of bacterial cells, indicating that direct, localized perception of *X. fastidiosa* was not the primary cause of tylose formation. The down-regulation of photosynthesis- and carbon-fixation-related genes and the occurrence of starch depletion as PD symptoms progressed indicate that *Vitis vinifera* grapevines likely undergo carbon starvation as a result of prolonged *X. fastidiosa* infection.

# Introduction

*Xylella fastidiosa* (*X. fastidiosa*) is a gram-negative proteobacteria that has evolved to exclusively colonize the xylem, a relatively nutrient poor niche, of its plant hosts. The xylem is comprised of many interconnected vessels of finite, variable length that are connected by bordered pits containing pit membranes (Thorne et al. 2006b, Tyree and Zimmerman 2002, Brett and Waldron 1996). Pit membranes are porous structures that allow the passage of water and small solutes, regulate the cavitation threshold, and prevent the free movement of air embolisms and pathogens (Stevenson et al. 2004, Tyree and Zimmerman 2002, Sperry et al. 1991). In order to systemically colonize the xylem, *X. fastidiosa* degrades pit membranes to move between vessels (Ingel et al. 2019, Perez-Donoso et al. 2010, Roper et al. 2007). Movement between hosts is facilitated by xylem-feeding hemipteran leafhopper insects such as the glassy-winged sharpshooter (*Homalodisca vitripennis*) (Hill and Purcell 1995). In several hosts, *X. fastidiosa* exists as an endophyte where it inhabits the xylem, but does not cause disease (Hopkins 1989). However, *X. fastidiosa* is the causal agent of many significant diseases such as Pierce's disease (PD) in grapevine (*Vitis vinifera*), citrus variegated chlorosis, coffee leaf scorch, and most recently, olive quick decline syndrome (Chang et al. 1993; Li et al. 2001, Saponari et al. 2013, Davis et al. 1978). The mechanism by which *X. fastidiosa* causes disease only in certain hosts has not been fully elucidated, though current evidence suggests compatibility between pit membrane carbohydrate composition and *X. fastidiosa*-secreted cell wall-degrading enzymes facilitates disease onset and progression (Ingel et al. 2019, Sun et al. 2011).

One symptom commonly seen in many hosts infected with *X. fastidiosa* is leaf scorching, a symptom similar to drought-induced water stress (McElrone et al. 2001; McElrone et al. 2003; Thorne et al. 2006a). During drought, reduced water uptake and increased transpiration lower xylem pressure to a point where cavitation occurs as air is pulled into the water column from adjacent air-filled spaces (air embolism) (Hopkins 1989, Mayr et al. 2014). Consequently, air embolisms can spread within the xylem if the pressure differential between embolized and water-filled vessels causes air seeding across the pit membrane or if pit membranes have been ruptured (Choat et al. 2003, Plavcová et al. 2013, Sperry and Tyree 1988). Interestingly, Perez-Donoso et al. (2007) determined that asymptomatic grapevines inoculated with *X. fastidiosa* experienced significantly more cavitation prior to symptom development relative to healthy control vines, indicating that the cause of cavitation was likely pathogen-induced. Furthermore, the authors speculated that the degradation of pit membranes by *X. fastidiosa* cell wall-degrading enzymes could facilitate the spread of air embolisms.

The spread of air embolisms within the xylem can be severely detrimental to hydraulic conductivity. As a result, plants produce tyloses in response to air embolisms caused by cavitation resulting from wounding or damage to the vascular tissue to seal affected vessels and divert water to other vessels (Zimmerman 1979, De Micco et al. 2016). Tyloses are outgrowths from adjacent ray parenchyma cells called contact cells (Chafe, 1974). These contact cells contain a protective layer composed of primary cell wall components that is deposited between the protoplast and the pit membrane (Meyer and Cote, 1968). Upon tylose induction, the protective layer expands beyond the pit

membrane and into the xylem vessel lumen via the incorporation of new primary cell wall components such as cellulose, hemicellulose, and pectin (Foster 1967, Murmanis 1975, Sachs 1970). Once the tylose is fully expanded, secondary cell wall components such as suberin or lignin are deposited, creating an impermeable barrier (Parameswaran et al. 1985, Sachs 1970). The mechanisms facilitating tylose formation have not been fully elucidated, though ethylene and jasmonic acid signaling pathways appear to be involved, as well as the down-regulation of pectin methylesterases (Leśniewska et al. 2017, McElrone et al. 2010, Sun et al. 2007).

Additionally, tyloses developed is response to biotic stress (air embolisms induced by pathogen-mediated vascular damage) can slow or prevent pathogen movement within the xylem, and the success of this defense is dependent on the rate of tylose formation relative to the rate of pathogen spread (Bonsen and Kučera 1990, Del Rio et al. 2001). Indeed, tyloses have been observed in grapevines infected with *X. fastidiosa*, and that cavitation events precede tylose formation at the early stage of PD (Fritschi et al. 2008, Sun et al. 2013, Perez-Donoso et al. 2016). However, the overproduction of tyloses in response to biotic stress can cause a detrimental reduction in hydraulic conductivity within the xylem (Collins et al. 2009 McElrone et al. 2010). Sun et al. (2013) also demonstrated this with *X. fastidiosa* in susceptible grapevines (cv. Chardonnay), which experienced significant tylose-induced-vessel occlusion and subsequent loss of hydraulic conductivity 12 weeks after inoculation.

Water stress induced by drought or vessel occlusion can have a significant effect on major physiological processes, subsequently affecting carbon uptake and utilization.

Often plants will reduce the rate of transpiration by closing their stomata to mitigate water loss and increased risk of cavitation, but the consequence of this is a significant reduction in photosynthesis (Pinheiro and Chaves 2010). Plant growth is also significantly affected, and despite the reduction in photosynthesis, the near cessation of plant growth causes an excess of carbon to accumulate as starch (Estiarte and Peñuelas 1999, Hummel et al. 2010). Under acute water stress conditions, plants can use this accumulated starch to continue essential processes such as respiration, metabolism, and defense (McDowell 2011). However, prolonged water stress caused by an increasing number of air embolisms and vessel blockages can result in a prolonged reduction in photosynthesis (Brodribb and Holbrook 2006, Hölttä et al. 2009). Without an adequate supply of carbon from the leaves over time, starch reserves begin to deplete as the amount of carbon required for survival becomes greater than the amount of carbon available (Gibon et al. 2009, McDowell 2011). This phenomenon is known as carbon starvation, and when combined with hydraulic failure from chronic water stress, can cause leaf shedding, disruption of xylem and phloem transport, and turgor loss, leading to plant death (Brodribb and Holbrook 2006, Tyree et al. 1993, Tyree and Sperry 1989, Sevanto 2014). These series of events can be further exacerbated by biotic stress from pathogen attack as carbon-rich defense production ceases due to carbon deficit, ultimately quickening plant death (Guérard et al. 2007, McDowell 2011, Poorter and Villar 1997).

The primary focus of *X. fastidiosa* research has predominantly involved the discovery of virulence factors (Chatterjee et al. 2008, Rapicavoli et al. 2018). While direct *X. fastidiosa*-mediated attack does play a significant role in PD symptom development, its

inability to completely occlude xylem vessels while causing drought-like symptoms indicates that host physiological response could contribute to PD (Nascimento et al. 2016, Sun et al. 2013). The major causes of water stress, cavitation and vessel occlusion, are present in grapevines infected with *X. fastidiosa* during PD symptom development, and while PD symptom development has been correlated with tylose production and loss of hydraulic conductivity, it remains unclear if vessel occlusion caused by tylose production facilitates prolonged water stress and induces carbon starvation as PD symptoms worsen. In this study, we demonstrate that both tylose production and tylose-induced vessel occlusion increase as PD symptoms progress, fulfilling the conditional requirement for prolonged water stress. Furthermore, we show that starch depletion occurs during the later phases of PD, indicating that grapevines infected with *X. fastidiosa* experience carbon starvation. Taken together, these data suggest that excessive tylose production caused by *X. fastidiosa* infection in grapevines contributes to prolonged water stress and carbon starvation, which ultimately leads to plant death.

## Materials and Methods

**Grapevines and bacterial strains.** *Vitis vinifera* cv. Cabernet sauvignon grapevines generously provided by Foundation Plant Services (UC Davis) were propagated from cuttings in vermiculite trays and transplanted into 1-gallon pots after root and shoot establishment. Vines were pruned to a single shoot, which was tied to a bamboo stake and allowed to grow to five feet tall under greenhouse conditions. Optimal water and nutrients were provided on a consistent basis.

*X. fastidiosa* Temecula 1 (wild type strain) was grown on PD3 agar media at 28°C for five days (Davis et al. 1981). Cells were harvested from PD3 agar plates with 1X PBS and the $OD600_{nm}$ was adjusted to 0.25 (approximately $1x10^8$ CFUs/ml).

***In planta* inoculations.** Grapevines were mechanically inoculated using a method adapted from Purcell and Sanders (1999). 20 µl of harvested *X. fastidiosa* cells ($OD600_{nm}$ = 0.25) was placed on the sixth internode of the stem, and the stem was pierced through the droplet using a 20-gauge needle. The needle was inserted to a depth where it penetrated the xylem, whereby the negative pressure of the xylem facilitated uptake of the inoculum droplet. Grapevines inoculated with 1X PBS served as negative controls, and all vines were randomized.

PD symptoms were rated on a weekly basis using the 0 – 5 PD rating scale established by Guilhabert and Kirkpatrick (2005) where 0= a healthy vine, 1= one or two leaves with scorching at the margins, 2= two or three leaves with more developed scorching, 3= all leaves with some scorching and a few matchstick petioles, 4= all leaves with heavy scorching and many matchstick petioles, and 5= a dead or dying vine. The trial was split up into three disease stage groups: Phase I (PD symptom score = 1-2), Phase II (PD symptom score = 2-3), and Phase III (PD symptom score = 3-4). Each disease stage group consisted of three biological replicates each containing three technical replicates, totaling nine wild type-inoculated vines and nine negative control vines.

**Grapevine tissue harvesting.** Once the average PD symptom score of the wild type-inoculated vines was within the established range for each Phase of PD, stem tissue was harvested for 1) tylose analysis via scanning electron microscopy (SEM), 2) starch analysis via microCT, and 3) transcriptomic analysis via RNAseq. The internode directly above the point of inoculation (POI) was excised from the vine and immediately immersed in liquid nitrogen for subsequent RNA extraction and RNAseq analysis. The second internode above the POI was excised was dried at 40°C for 24 hours in preparation for microCT analysis. The rest of the vine was used for SEM.

**Scanning electron microscopy.** Experimental vines for this study were inoculated with either PBS or wild-type *X. fastidiosa* (Temecula 1) and were visualized at either Phase I or Phase II of PD symptom development. Three vines from each inoculation type at each PD phase were used to investigate xylem structural features, detect *X. fastidiosa* distribution and quantify vascular occlusion of their stems. For each vine from Phase II (either inoculated with PBS or *X. fastidiosa*), five internode lengths of approximately 2 cm were sampled, respectively, from the 3rd, 7th, 11th, 13th and 17th internodes, counting upwards from the POI, which was considered internode zero (the same below). Sampling occurred in the same way for each vine from Phase I except that samples were collected from the 4th, 12th and 18th internodes. Samples from Phase I and Phase II were then fixed in PEM (50 mM PIPES, 5 mM EGTA, 5 mM MgSO4, pH 6.9) buffer containing 4% paraformaldehyde (PFA) and FAA (formalin-acetic acid-alcohol), respectively, for at least 24 hours. Then, multiple 1.0 mm thick stem disks and segments

exposing a radial or tangential surface were trimmed from each fixed sample. Sample trimming was conducted in 50 mM PIPES for the samples fixed with PFA and in 50% ethanol for those fixed with FAA. Trimmed specimens from PFA-fixed samples were dehydrated through an ethanol series of 10%, 30%, 50%, 70%, 85%, 90%, 95%, 100% and 100% with a 20 min stay at each step, while those from FAA-fixed samples started the dehydration process from 70% also with 20 min at each step. Dehydrated specimens were critical-point-dried with DCP-1 (Denton Vacuum, Inc., USA) or Autosamdri-931 (Tousimis Research Corp., Inc., USA) and then sputter-coated with Au/PD with Desk II (Denton Vacuum, Inc., USA) or CCU-010 Compact Coating Unit (Safematic GmbH, Switzerland). Coated specimens were examined and photographed under a scanning electron microscope (Hitachi S3400N, Hitachi Science Systems, Ltd., Japan) at an accelerating voltage of 8 kV.

Images of transverse sections of stem disks were used to quantify occluded xylem vessels. Stem disks from three vines were analyzed for each investigated internode of each inoculation type at either of the two phases. For each stem disk, one-third of the xylem sector of the whole stem transverse surface was randomly selected to count the total vessel number and the number of the vessels with tylose(s) or crystal(s), from which a percentage of vessels with vascular occlusion was calculated and used as a representative of the stem disk's vascular occlusion status. Each datum point of vascular occlusion status was presented as a mean with standard error of three samples/vines.

**X-ray micro-computed tomography.** Dried stems were scanned in a 21-keV synchrotron x-ray beam using a continuous tomography setting yielding 1,025 two-dimensional longitudinal images (resolution of 1.27 mm/pixel), which were captured on a complementary metaloxide semiconductor (CMOS) camera (PCO.edge; PCO) at 350 ms exposure time. Acquired raw images were reconstructed into transverse images using a custom software plugin for the image-processing software FIJI (www.fiji.sc; ImageJ) that was developed at the Advance Light Source (Lawrence Berkeley National Laboratory, Beamline 8.3.2). Quantitative analysis was conducted using the middle slice of image stacks reconstructed with standard gridrec Fourier reconstruction to determine starch depletion in ray parenchyma. Starch depletion was quantified using machine-learning algorithms developed by Earles et al. (2018).

**Statistical analysis of starch depletion.** A beta regression model was applied to the starch depletion data using time (phase) and treatment (*X. fastidiosa* and 1× PBS) as independent variables. Post-hoc analysis was performed using least square means to generate pairwise comparisons of Phase within treatment and comparisons between treatments. P-values were adjusted using the Tukey-Kramer method. Model generation and post-hoc analysis were performed in R using the betareg and emmeans packages (Cribari-Neto and Zeileis 2010, Lenth 2019, R Core Team 2019).

**RNA extraction and library preparation.** Total RNA was isolated using a CTAB-based extraction protocol as described in Blanco-Ulate et al. (2013). RNA concentration and

purity were measured using a Qubit fluorometer (Thermo Scientific) and a NanoDrop 2000c Spectrophotometer (Thermo Scientific), respectively. Libraries were prepared using the Illumina TruSeq RNA sample preparation kit v.2 (Illumina, CA, USA). Final libraries were evaluated for quantity and quality using the High Sensitivity DNA kit on a Bioanalyzer 2100 (Agilent Technologies, CA).

**RNA sequencing and downstream analysis.** cDNA libraries were sequenced using an Illumina HiSeq4000 sequencer (DNA Technologies Core, University of California, Davis, California, USA) as single-end 100-bp reads (Illumina, CA, USA). Illumina reads were trimmed using Trimmomatic v.0.36 (Bolger et al., 2014) with the options LEADING:3 TRAILING:3 SLIDINGWINDOW:10:20 MINLEN:20. Trimmed single-end reads were mapped onto the predicted protein-coding sequences of *V. vinifera* 'PN40024' (version V1 from http://genomes.cribi.unipd.it/grape/) using Bowtie2 v.2.3.4.1 (Langmead and Salzberg, 2012) with parameters: -q -end-to-end -sensitive -no-unal. Counts of reads mapping uniquely onto the grape reference transcriptome (i.e., with Q > 30) were extracted using sam2counts.py v.0.91 (https://github.com/vsbuffalo/sam2counts). Details on trimming and mapping results are reported in Table 4.1. The Bioconductor package DESeq2 v.1.16.1 (Love et al., 2014) was used for read count normalization and for statistical testing of differential gene expression. The VitisNet functional annotations were used to assign grape genes to functional categories (Grimplet *et al.*, 2009). Enrichment analyses of grape biological functions were computed in R using the classic Fisher method ($P$-value $\leq 0.05$).

## Results

**PD can be divided into three phases based symptom progression.** The 0 -5 PD rating index developed by Guilhabert and Kirkpatrick (2005) was divided into phases of PD symptom progression. A PD symptom score of 0-2 was considered Phase I, where PD symptoms first become apparent, with chlorosis and marginal leaf scorching present on a few leaves, usually near the POI (Fig. 4.1A). Phase II is defined by a PD symptom score of 2-4 where the entire vine is affected and all leaves have heavy chlorosis and leaf scorching, with a few petioles beginning to drop their leaves and displaying blackened tips (matchstick petioles) (Fig. 4.1B). Phase III is defined by a PD symptom score of 4-5 where the vine is steadily declining towards death, with most of the petioles having dropped their leaves and what leaves remaining are completely scorched (Fig. 4.1C).

**The percentage of tylose-occluded vessels increases from Phase I to Phase II of PD.** SEM was used to determine tylose formation, the percentage of occluded vessels, and *X. fastidiosa* distribution at multiple points above the POI during Phase I and Phase II of PD symptom progression. During Phase I of PD symptom progression, only 2% of xylem vessels in PBS-inoculated negative control vines have tyloses at the fourth internode above the POI, and are free of any occlusion (Fig. 4.2A; 4.3A, B). Similarly, only 3.7% of *X. fastidiosa*-inoculated vines have tyloses at the fourth internode above the POI, and are generally free of occlusion (Fig. 4.2A; 4.3B). Interestingly, small tyloses and crystalline structures were visible in some vessels of *X. fastidiosa*-inoculated vines, but were not present in PBS-inoculated negative control vines, indicating that PD-related

tylose formation may begin during this initial phase (Fig 4.3C-F). However, this phenomenon was not seen at the 12$^{th}$ internode above the POI (Fig. 4.3G), and the percentage of occluded vessels at this internode and the 18$^{th}$ internode were similar in both PBS-inoculated negative control vines and *X. fastidiosa*-inoculated vines (Fig. 4.2A).

During Phase II of PD symptom progression, the percentage of vessels with tyloses in PBS-inoculated negative control vines was 5% at the third internode above the POI, and vessels were free of occlusions (Fig. 4.2B; 4.4A, B). Similarly, tyloses were only present in 3 – 6% of vessels in PBS-inoculated vines at the 7$^{th}$, 11$^{th}$, 13$^{th}$, and 17$^{th}$ internodes, and vessels were free of any occlusions. Conversely, 35 – 50% of vessels at the same internodes above the POI in *X. fastidiosa*-inoculated vines contained tyloses (Fig. 4.2B). At the third internode above the POI, both clear and occluded vessels were seen, and the pattern of occluded vessels appears random (Fig. 4.4C). The tyloses in these occluded vessels are not sporadic clusters, but rather appear to completely fill the vessel (Fig. 4.4D, E). Interestingly, only in *X. fastidiosa*-inoculated vines during Phase II of PD symptom progression was this type of occlusion also present more distally at the 11$^{th}$ internode above the POI (Fig. 4.4F) and as far away as the 17$^{th}$ internode, indicating that tylose formation significantly increases throughout the vine between Phase I and Phase II (Fig. 4.2).

***X. fastidiosa* is randomly distributed throughout the xylem during Phase II of PD.** Despite PD symptom development during Phase I, *X. fastidiosa* cells were not visualized in the xylem vessels of infected vines (*data not shown*). However, by Phase II of PD

symptom progression, *X. fastidiosa* cells were visualized in approximately 10% of the vessels in infected vines, and were present throughout the vines (Fig. 4.5). At the 3rd and 11th internodes above the POI, *X. fastidiosa* cells appeared both as individual cells and as cell aggregates along the lateral wall of the corresponding xylem vessel (Fig. 4.5B-D). Interestingly, at the 17th internode, *X. fastidiosa* cell aggregates could be seen on top of a tylose, with some cell clusters forming biofilms, indicating that despite being defensive structures, tyloses can inadvertently provide an adequate surface for *X. fastidiosa* colonization (Fig. 4.5E, F). There does not appear to be a localized correlation between *X. fastidiosa* and tyloses as *X. fastidiosa* cells were found in vessels both with and without tyloses. Furthermore, several vessels were visualized that contained tyloses, but *X. fastidiosa* cells were not present. No *X. fastidiosa* cells were found in any vessels of the PBS-inoculated negative control vines (Fig. 4.5A).

***X. fastidiosa* infection induces starch depletion during the later phases of PD.** To determine if carbon starvation occurs as PD symptoms progress, microCT was used to visualize the ray parenchyma cells between xylem vessels where carbon is stored as starch. A machine-learning algorithm developed by Earles et al. (2018) was applied to the images to elucidate starch-depleted sections of the ray parenchyma during each Phase of PD (Fig. 4.6). In Phase I, the ray parenchyma cells in *X. fastidiosa*-inoculated vines are nearly all filled with starch, similar to the ray parenchyma cells in PBS-inoculated negative control vines. During Phase II, the starch levels in PBS-inoculated negative control vines appear similar to Phase I levels. However, the starch levels in *X. fastidiosa*-

inoculated vines have decreased from Phase I levels, indicating that starch depletion begins to occur during Phase II of PD. During Phase III, starch levels in PBS-inoculated vines appear to be slightly decreased from Phase I and II levels, but still remain mostly filled, while the starch levels in *X. fastidiosa*-inoculated vines show a marked decrease from Phase II starch levels.

To determine if the level of starch was significantly depleted from Phase I to Phase III seen in *X. fastidiosa*-inoculated vines relative to PBS-inoculated negative control vines, the machine learning algorithm was used to calculate the percentage of ray parenchyma still filled with starch. From Phase I to Phase III, the percentage of filled ray parenchyma in PBS-inoculated negative control vines only decreased from 94% to 90%, while the percentage of filled ray parenchyma in *X. fastidiosa*-inoculated vines decreased from 90% to 83% from Phase I to II, and from 83% to 76% from Phase II to III (Fig. 4.7).

The starch depletion data generated by the machine-learning algorithm conformed to a beta distribution with values ranging from 0-1 (Fig. 4.9A). A beta regression model applied to the data maintained the lowest Akaike information criterion and the Bayseian information criterion scores compared to alternative models and was considered the model of best fit based on via residual analysis (Fig. 4.9B). A least square means post hoc analysis with P-value adjustment via the Tukey-Kramer method was used to determine if starch depletion was significantly different from Phase I to Phase III in *X. fastidiosa*-inoculated vines relative and PBS-inoculated negative control vines. In PBS-inoculated vines, the starch levels during Phase I were not significantly different from starch levels during Phase III (P=0.074). However, the starch levels during Phase I were significantly

different from starch levels during Phase III (P=0.009) in *X. fastidiosa*-inoculated vines. Furthermore, the model was used to determine if starch depletion was significantly different in *X. fastidiosa*-inoculated vines relative to PBS-inoculated negative control vines during each phase of PD symptom development. During Phase I, the difference in starch levels was not significant (P=0.061), while starch levels were significantly less in *X. fastidiosa*-inoculated vines during Phase II (P=0.014) and Phase III (P=0.009). Taken together, these results indicate that starch depletion occurs as a result of PD.

**Transcriptomic profiling of *X. fastidiosa*-inoculated vines shows significant changes in genes related to water stress and carbon starvation.** Transcriptomes of *X. fastidiosa*- and PBS-inoculated vines were profiled using RNA sequencing (RNAseq) during Phase I and Phase II of PD symptom progression. An average of 12.8 ± 1.1 million high-quality reads was aligned to the grape transcriptome (Table 4.1). Differential gene expression analysis between *X. fastidiosa*- and PBS-inoculated vines was performed at both phases. A total of 5,651 differentially expressed genes (DEGs) were detected in response to *X. fastidiosa* infection, with a higher number of DEGs detected during Phase I (4,637) compared to Phase II (2,264) (Figure 4.10A). Moreover, we found that more genes were up-regulated rather than down-regulated during both phases. Comparison of the up- and down-regulated genes showed that about half (53%) of the DEGs detected during Phase II were also modulated during Phase I (Figure 4.10B). These results show that the major transcriptional re-programming caused by *X. fastidiosa* infection occurred during Phase I even though vascular symptoms, such as starch depletion and tylose

formation, were not yet observed during this phase of PD symptom development. However, the similarity of DEGs during Phase I and Phase II suggests a commonality of biological processes in the plant response throughout PD symptom progression.

The gene expression profiles of *X. fastidiosa*- and PBS-inoculated vines were compared at both phases, and differentially expressed genes were classified into six groups (I-VI) based on their expression patterns (Fig. 4.8A). Among the up-regulated genes, several functional categories (FCTs) were identified as significantly enriched (Fisher's exact test, $P$-value $\leq 0.05$) by *X. fastidiosa* infection only during Phase I, such as "Jasmonate signaling", "Carbohydrate metabolism", and "Starch and sucrose metabolism", while FCTs identified as significantly enriched by *X. fastidiosa* infection only during Phase II were related to the NBS-LRR superfamily. FCTs identified as significantly enriched by *X. fastidiosa* infection in both phases included "Biotic stress response", "Salicylic acid signaling", "Ethylene signaling", "Cell wall organization and biogenesis", "Monosaccharide metabolism", and "Drought response" (Fig. 4.8B).

Interestingly, *X. fastidiosa* infection triggered the up-regulation of genes involved in the biosynthesis of cell wall materials in both phases, including cellulose synthases, xylan synthases, and galacturonosyltransferases, as well as genes associated with hemicellulose and pectin rearrangement, including xyloglucan endotransglucosylase/hydrolases, pectate lyases, pectin methylesterases, pectinacetylesterases, and polygalacturonases (Fig. 4.11). Additionally, genes related to ethylene biosynthesis were also significantly up-regulated in both phases, including 1-

aminocyclopropane-1-carboxylate synthases and 1-aminocyclopropane-1-carboxylate oxidases (Table 4.2).

Genes related to carbohydrate, starch, and sucrose biosynthesis were only significantly up-regulated in *X. fastidiosa*-inoculated vines during Phase I, including an ADP-glucose pyrophosphorylase, sucrose synthases, glucose-6-phosphate translocators, vacuolar invertases, fructokinases, a phosphoglucomutase, and a 6-phosphofructokinase. Relatively few genes related to starch degradation were significantly up-regulated, and only included two α-amylases.

Several FCTs related to the photosynthetic process, such as "Photosynthesis", "Chlorophyll biosynthesis", and "Thylakoid organization and biogenesis", were only significantly down-regulated in *X. fastidiosa*-inoculated vines during Phase I, while FCTs related to aquaporins were only significantly down-regulated in *X. fastidiosa*-inoculated vines during Phase II. FCTs related to carbon fixation were significantly down-regulated in *X. fastidiosa*-inoculated vines during both phases (Fig. 4.8C). Over-represented FCTs up-regulated and down-regulated during Phase I are presented in Tables 4.2 and 4.3, respectively. Over-represented FCTs up-regulated and down-regulated during Phase II are presented in Tables 4.4 and 4.5, respectively.

## Discussion

Prolonged water stress is considered one of the main factors for plant decline and is defined as the inability to adequately move water from the roots to the foliage over an extended period of time (Sevanto et al, 2014). With regards to PD in grapevines, water

stress has been proposed as one of the major factors in symptom development and progression, and is thought to occur as a result of xylem vessel occlusion via *X. fastidiosa* biofilms or tylose formation in response to *X. fastidiosa* infection (Chatterjee et al. 2008, Sun et al. 2013). This study shows that during Phase I of PD when symptoms are first developing and affecting a few leaves near the POI, *X. fastidiosa* aggregates are not present and tyloses are only just beginning to form in a few vessels while most vessels remain clear of obstructions. These results imply that the initial PD symptoms are not related to water stress via vessel obstruction, and could instead be the product of direct host-microbe interactions related to host defense responses. However, between Phases I and II of PD, tylose production dramatically increases, with nearly 50% of xylem vessels occluded with tyloses. Furthermore, genes associated with ethylene production and cell wall biogenesis, processes that are necessary for tylose formation, are significantly up-regulated during both phases (De Micco et al. 2016, McElrone et al. 2010, Sun et al. 2007), as well as genes related to drought stress. Interestingly, genes related to photosynthesis and carbon fixation were down-regulated during Phase I, implying the cessation of plant growth, and thus, the cessation of new xylem vessel formation. Taken together, the significant increase in tylose occluded vessels from Phase I to Phase II of PD, unmitigated by new vessel production, suggests that *X. fastidiosa*-infected grapevines enter a period of tylose-mediated prolonged water stress that correlates with worsening symptoms.

The cause of tylose production in the course of PD is a subject of debate, in which the leading hypotheses are that tyloses are the result of either direct host-microbe

interactions or in response to *X.fastidiosa*-induced air embolisms (Fry and Milholland 1990, Perez-Donoso et al. 2016). As the percentage of tylose-occluded vessels increases from Phase I to Phase II, the percentage of vessels with *X. fastidiosa* also increases, though the percentage of *X. fastidiosa*-positive vessels remains low relative to the percentage of tylose occluded vessels. As a result, the percentage of vessels with both tyloses and *X. fastidiosa* cells is much lower than the percentage of vessels with tyloses alone, indicating that each instance of tylose formation is not the result of direct localized interactions between the vine and *X. fastidiosa*. Instead, these results could imply that tylose formation is triggered by direct interactions in one vessel, and a defensive signal could be sent to other vessels via the adjacent parenchyma cells. Alternatively, these results could imply that air embolisms induced by activities such as *X. fastidiosa* mediated cell wall degradation, are moving into adjacent vessels and triggering tylose formation (Bonsen and Kučera 1990). It has been well-documented that *X. fastidiosa* can be found beyond tylose-occluded vessels (Fritschi et al 2008), indicating that either this defensive tactic is inadequate despite host perception of *X. fastidiosa*, or direct perception of *X. fastidiosa* is not the primary reason for tylose formation.

Another hallmark of plant decline is carbon starvation, which is intimately linked to prolonged water stress (McDowell, 2011). During Phase I of PD, starch stores in the ray parenchyma remain full in *X. fastidiosa*-inoculated vines, which would be expected given that a prolonged water stress event has not occurred at this initial phase of PD. However, genes related to photosynthesis and carbon fixation are down-regulated, while genes related to starch accumulation are up-regulated. This indicates that acute water

stress is occurring during Phase I despite the absence of vessel occlusions, and could be the result of other factors such as air embolisms. By Phase II, tylose-mediated vessel occlusion has created prolonged water stress, creating the conditions necessary for carbon starvation to occur. Indeed, during Phase II, carbon fixation genes remain down-regulated, starch accumulation genes are no longer up-regulated, and the ray parenchyma cells are beginning to show signs of depletion. By Phase III, significant starch depletion is occurring in the ray parenchyma cells, indicating that carbon starvation is well underway during this phase of PD.

There is much debate about how *X. fastidiosa* interfaces with grapevines and how it facilitates PD. Here, we show that vessel occlusion does not occur during Phase I of PD symptom progression, but conditions for acute water stress are present, implying that air embolisms could be a contributing factor. During Phase II, nearly half of the vessels are occluded with tyloses and starch in the ray parenchyma cells is beginning to deplete, indicating prolonged water stress, and during Phase III, starch is significantly depleted, indicating carbon starvation. Induction of prolonged water stress and carbon starvation is not unique to PD, and similar physiological responses have been reported for vascular fungal pathogens such as *Neofusicoccum parvum*, (Massonnet *et al.*, 2017). Nonetheless, to the best of our knowledge, this is the first instance of a bacterial pathogen inducing these types of physiological responses. Tylose-mediated vessel occlusion appears to be the driving force behind the induction of prolonged water stress and subsequently, carbon starvation. The trigger for tylose formation still remains unclear, though our data suggest

that air embolisms may be the cause. However, elucidation of this mechanism requires further study.

# Literature Cited


Blanco-Ulate, B., Vincenti, E., Powell, A. L. T., and Cantu, D. 2013. Tomato transcriptome and mutant analyses suggest a role for plant stress hormones in the interaction between fruit and *Botrytis cinerea*. Front. Plant Sci. 4:142.

Brett, C. T., and Waldron, K. W. 1996. Physiology and biochemistry of plant cell walls. Springer Science & Business Media, Heidelberg.

Bolger, A. M., Lohse, M., and Usadel, B. 2014. Trimmomatic: a flexible trimmer for Illumina sequence data. Bioinformatics. 30:2114–2120.

Bonsen K. J. and Kučera L. J. 1990. Vessel occlusions in plants: morphological, functional and evolutionary aspects. IAWA J. 11: 393–399.

Brodribb, T. J. and Holbrook, N. M. 2006. Declining hydraulic efficiency as transpiring leaves desiccate: two types of response. Plant, Cell & Environment. *29*(12):2205-2215.

Chang, C. J., Garnier, M., Zreik, L., Rossetti, V., and Bové, J. M. 1993. Culture and serological detection of the xylem-limited bacterium causing citrus variegated chlorosis and its identification as a strain of *Xylella fastidiosa*. Current Microbiology. 27:137-142.

Chatterjee, S., Almeida, R. P. P., and Lindow, S. 2008. Living in two worlds: The plant and insect lifestyles of *Xylella fastidiosa*. Annual Review of Phytopathology. 46:243-271.

Choat, B., Ball, M., Luly, J. and Holtum, J. 2003. Pit membrane porosity and water stress-induced cavitation in four co-existing dry rainforest tree species. Plant Physiology. 131(1):41-48.

Collins, B. R., Parke, J. L., Lachenbruch, B. and Hansen, E. M. 2009. The effects of Phytophthora ramorum infection on hydraulic conductivity and tylosis formation in tanoak sapwood. Canadian journal of forest research. 39(9):1766-1776.

Cribari-Neto, F., Zeileis, A. 2010. Beta Regression in R. Journal of Statistical Software. 34(2):1-24. URL http://www.jstatsoft.org/v34/i02/.

Davis, M. J., Purcell, A.H. and Thomson, S.V. 1978. Pierce's disease of grapevines: isolation of the causal bacterium. Science. 199(4324):75-77.

Davis, M. J., French, W. J. and Schaad, N. W. 1981. Axenic culture of the bacteria associated with phony disease of peach and plum leaf scald. Current Microbiology. 6:309-314.

Del Rio J. A., Gonzales A., Fuster M. D., Botia J. M., Gomez P., Frias P. and Ortunio A. 2001. Tylose formation and changes in phenolic compounds of grape roots infected with *Phaemoniella chlamydospora* and *Phaeoacremonium* species. Phytopathol. Mediterr. 40: 394–399.

De Micco, V., Balzano, A., Wheeler, E. A. and Baas, P. 2016. Tyloses and gums: a review of structure, function and occurrence of vessel occlusions. IAWA journal. 37(2):186-205.

Earles, J. M., Knipfer, T., Tixier, A., Orozco, J., Reyes, C., Zwieniecki, M. A., Brodersen, C. R. and McElrone, A. J. 2018. *In vivo* quantification of plant starch reserves at micrometer resolution using X-ray micro CT imaging and machine learning. New Phytologist. 218(3):1260-1269.

Estiarte, M. and Peñuelas, J. 1999. Excess carbon: the relationship with phenotypical plasticity in storage and defense functions of plants. Orsis: organismes i sistemes. 14:159-203.

Foster, R. C. 1967. Fine structure of tyloses in three species of the Myrtaceae. Australian journal of botany. 15(1):25-34.

Fritschi, F. B., Lin, H. and Walker, M. A. 2008. Scanning electron microscopy reveals different response pattern of four *Vitis* genotypes to *Xylella fastidiosa* infection. Plant Disease. 92(2):276-286.

Fry, S. M. and Milholland, R.D. 1990. Response of resistant, tolerant, and susceptible grapevine tissues to invasion by the Pierce's disease bacterium, *Xylella fastidiosa*. Phytopathology. 80(1):66-69.

Gibon, Y., Pyl, E. T., Sulpice, R., Lunn, J. E., Hoehne, M., Guenther, M. and Stitt, M. 2009. Adjustment of growth, starch turnover, protein content and central metabolism to a decrease of the carbon supply when Arabidopsis is grown in very short photoperiods. Plant, Cell & Environment. 32(7):859-874.

Grimplet, J., Cramer, G. R., Dickerson, J. A., Mathiason, K., Van Hemert, J., and Fennell, A. Y. 2009. VitisNet: "omics" integration through grapevine molecular networks. PLoS ONE. 4:e8365.

Guérard, N., Maillard, P., Bréchet, C., Lieutier, F. and Dreyer, E. 2007. Do trees use reserve or newly assimilated carbon for their defense reactions? A $^{13}C$ labeling

approach with young Scots pines inoculated with a bark-beetle-associated fungus (*Ophiostoma brunneo ciliatum*). Annals of Forest Science. 64(6):601-608.

Guilhabert, M. R. and Kirkpatrick, B. C. 2005. Identification of *Xylella fastidiosa* antivirulence genes: Hemagglutinin adhesins contribute to *X. fastidiosa* biofilm maturation and colonization and attenuate virulence. Mol Plant-Microbe Interacts. 18(8):856-868.

Hill, B. L., and Purcell, A. H. 1995. Acquisition and retention of *Xylella fastidiosa* by an efficient vector, *Graphocephala atropunctata*. Phytopathology. 85:209-212.

Hölttä, T., Cochard, H., Nikinmaa, E. and Mencuccini, M. 2009. Capacitive effect of cavitation in xylem conduits: results from a dynamic model. Plant, Cell & Environment. 32(1):10-21.

Hopkins, D. L. 1989. *Xylella fastidiosa*: xylem-limited bacterial pathogen of plants. Annual review of phytopathology. 27(1):271-290.

Hummel, I., Pantin, F., Sulpice, R., Piques, M., Rolland, G., Dauzat, M., Christophe, A., Pervent, M., Bouteillé, M., Stitt, M. and Gibon, Y. 2010. Arabidopsis plants acclimate to water deficit at low cost through changes of carbon usage: an integrated perspective using growth, metabolite, enzyme, and gene expression analysis. Plant physiology. 154(1):357-372.

Ingel, B., Jeske, D. R., Sun, Q., Grosskopf, J. and Roper, C., 2019. Xylella fastidiosa Endoglucanases Mediate the Rate of Pierce's Disease Development in Vitis vinifera in a Cultivar-Dependent Manner. Mol Plant-Microbe Interacts. (ja).

Langmead, B., and Salzberg, S. L. 2012. Fast gapped-read alignment with Bowtie2. Nat. Methods. 9:357–359.

Lenth, R. 2019. emmeans: Estimated Marginal Means, aka Least-Squares Means. R package version 1.4.1. https://CRAN.R-project.org/package=emmeans

Leśniewska, J., Öhman, D., Krzesłowska, M., Kushwah, S., Barciszewska-Pacak, M., Kleczkowski, L. A., Sundberg, B., Moritz, T. and Mellerowicz, E. J. 2017. Defense responses in aspen with altered pectin methylesterase activity reveal the hormonal inducers of tyloses. Plant physiology. 173(2):1409-1419.

Li, W. B., Pria Jr, W. D., Teixeira, D. C., Miranda, V. S., Ayres, A. J., Franco, C. F., Costa, M. G., He, C. X., Costa, P. I., and Hartung, J. S. 2001. Coffee leaf scorch caused by a strain of *Xylella fastidiosa* from citrus. Plant Disease. 85:501-505.

Love, M. I., Huber, W., and Anders, S. 2014. Moderated estimation of fold change and dispersion for RNA-seq data with DESeq2. Genome Biol. 15:550.

Massonnet, M., Figueroa-Balderas, R., Galarneau, E. R., Miki, S., Lawrence, D. P., Sun, Q., Wallis, C. M., Baumgartner, K. and Cantu, D. 2017. *Neofusicoccum parvum* colonization of the grapevine woody stem triggers asynchronous host responses at the site of infection and in the leaves. Frontiers in plant science. 8:1117.

Mayr, S., Kartusch, B. and Kikuta, S. 2014. Evidence for air-seeding: watching the formation of embolism in conifer xylem. The journal of plant hydraulics. 1.

McDowell, N. G. 2011. Mechanisms linking drought, hydraulics, carbon metabolism, and vegetation mortality. Plant physiology. 155(3):1051-1059.

McElrone, A. J., Sherald, J. L., and Forseth, I. N. 2001. Effects of water stress on symptomatology and growth of *Parthenocissus quinquefolia* infected by *Xylella fastidiosa*. Plant Disease. 85:1160-1164.

McElrone, A. J., Sherald, J. L., and Forseth, I. N. 2003. Interactive effects of water stress and xylem-limited bacterial infection on the water relations of a host vine. Journal of Experimental Botany. 54:419-430.

McElrone, A. J., Grant, J. A. and Kluepfel, D. A. 2010. The role of tyloses in crown hydraulic failure of mature walnut trees afflicted by apoplexy disorder. Tree physiology. 30(6):761-772.

Meyer, R. W. and Côté, W. A. 1968. Formation of the protective layer and its role in tylosis development. Wood science and technology. 2(2):84-94.

Murmanis, L. 1975. Formation of tyloses in felled *Quercus rubra* L. Wood Science and Technology. 9(1):3-14.

Nascimento, R., Gouran, H., Chakraborty, S., Gillespie, H. W., Almeida-Souza, H. O., Tu, A., Rao, B. J., Feldstein, P. A., Bruening, G., Goulart, L. R. and Dandekar, A. M. 2016. The type II secreted lipase/esterase LesA is a key virulence factor required for *Xylella fastidiosa* pathogenesis in grapevines. Scientific reports. 6:18598.

Parameswaran, N., Knigge, H. and Liese, W. 1985. Electron microscopic demonstration of a suberized layer in the tylosis wall of beech *Fagus sylvatica* and oak *Quercus robur*. IAWA Bull. n.s. 6: 269–271.

Pérez-Donoso, A. G., Greve, L. C., Walton, J. H., Shackel, K. A. and Labavitch, J. M. 2007. *Xylella fastidiosa* infection and ethylene exposure result in xylem and water movement disruption in grapevine shoots. Plant Physiology. 143(2):1024-1036.

Perez-Donoso, A. G., Sun, Q., Roper, M. C., Greve, L. C., Kirkpatrick B. C., and Labavitch, J. M. 2010. Cell Wall-Degrading Enzymes Enlarge the Pore Size of Intervessel Pit Membranes in Healthy and *Xylella fastidiosa*-Infected Grapevines. Plant Physiology. 152:1748-1759.

Pérez-Donoso, A. G., Lenhof, J. J., Pinney, K. and Labavitch, J. M. 2016. Vessel embolism and tyloses in early stages of Pierce's disease. Australian journal of grape and wine research. 22(1):81-86.

Pinheiro, C. and Chaves, M. M. 2010. Photosynthesis and drought: can we make metabolic connections from available data? Journal of experimental botany. 62(3):869-882.

Plavcová, L., Jansen, S., Klepsch, M. and Hacke, U. G. 2013. Nobody's perfect: can irregularities in pit structure influence vulnerability to cavitation? Frontiers in Plant Science. 4:453.

Poorter, H. and Villar, R. 1997. The fate of acquired carbon in plants: chemical composition and construction costs. Plant resource allocation. 39-72.

Purcell, A. H., and Saunders, S. R. 1999. Fate of Pierce's disease strains of *Xylella fastidiosa* in common riparian plants in California. Plant Disease. 83:825-830.

R Core Team 2019. R: A language and environment for statistical computing. R Foundation for Statistical Computing, Vienna, Austria. URL https://www.R-project.org/.

Rapicavoli, J., Ingel, B., Blanco-Ulate, B., Cantu, D., and Roper, C. 2018. *Xylella fastidiosa*: an examination of a re-emerging plant pathogen. Molecular Plant Pathology. 19:786-800.

Roper, M. C., Greve, L. C., Warren, J. G., Labavitch, J. M., and Kirkpatrick, B. C. 2007. *Xylella fastidiosa* requires polygalacturonase for colonization and pathogenicity in *Vitis vinifera* grapevines. Mol Plant Microbe Interacts. 20:411-419.

Sachs, I., Kuntz, J., Ward, J., Nair, G. and Schultz, N. 1970. Tyloses structure. Wood and Fiber 2:259–268.

Saponari, M., Boscia, D., Nigro, F., and Martelli, G. P. 2013. Identification of DNA sequences related to *Xylella fastidiosa* in oleander, almond and olive trees

exhibiting leaf scorch symptoms in Apulia (Southern Italy). Journal of Plant Pathology. 95:659-668.

Sevanto, S. 2014. Phloem transport and drought. Journal of experimental botany. 65(7):1751-1759.

Sevanto, S., Mcdowell, N. G., Dickman, L. T., Pangle, R. and Pockman, W. T. 2014. How do trees die? A test of the hydraulic failure and carbon starvation hypotheses. Plant, cell & environment. 37(1):153-161.

Sperry, J. S., Perry, A. H. and Sullivan, J. E. M. 1991. Pit membrane degradation and air-embolism formation in ageing xylem vessels of *Populus tremuloides* Michx. Journal of Experimental Botany. 42(11):1399-1406.

Sperry, J. S. and Tyree, M. T. 1988. Mechanism of water stress-induced xylem embolism. Plant physiology. 88(3):581-587.

Stevenson, J. F., Matthews, M. A., and Rost, T. L. 2004. Grapevine susceptibility to Pierce's disease I: relevance of hydraulic architecture. American Journal of Enology and Viticulture. 55:228-237.

Sun, Q., Rost, T. L., Reid, M. S. and Matthews, M. A. 2007. Ethylene and not embolism is required for wound-induced tylose development in stems of grapevines. Plant Physiology. 145(4):1629-1636.

Sun, Q., Greve, L. C. and Labavitch, J. M. 2011. Polysaccharide compositions of intervessel pit membranes contribute to Pierce's disease resistance of grapevines. Plant Physiology. 155(4):1976-1987.

Sun, Q., Sun, Y., Walker, M. A. and Labavitch, J. M. 2013. Vascular occlusions in grapevines with Pierce's disease make disease symptom development worse. Plant physiology. 161(3):1529-1541.

Thorne, E. T., Stevenson, J. F., Rost, T. L., Labavitch, J. M., and Matthews, M. A. 2006a. Pierce's disease symptoms: comparison with symptoms of water deficit and the impact of water deficits. American Journal of Enology and Viticulture. 57:1-11.

Thorne, E. T., Young, B. M., Young, G. M., Stevenson, J. F., Labavitch, J. M., Matthews, M. A., and Rost, T. L. 2006b. The structure of xylem vessels in grapevine (Vitaceae) and a possible passive mechanism for the systemic spread of bacterial disease. American Journal of Botany. 93:497-504.

Tyree, M. T. and Sperry, J. S., 1989. Vulnerability of xylem to cavitation and embolism. Annual review of plant biology. 40(1):19-36.

Tyree, M. T., Cochard, H., Cruiziat, P., Sinclair, B. and Ameglio, T. 1993. Drought-induced leaf shedding in walnut: evidence for vulnerability segmentation. Plant, Cell & Environment. 16(7):879-882.

Tyree, M. T., and Zimmermann, M. H. 2002. Hydraulic architecture of whole plants and plant performance. Pages 175–214 in: Xylem Structure and the Ascent of Sap, Springer-Verlag Berlin Heidelberg, Berlin.

Zimmermann, M. H. 1979. The discovery of tylose formation by a Viennese lady in 1845. IAWA Bull. 1979/2: 51–56.


Figure 4.1 Phases of Pierce's Disease based on the rating index developed by Guilhabert and Kirkpatrick (2005). A) Phase I includes ratings from 0 – 2 where only a few leaves near the POI show signs of leaf scorching. B) Phase II includes ratings from 2 – 4 where leaf scorching affects the entire vine, with several matchstick petioles present. C) Phase III includes disease ratings from 4 – 5 when the vine is near death and only a few heavily scorched leaves remain.

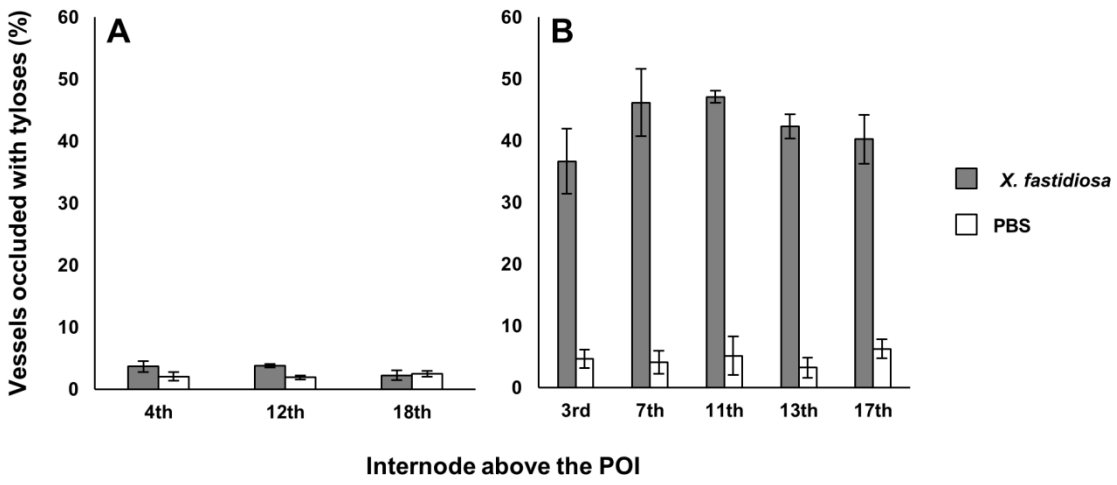


Figure 4.2 Quantitative comparison of tylose development based on percentage of occluded vessels in *Vitis vinifera* cv. Cabernet sauvignon vines inoculated with *X. fastidiosa* (Temecula 1; gray) or 1× PBS (negative control; white) during Phase I (A) and Phase II (B) of Pierce's Disease. Each datum point is presented as mean based on 3 - 5 samples from three vines. Bars represent the standard error of the mean.

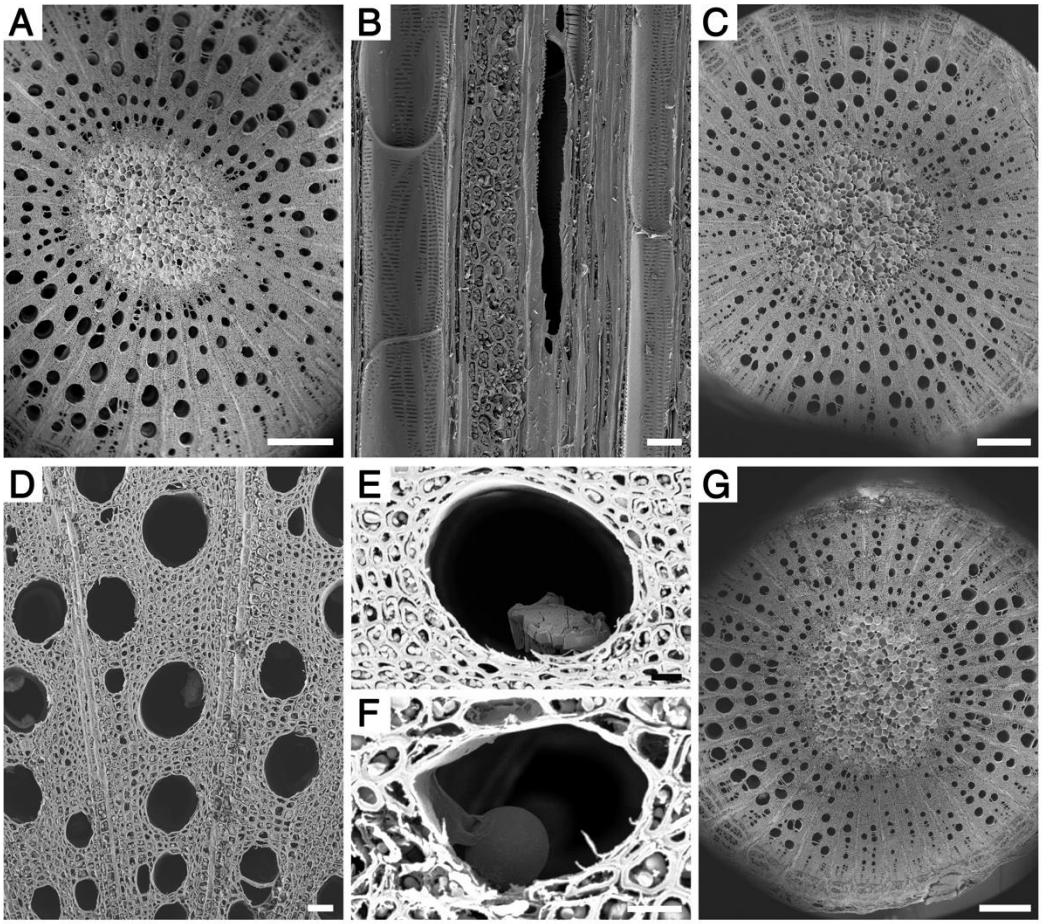


Figure 4.3 Vascular occlusion during Phase I of Pierce's Disease in *Vitis vinifera* cv. Cabernet sauvignon vines inoculated with 1× PBS (A-B) or *X. fastidiosa* (C-G), respectively. A, C-G: Transverse section of stem. B: Tangential longitudinal section of stem secondary xylem. A-F: Xylem tissue from the fourth internode counting upward from the POI (the same below). A) Vessels appear as open pores without visible occlusions. B) Several longitudinally transected vessels showing no tyloses and crystals inside. C) Xylem in a stem does not contain vessels with obvious occlusion. D) Most vessels are open with a crystal in one vessel. E) A small crystal in a vessel. F) A small tylose in a vessel lumen. G) Xylem tissue from the 12$^{th}$ internode showing most vessels are free of tyloses or crystals. Scale bar is 500 µm in A, C and G, 50 µm in B and D, and 20 µm in E and F.

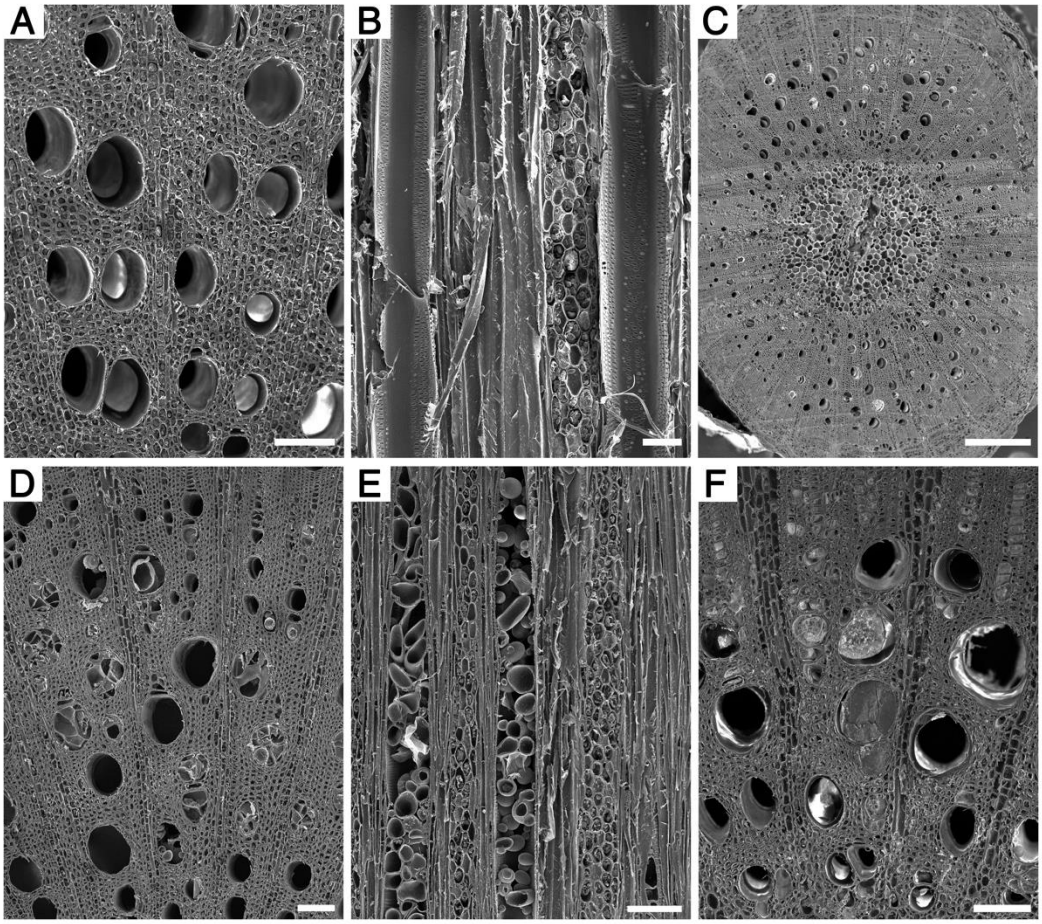


Figure 4.4 Vascular occlusion during Phase II of Pierce's Disease in *Vitis vinifera* cv. Cabernet sauvignon vines inoculated with 1× PBS (A-B) or X. fastidiosa (C-F), respectively. A, C, D and F: Transverse section of stem. B and E: Tangential longitudinal section of stem xylem. A and B: Xylem tissues from the third internode. A) Vessels are open without occlusions in the transverse section. B) Two longitudinally transected vessels are free of tyloses. C) Xylem tissue from the third internode. Both open and occluded vessels are present and occluded vessels occurred as patches dispersing among open vessels. D) Secondary xylem tissue, showing many vessels completely or partially occluded with tyloses. E) Two longitudinally transected vessels filled with tyloses along their lengths. F) Xylem tissue from the 11th internode, showing that some vessels are fully occluded. Scale bar is 50 µm in A and B, 100 µm in D-F, and 500 µm in C.

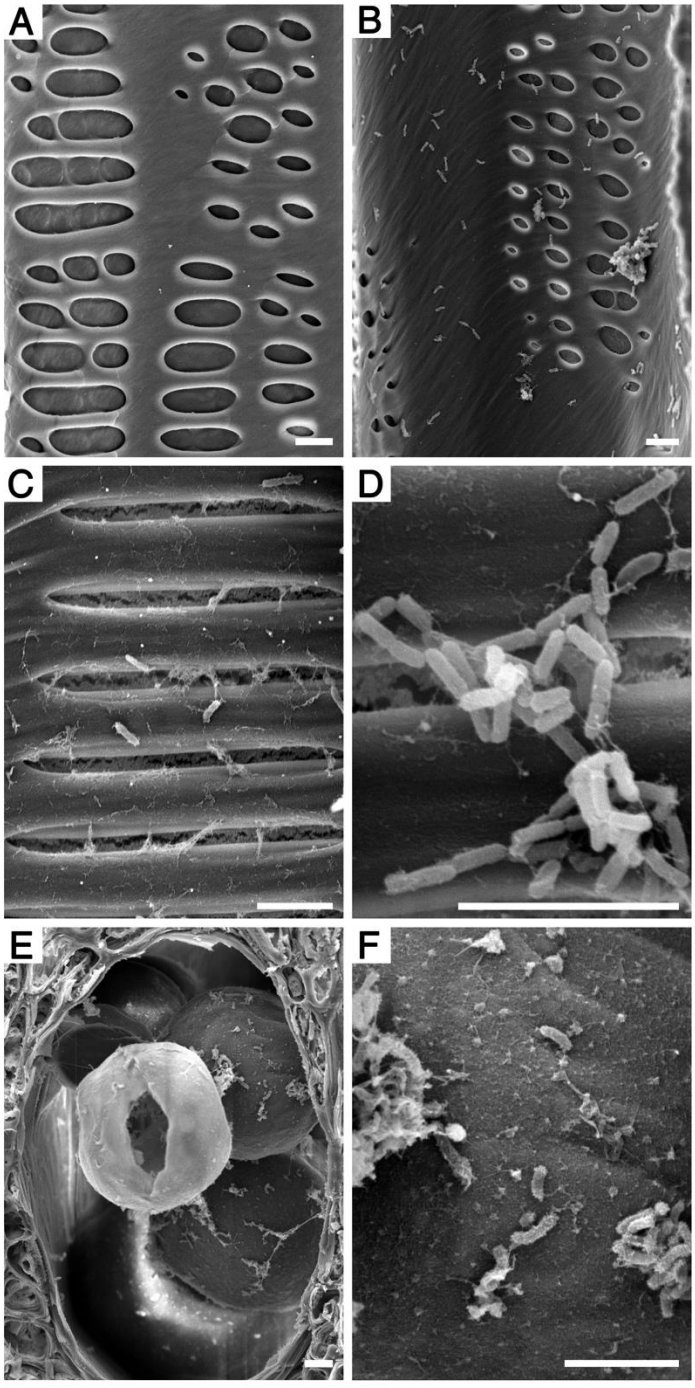
A
B
C
D
E
F

Figure 4.5 *X. fastidiosa* distribution during Phase II of Pierce's Disease in *Vitis vinifera* cv. Cabernet sauvignon vines inoculated with 1× PBS buffer (A) or *X. fastidiosa* (B-F), respectively. A-D: A lateral wall of a longitudinally transected vessel. E-F: Transverse section of a vessel. A) No *X. fastidiosa* cells in vessels of vines inoculated with 1× PBS. B) *X. fastidiosa* cells present both individually and in aggregates in a vessel from the 11$^{th}$ internode above POI. C-D: Vessel from the 3$^{rd}$ internode above the POI, showing that *X. fastidiosa* cells are present in small quantities either individually (C) or in small aggregates (D). E) A vessel from the 17$^{th}$ internode contains both tyloses and *X. fastidiosa* cells. F) An enlargement of the frame region in E, showing *X. fastidiosa* cells colonizing the surface of tyloses. Scale bar in all panels is 5 µm.

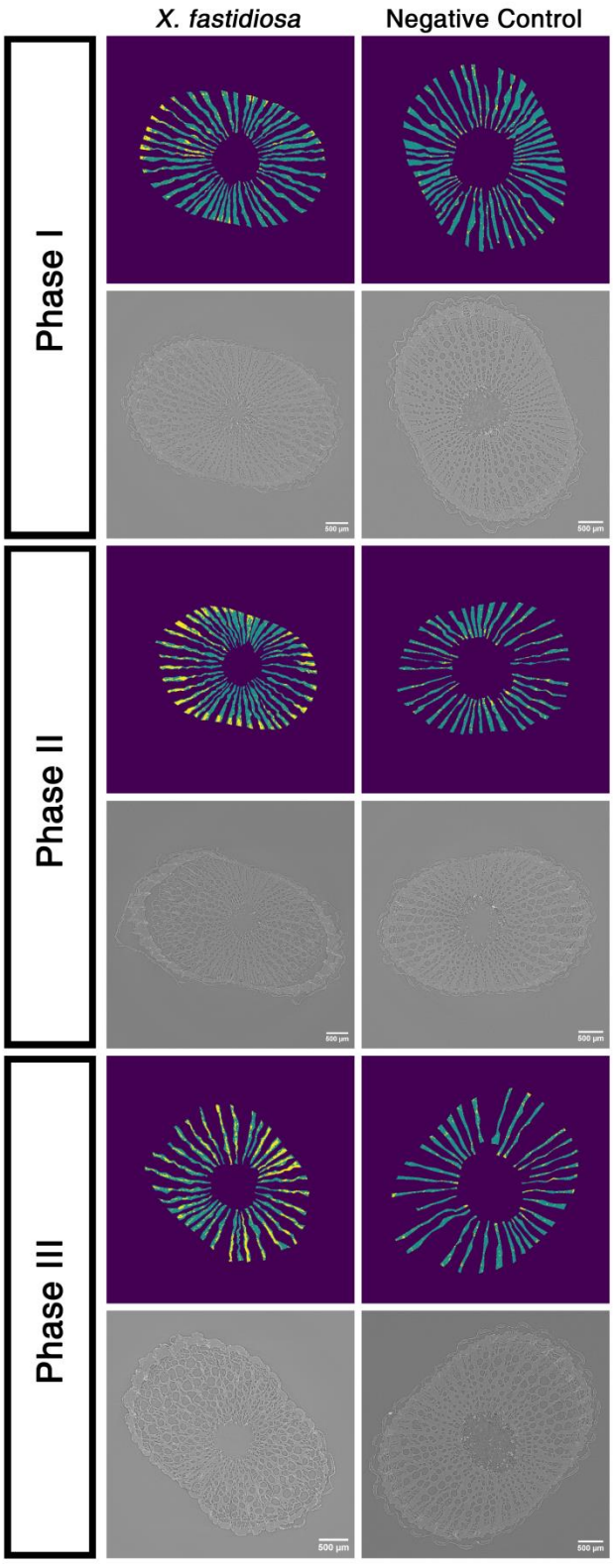
X. fastidiosa
Negative Control
Phase I
Phase II
Phase III
500 µm

Figure 4.6 Starch in the ray parenchyma of *X. fastidiosa*-inoculated vines depletes as PD symptoms progress. X-ray microCT and a machine-learning algorithm were used to predict starch depletion in *X.fastidiosa*- and 1× PBS-inoculated (negative control) vines during Phase I (top), Phase II (middle), and Phase III (bottom) of PD. For each Phase, the top row consists of spatial maps depicting the predicted starch-filled ray parenchyma (blue) and the predicted empty ray parenchyma (yellow). The bottom row for each Phase consists of the corresponding X-ray microCT images used with the machine-learning algorithm to generate the respective spatial maps above.

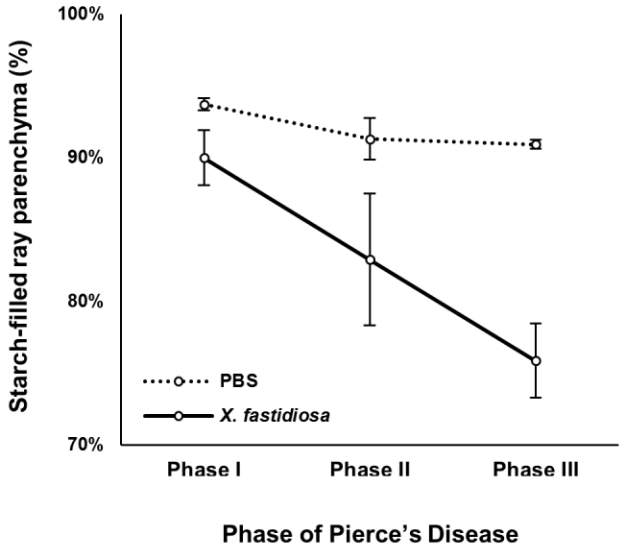


Figure 4.7 Percentage of starch-filled ray parenchyma during each phase of Pierce's Disease in vines inoculated with 1× PBS (dashed line) or *X. fastidiosa* (solid line). Data points at each phase represent the mean percentage of starch-filled ray parenchyma of 3 – 6 vines calculated by a machine learning algorithm developed by Earles et al. (2018). Bars represent the standard error of the mean.

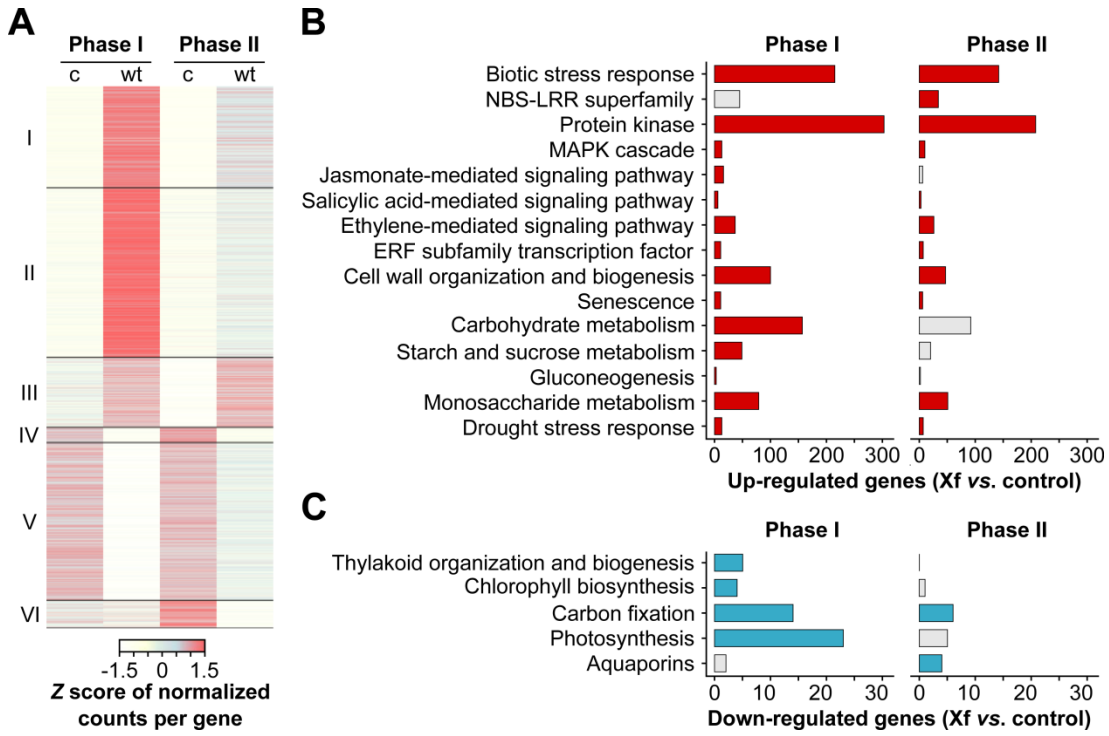


Figure 4.8 Grapevine transcriptomic response to *X. fastidiosa*. A) Differentially expressed genes (P-value ≤ 0.05) in response to *X. fastidiosa* (Temecula 1) when compared to 1× PBS control (c). Genes are classified in six groups (I-VI) based on their expression pattern. The colors of the heat map depict the *Z* score of the normalized counts per gene. Enriched grape functional categories (P-value ≤ 0.05) among genes up-regulated (red; B) and down-regulated (blue; C) in response to *X. fastidiosa* infection. Gray-colored bars represent functional categories that are not significantly overrepresented among the differentially expressed genes.

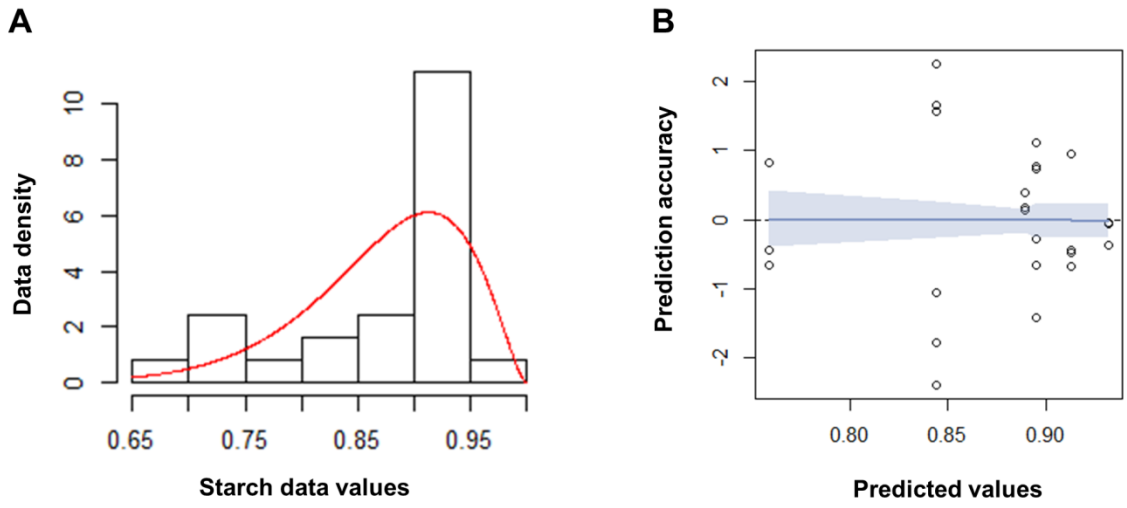


Figure 4.9 Validation of the beta regression model used to determine statistical significance of starch depletion. A) Histogram of starch-filled ray parenchyma percentage data conforms to a beta distribution (red line). B) Residual analysis of the beta regression model where model-predicted values (x-axis) are plotted against the accuracy of those predictions (residual = observed – predicted; y-axis), and appear to be randomly distributed, indicating the use of a linear model is warranted. Dashed line at 0 represents full prediction accuracy. The model (blue line) and 95% confidence intervals (light blue) are overlaid on top of the residuals to show accuracy of the model. An accurate model will completely overlap the dashed line.

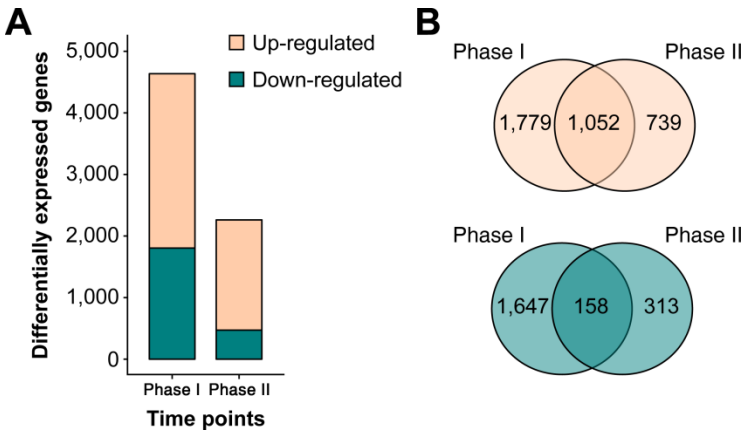


Figure 4.10 *Vitis vinivera* cv. Cabernet sauvignon transcriptional modulation in response to *X. fastidiosa* infection. (A) Number of genes differentially expressed between *X. fastidiosa*- and 1× PBS-inoculated vines during Phase I and Phase II of Pierce's Disease. (B) Comparison of the genes up- and down-regulated during Phase I and Phase II of Pierce's Disease.

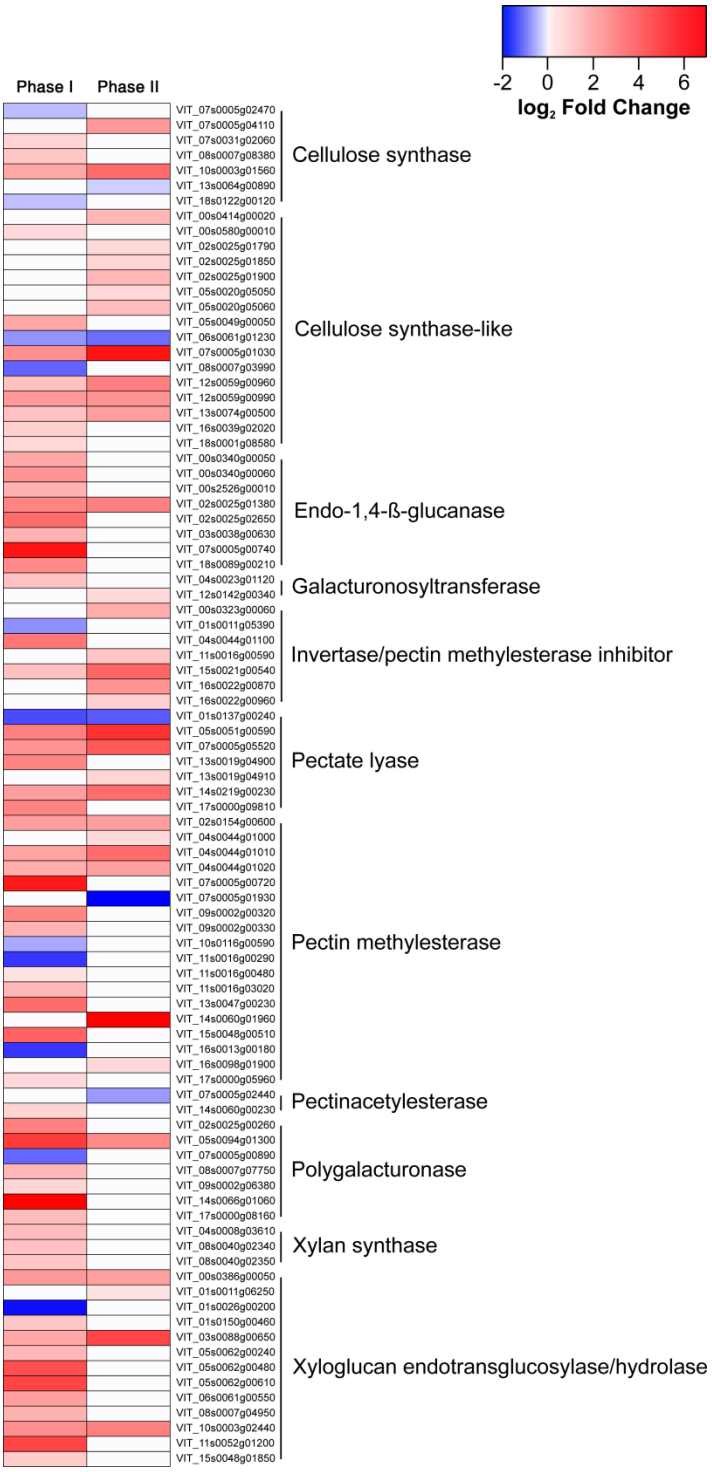
-2 0 2 4 6
log2 Fold Change
Phase I
Phase II
VIT_07s0005g02470
VIT_07s0005g04110
VIT_07s0031g02060
VIT_08s0007g08380
VIT_10s0003g01560
VIT_13s0064g00890
VIT_18s0122g00120
Cellulose synthase
VIT_00s0414g00020
VIT_00s0580g00010
VIT_02s0025g01790
VIT_02s0025g01850
VIT_02s0025g01900
VIT_05s0020g05050
VIT_05s0020g05060
VIT_05s0049g00050
VIT_06s0061g01230
VIT_07s0005g01030
VIT_08s0007g03990
VIT_12s0059g00960
VIT_12s0059g00990
VIT_13s0074g00500
VIT_16s0039g02020
VIT_18s0001g08580
Cellulose synthase-like
VIT_00s0340g00050
VIT_00s0340g00060
VIT_00s2526g00010
VIT_02s0025g01380
VIT_02s0025g02650
VIT_03s0038g00630
VIT_07s0005g00740
VIT_18s0089g00210
Endo-1,4-ß-glucanase
VIT_04s0023g01120
VIT_12s0142g00340
Galacturonosyltransferase
VIT_00s0323g00060
VIT_01s0011g05390
VIT_04s0044g01100
VIT_11s0016g00590
VIT_15s0021g00540
VIT_16s0022g00870
VIT_16s0022g00960
Invertase/pectin methylesterase inhibitor
VIT_01s0137g00240
VIT_05s0051g00590
VIT_07s0005g05520
VIT_13s0019g04900
VIT_13s0019g04910
VIT_14s0219g00230
VIT_17s0000g09810
Pectate lyase
VIT_02s0154g00600
VIT_04s0044g01000
VIT_04s0044g01010
VIT_04s0044g01020
VIT_07s0005g00720
VIT_07s0005g01930
VIT_09s0002g00320
VIT_09s0002g00330
VIT_10s0116g00590
VIT_11s0016g00290
VIT_11s0016g00480
VIT_11s0016g03020
VIT_13s0047g00230
VIT_14s0060g01960
VIT_15s0048g00510
VIT_16s0013g00180
VIT_16s0098g01900
VIT_17s0000g05960
Pectin methylesterase
VIT_07s0005g02440
VIT_14s0060g00230
Pectinacetylesterase
VIT_02s0025g00260
VIT_05s0094g01300
VIT_07s0005g00890
VIT_08s0007g07750
VIT_09s0002g06380
VIT_14s0066g01060
VIT_17s0000g08160
Polygalacturonase
VIT_04s0008g03610
VIT_08s0040g02340
VIT_08s0040g02350
Xylan synthase
VIT_00s0386g00050
VIT_01s0011g06250
VIT_01s0026g00200
VIT_01s0150g00460
VIT_03s0088g00650
VIT_05s0062g00240
VIT_05s0062g00480
VIT_05s0062g00610
VIT_06s0061g00550
VIT_08s0007g04950
VIT_10s0003g02440
VIT_11s0052g01200
VIT_15s0048g01850
Xyloglucan endotransglucosylase/hydrolase

Figure 4.11 Heat map of cell wall biosynthesis and organization-associated genes modulated during *X. fastidiosa* infection. Log2(Fold change) of differentially expressed genes between *X. fastidiosa*- and 1× PBS-inoculated steams during Phase I and Phase II of Pierce's Disease are depicted.

| Treatment | Bio-rep. | PD Phase | Year | fastq file ID | Raw reads | Parsed reads | % | Mapped ambiguously on *V. vinifera* | % |
|---|---|---|---|---|---|---|---|---|---|
| 1× PBS | 1 | I | 2016 | 16-4_S94_L006_R1_001.fastq.gz | 18,709,670 | 18,707,240 | 99.99 | 11,642,543 | 62.24 |
| 1× PBS | 2 | I | 2016 | 16-5_S110_L007_R1_001.fastq.gz | 18,078,656 | 18,076,633 | 99.99 | 12,572,464 | 69.55 |
| 1× PBS | 3 | I | 2016 | 16-6_S80_L006_R1_001.fastq.gz | 20,428,080 | 20,424,403 | 99.98 | 14,163,204 | 69.34 |
| 1× PBS | 1 | II | 2016 | 16-22_S103_L007_R1_001.fastq.gz | 17,922,538 | 17,920,454 | 99.99 | 12,654,441 | 70.61 |
| 1× PBS | 2 | II | 2016 | 16-23_S108_L007_R1_001.fastq.gz | 18,190,611 | 18,187,712 | 99.98 | 12,322,020 | 67.75 |
| 1× PBS | 3 | II | 2016 | 16-24_S73_L005_R1_001.fastq.gz | 20,251,192 | 20,249,310 | 99.99 | 13,717,827 | 67.74 |
| *X. fastidiosa* | 1 | I | 2016 | 16-7_S98_L007_R1_001.fastq.gz | 18,251,317 | 18,249,338 | 99.99 | 12,462,986 | 68.29 |
| *X. fastidiosa* | 2 | I | 2016 | 16-8_S95_L006_R1_001.fastq.gz | 19,212,870 | 19,210,989 | 99.99 | 13,537,493 | 70.47 |
| *X. fastidiosa* | 3 | I | 2016 | 16-9_S63_L005_R1_001.fastq.gz | 18,669,012 | 18,667,025 | 99.99 | 12,615,270 | 67.58 |
| *X. fastidiosa* | 1 | II | 2016 | 16-25_S66_L005_R1_001.fastq.gz | 22,029,756 | 22,026,964 | 99.99 | 15,153,593 | 68.80 |
| *X. fastidiosa* | 2 | II | 2016 | 16-26_S61_L005_R1_001.fastq.gz | 19,000,228 | 18,997,684 | 99.99 | 12,342,754 | 64.97 |
| *X. fastidiosa* | 3 | II | 2016 | 16-27_S58_L005_R1_001.fastq.gz | 16,493,055 | 16,490,834 | 99.99 | 11,148,892 | 67.61 |

Table 4.1 Summary of RNAseq data and mapping metrics. Reads were trimmed using Trimmomatic v.0.36 and trimmed single-end reads were mapped onto the predicted protein-coding sequences of *V. vinifera* 'PN40024' using Bowtie2 v.2.3.4.1. Counts of reads mapping uniquely onto the grape reference transcriptome (i.e., with Q > 30) were extracted using sam2counts.py v.0.91.

| Over-represented functional category (FCT) | *p*-value | Number of Genes | |
|---|---|---|---|
| | | FCT | Vines with *Xf* |
| Cellular process | 7.2E-09 | 301 | 2,332 |
| Cellular process.Cell growth and death | 1.6E-02 | 58 | 462 |
| Cellular process.Cell growth and death.Cell growth | 4.1E-02 | 8 | 42 |
| Cellular process.Cellular component organization and biogenesis | 1.4E-05 | 169 | 1,305 |
| Cellular process.Cellular component organization and biogenesis.Cell wall organization and biogenesis | 1.5E-12 | 100 | 511 |
| Cellular process.Cellular component organization and biogenesis.Cell wall organization and biogenesis.Cell wall metabolism | 3.7E-09 | 75 | 395 |
| Cellular process.Cellular component organization and biogenesis.Cell wall organization and biogenesis.Cell wall metabolism.Cell wall biosynthesis | 2.3E-04 | 27 | 139 |
| Cellular process.Cellular component organization and biogenesis.Cell wall organization and biogenesis.Cell wall metabolism.Cell wall biosynthesis.Cell wall glycan monomers generation | 1.3E-03 | 9 | 30 |
| Cellular process.Cellular component organization and biogenesis.Cell wall organization and biogenesis.Cell wall metabolism.Cell wall biosynthesis.Cellulose biosynthesis | 4.6E-02 | 14 | 91 |
| Cellular process.Cellular component organization and biogenesis.Cell wall organization and biogenesis.Cell wall metabolism.Cell wall biosynthesis.Xylan biosynthesis | 3.1E-03 | 3 | 4 |
| Cellular process.Cellular component organization and biogenesis.Cell wall organization and biogenesis.Cell wall metabolism.Cell wall catabolism | 1.5E-03 | 15 | 68 |
| Cellular process.Cellular component organization and biogenesis.Cell wall organization and biogenesis.Cell wall metabolism.Cell wall catabolism.Cellulose catabolism | 1.5E-02 | 8 | 35 |
| Cellular process.Cellular component organization and biogenesis.Cell wall organization and biogenesis.Cell wall metabolism.Cell wall catabolism.Pectin catabolism | 3.5E-02 | 5 | 20 |
| Cellular process.Cellular component organization and biogenesis.Cell wall organization and biogenesis.Cell wall metabolism.Cell wall modification | 3.7E-04 | 33 | 188 |
| Cellular process.Cellular component organization and biogenesis.Cell wall organization and biogenesis.Cell wall metabolism.Cell wall modification.Pectin modification | 2.8E-02 | 19 | 126 |
| Cellular process.Cellular component organization and biogenesis.Cell wall organization and biogenesis.Cell wall metabolism.Cell wall modification.Xyloglucan modification | 1.7E-03 | 11 | 43 |
| Cellular process.Cellular component organization and biogenesis.Cell wall organization and biogenesis.Cell wall structural protein | 1.5E-06 | 19 | 60 |
| Cellular process.Cellular component organization and biogenesis.Cytoskeleton organization and biogenesis | 8.1E-03 | 47 | 348 |
| Cellular process.Cellular component organization and biogenesis.Cytoskeleton organization and biogenesis.Microtubule organization and biogenesis | 8.1E-04 | 30 | 173 |
| Cellular process.Cellular component organization and biogenesis.Cytoskeleton organization and biogenesis.Microtubule organization and biogenesis.Microtubule-driven movement | 2.2E-06 | 28 | 115 |

| Over-represented functional category (FCT) | *p*-value | Number of Genes | |
|---|---|---|---|
| | | FCT | Vines with *Xf* |
| Cellular process.Cellular transport | 1.3E-02 | 71 | 578 |
| Cellular process.Cellular transport.Protein trafficking | 1.2E-02 | 71 | 574 |
| Development.Senescence | 5.7E-04 | 11 | 38 |
| Metabolism.Cellular metabolism.Esterase activity | 3.9E-03 | 12 | 54 |
| Metabolism.Cellular metabolism.Nitrogen and sulfur metabolism.Nitrogen metabolism | 3.4E-02 | 23 | 163 |
| Metabolism.Cellular metabolism.Shikimate metabolism | 1.3E-02 | 7 | 28 |
| Metabolism.Primary metabolism.Amino acid metabolism.Aromatic amino acid metabolism.Aromatic amino acid biosynthesis | 4.9E-02 | 20 | 143 |
| Metabolism.Primary metabolism.Carbohydrate metabolism | 2.3E-03 | 157 | 1,334 |
| Metabolism.Primary metabolism.Carbohydrate metabolism.Glycolysis Gluconeogenesis.Gluconeogenesis | 2.2E-02 | 3 | 7 |
| Metabolism.Primary metabolism.Carbohydrate metabolism.Monosaccharide metabolism | 2.5E-02 | 79 | 672 |
| Metabolism.Primary metabolism.Carbohydrate metabolism.Monosaccharide metabolism.Nucleotide sugar metabolism | 5.7E-04 | 16 | 69 |
| Metabolism.Primary metabolism.Carbohydrate metabolism.Monosaccharide metabolism.Xylose metabolism | 3.3E-02 | 3 | 8 |
| Metabolism.Primary metabolism.Carbohydrate metabolism.Monosaccharide metabolism.Xylose metabolism.Xylose biosynthesis | 3.3E-02 | 3 | 8 |
| Metabolism.Primary metabolism.Carbohydrate metabolism.Oligosaccharide metabolism | 2.3E-02 | 37 | 280 |
| Metabolism.Primary metabolism.Carbohydrate metabolism.Polysaccharide metabolism | 5.8E-04 | 55 | 372 |
| Metabolism.Primary metabolism.Carbohydrate metabolism.Polysaccharide metabolism.Beta-1,3 glucan metabolism | 1.7E-03 | 15 | 69 |
| Metabolism.Primary metabolism.Carbohydrate metabolism.Polysaccharide metabolism.Beta-1,3 glucan metabolism.Beta-1,3 glucan catabolism | 1.9E-04 | 15 | 57 |
| Metabolism.Primary metabolism.Carbohydrate metabolism.Polysaccharide metabolism.Starch and sucrose metabolism | 1.6E-03 | 49 | 337 |
| Metabolism.Primary metabolism.Coenzyme and prosthetic group metabolism.Nicotinate and nicotinamide metabolism | 8.7E-03 | 7 | 26 |
| Metabolism.Primary metabolism.Coenzyme and prosthetic group metabolism.Peptide derived compounds biosynthesis | 2.8E-02 | 21 | 143 |
| Metabolism.Primary metabolism.Coenzyme and prosthetic group metabolism.Peptide derived compounds biosynthesis.Glutathione metabolism | 2.8E-02 | 21 | 143 |
| Metabolism.Primary metabolism.Coenzyme and prosthetic group metabolism.Riboflavin metabolism | 2.1E-02 | 11 | 59 |
| Metabolism.Primary metabolism.Generation of metabolite precursors and energy.Photosynthesis.Antenna proteins | 3.0E-08 | 12 | 20 |

| Over-represented functional category (FCT) | *p*-value | Number of Genes | |
|---|---|---|---|
| | | FCT | Vines with *Xf* |
| Metabolism.Primary metabolism.Lipid metabolism.Ether lipid metabolism | 3.5E-02 | 10 | 56 |
| Metabolism.Primary metabolism.Lipid metabolism.Glycerolipid metabolism.Glycerophospholipid metabolism.Glycerophospholipid catabolism | 2.4E-03 | 7 | 21 |
| Metabolism.Primary metabolism.Lipid metabolism.Sphingolipid metabolism | 1.2E-02 | 16 | 92 |
| Metabolism.Primary metabolism.Protein metabolism and modification.Protein folding | 3.8E-04 | 70 | 493 |
| Metabolism.Primary metabolism.Protein metabolism and modification.Protein folding.Chaperone-mediated protein folding | 3.0E-05 | 51 | 301 |
| Metabolism.Primary metabolism.Protein metabolism and modification.Protein folding.Chaperone-mediated protein folding.HSP-mediated protein folding | 6.4E-06 | 45 | 240 |
| Metabolism.Primary metabolism.Protein metabolism and modification.Protein folding.Disulfide bond rearrangement | 8.3E-04 | 7 | 18 |
| Metabolism.Primary metabolism.Protein metabolism and modification.Protein processing in endoplasmic reticulum | 1.8E-04 | 38 | 219 |
| Metabolism.Primary metabolism.Protein metabolism and modification.Proteolysis.cytoplasmic and nuclear protein degradation.Ubiquitin-mediated proteolysis.Proteasome | 9.7E-04 | 14 | 59 |
| Metabolism.Primary metabolism.Protein metabolism and modification.Proteolysis.Peptidase-mediated proteolysis | 5.0E-02 | 56 | 475 |
| Metabolism.Secondary metabolism.Terpenoid metabolism.Terpenoid biosynthesis.Mevalonate biosynthesis | 1.4E-02 | 3 | 6 |
| Metabolism.Secondary metabolism.Terpenoid metabolism.Tetranotriterpenoid metabolism | 8.9E-03 | 2 | 2 |
| Regulation overview.Regulation of cell cycle | 2.0E-03 | 27 | 159 |
| Regulation overview.Regulation of gene expression.Regulation of transcription.Transcription factor.AP2 family transcription factor | 3.8E-02 | 20 | 139 |
| Regulation overview.Regulation of gene expression.Regulation of transcription.Transcription factor.AP2 family transcription factor.ERF subfamily transcription factor | 1.4E-02 | 11 | 56 |
| Regulation overview.Regulation of gene expression.Regulation of transcription.Transcription factor.bHLH family transcription factor | 2.9E-02 | 22 | 152 |
| Regulation overview.Regulation of gene expression.Regulation of transcription.Transcription factor.HSF family transcription factor | 1.2E-03 | 8 | 24 |
| Regulation overview.Regulation of gene expression.Regulation of transcription.Transcription factor.LIM family transcription factor | 2.1E-02 | 4 | 12 |
| Regulation overview.Regulation of gene expression.Regulation of transcription.Transcription factor.NAC family transcription factor | 4.0E-03 | 15 | 75 |
| Regulation overview.Regulation of gene expression.Regulation of transcription.Transcription factor.Orphans Response reg family transcription factor | 3.7E-02 | 4 | 14 |

| Over-represented functional category (FCT) | *p*-value | Number of Genes | |
|---|---|---|---|
| | | FCT | Vines with *Xf* |
| Regulation overview.Regulation of gene expression.Regulation of transcription.Transcription factor.PseudoARR-B family transcription factor | 4.1E-03 | 4 | 8 |
| Regulation overview.Regulation of gene expression.Regulation of transcription.Transcription factor.WRKY family transcription factor | 9.9E-11 | 25 | 62 |
| Regulation overview.Regulation of gene expression.Regulation of transcription.Transcription factor.Zinc finger C3HC4 family transcription factor | 1.5E-02 | 34 | 245 |
| Response to stimulus | 5.6E-27 | 348 | 2,093 |
| Response to stimulus.Stress response | 5.6E-27 | 348 | 2,093 |
| Response to stimulus.Stress response.Abiotic stress response | 2.7E-06 | 108 | 736 |
| Response to stimulus.Stress response.Abiotic stress response.Drought stress response | 1.9E-04 | 13 | 45 |
| Response to stimulus.Stress response.Abiotic stress response.Light stress response | 2.1E-02 | 4 | 12 |
| Response to stimulus.Stress response.Abiotic stress response.Temperature stress response | 7.4E-04 | 18 | 84 |
| Response to stimulus.Stress response.Biotic stress response | 2.0E-18 | 215 | 1,252 |
| Response to stimulus.Stress response.Biotic stress response.Plant-pathogen interaction | 2.4E-13 | 123 | 664 |
| Signaling | 7.1E-38 | 573 | 3,656 |
| Signaling.Hormone Signaling | 2.2E-04 | 152 | 1,218 |
| Signaling.Hormone Signaling.ABA Signaling | 8.4E-03 | 25 | 160 |
| Signaling.Hormone Signaling.ABA Signaling.ABA-mediated Signaling pathway | 1.5E-02 | 23 | 151 |
| Signaling.Hormone Signaling.Auxin Signaling.Auxin metabolism.Auxin inactivation by conjugation | 2.8E-02 | 5 | 19 |
| Signaling.Hormone Signaling.Auxin Signaling.Auxin transport | 8.3E-03 | 11 | 52 |
| Signaling.Hormone Signaling.Ethylene Signaling | 6.5E-03 | 37 | 257 |
| Signaling.Hormone Signaling.Ethylene Signaling.Ethylene-mediated Signaling pathway | 3.2E-03 | 37 | 246 |
| Signaling.Hormone Signaling.Jasmonate salicylate signaling | 1.1E-02 | 20 | 123 |
| Signaling.Hormone Signaling.Jasmonate salicylate signaling.Jasmonate Signaling | 2.8E-02 | 18 | 118 |
| Signaling.Hormone Signaling.Jasmonate salicylate signaling.Jasmonate Signaling.Jasmonate-mediated Signaling pathway | 5.0E-03 | 16 | 84 |
| Signaling.Hormone Signaling.Jasmonate salicylate signaling.Salicylic acid Signaling | 5.5E-06 | 12 | 29 |
| Signaling.Hormone Signaling.Jasmonate salicylate signaling.Salicylic acid Signaling.Salicylic acid-mediated Signaling pathway | 4.5E-06 | 6 | 7 |
| Signaling.Hormone Signaling.Jasmonate salicylate signaling.Salicylic acid Signaling.Salicylic acid-responsive | 2.8E-02 | 5 | 19 |
| Signaling.Signaling pathway | 3.8E-40 | 441 | 2,517 |
| Signaling.Signaling pathway.Calcium sensors and Signaling | 8.8E-09 | 70 | 366 |
| Signaling.Signaling pathway.Circadian clock Signaling | 2.6E-03 | 16 | 79 |

| Over-represented functional category (FCT) | *p*-value | Number of Genes | |
|---|---|---|---|
| | | FCT | Vines with *Xf* |
| Signaling.Signaling pathway.Protein kinase | 1.4E-35 | 303 | 1,557 |
| Signaling.Signaling pathway.Protein kinase.MAPK cascade | 2.8E-02 | 13 | 77 |
| Signaling.Signaling pathway.Protein phosphatase.PP2C | 6.7E-04 | 14 | 57 |
| Transport overview | 3.0E-04 | 388 | 3,500 |
| Transport overview.Channels and pores | 4.7E-03 | 51 | 373 |
| Transport overview.Channels and pores.a-Type channels | 1.0E-02 | 36 | 256 |
| Transport overview.Channels and pores.a-Type channels.Annexin | 6.8E-03 | 8 | 31 |
| Transport overview.Channels and pores.a-Type channels.Cation Channel-forming Heat Shock Protein-70 | 8.4E-03 | 8 | 32 |
| Transport overview.Channels and pores.Vesicle Fusion Pores | 6.8E-03 | 8 | 31 |
| Transport overview.Channels and pores.Vesicle Fusion Pores.Synaptosomal Vesicle Fusion Pore | 6.8E-03 | 8 | 31 |
| Transport overview.Electrochemical Potential-driven Transporters | 2.7E-04 | 124 | 966 |
| Transport overview.Electrochemical Potential-driven Transporters.Porters | 2.5E-04 | 124 | 964 |
| Transport overview.Electrochemical Potential-driven Transporters.Porters.Amino Acid-Polyamine-Organocation | 2.1E-02 | 4 | 12 |
| Transport overview.Electrochemical Potential-driven Transporters.Porters.Amino Acid-Polyamine-Organocation.Cationic Amino Acid Transporter | 1.5E-02 | 4 | 11 |
| Transport overview.Electrochemical Potential-driven Transporters.Porters.Amino Acid/Auxin Permease | 5.0E-03 | 16 | 84 |
| Transport overview.Electrochemical Potential-driven Transporters.Porters.Cation Diffusion Facilitator | 2.1E-02 | 4 | 12 |
| Transport overview.Electrochemical Potential-driven Transporters.Porters.Divalent Anion:Na+ Symporter | 4.7E-02 | 2 | 4 |
| Transport overview.Electrochemical Potential-driven Transporters.Porters.Drug/Metabolite Transporter.UDP-glucu/UDP-N-acgalactosamine Transporter Fam | 1.4E-02 | 3 | 6 |
| Transport overview.Electrochemical Potential-driven Transporters.Porters.Folate-Biopterin Transporter | 6.8E-04 | 5 | 9 |
| Transport overview.Electrochemical Potential-driven Transporters.Porters.Mitochondrial Carrier.Mitochondrial dicarboxilate Carrier | 4.7E-02 | 2 | 4 |
| Transport overview.Ion transport | 4.2E-02 | 64 | 546 |
| Transport overview.Ion transport.Anion transport | 2.4E-02 | 18 | 116 |
| Transport overview.Ion transport.Anion transport.Phosphate transport | 4.9E-02 | 7 | 36 |
| Transport overview.Macromolecule transport | 2.0E-02 | 156 | 1,409 |
| Transport overview.Macromolecule transport.Amino acid transport | 3.2E-03 | 18 | 95 |
| Transport overview.Macromolecule transport.Organic ion transport.Organic anion transport.Malate transport.Vacuolar malate transport | 8.9E-03 | 2 | 2 |
| Transport overview.Macromolecule transport.Protein transport | 3.8E-02 | 53 | 439 |
| Transport overview.Macromolecule transport.Protein transport.Tethering factors | 1.0E-02 | 18 | 106 |
| Transport overview.Macromolecule transport.Protein transport.Thylakoid targeting pathway | 7.1E-03 | 11 | 51 |

| Over-represented functional category (FCT) | *p*-value | Number of Genes | |
|---|---|---|---|
| | | FCT | Vines with *Xf* |
| Transport overview.Primary Active Transporters.P-P-bond hydrolysis-driven transporters.P-type ATPase (P-ATPase).Ca2+-ATPase (efflux) | 1.0E-02 | 8 | 33 |
| Transport overview.Transmembrane Electron Carriers | 1.9E-06 | 19 | 61 |
| Transport overview.Transmembrane Electron Carriers.Transmembrane 1-electron transfer carriers | 1.5E-06 | 19 | 60 |
| Transport overview.Transmembrane Electron Carriers.Transmembrane 1-electron transfer carriers.Phagocyte (gp91phox) NADPH Oxidase | 3.3E-02 | 3 | 8 |
| Transport overview.Transmembrane Electron Carriers.Transmembrane 1-electron transfer carriers.Plant Photosystem I Supercomplex | 2.4E-05 | 14 | 43 |

Table 4.2 List of over-represented functional categories (FCTs) up-regulated in *X. fastidiosa*-inoculated vines during Phase I of PD. Statistical analysis performed using Fisher's exact test; *p*-values $\leq 0.05$ considered significant.

| Over-represented functional category (FCT) | *p*-value | Number of Genes | |
|---|---|---|---|
| | | FCT | Vines with *Xf* |
| Cellular process.Cellular component organization and biogenesis.Organelle organization and biogenesis | 2.4E-03 | 20 | 166 |
| Cellular process.Cellular component organization and biogenesis.Organelle organization and biogenesis.Plastid organization and biogenesis | 1.7E-05 | 15 | 71 |
| Cellular process.Cellular component organization and biogenesis.Organelle organization and biogenesis.Plastid organization and biogenesis.Thylakoid organization and biogenesis | 7.1E-03 | 5 | 21 |
| Cellular process.Cellular component organization and biogenesis.Ribosome organization and biogenesis | 2.5E-03 | 15 | 110 |
| Cellular process.Cellular homeostasis.Heavy metal ion homeostasis | 1.3E-02 | 5 | 24 |
| Development | 3.7E-02 | 40 | 495 |
| Development.Reproductive development | 3.2E-02 | 32 | 377 |
| Development.Reproductive development.Flower development | 1.2E-02 | 21 | 205 |
| Metabolism | 9.0E-09 | 664 | 9,214 |
| Metabolism.Cellular metabolism.One-carbon metabolism | 4.6E-02 | 7 | 55 |
| Metabolism.Primary metabolism | 1.2E-14 | 603 | 7,668 |
| Metabolism.Primary metabolism.Amino acid metabolism.Beta-Alanine metabolism.Beta-Alanine biosynthesis | 2.0E-02 | 2 | 4 |
| Metabolism.Primary metabolism.Amino acid metabolism.Glycine, serine, and threonine metabolism.Glycine, serine, and threonine biosynthesis | 1.0E-02 | 2 | 3 |
| Metabolism.Primary metabolism.Carbohydrate metabolism.Glycolysis Gluconeogenesis.Glycolysis | 4.3E-02 | 6 | 43 |
| Metabolism.Primary metabolism.Carbohydrate metabolism.Monosaccharide metabolism.Monosaccharide catabolism | 4.4E-04 | 13 | 74 |
| Metabolism.Primary metabolism.Carbohydrate metabolism.Monosaccharide metabolism.Monosaccharide catabolism.Pentose-phosphate shunt | 4.4E-04 | 13 | 74 |
| Metabolism.Primary metabolism.Carbohydrate metabolism.Polysaccharide metabolism.Starch and sucrose metabolism.Starch biosynthesis catabolism | 3.8E-02 | 8 | 64 |
| Metabolism.Primary metabolism.Carbon fixation | 8.0E-03 | 14 | 113 |
| Metabolism.Primary metabolism.Cofactor metabolism | 1.5E-03 | 13 | 84 |
| Metabolism.Primary metabolism.Cofactor metabolism.Tetrapyrrole metabolism | 2.6E-03 | 12 | 79 |
| Metabolism.Primary metabolism.Cofactor metabolism.Tetrapyrrole metabolism.Chlorophyll metabolism | 5.9E-03 | 7 | 37 |
| Metabolism.Primary metabolism.Cofactor metabolism.Tetrapyrrole metabolism.Chlorophyll metabolism.Chlorophyll biosynthesis | 1.0E-02 | 4 | 15 |
| Metabolism.Primary metabolism.Generation of metabolite precursors and energy.Photosynthesis | 3.1E-03 | 23 | 205 |
| Metabolism.Primary metabolism.Generation of metabolite precursors and energy.Photosynthesis.Calvin cycle | 5.0E-03 | 8 | 45 |

| Over-represented functional category (FCT) | *p*-value | Number of Genes | |
|---|---|---|---|
| | | FCT | Vines with *Xf* |
| Metabolism.Primary metabolism.Generation of metabolite precursors and energy.Photosynthesis.Reaction center pigment biosynthesis | 2.5E-02 | 3 | 11 |
| Metabolism.Primary metabolism.Lipid metabolism.Glycolipid metabolism | 4.0E-02 | 4 | 22 |
| Metabolism.Primary metabolism.Nucleobase, nucleoside, nucleotide, nucleic acid metabolism | 9.5E-17 | 194 | 1,760 |
| Metabolism.Primary metabolism.Nucleobase, nucleoside, nucleotide, nucleic acid metabolism.Nucleic acid metabolism | 1.1E-14 | 168 | 1,521 |
| Metabolism.Primary metabolism.Nucleobase, nucleoside, nucleotide, nucleic acid metabolism.Nucleic acid metabolism.RNA metabolism | 2.4E-15 | 127 | 1,011 |
| Metabolism.Primary metabolism.Nucleobase, nucleoside, nucleotide, nucleic acid metabolism.Nucleic acid metabolism.RNA metabolism.RNA catabolism | 5.0E-06 | 34 | 245 |
| Metabolism.Primary metabolism.Nucleobase, nucleoside, nucleotide, nucleic acid metabolism.Nucleic acid metabolism.RNA metabolism.RNA catabolism.RNA surveillance | 1.8E-05 | 21 | 125 |
| Metabolism.Primary metabolism.Nucleobase, nucleoside, nucleotide, nucleic acid metabolism.Nucleic acid metabolism.RNA metabolism.RNA processing | 1.3E-08 | 53 | 382 |
| Metabolism.Primary metabolism.Nucleobase, nucleoside, nucleotide, nucleic acid metabolism.Nucleic acid metabolism.RNA metabolism.RNA processing.mRNA processing | 6.2E-09 | 49 | 332 |
| Metabolism.Primary metabolism.Nucleobase, nucleoside, nucleotide, nucleic acid metabolism.Nucleic acid metabolism.RNA metabolism.RNA processing.mRNA processing.mRNA splicing | 8.2E-08 | 45 | 317 |
| Metabolism.Primary metabolism.Nucleobase, nucleoside, nucleotide, nucleic acid metabolism.Nucleic acid metabolism.RNA metabolism.rRNA metabolism | 4.4E-03 | 4 | 12 |
| Metabolism.Primary metabolism.Nucleobase, nucleoside, nucleotide, nucleic acid metabolism.Nucleotide metabolism | 2.3E-04 | 27 | 214 |
| Metabolism.Primary metabolism.Nucleobase, nucleoside, nucleotide, nucleic acid metabolism.Nucleotide metabolism.Purine metabolism | 3.9E-03 | 17 | 138 |
| Metabolism.Primary metabolism.Nucleobase, nucleoside, nucleotide, nucleic acid metabolism.Nucleotide metabolism.Pyrimidine metabolism | 7.0E-03 | 13 | 100 |
| Metabolism.Primary metabolism.Organic acid metabolism | 2.2E-02 | 23 | 243 |
| Metabolism.Primary metabolism.Organic acid metabolism.Butanoate metabolism | 1.6E-02 | 10 | 76 |
| Metabolism.Primary metabolism.Organic acid metabolism.Butanoate metabolism.Butanoate biosynthesis | 2.0E-02 | 2 | 4 |
| Metabolism.Primary metabolism.Organic acid metabolism.Propanoate metabolism | 4.4E-02 | 8 | 66 |
| Metabolism.Primary metabolism.Protein metabolism and modification | 2.4E-06 | 202 | 2,450 |
| Metabolism.Primary metabolism.Protein metabolism and modification.Protein folding | 9.8E-03 | 43 | 493 |
| Metabolism.Primary metabolism.Protein metabolism and modification.Protein folding.Protein export | 2.2E-02 | 6 | 37 |

| Over-represented functional category (FCT) | *p*-value | Number of Genes | |
|---|---|---|---|
| | | FCT | Vines with *Xf* |
| Metabolism.Primary metabolism.Protein metabolism and modification.Protein modification.Protein methylation | 3.9E-02 | 6 | 42 |
| Metabolism.Primary metabolism.Protein metabolism and modification.Protein synthesis | 1.5E-12 | 90 | 678 |
| Metabolism.Primary metabolism.Protein metabolism and modification.Protein synthesis.Ribosome | 7.7E-13 | 66 | 419 |
| Metabolism.Primary metabolism.Protein metabolism and modification.Protein synthesis.Translation | 3.7E-03 | 28 | 270 |
| Metabolism.Primary metabolism.Protein metabolism and modification.Protein synthesis.Translation.Translational initiation | 1.6E-02 | 11 | 88 |
| Regulation overview | 1.7E-14 | 270 | 2,851 |
| Regulation overview.Regulation of cell cycle.Regulation of mitosis | 4.0E-02 | 4 | 22 |
| Regulation overview.Regulation of gene expression | 4.5E-14 | 257 | 2,699 |
| Regulation overview.Regulation of gene expression.Regulation of transcription | 9.0E-14 | 251 | 2,635 |
| Regulation overview.Regulation of gene expression.Regulation of transcription.Transcription factor | 6.8E-14 | 247 | 2,575 |
| Regulation overview.Regulation of gene expression.Regulation of transcription.Transcription factor.AUXIAA family transcription factor | 3.4E-07 | 10 | 23 |
| Regulation overview.Regulation of gene expression.Regulation of transcription.Transcription factor.BES1 family transcription factor | 2.1E-03 | 4 | 10 |
| Regulation overview.Regulation of gene expression.Regulation of transcription.Transcription factor.bZIP family transcription factor.AREB subfamily transcription factor | 1.0E-02 | 2 | 3 |
| Regulation overview.Regulation of gene expression.Regulation of transcription.Transcription factor.C2H2 family transcription factor | 2.9E-02 | 13 | 120 |
| Regulation overview.Regulation of gene expression.Regulation of transcription.Transcription factor.C3H family transcription factor | 1.3E-02 | 11 | 85 |
| Regulation overview.Regulation of gene expression.Regulation of transcription.Transcription factor.CO-like / B-box family transcriprion factor | 3.2E-02 | 3 | 12 |
| Regulation overview.Regulation of gene expression.Regulation of transcription.Transcription factor.FHA family transcription factor | 2.9E-02 | 4 | 20 |
| Regulation overview.Regulation of gene expression.Regulation of transcription.Transcription factor.GRF family transcription factor | 4.4E-03 | 4 | 12 |
| Regulation overview.Regulation of gene expression.Regulation of transcription.Transcription factor.Homeobox domain family transcription factor | 2.2E-02 | 11 | 92 |
| Regulation overview.Regulation of gene expression.Regulation of transcription.Transcription factor.MTERF | 1.7E-02 | 6 | 35 |
| Regulation overview.Regulation of gene expression.Regulation of transcription.Transcription factor.SET PCG family transcription factor | 4.6E-02 | 7 | 55 |

| Over-represented functional category (FCT) | *p*-value | Number of Genes | |
|---|---|---|---|
| | | FCT | Vines with *Xf* |
| Regulation overview.Regulation of gene expression.Regulation of transcription.Transcription factor.Trihelix family transcription factor | 1.6E-03 | 8 | 38 |
| Regulation overview.Regulation of gene expression.Regulation of transcription.Transcription factor.ZIM family transcription factor | 6.0E-03 | 4 | 13 |
| Regulation overview.Regulation of gene expression.Regulation of transcription.Transcription factor.Zinc finger AN1 family transcription factor | 4.0E-02 | 3 | 13 |
| Regulation overview.Regulation of gene expression.Regulation of transcription.Transcription factor.Zinc finger C3HC4 family transcription factor | 7.1E-03 | 25 | 245 |
| Regulation overview.Regulation of gene expression.Regulation of transcription.Transcription factor.Zinc finger SWIM family transcription factor | 1.0E-02 | 2 | 3 |
| Signaling.Hormone Signaling | 8.2E-03 | 94 | 1,218 |
| Signaling.Hormone Signaling.Auxin Signaling | 1.5E-02 | 37 | 422 |
| Signaling.Hormone Signaling.Auxin Signaling.Auxin metabolism.Auxin activation by conjugation hydrolysis | 1.4E-02 | 3 | 9 |
| Signaling.Hormone Signaling.Auxin Signaling.Auxin transport | 1.2E-02 | 8 | 52 |
| Signaling.Hormone Signaling.Ethylene Signaling.Ethylene responsive | 1.4E-02 | 3 | 9 |
| Signaling.Hormone Signaling.Ethylene Signaling.Ethylene-mediated Signaling pathway | 4.2E-02 | 22 | 246 |
| Signaling.Signaling pathway.Circadian clock Signaling | 1.6E-05 | 16 | 79 |
| Signaling.Signaling pathway.Light Signaling | 1.1E-03 | 10 | 53 |
| Signaling.Signaling pathway.Light Signaling.Red/Far red light Signaling | 2.1E-03 | 4 | 10 |
| Signaling.Signaling pathway.Protein phosphatase.PP2A | 3.2E-02 | 3 | 12 |
| Signaling.Signaling pathway.TOR Signaling pathway | 1.1E-02 | 6 | 32 |
| Transport overview | 8.0E-04 | 254 | 3,500 |
| Transport overview.Electrochemical Potential-driven Transporters | 1.5E-02 | 75 | 966 |
| Transport overview.Electrochemical Potential-driven Transporters.Porters | 1.4E-02 | 75 | 964 |
| Transport overview.Electrochemical Potential-driven Transporters.Porters.Glycoside-Pentoside-Hexuronide:Cation Symporter | 4.6E-02 | 2 | 6 |
| Transport overview.Electrochemical Potential-driven Transporters.Porters.Major Facilitator Superfamily | 1.8E-02 | 13 | 113 |
| Transport overview.Electrochemical Potential-driven Transporters.Porters.Major Facilitator Superfamily.Drug:H+ Antiporter-1 (12 Spanner) | 3.2E-02 | 3 | 12 |
| Transport overview.Electrochemical Potential-driven Transporters.Porters.Major Facilitator Superfamily.Organic Cation Transporter | 2.0E-02 | 2 | 4 |
| Transport overview.Electrochemical Potential-driven Transporters.Porters.Zinc (Zn2+)-Iron (Fe2+) Permease | 1.5E-03 | 6 | 22 |

| Over-represented functional category (FCT) | *p*-value | Number of Genes | |
|---|---|---|---|
| | | FCT | Vines with *Xf* |
| Transport overview.Group translocators | 2.2E-02 | 6 | 37 |
| Transport overview.Group translocators.Acyl CoA ligase-coupled transporters | 2.2E-02 | 6 | 37 |
| Transport overview.Group translocators.Acyl CoA ligase-coupled transporters.Proposed Fatty Acid Transporter | 2.2E-02 | 6 | 37 |
| Transport overview.Incompletely characterized transport systems.Putative transport protein.Putative Tripartite Zn2+ Transporter | 2.0E-02 | 2 | 4 |
| Transport overview.Ion transport.Cation transport.Heavy metal ion transport | 2.6E-03 | 11 | 69 |
| Transport overview.Ion transport.Cation transport.Heavy metal ion transport.Zinc transport | 1.3E-02 | 4 | 16 |
| Transport overview.Macromolecule transport | 2.3E-03 | 111 | 1,409 |
| Transport overview.Macromolecule transport.Carbohydrate transport | 9.0E-04 | 16 | 110 |
| Transport overview.Macromolecule transport.Carbohydrate transport.Sugar transport | 1.3E-03 | 15 | 103 |
| Transport overview.Macromolecule transport.Protein transport | 3.8E-02 | 36 | 439 |
| Transport overview.Macromolecule transport.Protein transport.Thylakoid targeting pathway | 1.9E-04 | 11 | 51 |
| Transport overview.Macromolecule transport.RNA transport | 1.6E-03 | 25 | 219 |
| Transport overview.Plastid membrane transport | 4.0E-02 | 3 | 13 |
| Transport overview.Plastid membrane transport.Plastid membrane protein transport | 4.0E-02 | 3 | 13 |
| Transport overview.Primary Active Transporters | 5.2E-04 | 67 | 736 |
| Transport overview.Primary Active Transporters.P-P-bond hydrolysis-driven transporters | 8.8E-06 | 61 | 567 |
| Transport overview.Primary Active Transporters.P-P-bond hydrolysis-driven transporters.Chloroplast Env Prot Translocase | 4.7E-02 | 6 | 44 |
| Transport overview.Primary Active Transporters.P-P-bond hydrolysis-driven transporters.General Secretory Pathway (Sec) | 2.4E-02 | 14 | 129 |
| Transport overview.Primary Active Transporters.P-P-bond hydrolysis-driven transporters.Nuclear mRNA Exporter | 1.2E-07 | 22 | 101 |

Table 4.3 List of over-represented functional categories (FCTs) down-regulated in *X. fastidiosa*-inoculated vines during Phase I of PD. Statistical analysis performed using Fisher's exact test; *p*-values ≤ 0.05 considered significant.

| Over-represented functional category (FCT) | *p*-value | Number of Genes | |
|---|---|---|---|
| | | FCT | Vines with *Xf* |
| Cellular process | 1.6E-07 | 199 | 2,332 |
| Cellular process.Cell growth and death | 9.4E-07 | 55 | 462 |
| Cellular process.Cellular component organization and biogenesis | 1.2E-05 | 116 | 1,305 |
| Cellular process.Cellular component organization and biogenesis.Cell wall organization and biogenesis | 2.3E-03 | 47 | 511 |
| Cellular process.Cellular component organization and biogenesis.Cell wall organization and biogenesis.Cell wall metabolism | 3.3E-02 | 33 | 395 |
| Cellular process.Cellular component organization and biogenesis.Cell wall organization and biogenesis.Cell wall metabolism.Cell wall biosynthesis | 1.9E-02 | 15 | 139 |
| Cellular process.Cellular component organization and biogenesis.Cell wall organization and biogenesis.Cell wall metabolism.Cell wall biosynthesis.Cellulose biosynthesis | 7.9E-03 | 12 | 91 |
| Cellular process.Cellular component organization and biogenesis.Cell wall organization and biogenesis.Cell wall metabolism.Cell wall catabolism.Pectin catabolism | 2.9E-02 | 4 | 20 |
| Cellular process.Cellular component organization and biogenesis.Cytoskeleton organization and biogenesis | 1.2E-10 | 54 | 348 |
| Cellular process.Cellular component organization and biogenesis.Cytoskeleton organization and biogenesis.Microtubule organization and biogenesis | 2.1E-12 | 38 | 173 |
| Cellular process.Cellular component organization and biogenesis.Cytoskeleton organization and biogenesis.Microtubule organization and biogenesis.Microtubule-driven movement | 7.2E-13 | 31 | 115 |
| Cellular process.Cellular component organization and biogenesis.Nucleus.Chromosome organization and biogenesis.Chromatin assembly | 1.2E-02 | 9 | 63 |
| Cellular process.Cellular transport.Protein trafficking.Vesicle-mediated trafficking.Phagosome | 5.0E-02 | 12 | 118 |
| Development.Senescence | 2.4E-02 | 6 | 38 |
| Diverse functions.Gene family with diverse functions.NBS-LRR superfamily | 4.3E-02 | 34 | 418 |
| Metabolism.Primary metabolism.Amino acid metabolism.Beta-Alanine metabolism.Beta-Alanine biosynthesis | 2.0E-02 | 2 | 4 |
| Metabolism.Primary metabolism.Amino acid metabolism.Glutamate metabolism | 3.7E-02 | 9 | 76 |
| Metabolism.Primary metabolism.Amino acid metabolism.Glutamate metabolism.Glutamate catabolism | 1.9E-02 | 3 | 10 |
| Metabolism.Primary metabolism.Amino acid metabolism.Serine metabolism.Serine catabolism | 4.6E-02 | 2 | 6 |
| Metabolism.Primary metabolism.Carbohydrate metabolism.Carbohydrate metabolism enzyme inhibitor | 1.9E-03 | 6 | 23 |

| Over-represented functional category (FCT) | *p*-value | Number of Genes | |
|---|---|---|---|
| | | FCT | Vines with *Xf* |
| Metabolism.Primary metabolism.Carbohydrate metabolism.Carbohydrate metabolism enzyme inhibitor.Invertase/pectin methylesterase inhibitor family | 1.9E-03 | 6 | 23 |
| Metabolism.Primary metabolism.Carbohydrate metabolism.Monosaccharide metabolism | 4.8E-02 | 51 | 672 |
| Metabolism.Primary metabolism.Carbohydrate metabolism.Monosaccharide metabolism.Amino sugar metabolism | 4.9E-02 | 9 | 80 |
| Metabolism.Primary metabolism.Carbohydrate metabolism.Polysaccharide metabolism.Beta-1,3 glucan metabolism | 7.3E-04 | 12 | 69 |
| Metabolism.Primary metabolism.Carbohydrate metabolism.Polysaccharide metabolism.Beta-1,3 glucan metabolism.Beta-1,3 glucan catabolism | 1.9E-03 | 10 | 57 |
| Metabolism.Primary metabolism.Generation of metabolite precursors and energy.Photosynthesis | 2.8E-03 | 23 | 205 |
| Metabolism.Primary metabolism.Generation of metabolite precursors and energy.Photosynthesis.Antenna proteins | 6.0E-08 | 10 | 20 |
| Metabolism.Primary metabolism.Lipid metabolism.Glycerolipid metabolism.Glycerolipid catabolism | 5.5E-03 | 6 | 28 |
| Metabolism.Primary metabolism.Lipid metabolism.Sphingolipid metabolism | 4.8E-02 | 10 | 92 |
| Metabolism.Primary metabolism.Nucleobase, nucleoside, nucleotide, nucleic acid metabolism.Nucleic acid metabolism.DNA metabolism.DNA replication | 2.5E-04 | 17 | 109 |
| Metabolism.Primary metabolism.Organic acid metabolism.Butanoate metabolism.Butanoate biosynthesis | 2.0E-02 | 2 | 4 |
| Regulation overview | 7.6E-12 | 257 | 2,851 |
| Regulation overview.Regulation of cell cycle | 1.8E-08 | 30 | 159 |
| Regulation overview.Regulation of gene expression | 6.1E-08 | 227 | 2,699 |
| Regulation overview.Regulation of gene expression.Regulation of transcription | 3.2E-08 | 224 | 2,635 |
| Regulation overview.Regulation of gene expression.Regulation of transcription.Transcription factor | 1.2E-08 | 222 | 2,575 |
| Regulation overview.Regulation of gene expression.Regulation of transcription.Transcription factor.AP2 family transcription factor.ERF subfamily transcription factor | 4.8E-02 | 7 | 56 |
| Regulation overview.Regulation of gene expression.Regulation of transcription.Transcription factor.AUXIAA family transcription factor | 4.5E-02 | 4 | 23 |
| Regulation overview.Regulation of gene expression.Regulation of transcription.Transcription factor.bHLH family transcription factor | 9.5E-03 | 17 | 152 |
| Regulation overview.Regulation of gene expression.Regulation of transcription.Transcription factor.C2C2-DOF family transcription factor | 5.0E-04 | 7 | 25 |

| Over-represented functional category (FCT) | *p*-value | Number of Genes | |
|---|---|---|---|
| | | FCT | Vines with *Xf* |
| Regulation overview.Regulation of gene expression.Regulation of transcription.Transcription factor.CO-like / B-box family transcriprion factor | 3.1E-02 | 3 | 12 |
| Regulation overview.Regulation of gene expression.Regulation of transcription.Transcription factor.CPP family transcription factor | 6.2E-03 | 3 | 7 |
| Regulation overview.Regulation of gene expression.Regulation of transcription.Transcription factor.Homeobox domain family transcription factor | 4.8E-02 | 10 | 92 |
| Regulation overview.Regulation of gene expression.Regulation of transcription.Transcription factor.LIM family transcription factor | 3.1E-02 | 3 | 12 |
| Regulation overview.Regulation of gene expression.Regulation of transcription.Transcription factor.NAC family transcription factor | 1.6E-03 | 12 | 75 |
| Regulation overview.Regulation of gene expression.Regulation of transcription.Transcription factor.PseudoARR-B family transcription factor | 7.3E-04 | 4 | 8 |
| Regulation overview.Regulation of gene expression.Regulation of transcription.Transcription factor.SBP family transcription factor | 2.9E-02 | 4 | 20 |
| Regulation overview.Regulation of gene expression.Regulation of transcription.Transcription factor.TRAF | 5.0E-02 | 5 | 34 |
| Regulation overview.Regulation of gene expression.Regulation of transcription.Transcription factor.WRKY family transcription factor | 1.3E-08 | 18 | 62 |
| Regulation overview.Regulation of gene expression.Regulation of transcription.Transcription factor.Zinc finger C3HC4 family transcription factor | 1.6E-04 | 30 | 245 |
| Response to stimulus | 7.7E-14 | 209 | 2,093 |
| Response to stimulus.Stress response | 7.7E-14 | 209 | 2,093 |
| Response to stimulus.Stress response.Abiotic stress response.Drought stress response | 1.7E-02 | 7 | 45 |
| Response to stimulus.Stress response.Abiotic stress response.Light stress response | 3.1E-02 | 3 | 12 |
| Response to stimulus.Stress response.Biotic stress response | 1.1E-13 | 142 | 1,252 |
| Response to stimulus.Stress response.Biotic stress response.Plant-pathogen interaction | 4.8E-12 | 87 | 664 |
| Response to stimulus.Stress response.Biotic stress response.Plant-pathogen interaction.R proteins from Plant-pathogen interaction | 2.6E-04 | 38 | 348 |
| Signaling | 1.6E-29 | 382 | 3,656 |
| Signaling.Hormone Signaling | 1.6E-05 | 109 | 1,218 |
| Signaling.Hormone Signaling.ABA Signaling | 1.5E-02 | 17 | 160 |

| Over-represented functional category (FCT) | *p*-value | Number of Genes | |
|---|---|---|---|
| | | FCT | Vines with *Xf* |
| Signaling.Hormone Signaling.ABA Signaling.ABA-mediated Signaling pathway | 1.9E-02 | 16 | 151 |
| Signaling.Hormone Signaling.Auxin Signaling | 4.8E-03 | 39 | 422 |
| Signaling.Hormone Signaling.Auxin Signaling.Auxin transport | 4.4E-05 | 12 | 52 |
| Signaling.Hormone Signaling.Auxin Signaling.Regulation of auxin transport | 4.6E-02 | 2 | 6 |
| Signaling.Hormone Signaling.Cytokinin Signaling.Cytokinin-mediated Signaling pathway | 6.9E-03 | 10 | 68 |
| Signaling.Hormone Signaling.Ethylene Signaling | 6.2E-03 | 26 | 257 |
| Signaling.Hormone Signaling.Ethylene Signaling.Ethylene-mediated Signaling pathway | 3.5E-03 | 26 | 246 |
| Signaling.Hormone Signaling.Ethylene Signaling.Regulation of ethylene biosynthesis | 3.2E-02 | 2 | 5 |
| Signaling.Hormone Signaling.Jasmonate salicylate signaling.Salicylic acid Signaling.Salicylic acid-mediated Signaling pathway | 6.2E-03 | 3 | 7 |
| Signaling.Signaling pathway | 1.2E-26 | 284 | 2,517 |
| Signaling.Signaling pathway.Calcium sensors and Signaling | 3.6E-04 | 39 | 366 |
| Signaling.Signaling pathway.Circadian clock Signaling | 3.4E-06 | 17 | 79 |
| Signaling.Signaling pathway.Light Signaling.Blue light Signaling | 3.2E-02 | 2 | 5 |
| Signaling.Signaling pathway.Protein kinase | 1.3E-28 | 208 | 1,557 |
| Signaling.Signaling pathway.Protein kinase.MAPK cascade | 1.6E-02 | 10 | 77 |
| Signaling.Signaling pathway.Protein phosphatase.PP2C | 6.4E-03 | 9 | 57 |
| Signaling.Signaling pathway.Signaling receptor | 3.1E-02 | 3 | 12 |
| Transport overview.Electrochemical Potential-driven Transporters | 4.4E-03 | 78 | 966 |
| Transport overview.Electrochemical Potential-driven Transporters.Porters | 4.1E-03 | 78 | 964 |
| Transport overview.Electrochemical Potential-driven Transporters.Porters.Amino Acid/Auxin Permease | 2.8E-02 | 10 | 84 |
| Transport overview.Electrochemical Potential-driven Transporters.Porters.Anion Exchanger | 1.7E-04 | 4 | 6 |
| Transport overview.Electrochemical Potential-driven Transporters.Porters.Auxin Efflux Carrier | 2.4E-03 | 6 | 24 |
| Transport overview.Electrochemical Potential-driven Transporters.Porters.Major Facilitator Superfamily.Drug:H+ Antiporter-1 (12 Spanner) | 4.3E-03 | 4 | 12 |
| Transport overview.Electrochemical Potential-driven Transporters.Porters.Major Facilitator Superfamily.Phosphate: H+ Symporter | 1.9E-02 | 3 | 10 |
| Transport overview.Electrochemical Potential-driven Transporters.Porters.Mitochondrial Carrier.Mitochondrial dicarboxilate Carrier | 2.0E-02 | 2 | 4 |

| Over-represented functional category (FCT) | *p*-value | Number of Genes | |
|---|---|---|---|
| | | FCT | Vines with *Xf* |
| Transport overview.Ion transport.Anion transport | 3.9E-03 | 15 | 116 |
| Transport overview.Macromolecule transport.Protein transport.Thylakoid targeting pathway | 3.0E-03 | 9 | 51 |
| Transport overview.Primary Active Transporters.P-P-bond hydrolysis-driven transporters.P-type ATPase (P-ATPase).Ca2+-ATPase (efflux) | 1.2E-02 | 6 | 33 |
| Transport overview.Transmembrane Electron Carriers | 5.2E-05 | 13 | 61 |
| Transport overview.Transmembrane Electron Carriers.Transmembrane 1-electron transfer carriers | 4.4E-05 | 13 | 60 |
| Transport overview.Transmembrane Electron Carriers.Transmembrane 1-electron transfer carriers.Plant Photosystem I Supercomplex | 3.3E-05 | 11 | 43 |

Table 4.4 List of over-represented functional categories (FCTs) up-regulated in *X. fastidiosa*-inoculated vines during Phase II of PD. Statistical analysis performed using Fisher's exact test; *p*-values $\leq 0.05$ considered significant.

| Over-represented functional category (FCT) | *p*-value | Number of Genes | |
|---|---|---|---|
| | | FCT | Vines with *Xf* |
| Cellular process.Cellular homeostasis | 1.9E-03 | 6 | 82 |
| Cellular process.Cellular homeostasis.Cell redox homeostasis | 1.1E-02 | 4 | 55 |
| Metabolism | 8.2E-09 | 203 | 9,214 |
| Metabolism.Cellular metabolism.Nitrogen and sulfur metabolism.Sulfur metabolism.Sulfate assimilation | 2.6E-02 | 2 | 16 |
| Metabolism.Primary metabolism | 2.8E-09 | 178 | 7,668 |
| Metabolism.Primary metabolism.Carbohydrate metabolism | 3.3E-04 | 38 | 1,334 |
| Metabolism.Primary metabolism.Carbohydrate metabolism.Glycolysis Gluconeogenesis | 7.0E-03 | 9 | 214 |
| Metabolism.Primary metabolism.Carbohydrate metabolism.Glycolysis Gluconeogenesis.Glycolysis | 4.6E-03 | 4 | 43 |
| Metabolism.Primary metabolism.Carbohydrate metabolism.Monosaccharide metabolism | 2.4E-03 | 21 | 672 |
| Metabolism.Primary metabolism.Carbohydrate metabolism.Monosaccharide metabolism.Pyruvate metabolism | 7.0E-04 | 10 | 184 |
| Metabolism.Primary metabolism.Carbohydrate metabolism.Oligosaccharide metabolism | 1.4E-02 | 10 | 280 |
| Metabolism.Primary metabolism.Carbon fixation | 9.0E-03 | 6 | 113 |
| Metabolism.Primary metabolism.Generation of metabolite precursors and energy.Citric acid cycle | 4.3E-03 | 5 | 68 |
| Metabolism.Primary metabolism.Generation of metabolite precursors and energy.Glyoxylate and dicarboxylate metabolism | 7.7E-03 | 5 | 78 |
| Metabolism.Primary metabolism.Lipid metabolism | 2.7E-04 | 27 | 818 |
| Metabolism.Primary metabolism.Lipid metabolism.Fatty acid metabolism | 2.1E-03 | 12 | 287 |
| Metabolism.Primary metabolism.Lipid metabolism.Fatty acid metabolism.Fatty acid biosynthesis | 2.1E-03 | 8 | 144 |
| Metabolism.Primary metabolism.Lipid metabolism.Fatty acid metabolism.Fatty acid biosynthesis.Unsaturated fatty acid biosynthesis | 4.4E-02 | 3 | 50 |
| Metabolism.Primary metabolism.Lipid metabolism.Synthesis and degradation of ketone bodies | 2.0E-02 | 2 | 14 |
| Metabolism.Primary metabolism.Organic acid metabolism | 1.5E-02 | 9 | 243 |
| Metabolism.Primary metabolism.Organic acid metabolism.Ascorbate and aldarate metabolism | 2.0E-02 | 4 | 66 |
| Metabolism.Primary metabolism.Protein metabolism and modification | 7.7E-05 | 63 | 2,450 |
| Metabolism.Primary metabolism.Protein metabolism and modification.Protein folding | 1.4E-05 | 22 | 493 |
| Metabolism.Primary metabolism.Protein metabolism and modification.Protein folding.Chaperone-mediated protein folding | 9.6E-05 | 15 | 301 |

| Over-represented functional category (FCT) | *p*-value | Number of Genes | |
|---|---|---|---|
| | | FCT | Vines with *Xf* |
| Metabolism.Primary metabolism.Protein metabolism and modification.Protein folding.Chaperone-mediated protein folding.HSP-mediated protein folding | 1.2E-04 | 13 | 240 |
| Metabolism.Primary metabolism.Protein metabolism and modification.Protein synthesis | 5.2E-04 | 23 | 678 |
| Metabolism.Primary metabolism.Protein metabolism and modification.Protein synthesis.Ribosome | 1.3E-04 | 18 | 419 |
| Metabolism.Primary metabolism.Protein metabolism and modification.Protein synthesis.Translation | 2.8E-02 | 9 | 270 |
| Metabolism.Secondary metabolism.Phenylpropanoid metabolism.Flavonoid metabolism | 2.4E-02 | 10 | 306 |
| Metabolism.Secondary metabolism.Phenylpropanoid metabolism.Flavonoid metabolism.Flavonoid biosynthesis | 6.0E-03 | 10 | 247 |
| Metabolism.Secondary metabolism.Phenylpropanoid metabolism.Lignin metabolism.Lignin biosynthesis | 2.3E-02 | 2 | 15 |
| Metabolism.Secondary metabolism.Polyamine metabolism.Polyamine biosynthesis | 4.6E-02 | 2 | 22 |
| Metabolism.Secondary metabolism.Terpenoid metabolism.Terpenoid biosynthesis.Mevalonate biosynthesis | 3.5E-03 | 2 | 6 |
| Metabolism.Secondary metabolism.Terpenoid metabolism.Terpenoid catabolism | 3.1E-02 | 1 | 2 |
| Metabolism.Secondary metabolism.Terpenoid metabolism.Terpenoid catabolism.Mevalonate catabolism | 3.1E-02 | 1 | 2 |
| Regulation overview.Regulation of gene expression.Regulation of transcription.Transcription factor.CO-like / B-box family transcriprion factor | 7.6E-04 | 3 | 12 |
| Regulation overview.Regulation of gene expression.Regulation of transcription.Transcription factor.CSD family transcription factor | 3.1E-02 | 1 | 2 |
| Signaling.Hormone Signaling.Ethylene Signaling.Ethylene metabolism | 2.5E-02 | 3 | 40 |
| Signaling.Hormone Signaling.Ethylene Signaling.Ethylene metabolism.Ethylene biosynthesis | 2.2E-02 | 3 | 38 |
| Signaling.Signaling pathway.Circadian clock Signaling | 3.6E-02 | 4 | 79 |
| Transport overview | 2.2E-03 | 76 | 3,500 |
| Transport overview.Channels and pores | 3.5E-02 | 11 | 373 |
| Transport overview.Channels and pores.a-Type channels | 7.6E-03 | 10 | 256 |
| Transport overview.Channels and pores.a-Type channels.Inward Rectifier K+ Channel | 4.6E-02 | 1 | 3 |
| Transport overview.Channels and pores.a-Type channels.Major Intrinsic Protein | 2.9E-03 | 4 | 38 |
| Transport overview.Electrochemical Potential-driven Transporters | 1.6E-04 | 31 | 966 |
| Transport overview.Electrochemical Potential-driven Transporters.Porters | 1.5E-04 | 31 | 964 |
| Transport overview.Electrochemical Potential-driven Transporters.Porters.Major Facilitator Superfamily | 3.3E-02 | 5 | 113 |

| Over-represented functional category (FCT) | *p*-value | Number of Genes | |
|---|---|---|---|
| | | FCT | Vines with *Xf* |
| Transport overview.Electrochemical Potential-driven Transporters.Porters.Major Facilitator Superfamily.Organic phosphate:Pi antiporter | 4.6E-02 | 1 | 3 |
| Transport overview.Electrochemical Potential-driven Transporters.Porters.Multidrug/Oligosaccharidyl-lipid/Polysaccharide Flippase | 8.2E-03 | 5 | 79 |
| Transport overview.Electrochemical Potential-driven Transporters.Porters.Multidrug/Oligosaccharidyl-lipid/Polysaccharide Flippase.Multi Antimicrobial Extrusion | 7.3E-03 | 5 | 77 |
| Transport overview.Electrochemical Potential-driven Transporters.Porters.Resistance-Nodulation-Cell Division | 2.4E-03 | 2 | 5 |
| Transport overview.Electrochemical Potential-driven Transporters.Porters.Resistance-Nodulation-Cell Division.Eukaryotic (Putative) Sterol Transporter | 2.4E-03 | 2 | 5 |
| Transport overview.Incompletely characterized transport systems.Putative transport protein | 1.6E-02 | 5 | 93 |
| Transport overview.Incompletely characterized transport systems.Putative transport protein.Testis-Enhanced Gene Transfer | 4.6E-02 | 1 | 3 |
| Transport overview.Incompletely characterized transport systems.Putative transport protein.YdjX-Z | 1.6E-02 | 1 | 1 |
| Transport overview.Macromolecule transport | 1.5E-02 | 33 | 1,409 |
| Transport overview.Macromolecule transport.Glycerol-3-phosphate transport | 3.1E-02 | 1 | 2 |
| Transport overview.Macromolecule transport.Multidrug transport.Anthocyanin transport | 3.5E-03 | 2 | 6 |
| Transport overview.Macromolecule transport.Oligopeptide transport | 3.5E-02 | 4 | 78 |
| Transport overview.Macromolecule transport.Protein transport.Thylakoid targeting pathway | 4.6E-02 | 3 | 51 |
| Transport overview.Water transport | 2.4E-03 | 4 | 36 |
| Transport overview.Water transport.Aquaporins | 2.4E-03 | 4 | 36 |
| Transport overview.Water transport.Aquaporins.PIP | 7.7E-03 | 3 | 26 |

Table 4.5 List of over-represented functional categories (FCTs) down-regulated in *X. fastidiosa*-inoculated vines during Phase II of PD. Statistical analysis performed using Fisher's exact test; *p*-values ≤ 0.05 considered significant.